Polymeric materials for catalysis applications

María Jesús García Fernández

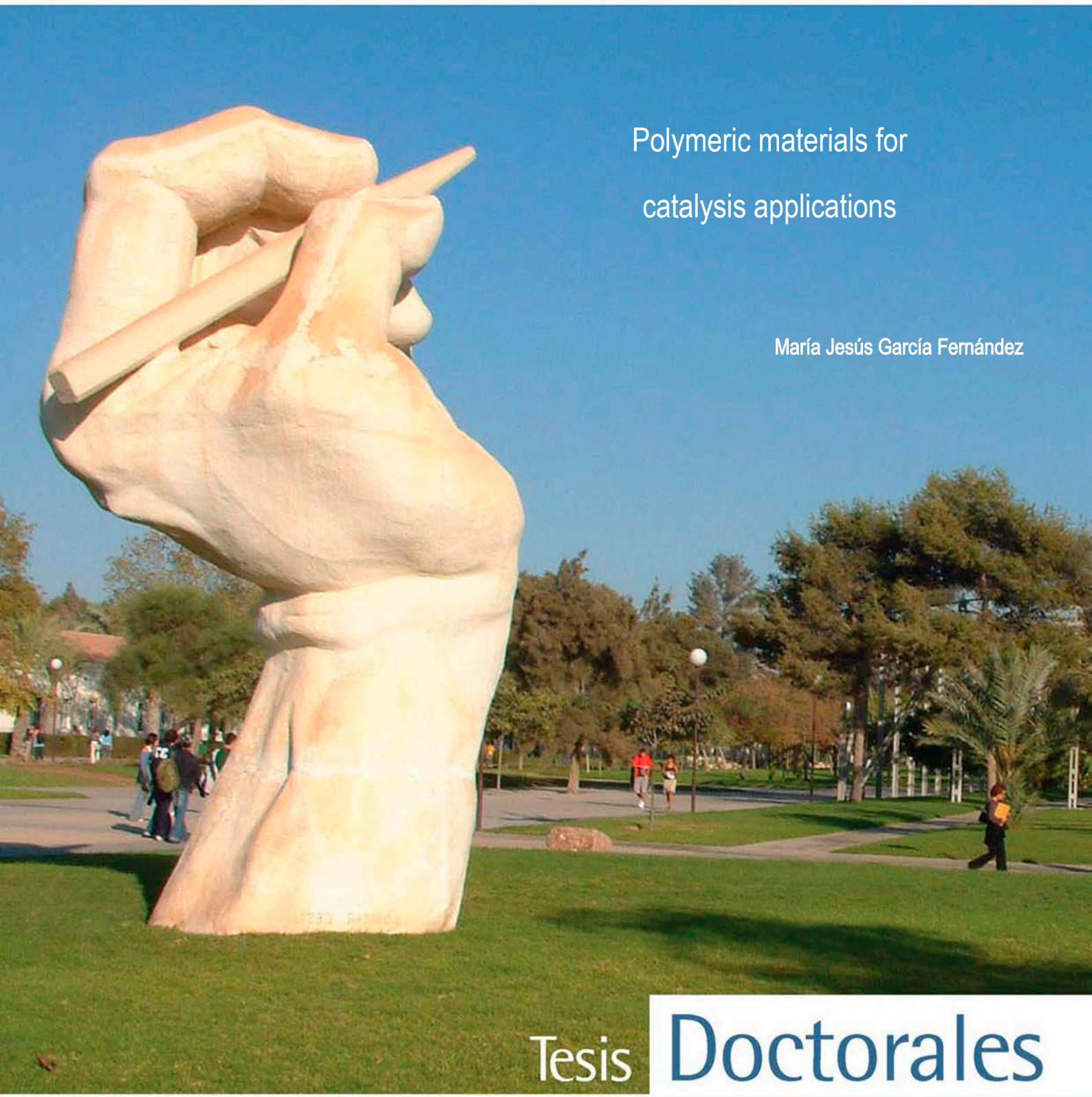

Universitat d'Alacant
Universidad de Alicante

Polymeric materials for catalysis applications

María Jesús García Fernández

Tesis presentada para aspirar al título de doctora
por la Universidad de Alicante

Doctorado en Ingeniería Química

Dirigida por:

Antonio Sepúlveda Escribano
Catedrático de Química Inorgánica

María de las Mercedes Pastor Blas
Catedrática de Química Inorgánica

Financiación:

Consellería de Educación (PROMETEO-2009-002)

Nada podrá descubrir quien pretenda negar lo inexplicable. La realidad es un pozo de enigmas.

Carmen Martín Gaite

Agradecimientos

A mis directores de tesis, el Dr. **Antonio Sepúlveda Escribano** y la Dra. **María Mercedes Pastor Blas**. Gracias por guiarme en esta aventura, por ayudarme y por el apoyo recibido.

A mis compañeros del departamento de Química Inorgánica, del Laboratorio de Materiales Avanzados y a los técnicos de laboratorio.

A la Dra. **Florence Epron** (*Institut de Chimie des Milieux et Matériaux de Poitiers, IC2MP-CNRS-Université de Poitiers, France*) por permitirme colaborar con ellos y hacer uso de las instalaciones de sus laboratorios para hacer de mi investigación un trabajo más completo.

A mis compañeros de laboratorio de la Universidad de Poitiers.

A mis amigos, por estar ahí.

Y, cómo no, a **mi familia** (especialmente a mis **padres** y a mi **hermano**). Gracias por ser los pilares fundamentales de mi vida y por hacerme ser feliz cada día.

Índice / Table of Contents

Índice / Table of contents

Summary

Chapter I. Introduction

The increasing use of nitrogenous fertilizers is responsible for nitrogen species permeation through the soil layers and contamination of groundwater. Methemoglobinemia and cancer are diseases produced by the human consumption of water exceeding the maximum permitted level of nitrate of 50 $mg \cdot L^{-1}$. Nitrates may be reduced to nitrites within the human body. Nitrite combines with hemoglobin, which contains the ferrous (Fe^{2+}) ion, to form methemoglobin, which contains the ferric (Fe^{3+}) form of iron. The increased affinity for oxygen of methemoglobin leads to an overall reduced ability of the red blood cells to release oxygen to tissues. When methemoglobin concentration is too high in red blood cells, tissue hypoxia may occur. This disease, known as the blue baby syndrome, is fatal to the new born. Physico-chemical, biological and catalytic processes are available for removing nitrates from water. Physico-chemical methods as ion-exchange, reverse osmosis and electro-dialysis remove nitrates from drinking water, but concentrate them elsewhere, with the subsequent disposal problem of the generated nitrate waste brine. Biological denitrification transforms nitrates into molecular nitrogen but is difficult to operate and may become another source of contamination of water with bacteria.

Catalytic reduction of nitrate species to form nitrogen has been considered as an alternative technology for nitrate abatement. Nitrate reduction is generally carried out with hydrogen (H_2) in the presence of metal catalysts. Monometallic systems based on Pt or Pd can be used, and also bimetallic systems combining a hydrogenating metal (Pd, Pt) and a promoter metal (Cu, In, Sn) dispersed on different supports with a relatively high surface area as activated carbons, carbon nanotubes, zeolites and metal oxides, as well as cation exchange resins. It has been demonstrated that the reaction progresses through intermediate nitrite (NO_2^-), and that nitrogen (N_2) and ammonium (NH_4^+) are the principal products of the catalytic reduction of nitrate (NO_3^-) with dyhidrogen (H_2).

In many cases, the efficiency of the studied catalysts is not satisfactory, as high concentrations of toxic nitrites or ammonia by-products instead of the desired N_2 are produced. The activity and selectivity of the catalysts is highly dependent on the preparation method, on the way the noble metal is promoted, on the metal/promoter ratio

and on the operation conditions. Moreover, the support also affects the catalytic performance.

The aim of this research work is to determine the ability of some conducting polymers (polypyrrole, polyaniline and polythiophene), for removing nitrates from water by adsorption and reduction, preferably without the need of a metal catalyst and producing molecular nitrogen as the only product.

Chapter II. Experimental

In this chapter, the synthesis of the materials and the characterization techniques used in this research work are described, as well as the experimental procedure used to study their ability for removal of nitrates in water.

Chapter III. Plasma-assisted preparation of polypyrrole-supported catalysts and their application to nitrate removal in water

This chapter is extracted from the publication: R. Buitrago-Sierra, **M.J. García-Fernández**, M.M. Pastor-Blas, A. Sepúlveda-Escribano, "Environmentally friendly reduction of a platinum catalysts precursor supported on polypyrrole", *Green Chemistry*. **2013**, *15*, 1981-1990.

Supported metal catalysts are traditionally prepared by impregnating a support material with the metal precursor solution, followed by reduction in hydrogen at high temperatures. In this chapter, a polymeric support has been considered. Polypyrrole (PPy) has been chemically synthesized using $FeCl_3$ as a doping agent, and it has been impregnated with a H_2PtCl_6 solution to prepare a catalyst precursor. The restricted thermal stability of polypyrrole does not allow using the traditional reduction in hydrogen at elevated temperature, and chemical reduction under mild conditions using sodium borohydride implies environmental concerns. Therefore, cold RF plasma has been considered as an environmentally friendly alternative. Argon (Ar) plasma leads to a more effective reduction of platinum ions in the chloroplatinic complex anchored onto the polypyrrole chain after impregnation than reduction with sodium borohydride, as has been evidenced by XPS. The increase of RF power enhanced the effectiveness of the Ar plasma treatment. A homogeneous distribution of platinum nanoparticles has been

observed by TEM after the reduction treatment with plasma. The PPy/Pt catalyst reduced by Ar plasma at 200 W effectively catalyzed the aqueous reduction of nitrates with H_2 to yield N_2, with a very low selectivity to undesired nitrites and ammonium by-products.

Chapter IV. Optimization of the platinum loading and the argon plasma treatment

The size and distribution of the metal nanoparticles on the support depend on the nature and concentration of the reducing agent, the reduction procedure and the metal loading. In the previous chapter, a metal loading of 1 wt. % was selected and reduction using sodium borohydride ($NaBH_4$) as a mild chemical reducing agent has been compared with Ar cold plasma reduction. It has been concluded that electrons in the plasma are responsible for the more effective reduction of platinum ions to the metallic state than reduction with borohydride. Different RF powers (100 W, 150 W and 200 W) and also a repetitive plasma treatment were studied. The experimental results show that the increase of the Ar plasma power results in a more effective reduction of platinum ions into is zero-valent metallic state, and that the manual mixing between repetitive treatments assure an even exposure to the plasma.

In this chapter, the RF power has been set to 200 W, and the influence of the length of the plasma treatment and the platinum loading has been analysed. As a result, the optimal experimental conditions have been established: 2 wt. % platinum loading and an argon plasma treatment at 200 W carried out for 3 h (5 min x 36 times) with manual mixing between treatments to assure an even exposure to the Ar plasma.

Chapter V. Comparative study of the nitrate removal in water using monometallic and bimetallic catalysts supported on polypyrrole

This chapter is extracted from the publication: **M.J. García-Fernández**, R. Buitrago-Sierra, M.M. Pastor-Blas, O.S.G.P. Soares, M.F.R. Pereira, A. Sepúlveda-Escribano, "Green synthesis of polypyrrole-supported metal catalysts: application to nitrate removal in water", *RSC Advances*. **2015**, *5*, 32706-32713.

Pt and Pt/Sn nanoparticles supported on polypyrrole (PPy) have been prepared using Ar plasma to reduce the metal precursors dispersed on the polymer. The PPy

support was synthesized by chemical polymerization of pyrrole with $FeCl_3 \cdot 6H_2O$, this leading to the conducting form of the polymer (assessed by conductimetric measurements). The Ar plasma treatment produced a partial reduction of platinum ions, anchored as platinum chloro-complexes to the PPy chain, into metallic platinum. A homogeneous distribution of Pt and Sn nanoparticles was observed by TEM. The catalytic activity of the PPy-supported catalysts was evaluated in the reduction of aqueous nitrate with H_2 at room temperature. Nitrate concentration in water below the maximum acceptable level of 50 $mg \cdot L^{-1}$ was achieved with all catalysts. However, considering not only efficiency in nitrate reduction, but also minimized concentrations of undesired nitrite and ammonium, the monometallic Pt catalyst seems to be the most promising one.

Chapter VI. Metal-free procedure for the removal of nitrates from water: effect of the oxidant used in the synthesis of polypyrrole

Polypyrrole (PPy) has been synthesized by chemical polymerization of pyrrole (C_4H_5N) using ferric chloride ($FeCl_3 \cdot 6H_2O$) or potassium peroxydisulfate ($K_2S_2O_8$) as oxidants and dopants. The influence of the counterion acting as dopant, chloride (Cl^-) or sulfate (SO_4^{2-}), in the process of nitrate removal by adsorption/reduction has been determined, and it has been observed that the ion-exchange and the redox properties of PPy are strongly affected by the oxidant used in the polymer synthesis. The initial oxidation degree of the polymer is determined by the oxidant, and it defines the ability of the polymer to carry out the reduction of nitrate by electron transfer from the polymeric chain. The reduction process, the selectivity to desired nitrogen and to un-desired nitrite and ammonium are also affected by the oxidant used.

Chapter VII. Proposed mechanisms for the hydrogenation of nitrate catalyzed by platinum nanoparticles supported on polypyrrole and polyaniline

This chapter is extracted from the publication: **M.J. García-Fernández**, M.M. Pastor-Blas, F. Epron, A. Sepúlveda-Escribano, "Proposed mechanisms for the removal of nitrate from water by platinum catalysts supported on polyaniline and polypyrrole", *Applied Catalysis B: Environmental*. **2018**, *225*, 162-171.

Platinum nanoparticles have been synthesized on polyaniline (PANI) and polypyrrole (PPy) as supports using H_2PtCl_6 as metal precursor and a reducing treatment with cold Ar plasma. The catalytic activity of the polymer-supported catalysts in the reduction of aqueous nitrate with H_2 at room temperature was evaluated. These systems are able to considerably decrease the concentration of nitrate in water in only 5 minutes. The mechanism of the nitrate abatement process is determined by the nature of the conducting polymer. The nitrogen functionalities in polyaniline are external to the ring system, and favor nitrate retention at the platinum complex either by the formation of an adduct or by nitrate participating as a ligand. In contrast, polypyrrole possesses aromatic nitrogen atoms with a considerably more important steric hindrance. In this case, ion exchange between the counterions in the doped polymer (SO_4^{2-}) and nitrate ion from water is produced, followed by reduction of nitrate by hydrogen chemisorbed on the platinum nanoparticles.

Chapter VIII. Surfactant-assisted synthesis of conducting polymers and their application to the removal of nitrates from water

This chapter is extracted from the publication: **M.J. García-Fernández**, S. Sancho-Querol, M.M. Pastor-Blas, A. Sepúlveda-Escribano, "Surfactant-assisted synthesis of conducting polymers. Application to the removal of nitrates from water", *Journal of Colloid and Interface Science*. **2017**, *494*, 98-106.

Three different conducting polymers, polythiophene (PT), polypyrrole (PPy) and polyaniline (PANI) have been synthesized via oxidative chemical polymerization in aqueous media, in such a way that the synthesis protocol did not involve any toxic solvents. They have been tested in the abatement of nitrates from an aqueous solution without the need of any metal catalyst. The N-containing polymers (PANI and PPy) were able to remove nitrates to a level that accomplishes the European legislation requirements; however, the nature of each polymer greatly influenced the process mechanism. Whereas ion exchange between Cl^- and SO_4^{2-} counterions in the polymer and NO_3^- from water is the main responsible for the effective nitrate removal in PANI, as assessed by FTIR and XPS analyses, the nitrate removal mechanism on PPy is based in an electron transfer from the polymer to nitrate through N sites located in the pyrrolic ring. On the other hand, PT was not able to exchange nitrate unless it was synthesized with $FeCl_3$ as oxidant/dopant

and an anionic surfactant (sodium dodecyl sulfate -SDS-) is used. In that case, the electrostatic attraction between sulfate (OSO_3^-) groups from the surfactant and Fe^{3+} ions from $FeCl_3$ produced the anchoring of Cl^- to the oxidized PT growing chain, this favoring ion exchange with nitrate in the aqueous solution, followed by a redox process.

Chapter IX. Synthesis of conducting polymer-TiO_2 hybrid materials for their application in the removal of nitrate from water

This chapter is extracted from the publication: J.J. Villora-Picó, V. Belda-Alcázar, **M.J. García-Fernández**, E. Serrano, A. Sepúlveda-Escribano, M.M. Pastor-Blas, "Conducting polymer-TiO_2 hybrid materials: application in the removal of nitrates from water", *Langmuir*. **2019**, *35*, 6089-6105.

Materials able to produce the reduction of nitrate from water without the need of a metal catalyst and avoiding the use of gaseous hydrogen have been developed by combining the synergistic properties of titania and two conducting polymers. Polymerization of aniline and pyrrole on titanium dioxide in the presence of two different oxidants/dopants (iron trichloride or potassium peroxydisulfate) has been evaluated. The resulting hybrid materials have good thermal stability imparted by the titania counterpart, and a considerable conductivity provided by the conducting polymers. The capability of the hybrid materials of reducing aqueous nitrate has been assessed and compared to the catalytic hydrogenation of nitrate using a platinum catalyst supported on these hybrid materials. The mechanism of nitrate abatement implies adsorption of nitrate on the polymer by ion-exchange with the dopant anion, followed by the reduction of nitrate. The electron transfer from titania to the conducting polymer in the hybrid material favors the reductive ability of the polymer, in such a way that nitrate is selectively reduced with a very low production of undesirable side products. The obtained results show that the activity and selectivity of the catalytic reduction of nitrate with dihydrogen in the presence of a platinum catalyst supported on the hybrid materials is considerably lower than those of the metal-free nanocomposites.

Resumen

Capítulo I. Introducción

El uso creciente de fertilizantes nitrogenados es responsable de la permeación de especies de nitrógeno a través de las capas del suelo y de la contaminación de las aguas subterráneas. El consumo humano de agua con altos niveles de nitratos (el nivel máximo permitido es de 50 $mg \cdot L^{-1}$) puede producir metahemoglobinemia y hasta cáncer. Los nitratos pueden reducirse a nitritos en el cuerpo humano. El nitrito se combina con la hemoglobina, que contiene el ion ferroso (Fe^{2+}), para formar la metahemoglobina, que contiene la forma férrica (Fe^{3+}) del hierro. La mayor afinidad de la metahemoglobina por el oxígeno conduce a una reducción general de la capacidad de los glóbulos rojos para liberar oxígeno a los tejidos. Cuando la concentración de metahemoglobina es demasiado alta en los glóbulos rojos, se puede producir hipoxia tisular. Esta enfermedad, conocida como el síndrome del bebé azul, es fatal para el recién nacido. Se dispone de procesos fisicoquímicos, biológicos y catalíticos para eliminar los nitratos del agua. Los métodos fisicoquímicos, como el intercambio iónico, la ósmosis inversa y la electrodiálisis, eliminan los nitratos del agua potable, pero los concentran en otros lugares, con el consiguiente problema de eliminación de la salmuera generada de los residuos de nitratos. La desnitrificación biológica transforma los nitratos en nitrógeno molecular, pero es difícil de realizar y puede convertirse en otra fuente de contaminación del agua con bacterias.

La reducción catalítica de las especies de nitrato para formar nitrógeno se ha considerado como una tecnología alternativa para la reducción de nitratos. La reducción de nitratos se realiza generalmente con hidrógeno (H_2) en presencia de catalizadores metálicos. Se pueden utilizar sistemas monometálicos como Pt o Pd, y también sistemas bimetálicos que combinan un metal hidrogenante (Pd, Pt) y un metal promotor (Cu, In, Sn), dispersados en diferentes soportes con una superficie específica relativamente alta, como los carbones activados, nanotubos de carbono, zeolitas y óxidos metálicos, así como resinas de intercambio catiónico. Se ha demostrado que la reacción transcurre a través del intermedio nitrito (NO_2^-), y que el nitrógeno (N_2) y el amonio (NH_4^+) son los principales productos de la reducción catalítica de nitrato (NO_3^-) con hidrógeno (H_2).

En muchos casos, la eficiencia de los catalizadores estudiados no es satisfactoria, ya que se producen elevadas concentraciones de nitritos tóxicos o de amoniaco/amonio

en lugar del N_2 deseado. La actividad y la selectividad de los catalizadores depende en gran medida del método de preparación, de cómo se promueve el metal noble, de la proporción metal/promotor y de las condiciones de trabajo. Además, el soporte también afecta a la efectividad del catalizador.

El objetivo de este trabajo de investigación es determinar la capacidad de los polímeros conductores (polipirrol, polianilina y politiofeno) para eliminar los nitratos del agua por adsorción y reducción, preferiblemente sin la necesidad de un catalizador metálico, y producir nitrógeno molecular como único producto.

Capítulo II. Experimental

En este capítulo se describen los procedimientos de síntesis y las técnicas de caracterización empleadas en este trabajo de investigación, así como el proceso experimental para la eliminación de nitratos en agua.

Capítulo III. Preparación de catalizadores soportados en polipirrol mediante plasma y su aplicación en la eliminación de nitratos en agua

Este capítulo se ha extraído de la publicación: R. Buitrago-Sierra, **M.J. García-Fernández**, M.M. Pastor-Blas, A. Sepúlveda-Escribano, "Environmentally friendly reduction of a platinum catalysts precursor supported on polypyrrole", *Green Chemistry*. **2013**, *15*, 1981-1990.

Los catalizadores metálicos soportados se preparan tradicionalmente impregnando un material sólido (soporte) con una disolución del precursor del metal, seguido de una reducción con hidrógeno a temperaturas elevadas. En este capítulo se ha empleado un soporte polimérico. Se ha sintetizado químicamente el polipirrol (PPy) usando $FeCl_3$ como agente dopante y, posteriormente, se ha impregnado con una disolución de H_2PtCl_6 para preparar el precursor del catalizador. La baja estabilidad térmica del polipirrol no permite el uso de la reducción tradicional con hidrógeno a elevada temperatura, y la reducción química en condiciones suaves utilizando borohidruro de sodio conlleva problemas medioambientales. Por lo tanto, se ha considerado el plasma frío de radiofrecuencia (RF) como una alternativa respetuosa con el medio ambiente. El plasma de argón (Ar) produce una reducción más efectiva de los

iones platino en el complejo cloroplatínico que se encuentra anclado en la cadena de polipirrol después de la impregnación, en comparación con la reducción con borohidruro de sodio, como se evidencia mediante XPS. El aumento de la potencia de RF mejora la efectividad del tratamiento con plasma de Ar. Mediante TEM se observa una distribución homogénea de las nanopartículas de platino tras el tratamiento de reducción con plasma. El catalizador PPy/Pt reducido con plasma de Ar a 200 W catalizó de manera efectiva la reducción de nitratos con H_2 en disolución acuosa para dar N_2, con una selectividad muy baja hacia los productos no deseados nitrito y amonio.

Capítulo IV. Optimización del tratamiento con plasma de argón y del contenido en platino

El tamaño y la distribución de las nanopartículas metálicas en el soporte dependen de la naturaleza y de la concentración del agente reductor, del procedimiento de reducción y del contenido en metal. En el capítulo anterior se seleccionó un contenido metálico del 1 % en masa y se comparó la reducción con borohidruro de sodio ($NaBH_4$) como agente reductor químico suave con la reducción con plasma frío de Ar. Se concluyó que los electrones en el plasma son los responsables de que la reducción de iones platino al estado metálico sea más efectiva que la reducción con borohidruro. Se estudiaron diferentes potencias de RF (100 W, 150 W y 200 W) y también un tratamiento repetitivo con plasma. Los resultados experimentales mostraron que el aumento de la potencia del plasma de Ar implica una reducción más efectiva de los iones platino a su estado metálico, y que la mezcla manual entre tratamientos repetitivos asegura una exposición uniforme al plasma.

En este capítulo se ha ajustado la potencia de RF a 200 W y se ha analizado la influencia de la duración del tratamiento de plasma y del contenido en platino. Como resultado, se han establecido las condiciones experimentales óptimas: contenido en platino del 2 % en masa y tratamiento con plasma de argón a 200 W durante 3 h (5 min x 36 repeticiones) realizando una homogeneización de la muestra de forma manual entre tratamientos para asegurar una exposición uniforme al plasma de Ar.

Capítulo V. Estudio comparativo de la eliminación de nitratos en agua utilizando catalizadores monometálicos y bimetálicos soportados en polipirrol

Este capítulo se ha extraído de la publicación: **M.J. García-Fernández**, R. Buitrago-Sierra, M.M. Pastor-Blas, O.S.G.P. Soares, M.F.R. Pereira, A. Sepúlveda-Escribano, "Green synthesis of polypyrrole-supported metal catalysts: application to nitrate removal in water", *RSC Advances*. **2015**, *5*, 32706-32713.

Se han preparado nanopartículas de Pt y de Pt/Sn soportadas en polipirrol (PPy) utilizando plasma de Ar para reducir los precursores metálicos dispersos en el polímero. El soporte de PPy se ha sintetizado mediante polimerización química del pirrol con $FeCl_3 \cdot 6H_2O$, lo que genera la forma conductora del polímero (determinado mediante medidas conductimétricas). El tratamiento con plasma de Ar produce una reducción parcial de los iones platino que se encuentran anclados a la cadena de PPy en forma de clorocomplejos hasta platino metálico. Mediante TEM se observa una distribución homogénea de las nanopartículas de Pt y de Sn. Se ha evaluado la actividad de los catalizadores soportados en PPy en la reducción de nitrato acuoso con H_2 a temperatura ambiente. Con todos los catalizadores se consiguió una concentración de nitrato en agua inferior al nivel máximo permitido de 50 $mg \cdot L^{-1}$. Sin embargo, considerando no sólo la eficiencia en la reducción de nitrato sino también la minimización de las concentraciones de los productos no deseados nitrito y amonio, el catalizador monometálico de Pt parece ser el más prometedor.

Capítulo VI. Procedimiento libre de metal para la eliminación de nitratos del agua: efecto del oxidante usado en la síntesis de polipirrol

Se ha sintetizado polipirrol (PPy) mediante polimerización química del pirrol (C_4H_5N), utilizando cloruro férrico ($FeCl_3 \cdot 6H_2O$) o peroxidisulfato de potasio ($K_2S_2O_8$) como oxidantes y dopantes. Se ha determinado la influencia del contraión que actúa como dopante, cloruro (Cl^-) o sulfato (SO_4^{2-}), en el proceso de eliminación de nitratos por adsorción/reducción, y se ha observado que el intercambio de iones y las propiedades redox del PPy se ven fuertemente afectados por el oxidante empleado en la síntesis del polímero. El grado de oxidación inicial del polímero está determinado por el oxidante, y define la capacidad del polímero para llevar a cabo la reducción de nitrato por

transferencia de electrones de la cadena polimérica. El proceso de reducción y la selectividad al producto deseado, nitrógeno, y a los no deseados nitrito y amonio, también se ven afectados por el oxidante utilizado.

Capítulo VII. Mecanismo de la hidrogenación de nitratos catalizada por nanopartículas de platino soportadas en polipirrol y en polianilina

Este capítulo se ha extraído de la publicación: **M.J. García-Fernández**, M.M. Pastor-Blas, F. Epron, A. Sepúlveda-Escribano, "Proposed mechanisms for the removal of nitrate from water by platinum catalysts supported on polyaniline and polypyrrole", *Applied Catalysis B: Environmental*. **2018**, *225*, 162-171.

Se han sintetizado nanopartículas de platino sobre soportes como polianilina (PANI) y polipirrol (PPy) utilizando H_2PtCl_6 como precursor metálico y un tratamiento de reducción con plasma frío de Ar. Se ha evaluado la actividad catalítica de los catalizadores poliméricos soportados en la reducción de nitrato acuoso con H_2 a temperatura ambiente. Estos sistemas son capaces de disminuir considerablemente la concentración de nitratos en agua en sólo 5 min. El mecanismo del proceso de eliminación de nitratos está determinado por la naturaleza del polímero conductor. En la polianilina, las funcionalidades del nitrógeno son externas al anillo y favorecen la retención del nitrato en el complejo de platino, ya sea por la formación de un aducto o por la participación del nitrato como ligando. Por el contrario, el polipirrol posee átomos de nitrógeno aromáticos con un impedimento estérico considerablemente mayor. En este caso, se produce un intercambio iónico entre los contraiones del polímero dopado (SO_4^{2-}) y el anión nitrato en el agua, seguido de una reducción del nitrato por el hidrógeno quimisorbido en las nanopartículas de platino.

Capítulo VIII. Síntesis de polímeros conductores asistida por un surfactante y su aplicación en la eliminación de nitratos del agua

Este capítulo se ha extraído de la publicación: **M.J. García-Fernández**, S. Sancho-Querol, M.M. Pastor-Blas, A. Sepúlveda-Escribano, "Surfactant-assisted synthesis of conducting polymers. Application to the removal of nitrates from water", *Journal of Colloid and Interface Science*. **2017**, *494*, 98-106.

Se han sintetizado tres polímeros conductores diferentes, politiofeno (PT), polipirrol (PPy) y polianilina (PANI), mediante polimerización química oxidativa en medio acuoso, de modo que el protocolo de síntesis no incluya ningún disolvente tóxico. Dichos polímeros se han probado en la eliminación de nitratos de una disolución acuosa sin la necesidad de ningún catalizador metálico. Los polímeros que contienen N (PANI y PPy) fueron capaces de eliminar los nitratos a un nivel que cumplía los requerimientos de la legislación europea; sin embargo, el mecanismo del proceso se encuentra en gran medida influenciado por la naturaleza de cada polímero. Mientras que en la PANI el principal responsable de la efectiva eliminación de los nitratos es el intercambio iónico entre los contraiones del polímero, cloruro (Cl^-) y sulfato (SO_4^{2-}) y el nitrato (NO_3^-) del agua, como se demuestra mediante los análisis FTIR y XPS, el mecanismo de eliminación de nitratos en el PPy está basado en la transferencia electrónica del polímero al nitrato a través de los sitios N localizados en el anillo pirrólico. Por otra parte, el PT no fue capaz de intercambiar nitratos a menos que se sintetizara con cloruro férrico ($FeCl_3$) como dopante/oxidante y utilizando un surfactante aniónico (sulfato de dodecilo sódico –SDS–). En ese caso, la atracción electrostática entre los grupos sulfato (OSO_3^-) del surfactante y los iones Fe^{3+} del $FeCl_3$ produce el anclaje de Cl^- a la cadena de crecimiento del PT oxidado, lo que favorece el intercambio iónico con el nitrato en la disolución acuosa, seguido de un proceso redox.

Capítulo IX. Síntesis de materiales híbridos polímero conductor-TiO_2 para su aplicación en la eliminación de nitratos del agua

Este capítulo se ha extraído de la publicación: J.J. Villora-Picó, V. Belda-Alcázar, **M.J. García-Fernández**, E. Serrano, A. Sepúlveda-Escribano, M.M. Pastor-Blas, "Conducting polymer-TiO_2 hybrid materials: application in the removal of nitrates from water", *Langmuir*. **2019**, *35*, 6089-6105.

Se han desarrollado materiales capaces de producir la reducción del nitrato del agua sin la necesidad de un catalizador metálico y evitando el uso de hidrógeno gaseoso, mediante la combinación de las propiedades sinérgicas de la titania y de dos polímeros conductores. Se ha evaluado la polimerización de anilina y de pirrol sobre el dióxido de titanio en presencia de dos oxidantes/dopantes diferentes (tricloruro de hierro o peroxidisulfato de potasio). Los materiales híbridos resultantes tienen una buena

estabilidad térmica debida a la titania y una conductividad considerable proporcionada por los polímeros conductores. Se ha evaluado la capacidad de estos materiales híbridos de reducir el nitrato acuoso, y se ha comparado con la hidrogenación catalítica del nitrato utilizando un catalizador de platino soportado en estos materiales híbridos. El mecanismo de eliminación de nitratos implica la adsorción de nitrato en el polímero mediante intercambio iónico con el anión dopante, seguido de la reducción del nitrato. La transferencia de electrones de la titania al polímero conductor en el material híbrido favorece la capacidad reductora del polímero, de forma que el nitrato se reduce selectivamente con una producción muy baja de productos secundarios no deseados. Los resultados obtenidos muestran que la actividad y la selectividad de la reducción catalítica del nitrato con dihidrógeno en presencia de un catalizador de platino soportado en estos materiales híbridos es considerablemente menor que la de los nanocompuestos libres de metal.

Capítulo I. Introducción

1. ANTECEDENTES

1.1. Polímeros conductores

Los polímeros son compuestos orgánicos que presentan una elevada ductilidad (equiparable a la que poseen los metales) y una menor temperatura de fusión y mayor reactividad química que las cerámicas [1]. La mayoría de estos materiales posee una pobre conductividad eléctrica debido a la baja disponibilidad de electrones libres, lo que hace que sean generalmente conocidos por su eficacia como aislantes eléctricos. No obstante, siempre se planteó la idea de que los polímeros que poseyeran una estructura apropiada deberían ser capaces de conducir la electricidad, aunque esas mismas características que podrían permitir ese fenómeno implicarían dificultades en el tratamiento y procesado de dichos materiales [2].

Sin embargo, en los últimos años se han sintetizado polímeros que presentan conductividades eléctricas mucho más elevadas, los cuales que reciben el nombre de *polímeros conductores*. Estos nuevos materiales combinan excelentes propiedades económicas (fácil preparación y bajo coste de fabricación), mecánicas (flexibilidad, ligereza y resistencia al impacto) y químicas (resistencia a la corrosión). Fueron descubiertos a finales de la década de los 70, reconociéndose este interés científico en el año 2000, cuando se otorgó el Premio Nobel de Química a los investigadores Alan J. Heeger, Alan G. MacDiarmid y Hideki Shirakawa por el "descubrimiento y desarrollo de los polímeros conductores". Ello hizo que, a partir de ese momento, el desarrollo de estos materiales modificase extraordinariamente el campo de los polímeros y que actualmente presenten un interés creciente en el campo de la investigación [3-5].

Los polímeros conductores presentan dobles enlaces conjugados, con frecuencia en un grupo aromático (en ocasiones, heterociclo), que permiten el paso de un flujo de electrones [6]. Para que exista conductividad eléctrica en este tipo de materiales es necesario que la carga se transfiera a lo largo de la cadena conjugada y entre las cadenas [2]. No obstante, dicha conjugación no es suficiente para permitir que el polímero sea conductor, con lo que resulta imprescindible la introducción en el material de transportadores de carga a través de un proceso de *dopado*, ya sea en forma de huecos (material *p*-dopado) o de electrones extra (material *n*-dopado). Hay que tener en cuenta que los huecos son posiciones con deficiencia de electrones, de modo que la conducción

se lleva a cabo mediante un mecanismo de saltos, a través del cual un hueco se llena con un electrón de una posición vecina, generándose un nuevo hueco y dando lugar a la migración de la carga. A este grupo pertenecen polímeros como el polipirrol (PPy), la polianilina (PANI) y el politiofeno (PT), entre otros.

Los polímeros conductores poseen propiedades que los hacen altamente interesantes. Su alta conductividad eléctrica, su capacidad de alternar de forma reversible entre varios estados redox, la posibilidad de modificar sus propiedades mediante procesos de dopado/desdopado, así como su ligereza, flexibilidad y bajo coste de producción determinan su gran número de aplicaciones. Entre ellas, cabe destacar su uso en pinturas y adhesivos conductores, como electrodos en pilas de combustible, sensores electrocrómicos, condensadores, membranas selectivas, intercambiadores iónicos, dispositivos fotovoltaicos, soportes de catalizador, etc. [7].

Entre los métodos de síntesis más habituales de polímeros conductores se encuentran la síntesis directa, la oxidación química del monómero, la oxidación electroquímica, la oxidación en plasma y la obtención a partir de precursores. También existen otros métodos menos comunes como son pirólisis parcial de polímeros no conductores, polimerizaciones fotoiniciadas, polimerizaciones por condensación, etc. [8].

Sin embargo, la metodología más habitual de síntesis de este tipo de polímeros es la polimerización química en disolución usando un oxidante químico. En una primera etapa se oxida el monómero, formándose un catión radicalario. Estos cationes radicalarios se acoplan para dar un dímero. Seguidamente, se produce una desprotonación de este dímero. En pasos sucesivos, el dímero se oxida para acoplarse con nuevo monómero oxidado, dando lugar a oligómeros sucesivamente más largos.

En el Esquema 1.1 se muestran las condiciones más habituales de síntesis mediante polimerización oxidativa del tiofeno, del pirrol y de la anilina, para dar lugar a los polímeros correspondientes.

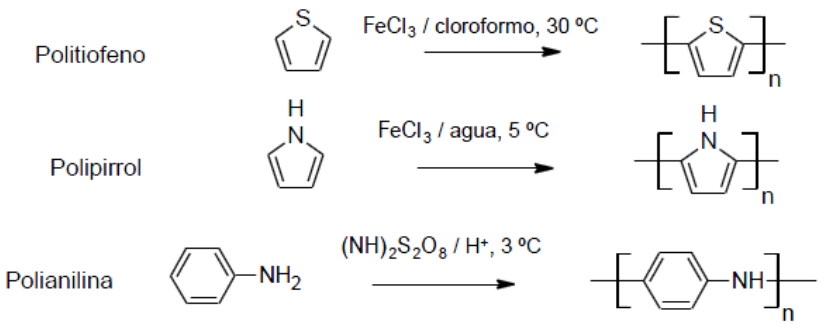

Esquema 1.1. Esquema que muestra la síntesis vía oxidación química de politiofeno, polipirrol y polianilina [8].

Las polimerizaciones del pirrol y de la anilina se producen fácilmente en presencia de diferentes oxidantes como persulfato amónico [$(NH_4)_2S_2O_8$], persulfato potásico ($K_2S_2O_8$) o tricloruro de hierro hidratado ($FeCl_3 \cdot 6H_2O$). La ventaja de esta vía de síntesis es que se llevan a cabo simultáneamente los procesos de polimerización del monómero, así como el proceso de oxidación y dopado, ya que el oxidante también actúa como dopante y esto es importante, puesto que determina las propiedades finales del polímero [9]. Tanto el polipirrol como la polianilina pueden sintetizarse fácilmente en medio acuoso, (la polianilina requiere condiciones ácidas) [10]. Sin embargo, dada la baja solubilidad del tiofeno en agua, su polimerización catalizada por Fe^{3+} para producir politiofeno se suele realizar empleando $FeCl_3$ anhidro y en disolventes apolares como el cloroformo [11].

En este trabajo se han sintetizado polipirrol (PPy), polianilina (PANI) y politiofeno (PT) mediante polimerización química oxidativa en medio acuoso, con el fin de que el proceso sea respetuoso con el medio ambiente. En la síntesis del politiofeno, que es especialmente complicada en medio acuoso, se han empleado diferentes agentes tensioactivos.

A continuación, se detalla el mecanismo de conducción en el PPy. En capítulos posteriores, se describirán las propiedades conductoras de la PANI y del PT.

Como se ha señalado anteriormente, el PPy es un polímero conductor intrínseco, pudiéndose considerar como un semiconductor, con una banda de valencia llena y una banda de conducción vacía separadas por un intervalo de energía de 3,16 eV [12,13]. Dicho valor es demasiado grande para que, a temperatura ambiente, tenga lugar el salto

de electrones desde la banda de valencia hasta la banda de conducción (Fig. 1.1). Por ese motivo, durante la síntesis química del PPy se llevan a cabo simultáneamente los procesos de polimerización del pirrol y los de oxidación y dopado del polipirrol. En muchas ocasiones, el mismo agente puede actuar como dopante y oxidante. Por ello, la elección del dopante es importante, ya que determina las propiedades finales del polímero. En este trabajo se han utilizado dos agentes oxidantes/dopantes diferentes: tricloruro de hierro ($FeCl_3 \cdot 6H_2O$) y peroxidisulfato de potasio ($K_2S_2O_8$) (Fig. 1.2).

El PPy es aislante en su forma reducida; por tanto, es necesario que se creen nuevas bandas dentro del intervalo energético existente entre la banda de valencia y la de conducción, ya que entre ellas se produce el movimiento de los electrones. De esta forma, se consigue un incremento de la conductividad del material gracias al proceso de dopado, observándose que el PPy conduce la electricidad cuando se encuentra en su forma oxidada. Así, cuando un electrón se mueve desde la parte superior de la banda de valencia debido al proceso de dopado, origina una vacante (hueco o radical catión) que produce una deslocalización parcial, extendiéndose a lo largo de varias unidades monoméricas y produciendo una deformación estructural. Este radical catión se encuentra parcialmente deslocalizado sobre un segmento del polímero y se llama *polarón* (Fig. 1.2b). El nivel de energía que tiene asociado se encuentra en el intervalo de la barrera energética entre bandas (Fig. 1.1b). Posteriormente, debido a que el proceso de oxidación continúa, se produce la eliminación de otro electrón de la cadena de PPy que ya contiene un polarón, dando lugar a la formación de un dicatión llamado *bipolarón* (Fig. 1.2c), cuya formación está energéticamente más favorecida que la de dos polarones. Numerosos estudios demuestran que un bipolarón se extiende a lo largo de cuatro unidades de pirrol [13]. Los bipolarones juegan un papel imprescindible en las propiedades electrónicas de los polímeros conductores, ya que son los responsables de la reducción del intervalo energético entre bandas (Fig. 1.1c), lo que facilita el transporte de carga a través de las cadenas conjugadas del polímero y también entre las cadenas del mismo [14]. El diagrama de energía que se muestra en la Figura 1.1d corresponde al estado con un nivel de dopado de aproximadamente 33 %mol., que está cerca del valor máximo encontrado en el PPy oxidado electroquímicamente [13].

De esta forma, la conductividad eléctrica que presentan este tipo de materiales depende del número de cargas que posean y de su movilidad relativa. Dichas cargas se

encuentran estabilizadas en el polímero gracias a la presencia de contraiones procedentes del dopante, con lo que las condiciones de preparación de los polímeros conductores tales como el tipo de dopante utilizado, la concentración del contraión y el nivel de dopado alcanzado son factores que van a influir en la conductividad eléctrica de los polímeros conductores intrínsecos. Diversos estudios [14-17] señalan que el efecto del contraión utilizado y de las condiciones de preparación del medio son los responsables de las diferencias en los valores de conductividad de los polímeros conductores, estableciéndose un rango de conductividad entre 10^{-7} – 10^{2} $S \cdot cm^{-1}$, típico de materiales semiconductores.

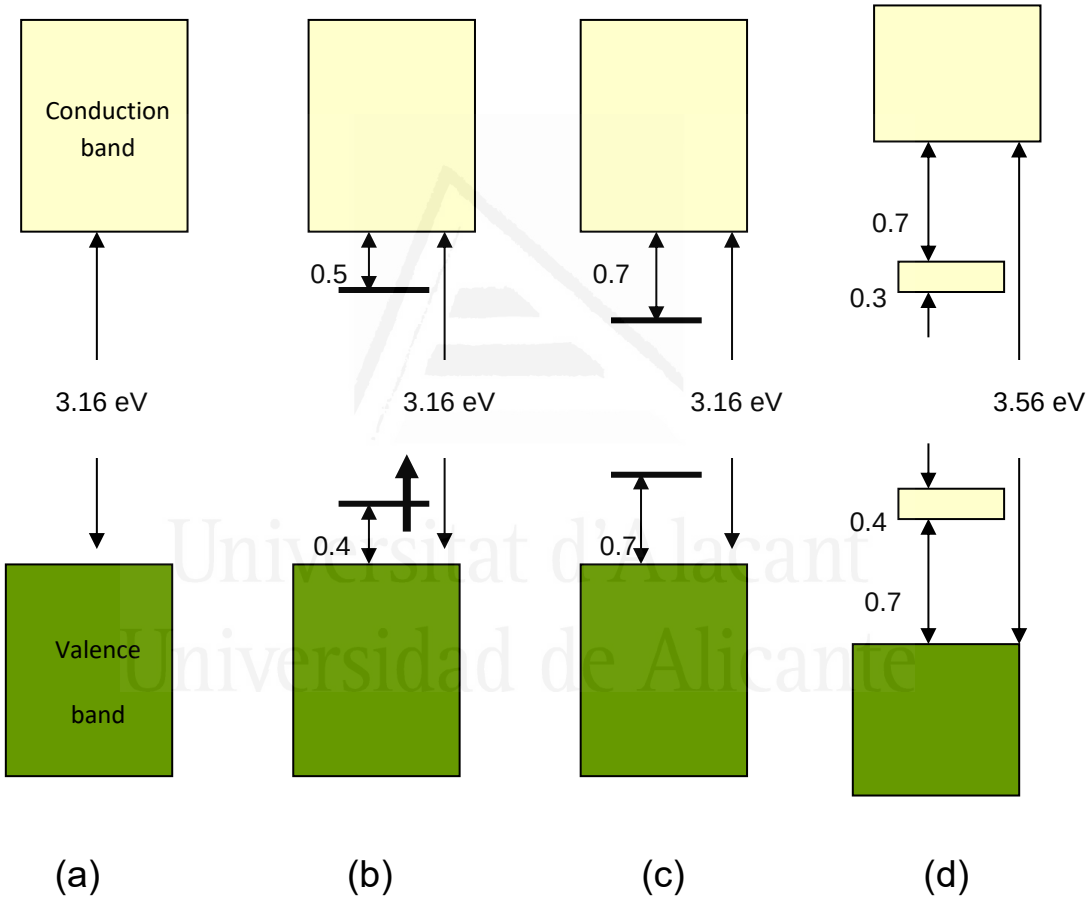

Figura 1.1. Diagrama de bandas de energía (eV) de: (a) PPy neutro, (b) polarón, (c) bipolarón y (d) PPy completamente dopado (adaptada de [13]).

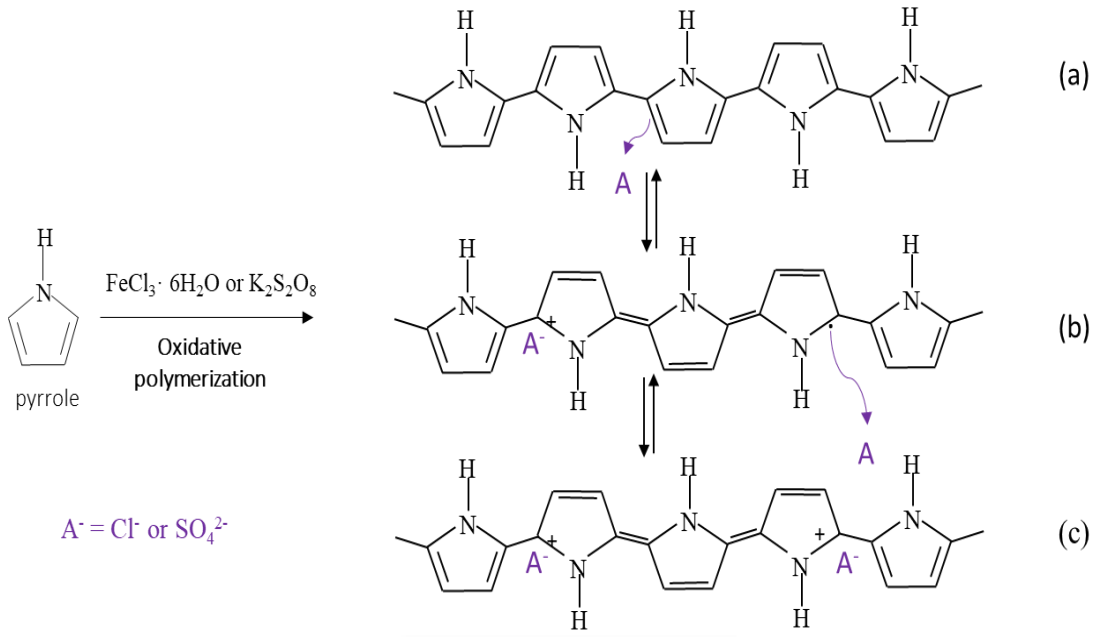

Figura 1.2. Estructuras electrónicas de: (a) PPy neutro, (b) polarón del PPy parcialmente dopado y (c) bipolarón del PPy completamente dopado (adaptada de [13]).

1.2. Eliminación de nitratos del agua

El nitrato está presente de forma natural en el medio ambiente como consecuencia del ciclo del nitrógeno, pero éste puede verse alterado por diversas actividades agrícolas e industriales, entre las que se encuentran la utilización de fertilizantes nitrogenados en la agricultura y los vertidos orgánicos no sometidos a tratamientos de depuración adecuados. En consecuencia, la mayor parte del agua que se utiliza para consumo humano, especialmente aquélla que proviene del subsuelo, es proclive a contaminarse con nitratos.

La legislación europea establece en 50 $mg \cdot L^{-1}$ la concentración máxima permitida de nitratos en el agua potable [18], por lo que se hace necesaria su eliminación debido al aumento de la contaminación en las reservas naturales de agua para consumo humano.

La toxicidad del nitrato (NO_3^-) viene determinada por su reducción a nitrito (NO_2^-) que se produce en el interior del organismo por acción bacteriana, ya que éste puede dar lugar a trastornos y enfermedades como hipertensión, metahemoglobinemia (por oxidación del Fe^{2+} de la hemoglobina) o cáncer (el nitrito puede reaccionar con aminas o amidas para formar nitrosocompuestos y la mayoría de ellos son potentes carcinógenos) [19,20].

Es posible tratar el agua subterránea contaminada, aunque puede ser un proceso difícil, caro y no totalmente efectivo. Las tecnologías más comunes para la eliminación de nitratos se pueden dividir en procesos físico-químicos, procesos biológicos y procesos catalíticos. La principal desventaja de los procesos físico-químicos como la electrodiálisis, el intercambio iónico o la ósmosis inversa es que los nitratos no se transforman en compuestos inofensivos, sino que simplemente se extraen del agua, pero finalmente tendrán que ser tratados de alguna manera. A pesar de esto se utilizan por razones económicas, pero se deben evitar por razones ecologistas. La manera más favorable de eliminar los nitratos desde el punto de vista ecológico es convertir los nitratos en un producto que respete la salud y el medio ambiente como el nitrógeno (N_2). Esto se puede conseguir mediante desnitrificación biológica, un proceso selectivo a la reducción de nitrato, lo que no altera la composición del agua. Sin embargo, aparecen problemas como pueden ser la formación de NO_2^-, NO_x o N_2O por una desnitrificación incompleta. También lleva asociados una serie de inconvenientes como pueden ser la necesidad de controlar de manera estricta algunos parámetros como la concentración o el pH, así como la dificultad y el coste de los tratamientos posteriores a la reacción como son la eliminación de la biomasa o de la turbidez.

Una manera de llevar a cabo la reducción de nitratos a nitrógeno con un menor coste económico es su eliminación catalítica. La eliminación catalítica de nitratos en agua consiste en la reducción de nitrato a nitrógeno en presencia de un agente reductor. Existen diferentes agentes que pueden actuar como reductores de nitratos, entre los que se encuentran metales activos, amoníaco, borohidruro, formiato, hidrazina, hidroxilamina, hierro (II) e hidrógeno, siendo este último el más extendido en la actualidad [19,20]. Aunque la reacción de reducción está favorecida termodinámicamente, el nitrato no se reduce a una velocidad apreciable en ausencia de un catalizador.

En algunos trabajos encontrados en la bibliografía [19] se comenta la necesidad de activación del metal noble que actúa como catalizador para incrementar la selectividad de la reacción de reducción de nitrato a nitrógeno. Por ese motivo, generalmente esta reacción se lleva a cabo utilizando catalizadores bimetálicos compuestos por un metal noble (Pt o Pd) y un metal promotor (Sn, Cu, In, etc.). Pero, por otro lado, también se ha señalado la influencia del soporte del catalizador (alúmina, titania, ceria, carbón activado, nanotubos de carbono, entre otros) en la eficiencia y selectividad del catalizador [21,22].

Una de las mayores ventajas de la reducción catalítica es que no se forman residuos, ni sólidos ni líquidos. Sin embargo, la reducción de nitrato puede dar lugar a nitrito como intermedio de reacción y a amonio (NH_4^+) como subproducto, ambos de ellos indeseables pues son perjudiciales para el organismo (Esquema 1.2).

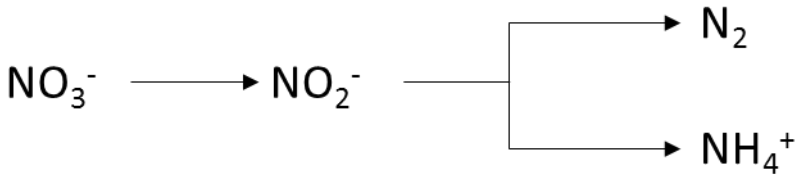

Esquema 1.2. Esquema general de la reducción de nitrato.

También se ha propuesto la presencia de otros intermedios de reacción, como óxido nitroso (N_2O), que continúa su reducción hacia N_2 y no hacia NH_4^+ [23], e hidroxilamina (NH_2OH), que continúa reduciéndose a amonio [24]. La concentración máxima permitida de nitrito y de amonio en agua potable es de 0,5 $mg \cdot L^{-1}$ para cada uno de ellos. Interesa, por tanto, que la reacción de reducción de nitrato sea altamente selectiva a nitrógeno. Por otro lado, la formación de iones hidroxilo (OH^-), que se da según las reacciones:

$$NO_3^- + H_2 \rightarrow NO_2^- + H_2O$$

$$NO_2^- + \frac{3}{2} H_2 \rightarrow \frac{1}{2} N_2 + H_2O + OH^-$$

$$NO_3^- + 4\,H_2 \rightarrow NH_4^+ + H_2O + 2\,OH^-$$

$$NO_2^- + 3\,H_2 \rightarrow NH_4^+ + 2\,OH^-$$

produce un incremento indeseado del pH, que puede llegar a alcanzar un valor de 10-11, lo que es inaceptable para el agua de bebida. Además, un pH básico produce una disminución de la actividad y selectividad a nitrógeno e incrementa la selectividad a amonio. Por ese motivo, generalmente, además de emplear hidrógeno gaseoso como reductor, se puede añadir HCl o se puede emplear una corriente de CO_2 para tamponar la disolución.

2. MOTIVACIÓN DEL TRABAJO

En este estudio se han empleado polímeros conductores para producir la eliminación del nitrato del agua. Dado que la reducción catalítica del nitrato con hidrógeno es el método más ampliamente extendido en la actualidad, en un principio se consideró utilizar polímeros conductores como soporte del catalizador, ya que la estructura regular de la cadena polimérica favorece un alto grado de dispersión de la fase metálica activa. Estudios realizados con otros soportes indican que es necesaria la presencia de un promotor a la fase activa del catalizador para producir la hidrogenación del nitrato. Por ese motivo se prepararon catalizadores bimetálicos de Pt:Sn (platino:estaño) y se comparó su efectividad con la de un catalizador monometálico de Pt.

Los catalizadores metálicos se prepararon mediante la impregnación del soporte con una sal metálica, la cual es necesario reducir para producir nanopartículas metálicas altamente dispersas. Generalmente se emplea un tratamiento reductor con hidrógeno a elevada temperatura. Sin embargo, dada la limitada estabilidad térmica de los polímeros, es necesario realizar un tratamiento reductor suave de los precursores metálicos empleados. Aunque es posible emplear reductores suaves como el borohidruro sódico, en este trabajo se ha implementado un tratamiento de reducción mediante un plasma frío de radiofrecuencias. De este modo se evitan los posibles problemas de contaminación inherentes a los reductores químicos, ya que el tratamiento con plasma de argón es respetuoso con el medio ambiente. Sin embargo, al tratarse de un tratamiento novedoso, fue necesario estudiar las distintas variables experimentales que influyen en la efectividad de la reducción del precursor metálico con plasma de argón. Un estudio sistemático de la potencia del plasma, del tiempo del tratamiento y del grado de homogeneización del material tratado permitió seleccionar las condiciones óptimas para la síntesis de los catalizadores mono y bimetálicos soportados en los polímeros conductores. Éstos se emplearon en la reacción de reducción catalítica de nitrato con hidrógeno (H_2). Se estudió su actividad y su selectividad frente a nitrógeno y se evaluó su idoneidad considerando la legislación en términos de concentraciones máximas permitidas de nitrato, nitrito y amonio en el agua potable.

Seguidamente, y con el objetivo de desarrollar un procedimiento de eliminación del nitrato del agua limpio y respetuoso con el medio ambiente, se estudió la posibilidad de eliminar el uso de la fase metálica, aprovechando las propiedades intercambiadoras de iones y redox de los polímeros conductores por sí mismos. Se estudiaron los mecanismos de reacción que permiten discernir si la eliminación se produce mediante un simple intercambio iónico entre el nitrato y el contraión de la cadena polimérica semioxidada (que daría lugar a una necesaria regeneración del polímero y un consecuente problema de eliminación del nitrato intercambiado) o, si por el contrario, la cadena polimérica semioxidada es capaz de producir la reducción del nitrato sin necesidad de adicionar un catalizador metálico ni un agente reductor externo.

Para ello fue necesario estudiar cómo afecta la naturaleza del contraión proporcionado por el oxidante. Se sintetizó PPy a partir de pirrol empleando dos oxidantes ($FeCl_3 \cdot 6H_2O$ o $K_2S_2O_8$) que proporcionaran contraiones con diferente capacidad intercambiadora con el nitrato de la disolución. Se ha demostrado que el oxidante empleado afecta a la conductividad eléctrica, a la capacidad intercambiadora y a las propiedades redox del polímero final. Estas propiedades determinan a su vez su comportamiento en la eliminación de nitrato del agua en términos tanto de actividad como de selectividad frente a nitrógeno o amoníaco.

A continuación, se amplió el estudio a otros polímeros conductores. Se comenzó comparando la actividad y la selectividad del catalizador de Pt soportado sobre PPy y sobre PANI. Ambos polímeros poseen un átomo de nitrógeno en su estructura, sin embargo, la localización del nitrógeno dentro o fuera del anillo determina el anclaje del precursor metálico (H_2PtCl_6). Se concluyó que el Pt bloquea las posiciones de N a través de las cuales se produce la transferencia de electrones desde la cadena polimérica al nitrato. Ello sugiere que se produce una reducción de nitrato más efectiva en ausencia de Pt, pero que la naturaleza del polímero es determinante tanto en la actividad como en la selectividad de la reacción de reducción de nitrato.

Por ese motivo, se consideró un polímero que contuviera un heteroátomo de S en lugar de N. Así, se estudiaron PPy, PANI y PT. Sin embargo, la síntesis acuosa del PT no es sencilla, dada la limitada solubilidad del monómero de tiofeno. Fue necesario diseñar cuidadosamente la síntesis del PT y recurrir al uso de surfactantes de distinta naturaleza.

Los tres polímeros se probaron para la eliminación de nitrato del agua sin necesidad de emplear ni catalizador metálico ni agente reductor externo. Los polímeros funcionales con N son capaces de eliminar nitrato hasta niveles en agua satisfactorios con la legislación vigente. Sin embargo, la naturaleza del polímero afecta en gran medida al mecanismo de eliminación. En la PANI, con el átomo de N externo al anillo, se produce preferentemente el intercambio de sus contraiones (Cl^- y SO_4^{2-}) por el nitrato de la disolución, que queda retenido en el polímero, lo que implica la necesidad de la posterior regeneración del polímero con el fin de poder ser reutilizado. Además, en ese caso no se soluciona el problema de la eliminación posterior del nitrato anclado al polímero. Sin embargo, el PPy es capaz de producir la reducción selectiva del nitrato previamente intercambiado por Cl^-, con mínima producción de amonio. Se ha determinado que el mecanismo de reacción se basa en la transferencia de electrones de la cadena polimérica al nitrato a través del átomo de N polimérico. Por otro lado, el PT no es capaz de intercambiar nitrato a menos que se sintetice empleando $FeCl_3$ como oxidante/dopante y un surfactante aniónico (sulfato de dodecil sodio – SDS). En este caso, la atracción electrostática entre los grupos sulfato del surfactante y los cationes Fe^{3+} procedentes del oxidante favorece el anclaje del Cl^- a la cadena en crecimiento del PT durante su síntesis y su posterior intercambio por NO_3^-. El nitrato intercambiado es efectivamente reducido por los electrones transferidos desde el PT a través del átomo de S.

Por último, se han desarrollado materiales híbridos titania/polímero conductor con excelente estabilidad térmica, debido a la presencia de la titania, capaces de producir la reducción del nitrato del agua sin necesidad de catalizador metálico ni reductor externo. Se han propuesto mecanismos de reacción basados en la transferencia electrónica entre la titania y el polímero conductor. La sinergia entre las propiedades de la titania y del polímero conductor dotan a estos materiales de alta estabilidad térmica, de propiedades conductoras de la electricidad y de capacidad intercambiadora de iones, que los hace susceptibles de ser aplicados en otras reacciones catalíticas a temperaturas más elevadas que la estudiada en este trabajo.

3. BIBLIOGRAFÍA

[1] M.A. Cotarelo-Méndez. Tesis doctoral *Síntesis de polímeros conductores obtenidos a partir de dímeros de anilina*. Universidad de Alicante. **2008**.

[2] D. Walton, P. Lorimer. *Polymers*. Oxford University Press. **2000**, Chap. 6, *Functional polymers*, p. 130.

[3] G.A. Rimbu, I. Stamatin, C.L. Jackson, K. Scott. *J. Optoelectron. Adv. M*. **2006**, *8(2)*, 670-674.

[4] G. Inzelt. *Conducting polymers. A new era in electrochemistry*. 2nd ed. Springer, Budapest, Hungary. **2008**, Chap. 2, *Classification of electrochemically active polymers*, p. 7-45.

[5] K.M. Ismail, Z.M. Khalifa, M.A. Azzem, W.A. Badawy. *Electrochim. Acta*. **2002**, *47(12)*, 1867-1873.

[6] M. Innocenti, F. Loglio, L. Pigani, R. Seeber, F. Terzi, R. Udisti. *Electrochim. Acta*. **2005**, *50(7-8)*, 1497-1503.

[7] J. Rodríguez, H.J. Grande, T.F. Otero. *Handbook of organic conductive molecules and polymers*. Vol. 2, *Conductive polymers: synthesis and electrical properties*. H.S. Nalwa (Ed.), Wiley. **1997**, Chap. 10, *Polypyrroles: from basic research to technological applications*, p. 415-468.

[8] T.F. Otero. *Polímeros conductores: síntesis, propiedades y aplicaciones electroquímicas*. *Revista Iberoamericana de Polímeros*. **2003**, *4(4)*, 1-32.

[9] D.V. Brezoi. *Journal of Science and Arts*. **2010**, *1(12)*, 53-58.

[10] H.J. Salavagione, C. Sanchís, E. Morallón. *J. Phys. Chem. C*. **2007**, *111(33)*,12454-12460.

[11] G. Inzelt. *Conducting polymers. A new era in electrochemistry*. 2nd ed. Springer, Budapest, Hungary. **2008**, Chap. 1, *Introduction*, p. 1-6.

[12] J. Yepes-Martínez, R.J. Camargo-Amado, R.A. Vargas. *Revista Colombiana de Física*. **2011**, *43(1)*, 127-133.

[13] T.A. Skotheim, J.R. Reynolds. *Recent advances in polypyrrole* in *Handbook of conducting polymers. Conjugated polymers: theory, synthesis, properties, and characterization*. 3rd ed. CRC Press: Boca Raton, FL, USA. **2007**, Chap. 8.

[14] B. Sari, M. Talu. *Synth. Met*. **1998**, *94(2)*, 221-227.

[15] N. Dubey, M. Leclerc. *J. Polym. Sci., Part B: Polym. Phys*. **2011**, *49(7)*, 467-475.

[16] C. Sanchís, H.J. Salavagione, J. Arias-Pardilla, E. Morallón. *Electrochim. Acta*. **2007**, *52(9)*, 2978-2986.

[17] P. Mavinakuli, S. Wei. Q. Wang, A.B. Karki, S. Dhage, Z. Wang, D.P. Young, Z. Guo. *J. Phys. Chem. C*. **2010**, *114*, 3874-3882.

[18] Directiva Europea 91/676/CEE traspuesta a la legislación española a través del Real Decreto 261/1996.

[19] I. Dodouche, D.P. Barbosa, M.C. Rangel, F. Epron. *Appl. Catal., B : Env.* **2009**, *93(1-2)*, 50-55.

[20] O.S.G.P. Soares, E.O. Jardim, A. Reyes-Carmona, J. Ruiz-Martínez, J. Silvestre-Albero, E. Rodríguez-Castellón, J.J.M. Órfão, A. Sepúlveda-Escribano, M.F.R. Pereira. *J. Colloid Interface Sci*. **2012**, *369(1)*, 294-301.

[21] J. Sá, J.A. Anderson. *Appl. Catal., B: Env.* **2008**, *77(3-4)*, 409-417.

[22] O.S.G.P. Soares, J.J.M. Órfão, M.F.R. Pereira. *Ind. Eng. Chem. Res.* **2010**, *49(16)*, 7183-7192.

[23] R. Zhang, D. Shuai, K.A. Guy, J.R. Shapley, T.J. Strathmann, C.J. Werth. *ChemCatChem*. **2013**, *5(1)*, 313-321.

[24] K. Wada, T. Hirata, S. Hosokawa, S. Iwamoto, M. Inoue. *Catal. Today*. **2012**, *185(1)*, 81-87.

Capítulo II. Experimental

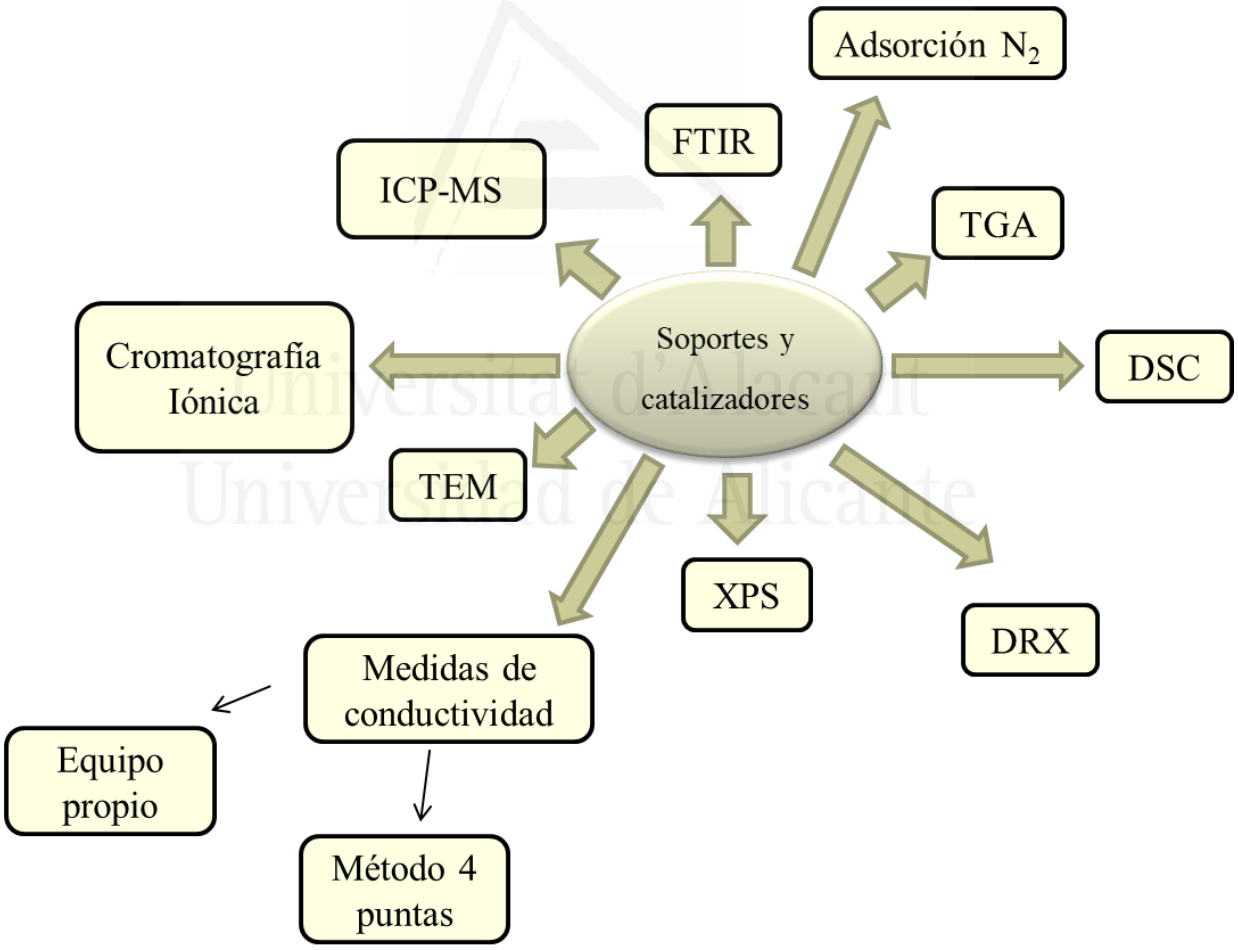

1. MATERIALES Y MÉTODOS

1.1. Preparación de los polímeros conductores

1.1.1. Síntesis de polipirrol

El polipirrol se ha preparado mediante polimerización química oxidativa utilizando como oxidante/dopante tricloruro de hierro hexahidratado o peroxidisulfato potásico [1]. El oxidante se adiciona en una proporción molar oxidante/monómero de 2,33 [2]. Para ello se disuelven 9 g de oxidante ($FeCl_3 \cdot 6H_2O$, M_m = 270,30 g·mol^{-1}, *Sigma-Aldrich* o $K_2S_2O_8$, M_m = 270,30 g·mol^{-1}, *Sigma-Aldrich*) en 200 mL de agua ultrapura. A continuación, se añade gota a gota 1 mL de pirrol (C_4H_5N, M_m = 67,09 g·mol^{-1}, ρ = 0,967 g·mL^{-1}, 98 % pureza, *Sigma-Aldrich*), con lo que la disolución adquiere coloración negra. Dicha disolución se mantiene en agitación suave durante 6 horas a temperatura ambiente. Tras ese tiempo, el precipitado obtenido se filtra a vacío y se lava repetidamente con agua destilada hasta que las aguas de filtrado no presentan coloración amarilla, para asegurar la ausencia de cloruros en la disolución. Finalmente, el precipitado se seca en estufa a 80 °C durante 12 horas.

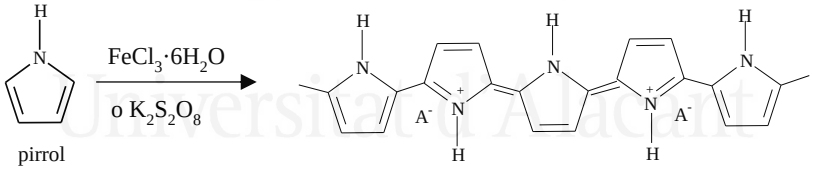

Esquema 2.1. Reacción de polimerización del pirrol para dar su forma conductora. A^- puede ser Cl^- o SO_4^{2-} dependiendo del oxidante empleado (cloruro férrico o peroxidisulfato potásico, respectivamente).

1.1.2. Síntesis de polianilina

La polimerización química oxidativa de la anilina se ha realizado siguiendo el proceso experimental que se indica a continuación [1], donde el oxidante se adiciona en una proporción molar oxidante/monómero de 1,25 [2]. Se disuelven 3,7 g de peroxidisulfato de potasio ($K_2S_2O_8$, M_m = 270,30 g·mol^{-1}, *Sigma-Aldrich*) en 75 mL de ácido clorhídrico (HCl, 0,2 mol·L^{-1}). Mientras se mantiene la agitación de dicha disolución, se añade gota a gota 1 mL de anilina ($C_6H_5NH_2$, M_m = 93,13 g·mol^{-1}, *Sigma-Aldrich*). La disolución presenta un color verde azulado que se va oscureciendo con el paso del tiempo (en cuestión de segundos), lo que es indicativo de la formación de la sal de emeraldina. Se mantiene la agitación durante 20 horas a temperatura ambiente. El

precipitado obtenido se lava varias veces con HCl 0,2 mol·L^{-1} hasta que las aguas de filtrado no muestran coloración amarilla. Finalmente, el precipitado se seca en estufa a 80 °C durante 12 horas.

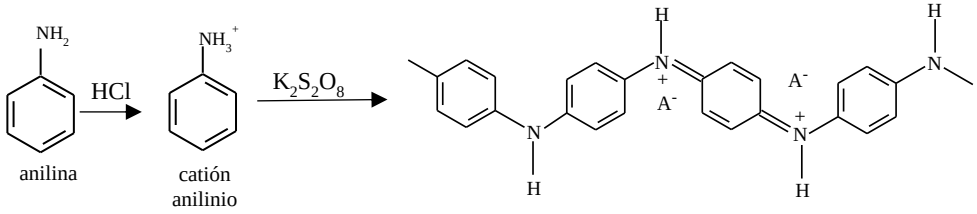

Esquema 2.2. Reacción de polimerización de la anilina con peroxidisulfato potásico en medio ácido. A^- puede ser Cl^- (del HCl) o SO_4^{2-} (por reducción del anión peroxidisulfato por la cadena polimérica).

1.1.3. Síntesis de politiofeno

Como se ha comentado con anterioridad, la polimerización oxidativa de tiofeno en un medio acuoso es complicada debido a la escasa solubilidad en agua del tiofeno, a la baja actividad oxidante de los catalizadores y a una conversión extremadamente pequeña. En este trabajo se ha empleado una ruta de síntesis alternativa a la polimerización oxidativa de tiofeno convencional en cloroformo. El método empleado [3] incluye una combinación de dos oxidantes, $FeCl_3$ anhidro y H_2O_2 en proporción $FeCl_3/H_2O_2$ de 0,00422 (0,1 mmoles de $FeCl_3$ y 7,5 mL de H_2O_2 al 30 %). Al reducir la concentración de $FeCl_3$, el Fe^{3+} puede actuar como catalizador de la polimerización del tiofeno, pero se minimiza la concentración de Cl^-. De esta manera, se reduce la posibilidad de intercambio iónico con el NO_3^- de la disolución de nitrato y se puede analizar la capacidad reductora del polímero en la reducción del nitrato del agua.

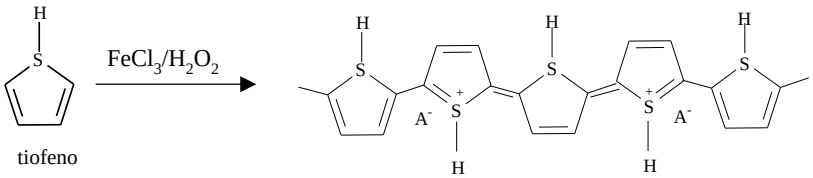

Esquema 2.3. Reacción de polimerización del tiofeno. A^- es Cl^-.

El proceso experimental empleado es el que se describe a continuación (Fig. 2.1): se disuelven 1,9 mL del monómero de tiofeno (C_4H_4S, M_m = 84,14 g·mol^{-1}, > 99 % pureza, *Sigma-Aldrich*) en 60 mL de agua ultrapura, y la disolución se añade al reactor. Posteriormente, se adicionan 7,5 mL de peróxido de hidrógeno (H_2O_2, 50 % disolución

acuosa, *Sigma-Aldrich*) a la disolución de la mezcla reaccionante. Por otra parte, se disuelven 16 mg de tricloruro de hierro anhidro ($FeCl_3$, M_m = 162,20 g·mol^{-1}, 97 % pureza, *Sigma-Aldrich*) en 5 mL de agua ultrapura y se añaden a la disolución de la mezcla reaccionante gota a gota con ayuda de una pipeta durante 60 minutos. Se mantiene la agitación a 300 rpm durante 12 horas a 50 °C.

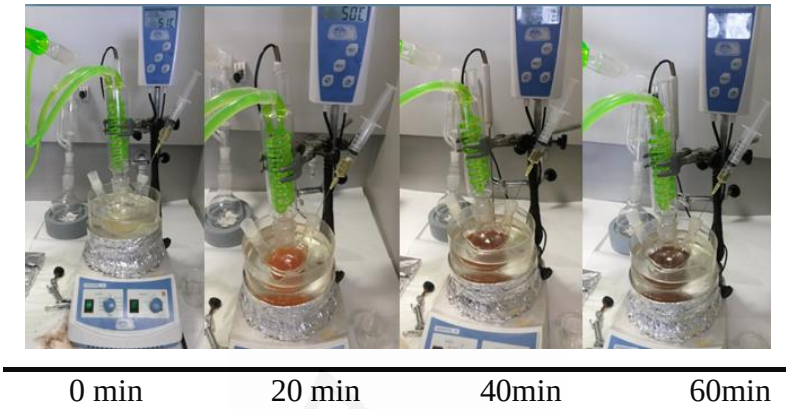

Figura 2.1. Imágenes del proceso de polimerización del tiofeno en disolución acuosa (50 °C, 300 rpm).

A medida que se va añadiendo el $FeCl_3$, la coloración de la disolución pasa de incolora en ausencia de éste, a una tonalidad amarillenta, hasta ser finalmente marrón. A continuación, se filtra y el precipitado obtenido se seca en estufa a 50 °C durante 24 horas. En presencia de H_2O_2, una pequeña cantidad de $FeCl_3$ es suficiente para obtener un alto rendimiento, debido a la regeneración continua del Fe^{3+} a través de la oxidación del Fe^{2+} formado en la reacción de H_2O_2.

Adicionalmente, también se ha realizado la síntesis de politiofeno con surfactantes de distinta naturaleza: aniónica (sulfato de dodecil sodio – SDS –, $NaC_{12}H_{25}SO_4$, M_m = 288,38 g·mol^{-1}, *Sigma-Aldrich*), catiónica (bromuro de cetiltrimetilamonio – CTAB –, $C_{19}H_{42}BrN$, M_m = 364,45 g·mol^{-1}, *Sigma-Aldrich*) y no iónica (polietilenglicol tert-octifenil éter –Tritón X-100–, *t*-Oct-C_6H_4-$(OCH_2CH_2)_xOH$, x= 9-10, ρ = 1,07 g·mL^{-1}, *Sigma-Aldrich*). La adición de surfactantes permite la formación de nanopartículas de politiofeno mediante la polimerización oxidativa catalizada por Fe^{3+} de tiofeno en el interior de las gotitas de tamaño nanométrico, que actúan como nanorreactores dispersos en la fase acuosa. Cuando se emplean surfactantes en la síntesis del politiofeno, el montaje experimental es idéntico al descrito más arriba, pero se disuelven 0,1 g de surfactante en 60 mL de agua ultrapura antes de añadir el monómero de tiofeno.

1.2. Preparación de los precursores metálicos

La preparación de los metales soportados se ha llevado a cabo mediante el proceso de impregnación húmeda, a través del cual se persigue el anclaje del precursor metálico a la estructura del polímero a través del átomo de nitrógeno. Aunque se pueden emplear precursores de platino de distinta naturaleza, se ha seleccionado el ácido hexacloroplatínico ($H_2PtCl_6 \cdot 6H_2O$), ya que se puede anclar a la cadena polimérica a través del anión complejo $[PtCl_n]^{2-}$ (Esquema. 2.4) [4]. En algunos casos, se ha realizado una impregnación con dicloruro de estaño ($SnCl_2 \cdot 2H_2O$), con el fin de obtener catalizadores bimetálicos Pt/Sn.

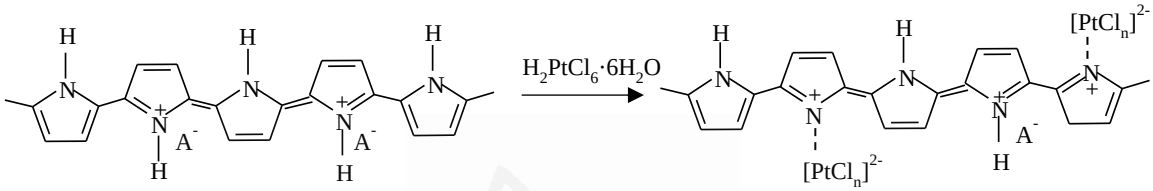

Esquema 2.4. Formación de un complejo de cloroplatinato anclado al polipirrol.

1.2.1. Precursor monometálico soportado en el polímero conductor

Para la preparación del sistema monometálico soportado en el polímero conductor se ha disuelto en agua ultrapura la cantidad necesaria del precursor de platino $H_2PtCl_6 \cdot 6H_2O$, ($M_{m(precursor)}$ = 517,912 g·mol^{-1}, *Alfa-Aesar*) para obtener el contenido en peso de platino deseado y, seguidamente, se ha añadido el polímero (25 mL de agua ultrapura·g^{-1} de polímero). La suspensión se mantiene en agitación durante 12 horas a temperatura ambiente para garantizar la impregnación y, posteriormente, se evapora el disolvente a vacío en un rotavapor. Finalmente, el precipitado se seca en estufa a 80 °C durante 12 horas. El polímero impregnado con el precursor de platino se ha sometido al tratamiento de reducción que se describe en el Apartado 1.3 de este capítulo para obtener partículas metálicas dispersas en el soporte polimérico.

A continuación se muestra, como ejemplo, el proceso de cálculo para la preparación del catalizador monometálico con un contenido del 2 % en masa de Pt soportado (ecuación 2.1):

$$0{,}02 = \frac{m_{Pt}}{m_{precursor} + m_{polímero}} \qquad (2.1)$$

donde m_{Pt} es la masa de platino metálico, $m_{precursor}$ es la masa de precursor de platino ($H_2PtCl_6 \cdot 6H_2O$) y $m_{polímero}$ es la masa de polímero.

Hay que considerar que cada mol de precursor proporciona un mol de platino (ecuación 2.2):

$$n_{precursor} = n_{Pt} \rightarrow \frac{m_{precursor}}{M_{m(precursor)}} = \frac{m_{Pt}}{M_{at(Pt)}} \rightarrow m_{Pt} = \frac{m_{precursor} \cdot M_{at(Pt)}}{M_{m(precursor)}} \qquad (2.2)$$

donde $n_{precursor}$ y n_{Pt} son el número de moles de precursor de platino y el número de moles de platino, respectivamente.

Así, sustituyendo la ecuación 2.2 en la ecuación 2.1 se obtiene la expresión (ecuación 2.3):

$$0{,}02 = \frac{m_{precursor} \cdot M_{at(Pt)}}{M_{m(precursor)} \cdot \left[m_{precursor} + m_{polímero}\right]} \qquad (2.3)$$

De esta forma, si se desease preparar el catalizador a partir de una $m_{polímero}$ = 1 g, sería necesaria una $m_{precursor}$ = 0,056 g.

1.2.2. Precursor bimetálico soportado en el polímero conductor

La preparación del sistema bimetálico soportado en el polímero conductor se ha llevado a cabo mediante una co-impregnación en disolución acuosa de $H_2PtCl_6 \cdot 6H_2O$ (M_m = 517,912 g·mol^{-1}, *Alfa-Aesar*) y $SnCl_2 \cdot 2H_2O$ (M_m = 225,63 g·mol^{-1}, 98 %, *Sigma-Aldrich*) en relaciones atómicas Pt:Sn 3:1 y 1:1, siguiendo el mismo procedimiento que el descrito en el Apartado 1.2.1 de este capítulo. Tras el proceso de impregnación, se ha realizado la reducción de los precursores metálicos como se describe a continuación.

1.3. Reducción del precursor metálico

Generalmente, los catalizadores metálicos soportados se preparan mediante la impregnación del soporte con la disolución precursora del metal, seguido por una reducción con hidrógeno a alta temperatura. En este trabajo, la limitada estabilidad

térmica del soporte polimérico en comparación con otros soportes cerámicos o carbonosos, hace necesaria la reducción del precursor del metal utilizando un método de reducción alternativo. Aunque es posible utilizar una disolución de un agente químico reductor como el borohidruro sódico [5], su uso implica potenciales problemas medioambientales. Por ese motivo, en este trabajo se ha estudiado la posibilidad de utilizar un tratamiento de reducción alternativo, que sea respetuoso con el medio ambiente y que no implique el uso de reactivos químicos [6,7]. Para ello se ha empleado un plasma frío de radiofrecuencias (RF). La generación del plasma se consigue sometiendo un flujo de gas (en este caso, argón) a la acción de un campo magnético oscilante, inducido por una corriente que fluctúa a elevada frecuencia. En el proceso de generación del plasma, los iones de argón (Ar) y los electrones libres son acelerados siguiendo trayectorias anulares, debido a la alternancia del campo magnético presente creado por el generador de radiofrecuencia.

Para ello se ha empleado un equipo de plasma de radiofrecuencias *Tucano (Gambetti Kenologia,* Italia) provisto de una cámara de reacción tipo barril y de un generador de radiofrecuencias que funciona a 13,56 MHz, con una potencia variable entre 0 y 200 W. Está equipado con medidores de flujo másico (MFC) para controlar el flujo de gas que se introduce en la cámara, y con una puerta de aluminio anodizado. La muestra se deposita en un recipiente de aluminio, que se sitúa en el centro de la bandeja de acero inoxidable y se introduce en la cámara de reacción. Dicha cámara se evacúa hasta alcanzar un vacío de 0,15 Torr utilizando para ello una bomba rotatoria *Pfeiffer* (modelo PK D41 029C-Duo 2,5 con lubricante Fomblin F4 YL VAC 25/6). Seguidamente, se introduce argón (99,9999 % de pureza mínima, *Air-liquide*), manteniendo una presión de 0,5 mbar en el interior de la cámara, que se ha purgado previamente durante 10 minutos antes de activar la fuente de radiofrecuencias. Se ha controlado la temperatura de la superficie de la muestra tratada con plasma mediante un termómetro infrarrojo de no contacto (*PCE Instruments*, modelo PCE-888).

1.4. Eliminación de nitrato del agua

Se ha evaluado la actividad catalítica de las muestras preparadas en la reacción de eliminación de nitrato del agua empleando hidrógeno como agente reductor. El proceso se ha realizado a presión atmosférica y temperatura ambiente en un reactor semicontinuo

equipado con un agitador magnético (Fig. 2.2). Inicialmente, se adicionan al reactor 592,5 mL de agua ultrapura y 300 mg de catalizador. Manteniendo una agitación de 700 rpm, se burbujea durante 15 minutos una mezcla de H_2 y CO_2 con un flujo de 75 $cm^3 \cdot min^{-1}$ cada uno, con el fin de eliminar el oxígeno. Posteriormente, se adicionan 7,5 mL de una disolución de nitrato de sodio ($NaNO_3$, M_m = 84,99 $g \cdot mol^{-1}$, *PANREAC*) preparada de forma que la concentración inicial de nitrato en el reactor sea 100 $mg \cdot L^{-1}$. Durante todo el proceso se mantiene el flujo de hidrógeno (que actúa como reductor) y de CO_2 (que tampona la disolución con el fin de obtener un pH próximo a 5). A diferentes fracciones de tiempo se extraen alícuotas de 1 mL, se determina su pH y se filtran antes de determinar la concentración de iones nitrato, nitrito y amonio mediante cromatografía iónica. Una vez finalizada la reacción, se cierra el paso de H_2 y CO_2 y se extrae una alícuota de 5 mL para comprobar mediante ICP-MS [8] si existe lixiviado de metales (*leaching*) a la disolución.

Figura 2.2. Reactor utilizado en la reacción de eliminación de nitrato.

2. TÉCNICAS DE CARACTERIZACIÓN

La caracterización de las muestras preparadas (polímeros y catalizadores mono y bimetálicos soportados en los polímeros) se ha realizado empleando las técnicas que se indican a continuación.

2.1. Espectroscopía Infrarroja con Transformada de Fourier en el modo de Reflectancia Total Atenuada (FTIR-ATR)

Se ha empleado un espectrómetro IR *Bruker Tensor 27* (*Bruker Optics*, Billerica, MA USA) con un ATR horizontal de ZnSe. Las medidas se han realizado en el rango comprendido entre 600 y 4000 cm^{-1}, empleando 200 barridos y una resolución de 4 cm^{-1}. Los espectros infrarrojos obtenidos se han analizado mediante el programa informático OMNIC 6.0.

2.2. Adsorción de nitrógeno a -196 °C

La textura porosa de los polímeros sintetizados se ha determinado mediante adsorción de nitrógeno a -196 °C en un equipo automatizado diseñado y construido en el *Laboratorio de Materiales Avanzados* del Departamento de Química Inorgánica de la Universidad de Alicante. Previamente al experimento de adsorción, las muestras se han desgasificado a 150 °C durante 4 horas. Se ha empleado una presión de nitrógeno de 15 Torr, un tiempo de equilibrio de 120 s y una rampa de calentamiento de 5 °C·min^{-1}.

A partir de los datos de las isotermas de adsorción es posible determinar la superficie específica (S) de las muestras mediante la ecuación BET (Brunauer-Emmett-Teller) (ecuación 2.4) y la ecuación 2.5:

$$\frac{P/P_o}{n\cdot\left[1-\left(P/P_o\right)\right]} = \frac{1}{n_m\cdot C} + \frac{C-1}{n_m\cdot C}\cdot\frac{P}{P_o} \qquad (2.4)$$

donde P/P_0 es la presión relativa de equilibrio (adimensional), n es el número de moles de gas (en este caso, N_2) adsorbido por gramo de adsorbente a la presión de equilibrio (mol·g^{-1}), n_m es la capacidad específica de la monocapa de adsorbato (mol·g^{-1}), C es un parámetro (adimensional) y:

$$S = n_m \cdot A_m \cdot N_A \cdot 10^{-18} \qquad (2.5)$$

donde S es la superficie específica (m^2·g^{-1}), n_m la capacidad específica de la monocapa de adsorbato (mol·g^{-1}), A_m es el área ocupada por una molécula de nitrógeno (0,162 nm^2·$molécula^{-1}$), N_A es el número de Avogadro ($6{,}022\cdot10^{23}$ moléculas·mol^{-1}) y 10^{-18} es el factor de conversión para pasar de nm^2 a m^2.

2.3. Análisis Termogravimétrico (TGA)

La estabilidad térmica de los materiales preparados se ha determinado mediante análisis termogravimétrico tanto en atmósfera de nitrógeno como de aire. Para ello se ha empleado una rampa de calentamiento de 10 °C·min^{-1} y un flujo de 100 mL·min^{-1} de N_2 o de aire. Se ha utilizado un crisol de alúmina de 70 μL y una masa de muestra de 3 – 4 g. Los ensayos se han realizado en un rango de temperatura comprendido entre los 25 y 1200 °C para atmósfera de nitrógeno, y entre 25 y 800 °C en el caso de aire. Para asegurar la reproducibilidad de los resultados se han comparado los análisis obtenidos en un equipo SDT 2960 (*TA Instruments*, Delaware, NC USA) del *Laboratorio de Materiales Avanzados* con los obtenidos en un equipo *Mettler-Toledo*, modelo TGA/SDTA851e/LF/ 1600) de los Servicios Técnicos de Investigación de la Universidad de Alicante [8].

2.4. Calorimetría Diferencial de Barrido (DSC)

El análisis calorimétrico de las distintas muestras se ha realizado simultáneamente al análisis TGA en el equipo SDT 2960 (*TA Instruments*, Delaware, NC USA) en atmósferas de nitrógeno y de aire. En el primer caso, se ha realizado una isoterma a 25 °C durante 20 minutos para estabilizar la temperatura del equipo y, posteriormente, un barrido entre 25 y 1200 °C (en atmósfera de nitrógeno) o entre 25 y 800 ºC (si la atmósfera empleada es aire) con una rampa de calentamiento de 10 °C·min^{-1}. La masa de muestra utilizada es de aproximadamente 3 – 4 g.

2.5. Difracción de Rayos X (XRD)

El análisis mediante XRD de las distintas muestras se ha realizado en un equipo *Bruker*, modelo *D8-Advance*, de los Servicios Técnicos de Investigación de la Universidad de Alicante [8], provisto de un ánodo de cobre y un espejo Göebel, que evita la necesidad de eliminar la radiación K_β del cobre con un filtro de níquel. Se ha utilizado la radiación K_α del Cu (λ = 1,5406 Å), realizándose un barrido 2θ entre 6 º y 90 º a una velocidad de 1 º·min^{-1} y un tiempo de paso de 3 s.

El espaciado interplanar se puede calcular a partir de la *ecuación de Bragg* (ecuación 2.6):

$$n \cdot \lambda = 2 \cdot d_{hkl} \cdot sen\theta \qquad (2.6)$$

donde *n* es el orden de difracción (*n* = 1), λ es la longitud de onda de la radiación X utilizada (λ= 1,5406 Å, radiación K_α del Cu), d_{hkl} es el espaciado interplanar (nm) y θ es el ángulo de difracción (º) del pico principal centrado, también conocido como el *ángulo de Bragg*.

El tamaño medio de cristalito (*L*) se puede estimar a partir de la anchura a media altura (FWHM, del inglés *full width at half maximum*) empleando la *ecuación de Scherrer* (ecuación 2.7):

$$\tau = \frac{\kappa\lambda}{\beta \cos\theta} \qquad (2.7)$$

donde τ es el tamaño medio de los dominios cristalinos, κ es un factor de forma adimensional (suele tener un valor típico de 0,9), λ es la longitud de onda de la radiación X utilizada (λ = 1,5406 Å, radiación K_α del Cu), β es el ensanchamiento de la línea a la anchura a media altura (FWHM) en radianes y θ es el *ángulo de Bragg* (º).

2.6. Espectroscopía Fotoelectrónica de Rayos X (XPS)

Los análisis XPS se han llevado a cabo en un espectrómetro *K-Alpha* (*Thermo-Scientific*) totalmente automatizado, perteneciente a los Servicios Técnicos de Investigación de la Universidad de Alicante [8], provisto de un monocromador de alta resolución. Se ha utilizado la radiación K_α del Al (1486,6 eV) como fuente de rayos X y se ha operado en condiciones de ultra alto vacío. El equipo dispone de un analizador alfa hemisférico que opera en modo de energía constante con una energía de paso de 200 eV para la obtención del espectro completo y de 50 eV para la realización de un barrido estrecho que permite medir selectivamente cada elemento. Se ha registrado el espectro global de energías de enlace (*survey spectra*) entre 0 y 1350 eV (con una precisión de ± 0,2 eV) y se ha realizado el ajuste de las curvas mediante la deconvolución de los picos principales. Se ha tomado como referencia la energía de enlace del C 1s para las especies C-C y C-H a 284,5 eV.

2.7. Medidas de conductividad

La baja resistencia mecánica de las pastillas de polímero ha hecho necesario el diseño de un equipo de cuatro cables de fabricación propia (Fig. 2.3) compuesto por un soporte de teflón con una oquedad cilíndrica en su interior, a través de la cual se introduce

la muestra. Dos piezas de cobre metálico cierran el circuito y un multímetro *2000 Multimeter* (*idm*, Madrid) permite realizar las medidas de resistencia y, a partir de ellas, calcular la conductividad.

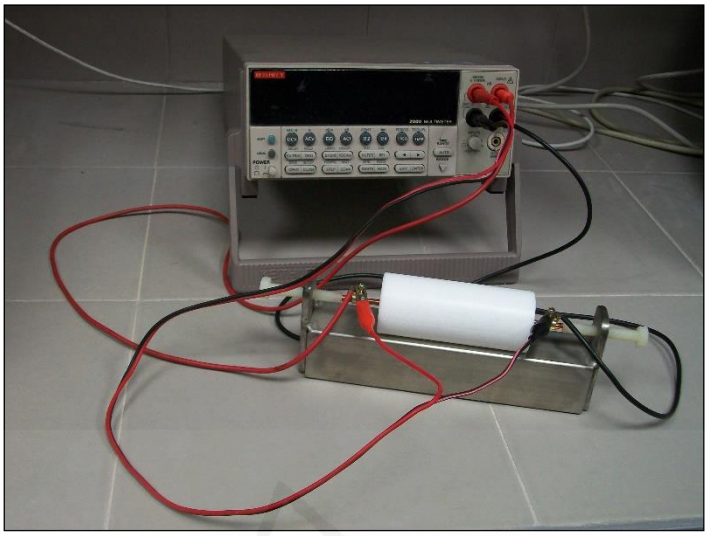

Figura 2.3. Equipo para realizar las medidas de conductividad.

2.8. Microscopía Electrónica de Transmisión (TEM)

Las imágenes TEM se han obtenido en un microscopio *JEM2010* (*JEOL* Ltd., Tokio, Japón) perteneciente a los Servicios Técnicos de Investigación de la Universidad de Alicante [8], que opera a 120 kV. Se deposita una gota de suspensión acuosa de la muestra molida sobre una película delgada de carbón y ésta se soporta sobre una rejilla de cobre. Un detector *OXFORD* (modelo *INCA Energy TEM 100*) de energía dispersiva de rayos X (EDX) permite realizar el análisis elemental de las muestras.

2.9. Cromatografía Iónica

La cromatografía iónica permite determinar la concentración de iones nitrato (NO_3^-), nitrito (NO_2^-) y amonio (NH_4^+) presentes en las alícuotas extraídas a distintos tiempos de disolución acuosa de nitrato. Para ello se ha utilizado un cromatógrafo iónico con supresión química de conductividad y detección conductimétrica y amperométrica *Metrohm 850 ProfIC AnCat-MCS* de los Servicios Técnicos de Investigación de la Universidad de Alicante [8]. Para el análisis de los aniones nitrato y nitrito se ha empleado una columna *Metrosep ASSUP-7 (250 mm x 4 mm)* y para analizar los cationes amonio, una columna *Metrosep C3 (250 mm x 4 mm).*

A partir de los datos experimentales obtenidos se ha calculado la conversión del nitrato y la selectividad de los catalizadores hacia nitrito y amonio únicamente, ya que no es posible determinar la producción de nitrógeno. La conversión de nitrato ($\chi_{NO_3^-}$), expresada en tanto por cien, se ha calculado empleando la siguiente ecuación:

$$\chi_{NO_3^-} = \frac{[NO_3^-]_0 - [NO_3^-]_t}{[NO_3^-]_0} \cdot 100 \qquad (2.8)$$

donde $[NO_3^-]_0$ y $[NO_3^-]_t$ son las concentraciones de nitrato ($mg \cdot L^{-1}$) inicial y a tiempo *t* (min), respectivamente.

Las selectividades a nitrito ($S_{NO_2^-}$) y a amonio ($S_{NH_4^+}$), expresadas en tanto por cien, se han calculado con las siguientes ecuaciones:

$$S_{NO_2^-} = \frac{(n_{NO_2^-})_t}{(n_{NO_3^-})_0 - (n_{NO_3^-})_t} \cdot 100 \qquad (2.9)$$

$$S_{NH_4^+} = \frac{(n_{NH_4^+})_t}{(n_{NO_3^-})_0 - (n_{NO_3^-})_t} \cdot 100 \qquad (2.10)$$

donde $(n_{NO_3^-})_0$ es la cantidad de nitrato inicial (mol) y $(n_{NO_3^-})_t$, $(n_{NO_2^-})_t$ y $(n_{NH_4^+})_t$ son las cantidades de las especies respectivas (mol) a tiempo *t* (min).

La selectividad frente a nitrógeno (S_{N_2}), expresada en tanto por cien, se puede estimar a partir de las selectividades frente a nitrito y a amonio, asumiendo que en las condiciones de reacción no hay ninguna otra especie intermedia como N_2O o NO.

$$S_{N_2} = 100 - S_{NO_2^-} - S_{NH_4^+} \qquad (2.11)$$

2.10. Espectrometría de Masas por Plasma de Acoplamiento Inductivo (ICP-MS)

Para comprobar que no existe lixiviado (*leaching*) de platino y/o estaño desde el soporte hacia la disolución, se ha analizado mediante ICP-MS una alícuota al finalizar la reacción de reducción de nitratos. Esta técnica permite determinar de forma cuantitativa gran parte de elementos a niveles de traza y ultratraza en muestras en disolución acuosa. Para ello se ha empleado un equipo *7700x* (*Agilent*) de los Servicios Técnicos de Investigación de la Universidad de Alicante [8] que incluye una matriz HMI (High Matrix Introduction). Se opera en modo ORS (Sistema de Reacción Octopolar) con estándar de

helio, una potencia RF de 1550 W, un caudal de gas de 0,99 $L \cdot min^{-1}$ y un caudal de líquido de 0,3 $mL \cdot min^{-1}$.

3. BIBLIOGRAFÍA

[1] I. Dodouche, F. Epron. *Appl. Catal., B: Env.*. **2007**, *76(3-4)*, 291-299.

[2] R. Ansari. *E-J. Chem*. **2006**, *3(4)*, 186-201.

[3] S.J. Lee, J.M. Lee, I.W. Cheong, H. Lee, J.H. Kim. *J. Polym. Sci., Part A: Polym. Chem*. **2008**, *46(6)*, 2097-2107.

[4] Y. Verde, G. Alonso, V. Ramos, H. Zhang, A.J. Jacobson, A. Keer. *Appl. Catal., A : Gen*. **2004**, *277(1-2)*, 201-207.

[5] M. Králik, A. Biffis. *J. Mol. Catal. A: Chem*. **2001**, *177(1)*, 113-138.

[6] J.J. Zou, Y.P. Zhang, C.J. Liu. *Langmuir*. **2006**, *22(26)*, 11388-11394.

[7] R. Buitrago-Sierra, M.J. García-Fernández, M.M. Pastor-Blas, A. Sepúlveda-Escribano. *Green Chem.* **2013**, *15*, 1981-1990.

[8] Servicios Técnicos de Investigación de la Universidad de Alicante (España) https://sstti.ua.es/es/instrumentacion-cientifica/area-de-instrumentacion-cientifica.html

Chapter III. Plasma-assisted preparation of polypyrrole-supported catalysts and their application to nitrate removal in water

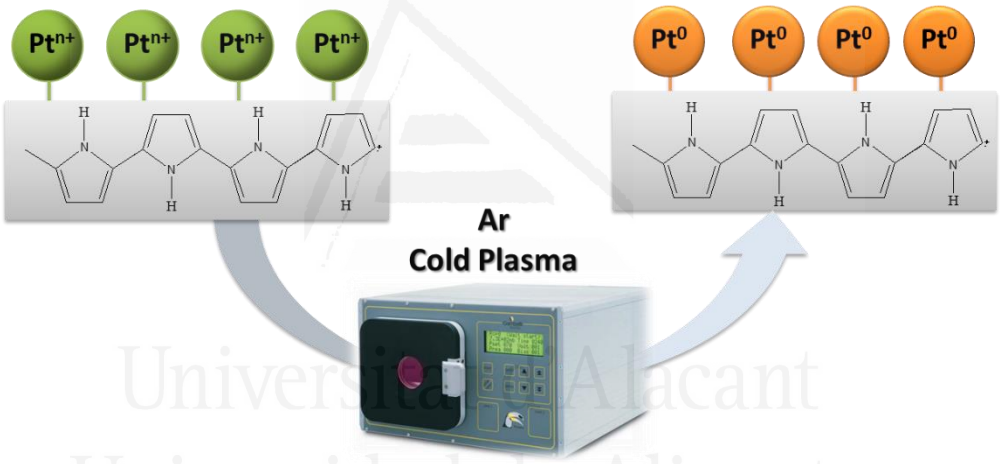

R. Buitrago-Sierra, **M.J. García-Fernández**, M.M. Pastor-Blas, A. Sepúlveda-Escribano, "Environmentally friendly reduction of a platinum catalysts precursor supported on polypyrrole", *Green Chemistry*. **2013**, *15*, 1981-1990.

1. INTRODUCTION

Plasma treatment is a simple, easy to manipulate green technique which may become an environmentally friendly alternative to processes that involve the use of hazardous solvents and chemicals. In this chapter, the application of plasma techniques in the preparation of highly dispersed supported metal catalysts has been investigated.

Supported metals are traditionally prepared by impregnating a support material with the metal precursor solution, followed by reduction in hydrogen at relatively high temperature. The resulting metal particles are usually heterogeneously dispersed, with a broad particle size distribution. However, the thermal stability of polymer-based supports often determines that the reduction treatment has to be carried out under mild conditions in the liquid phase. The most frequently employed reducing agents for low temperature reduction are sodium borohydride, hydrazine, alcohols and formaldehyde [1]. But the use of these chemicals implies environmental concerns [2]. Therefore, cold RF plasma has been considered in this work to treat a polymer-supported metal precursor (Pt on polypyrrole). Hydrogen plasma has excellent abilities to reduce metal ions due to the strong reducing nature of the H radicals or atoms that are produced in the plasma [3]. However, Ar plasma is also a potential reductor, and it is much greener [4]. In addition, plasma reduction is simple, easy to manipulate and compatible with the commonly used impregnation processes.

Polypyrrole is a conducting polymer with high electrical conductivity and appreciable environmental stability [3]. Although PPy can also be prepared electrochemically, the chemical oxidation method is suitable for its commercial mass production, and it provides much greater feasibility to control the molecular weight and structural features of the resulting polymer. In the chemical oxidation method, an oxidizing agent is added to a solution containing pyrrole and a dopant, resulting in the precipitation of a doped polypyrrole powder [5]. Sometimes, the same compound can provide the dopant as well as result in oxidation of the polymeric chain. The purpose of oxidizing pyrrole is to complete the oxidative polymerization of unreacted pyrrole and to achieve its oxidative doping [3]. Several oxidants have been used in the literature, each of them providing different dopants. In this way, polypyrrole doped with *p*-toluenesulfonate, tetrafluoroborate and perchlorate anions has been studied [6,7]. For

instance, potassium peroxydisulfate ($K_2S_2O_8$) provides either $S_2O_8^{2-}$ anions if the oxidant is in excess, or SO_4^{2-} anions resulting from the redox reaction between the persulfate and the pyrrole monomer [8]. In Scheme 3.1 is interesting to observe that ferric chloride ($FeCl_3 \cdot 6H_2O$) acts as an oxidant and also provides Cl^- as counterion to be incorporated in the *p*-doped polypyrrole ring.

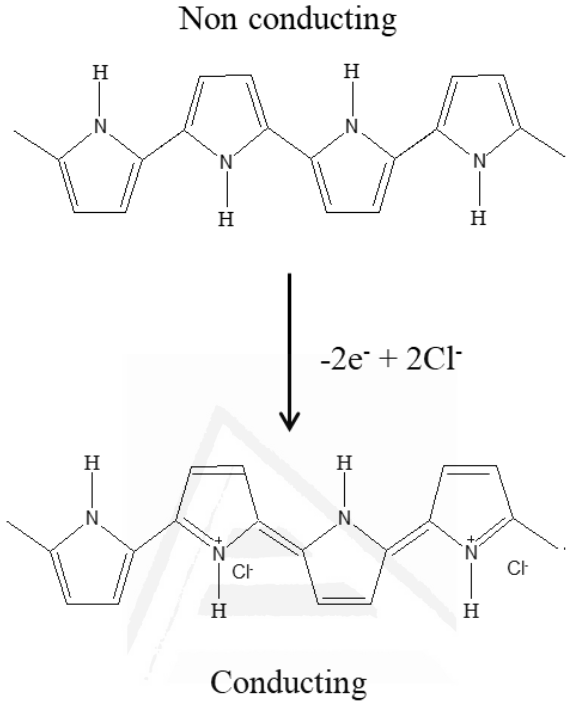

Scheme 3.1. Scheme showing reduced (non-conducting) and oxidized (conducting) forms of polypyrrole chemically synthesized using $FeCl_3$. To maintain charge neutrality, Cl^- anions are incorporated into the growing chain during polymerization, thus producing a bipolaron.

Conducting polymers are important materials emerging in lots of applications in various fields. Polypyrrole has been widely used in gas sensors, biosensors, electromagnetic irradiation shielding materials, actuators and artificial muscles, electrode materials, photovoltaic cells, coating materials, corrosion inhibitors [9], chromatographic stationary phases, light-weight batteries, membrane separation, and counter-electrode in electrolytic capacitors [7]. However, applications of this polymer as catalyst support have been scarcely investigated. Thus, the main objective of this chapter has been to use polypyrrole as a support for effectively dispersing platinum, and to analyze the reduction of the catalyst precursor using Ar plasma treatments.

The catalytic behavior of the platinum nanoparticles supported on polypyrrole has been evaluated in the reduction of nitrates in water using hydrogen as a reductive agent.

This reaction proceeds through the production of nitrite ion as intermediate, as shown below:

$$NO_3^- + 2\,H^+ + 2\,e^- \rightarrow NO_2^- + H_2O$$

Further reduction of nitrite may produce nitrogen (desired product):

$$2\,NO_2^- + 8\,H^+ + 6\,e^- \rightarrow N_2 + 4\,H_2O$$

or ammonium ions (undesired product):

$$NO_2^- + 8\,H^+ + 6\,e^- \rightarrow NH_4^+ + 2\,H_2O$$

Taking into account that nitrites and ammonium are also toxic compounds, the selective reduction of nitrates to nitrogen has to be achieved. Although it has been reported [10] that to selectively reduce nitrates to nitrogen it is necessary to activate the precious metal (Pt or Pd) by the addition of a promoter such as tin or copper, also monometallic catalysts have been shown to be active when an adequate support such as TiO_2 is used [11]. In this chapter, preliminary results on the ability of a PPy/Pt catalyst obtained after treatment with Ar plasma to reduce nitrates in water are reported.

2. EXPERIMENTAL

2.1. Materials preparation

Polypyrrole was prepared by chemical polymerization of pyrrole (C_4H_5N) with ferric chloride ($FeCl_3 \cdot 6H_2O$) as an oxidant. The experimental procedure was described in Chapter II, Section 1.1.1 [8]. The precursor of the polymer-supported platinum catalyst (PPy/Pt) was prepared by wet impregnation in excess of solvent, using $H_2PtCl_6 \cdot 6H_2O$ as the metal precursor. The appropriate amount of this salt to obtain 1 wt. % Pt loading was dissolved in ultrapure water, and then it was put into contact with polypyrrole as described in Chapter II, Section 1.2.1. The obtained material was split into two portions; one of them was treated in Ar plasma and the other one was treated with a mild reducing chemical, sodium borohydride ($NaBH_4$).

Ar plasma treatment of PPy/Pt was carried out at several discharge powers (100, 150 and 200 W). The duration of each plasma treatment was 60 min, but the effectiveness of a whole 60 min treatment was compared to a repetitive treatment of the sample during

10 min for 6 times, *i.e.* the plasma treatment was for 10 min, and each sample was treated 6 times, with manual mixing of the sample between treatments to assure an even exposure to the plasma [12]. The temperature of the sample after the plasma treatment remained below 50 °C in all cases (Chapter II, Section 1.3).

Reduction with sodium borohydride was carried out by treating the polypyrrole-supported catalyst precursor (PPy/Pt) (500 mg) with 50 mL of an aqueous solution of ice cold 0.1 $mol \cdot L^{-1}$ $NaBH_4$ with continuous stirring during 60 min, followed by washing with high purity water, as reported elsewhere [13].

2.2. Materials characterization

The polypyrrole support (PPy) and the catalyst precursor (PPy/Pt) were characterized by infrared spectroscopy (FTIR), X-ray diffraction (XRD), transmission electron microscopy (TEM), thermogravimetric analysis (TGA), differential scanning calorimetry (DSC) and X-ray photoelectron spectroscopy (XPS), which were described in Chapter II, Section 2.

2.3. Catalyst evaluation

Catalytic activity of the polypyrrole-supported Pt catalyst obtained after treatment with Ar plasma at 200 W was evaluated in the aqueous reduction of nitrate with H_2 at room temperature. The reaction was carried out in a semi-batch reactor equipped with a magnetic stirrer (700 rpm) as it is detailed in Chapter II, Section 1.4. Small samples (1 mL) were withdrawn at different times from the reactor and immediately filtered for determination of nitrate, nitrite and ammonium concentrations by ion chromatography (Chapter II, Section 2.9).

3. RESULTS AND DISCUSSION

3.1. Characterization of polypyrrole

The X-ray diffraction pattern of PPy (Fig. 3.1) shows a broad peak centered at $2\theta \approx 26.0$ º, which is characteristic of amorphous polypyrrole and is due to the scattering

from PPy chains at the interplanar spacing [14]. The *d*-spacing can be calculated from the Bragg's equation (equation 2.6 in Chapter II, Section 2.5) and for PPy is d = 0.36 nm.

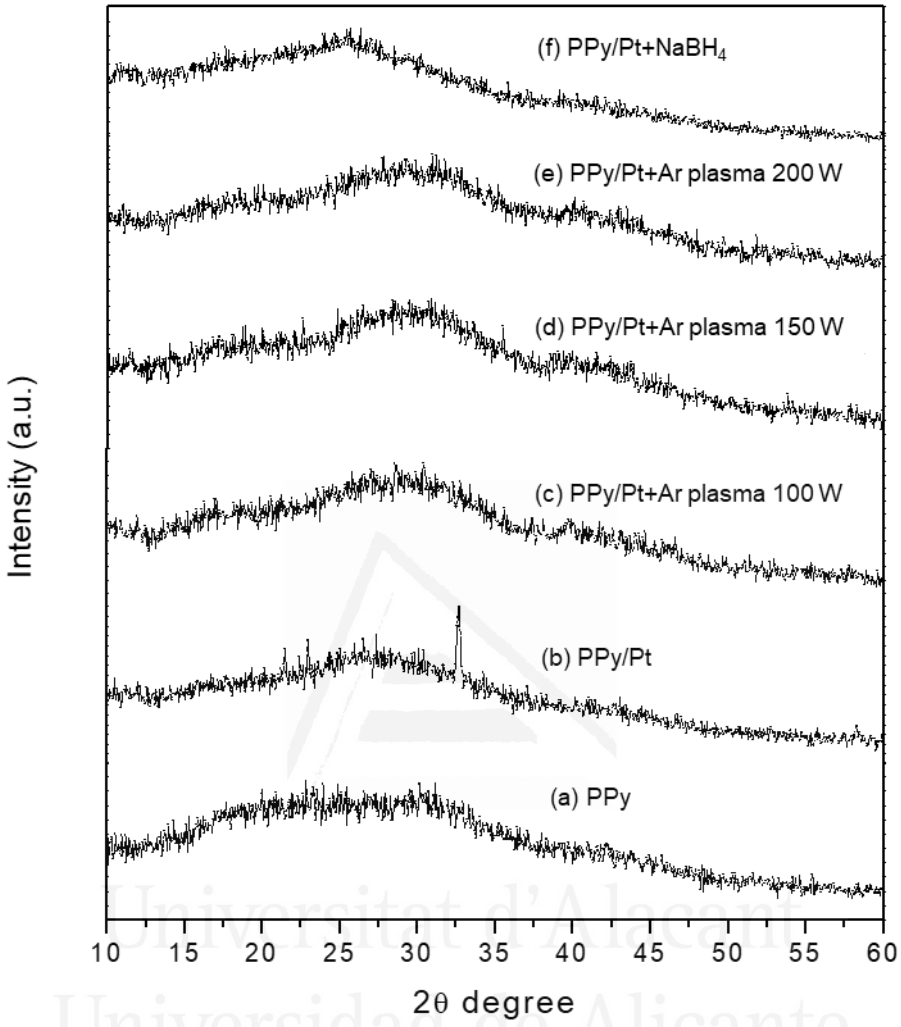

Figure 3.1. XRD patterns of: (a) chemically synthesized polypyrrole; (b) polypyrrole impregnated with H_2PtCl_6; (c-e) polypyrrole impregnated with H_2PtCl_6 and treated with Ar plasma 10 min x 6 times at 100, 150 and 200 W; (f) polypyrrole impregnated with H_2PtCl_6 and treated with $NaBH_4$.

The average crystallite size (L) has been estimated using the Scherrer's equation (equation 2.7 in Chapter II, Section 2.5). It results in 0.41 nm, and similar values have been obtained by Dodouche et al. [8] in the synthesis of polypyrrole with $K_2S_2O_8$ and $FeCl_3$.

The DSC profile of polypyrrole under nitrogen atmosphere is shown at Figure 3.2. After removing its thermal history, a second run between 25 to 400 °C shows a broad endothermic peak at 80 °C corresponding to the glass transition temperature (T_g). Above

250 °C, the polymer degrades. However, the DSC profile shows that chemically synthesized PPy is mainly amorphous, which is consistent with XRD analysis.

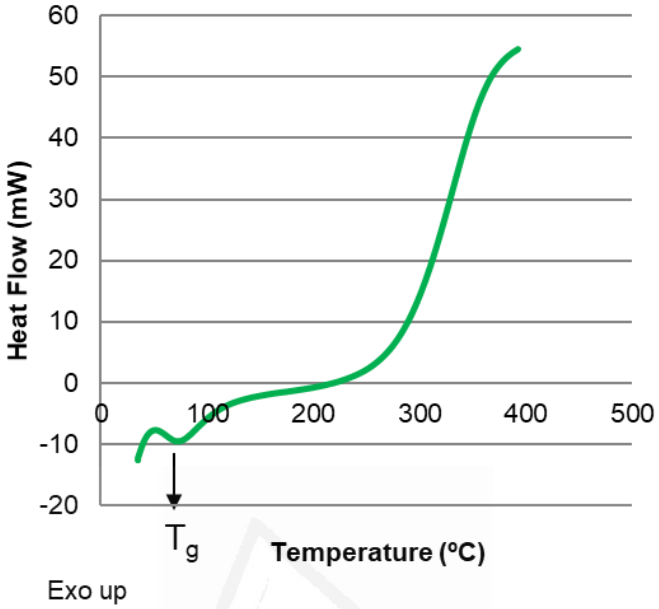

Figure 3.2. DSC profile in N_2 atmosphere of chemically synthesized polypyrrole with $FeCl_3$ as oxidant.

The FTIR spectrum of PPy (Fig. 3.3) shows the typical bands of this material [8]: C=N in-plane bending (1563 cm^{-1}), C=C stretching (1479 cm^{-1}), in-plane bending of =C-H bond (1327 cm^{-1}), C-C stretching and C-N stretching (1107 cm^{-1}), =C-H out of plane bending (1047 cm^{-1}) [4,15], N-H bending (793 cm^{-1}) and C-H out of plane bending (695 cm^{-1}) [16]. The bands at 1206 and 931 cm^{-1} correspond to C-N^+ stretching and C=N^+-C stretching, respectively, and have been attributed to the bipolaron bands characteristic of the doping [17], which suggests that the PPy support is in its oxidized state and contains positive charges (N^+ moieties) [15].

The band at 1704 cm^{-1} can be attributed to C=O stretching due to polypyrrole backbone oxidation through free radical oxygen insertion and dopant degradation [6]. Radical generation favors nucleophilic attack to the cations (bipolarons) present in the polymer, producing degradation [18]:

$PPy^{+}\bullet + OH^{-} \rightarrow PPy\text{-}OH + H^{+}$

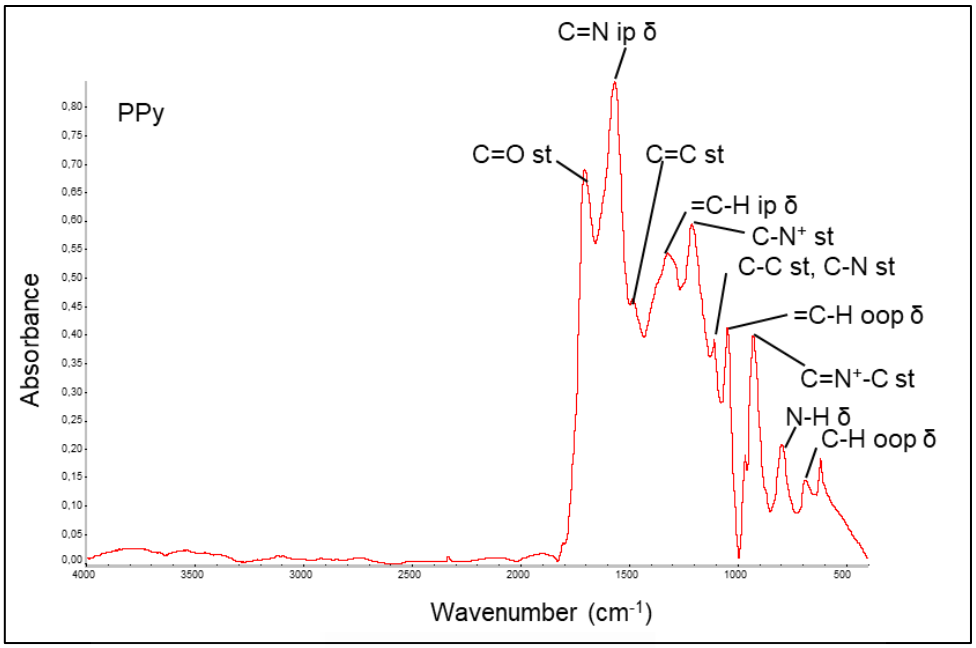

Figure 3.3. FTIR-ATR spectra of polypyrrole chemically synthesized with $FeCl_3$ as oxidant.

OH^- may come from the aqueous solution or be present in the polymer channels due to its high hygroscopic character. Scheme 3.2 shows a scheme of polypyrrole degradation by OH radicals and the consequent creation of C=O moieties. On the other hand, some degree of surface oxidation may also be produced by exposure of the polymer to air.

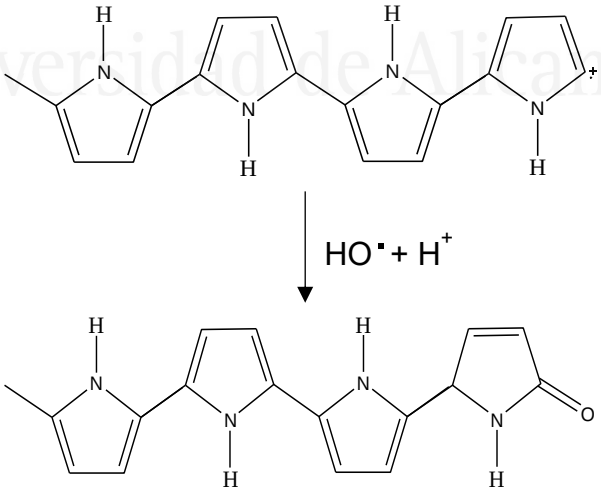

Scheme 3.2. Scheme showing polypyrrole degradation by OH radicals, with the subsequent formation of C=O moieties.

Furthermore, a high concentration of cationic polymeric radicals might produce reticulation of PPy chains:

$$PPy^{+}\bullet + PPy^{+}\bullet \rightarrow PPy\text{-}PPy + 2\,H^{+}$$

In our case, insolubility of the chemically synthesized PPy indicates that reticulation of polymeric chains has been produced during the chemical oxidative polymerization.

3.2. Characterization of PPy/Pt

Impregnation of polypyrrole with H_2PtCl_6 leads to a homogeneous distribution and good dispersion of platinum species on the support, as observed from the dark spots in TEM images (Fig. 3.4). EDX spectra recorded on dark spots reveals the presence of C and N from PPy, Pt from the catalyst precursor and O, which is consistent with the PPy oxidation as observed by FTIR. The Pt loading calculated with EDX is 0.3 at. % (5 wt. %).

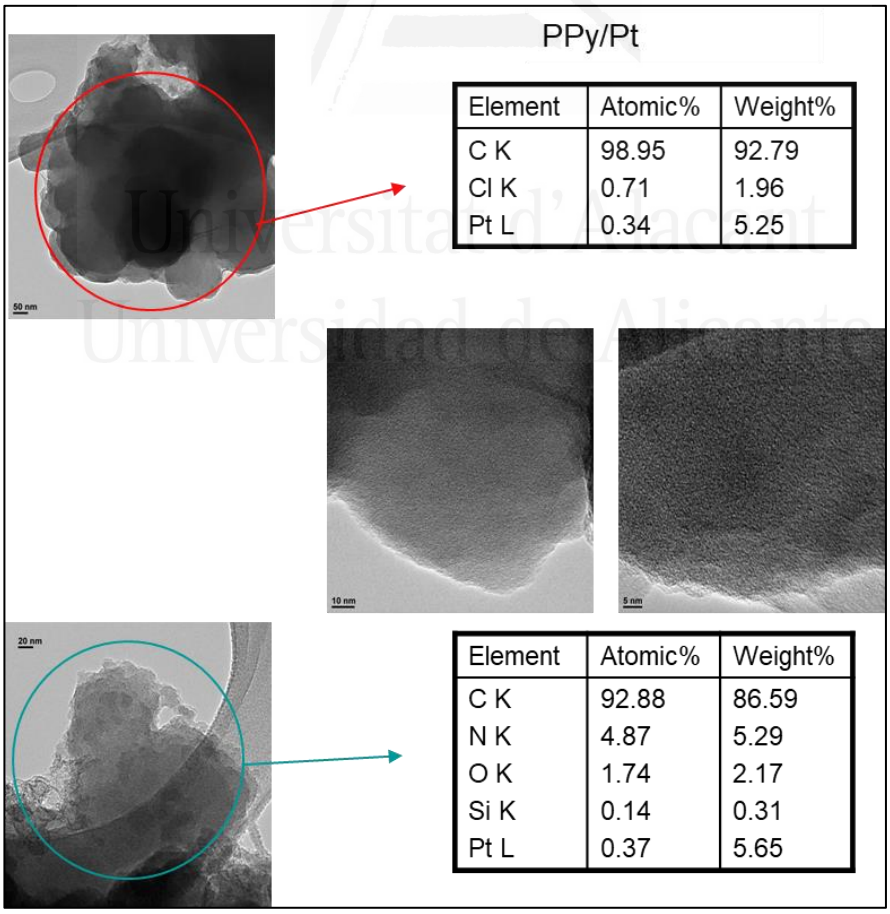

Figure 3.4. TEM images and EDX analysis of polypyrrole impregnated with H_2PtCl_6 (PPy/Pt).

One of the aims to use this kind of polymers as supports for metal particles is the possibility of anchoring the metal precursor on specific sites at the polymer's surface in a controlled way. In this sense, a high metal dispersion could be achieved. TEM images of the impregnated polymer reveal that only tiny particles, well dispersed over the polymer surface, are observed.

Polypyrrole is able to reversibly transform between its oxidized (positively charged) and reduced (neutral) states (Scheme 3.1). Polypyrrole is oxidized by doping with $FeCl_3$. Consequently, oxidation of -NH- amine groups in the PPy chain to N^+ would be expected. Surface characterization performed by X-ray photoelectron spectroscopy (XPS) allows detailed investigation into changes in chemical states of surface atoms.

XPS analysis of chemically synthesized polypyrrole (Table 3.1) shows the presence of C and N from the polymer and Cl from the doping with $FeCl_3$. The analysis of the C 1s (Fig. 3.5a) and O 1s (Fig. 3.6a) levels shows the presence of C=O and C-O moieties (Table 3.2), which support PPy degradation and/or surface oxidation (Scheme 3.2) and is in agreement with FTIR and EDX.

Table 3.1. XPS surface chemical composition (atomic %) of the different samples.

Binding energy (eV)	**Element**	**PPy**	**PPy/Pt**	**PPy/Pt/ $NaBH_4$**	**PPy/Pt/Plasma**			
					60 min	**10 min x 6 times**		
					100 W	**100 W**	**150 W**	**200 W**
284.5	C 1s	87.2	78.2	81.2	56.4	65.5	62.1	63.0
531.5	O 1s	7.2	15.1	12.6	25.3	23.1	21.2	20.4
398.1	N 1s	4.6	6.4	5.3	14.6	10.8	13.9	13.1
198.5	Cl 2p	1.0	0.2	0.3	2.6	0.4	1.5	1.7
71.2	Pt 4f	-	0.1	0.5	1.1	0.2	1.3	1.8
710.9	Fe 2p	0.0	0.0	0.0	0.0	0.0	0.0	0.0
1072.1	Na 1s	-	-	0.1	-	-	-	-
531.5/284.5	O/C	0.08	0.19	0.16	0.45	0.35	0.34	0.32

On the other hand, N 1s curve fit (Fig. 3.7a) shows the presence of –NH- of polypyrrole (399.8 eV) and also positively charged nitrogen, N^+ (401.2 eV). Table 3.2 shows that 23.3 at. % of total nitrogen is positively charged in the prepared PPy. Lower binding energy components (≈ 397.5 eV) of uncharged deprotonated imine (=N-) nitrogen atoms or due to imine defects responsible for interruption of effective conjugation of PPy are not present in the N 1s level XPS spectrum of PPy [16,19].

Table 3.2. Percentages (%) of the different surface species estimated from the areas of the contributions to the XPS spectra corresponding to the C 1s, O 1s, N 1s and Pt $4f_{7/2}$ levels.

Binding energy (eV)	Species	PPy	PPy/ Pt	PPy/Pt/ $NaBH_4$	PPy/Pt/Plasma			
					60 min	10 min x 6 times		
					100 W	100 W	150 W	200 W
C 1s								
284.5	C-C, C-H, C-N	52.8	68.7	21.5	48.4	58.0	45.2	45.2
286.2	C-O	30.6	21.6	69.1	22.9	22.4	25.7	22.9
288.1	C=O	16.6	9.7	9.4	18.8	19.6	15.7	16.8
289.2	RO-C=O	-	-	-	9.9	-	13.4	15.1
O 1s								
531.5	O=C, O-H	38.3	48.8	22.2	39.1	55.4	44.6	43.4
533.0	O-C	41.6	40.4	44.2	38.8	44.6	32.9	36.4
534.0	O-C	20.1	10.8	33.6	22.1	-	22.5	20.2
N 1s								
399.8	-NH-	76.7	50.5	32.3	59.9	62.8	78.5	69.6
401.2	N^+	23.3	49.5	67.7	40.1	37.2	21.5	30.4
	N^+/-NH-	0.30	0.98	2.10	0.67	0.59	0.27	0.44
Pt 4f$_{7/2}$								
71.2	Pt^o	-	0	37.8	40.8	51.9	72.8	77.8
72.9	Pt^{n+}	-	100	62.2	59.2	48.1	27.2	22.2
	Pt^o/Pt^{n+}	-	0	0.61	0.69	1.08	2.68	3.50

The XPS spectra of polypyrrole doped with $FeCl_3$ and impregnated with H_2PtCl_6 (PPy/Pt) shows the presence of C and N from polypyrrole and Cl from the dopant. The C 1s band (Fig. 3.5b) shows a decrease of C-O and C=O species when compared to synthesized polypyrrole. The O 1s band (Fig. 3.6b) also shows a decrease of O-C and O=C moieties after impregnation of the PPy support. There is also a slight decrease in Cl percentage after impregnation with H_2PtCl_6 (1.0 at. % in PPy *vs.* 0.2 at. % in PPy/Pt, Table 3.1). Therefore, Cl may come mainly from $FeCl_3$ oxidant during the chemical polymerization of PPy.

On the other hand, the XPS N 1s spectra (Fig. 3.7b) shows that there is an increase of positively charged N^+ species (401.2 eV) in the platinum impregnated polypyrrole (PPy/Pt), *ca.* 49.5 at. %, when compared to the parent PPy, *ca.* 23.3 at. % (Table 3.2).

The platinum content calculated from XPS data is 0.1 at. %; this corresponds to 1.4 wt. % (Table 3.1), which is in agreement with the nominal platinum loading of 1 wt. %. The XPS spectra corresponding to the Pt 4f level can be deconvoluted into two bands (Fig. 3.8a), at 72.9 eV (Pt $4f_{7/2}$) and 76.3 eV (Pt $4f_{5/2}$), which correspond to ionic platinum, Pt(II) [2], thus confirming the absence of metallic platinum which should appear at lower

binding energies (Table 3.2). Considering the redox potentials of PPy (PPy^{+}/PPy, E° = 0.150 V, at pH = 0) and platinum ($[PtCl_6]^{2-}/[PtCl_4]^{2-}$, E° = 0.726 V; $[PtCl_4]^{2-}/Pt$, E° = 0.758 V) a partial reduction of Pt(IV) to Pt(II) and the oxidation of the polypyrrole polymeric chain (from -NH- to N^{+}) upon the impregnation with H_2PtCl_6 might be possible [20]. This result is similar to those reported in the literature showing the partial reduction of Pt(IV) in H_2PtCl_6 upon impregnation on a carbonaceous support and ulterior drying [21,22].

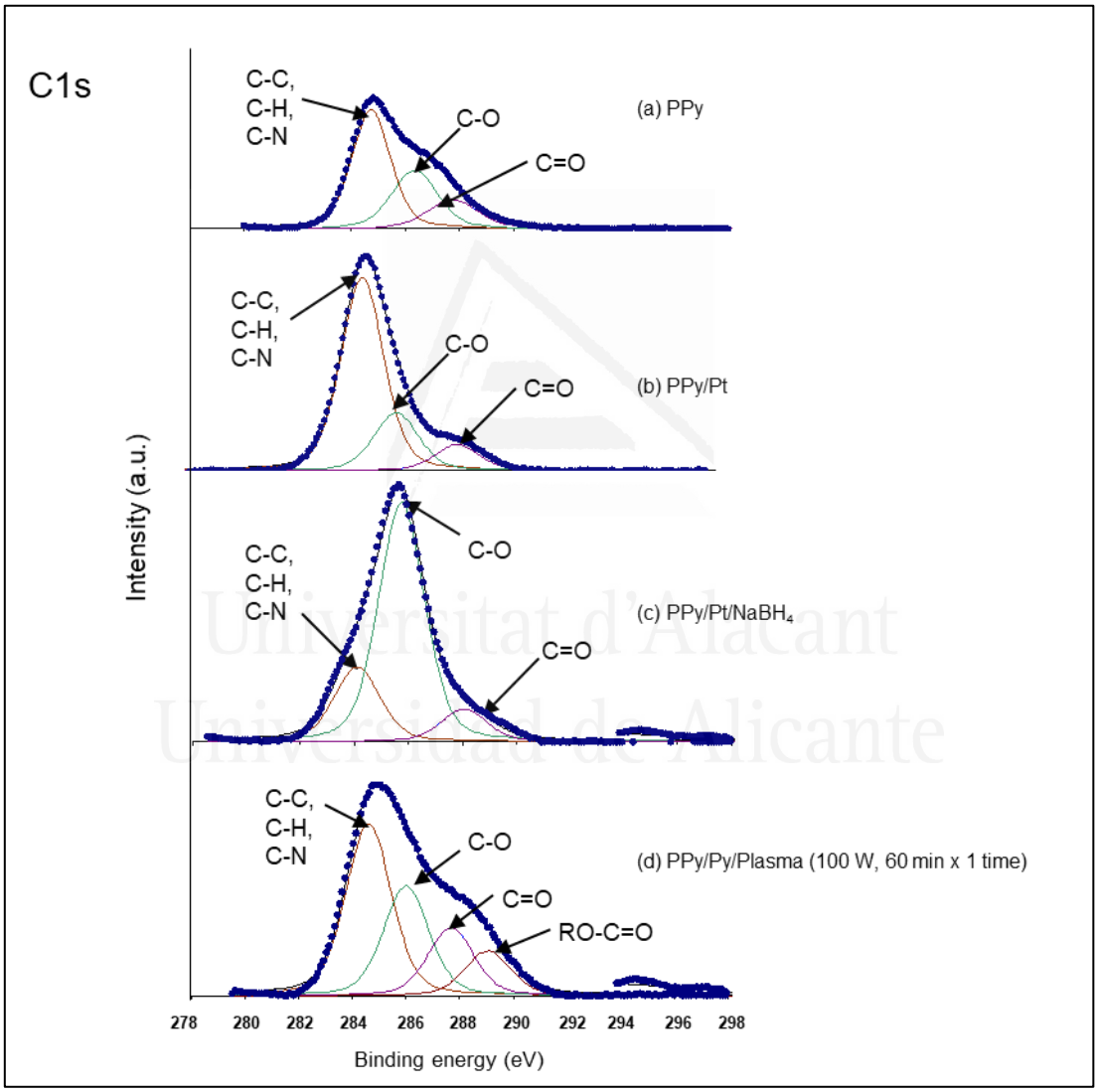

Figure 3.5. XPS C 1s spectra of (a) polypyrrole, (b) polypyrrole impregnated with H_2PtCl_6, (c) polypyrrole impregnated with H_2PtCl_6 and treated with $NaBH_4$, and (d) polypyrrole impregnated with H_2PtCl_6 and treated with Ar plasma 60 min x 1 time at 100 W.

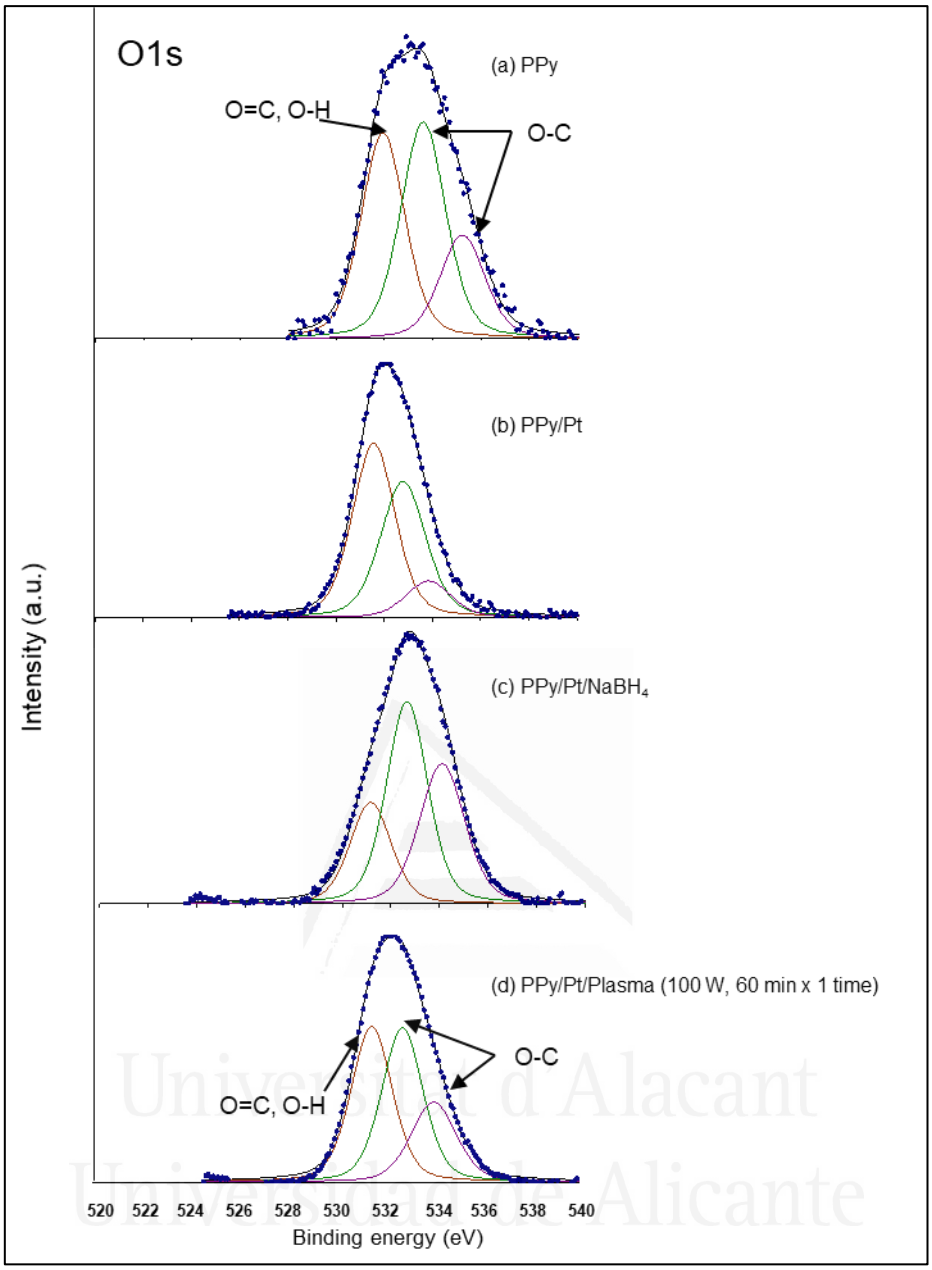

Figure 3.6. XPS O 1s spectra of (a) polypyrrole, (b) polypyrrole impregnated with H_2PtCl_6, (c) polypyrrole impregnated with H_2PtCl_6 and treated with $NaBH_4$, and (d) polypyrrole impregnated with H_2PtCl_6 and treated with Ar plasma 60 min x 1 time at 100 W.

Therefore, these data suggest that impregnation of PPy with H_2PtCl_6 leads to the anchoring of the platinum chlorocomplex on the polypyrrole, maybe by interaction with the N^+ moieties in the polymer structure. However, platinum is still in an ionic state, Pt(II), and, although some catalytic reactions could use this system as it is [23], for the main part of applications the presence of metallic platinum is required. Thus, a reductive treatment has to be applied.

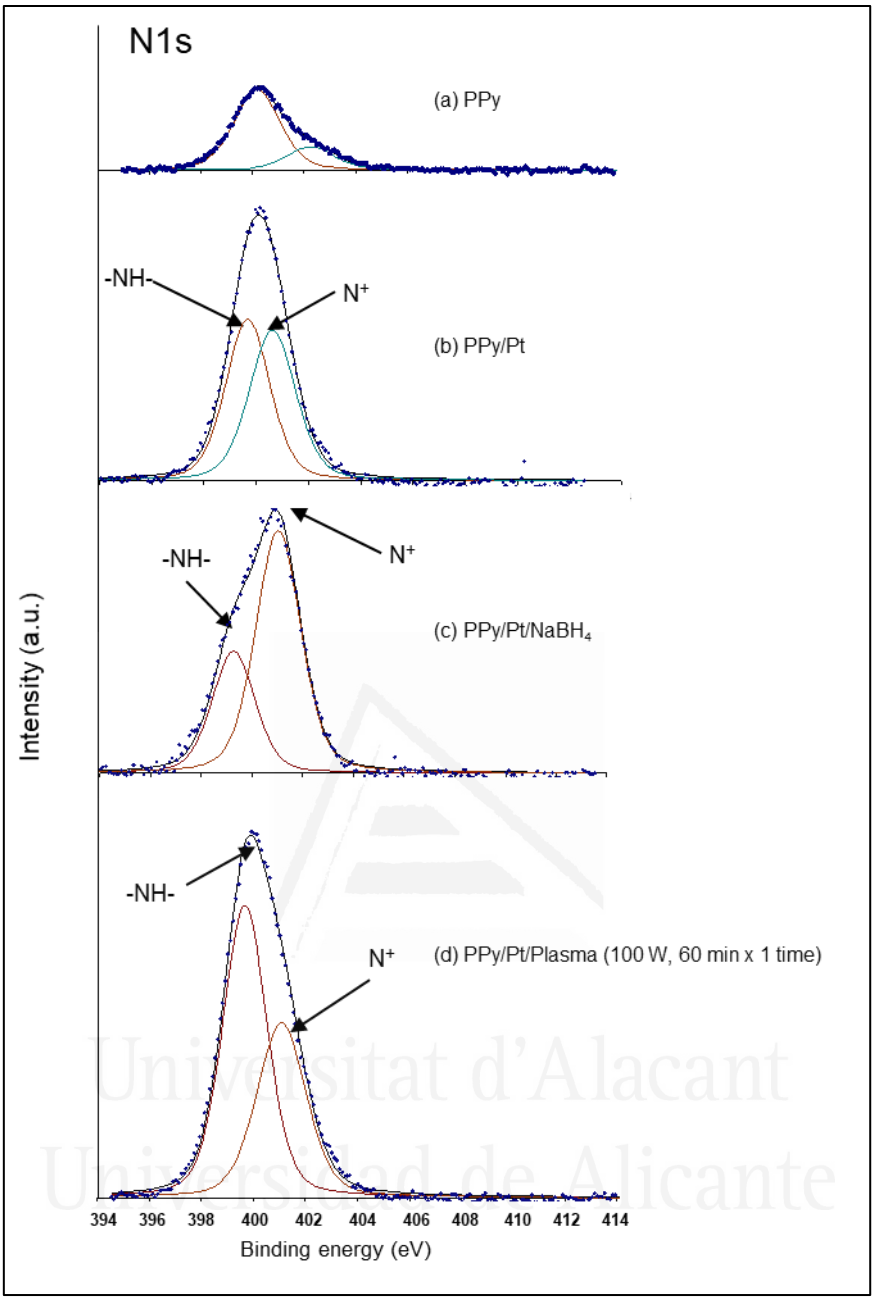

Figure 3.7. XPS N 1s spectra of (a) polypyrrole, (b) polypyrrole impregnated with H_2PtCl_6, (c) polypyrrole impregnated with H_2PtCl_6 and treated with $NaBH_4$, and (d) polypyrrole impregnated with H_2PtCl_6 and treated with Ar plasma 60 min x 1 time at 100 W.

Due to the relatively low thermal stability of the polymer support, as well as the necessity to swell the polymeric support in order to guarantee the accessibility of the metal, reduction is usually carried out in the liquid phase, in a solvent that is compatible with the polymer. The peculiar structure of polymeric supports compared to traditional inorganic supports determines that the growth of the metal nanoparticles during reduction becomes limited by the steric restrictions imposed by the three-dimensional polymer

network, which would allow controlling the nanoparticle size. The size and distribution of the metal nanoparticles throughout the particles of the support can depend on the nature and concentration of the reducing agent, the reduction procedure and the metal concentration. The most frequently used reducing agents are sodium borohydride, hydrazine, alcohols and formaldehyde [1]. In this work, reduction using sodium borohydride ($NaBH_4$) as a mild chemical reducing agent has been compared with Ar cold plasma reduction.

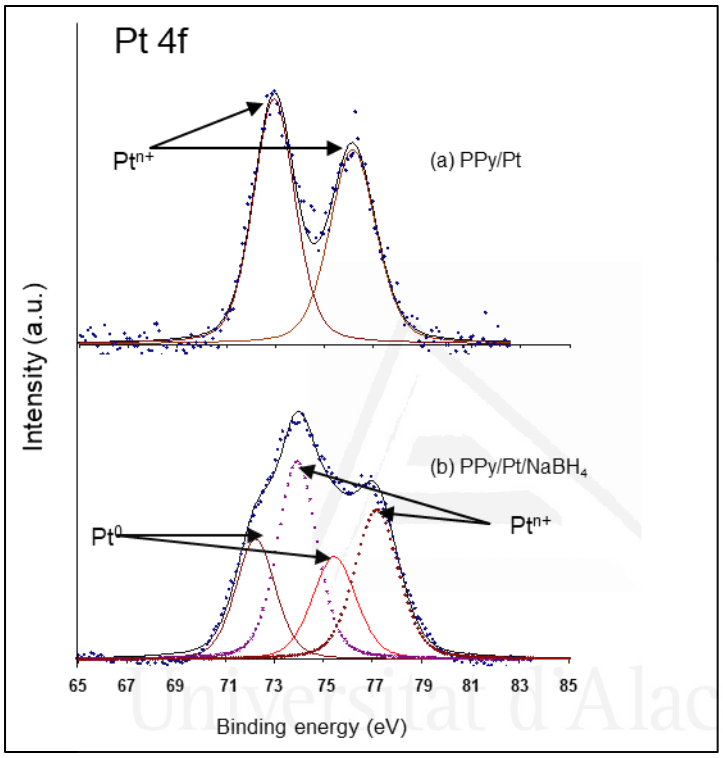

Figure 3.8. XPS Pt 4f spectra of (a) polypyrrole impregnated with H_2PtCl_6 and (b) polypyrrole impregnated with H_2PtCl_6 and treated with $NaBH_4$.

Considering the redox potentials of platinum species (see above) and of borohydride (BH_4^-/H_3BO_3, E° = -0.481 V at pH = 0 and E° = -1.240 V at pH = 14) [24] the reduction of the anionic platinum chlorocomplex with sodium borohydride is possible. The XPS spectra of the Pt 4f level (Fig. 3.8b) shows that the treatment with $NaBH_4$ leads to the partial reduction of the platinum species in the PPy/Pt catalyst precursor. From the comparison of the areas of the Pt $4f_{7/2}$ bands corresponding to metallic platinum (71.2 eV) and oxidized platinum species (72.9 eV) it can be concluded that the liquid phase reduction treatment yields a 38 % of metallic platinum (Table 3.2).

The involved redox processes might be as follows:

$$2\ PtCl_6^{2-} + BH_4^- + 3\ H_2O \rightarrow 2\ Pt + H_3BO_3 + 7\ H^+ + 12\ Cl^-$$

$$4\ PtCl_4^{2-} + BH_4^- + 3\ H_2O \rightarrow 4\ Pt + H_3BO_3 + 7\ H^+ + 16\ Cl^-$$

This might require ligand dissociation of the anionic platinum chlorocomplex anchored onto the polypyrrole chain, followed by reduction of the metal ion. On the other hand, Khain [25] reported that reactions of borohydride ions with metal ions can be classified as reactions taking place *via* bridge active complexes; that is, by an inner sphere mechanism. The first stage is the replacement of ligands by BH_4^-, with a subsequent stage involving a spontaneous redox reaction of electron transfer of the intermediate complex [24].

The XPS spectrum of the Pt 4f level (Fig. 3.8b) shows the presence of both Pt ions and metallic Pt on the borohydride-treated catalyst precursor; however, atomic percentages of C, O, N and Pt obtained from its survey spectra are similar to those of the as impregnated polypyrrole (PPy/Pt, Table 3.1). Therefore, borohydride reduction mainly affects the chemical state of platinum, without affecting the support. Furthermore, the XPS C 1s spectrum (Fig. 3.5c) after the reduction treatment shows an increase of C-O moieties (69.1 %) as compared to the as-impregnated polypyrrole (21.6 %). The XPS spectrum of the O 1s level (Fig. 3.6c) also shows an increase of oxygen moieties (O-C) after reduction with borohydride. This is consistent with polypyrrole degradation by aqueous borohydride solution. On the other hand, the XPS spectrum of the N 1s level (Fig. 3.7c) reveals an increase of N^+ moieties with the reduction treatment (67.7 %), which represents a N^+/-NH- ratio of 2.1 (Table 3.2). This evidences that the polymer support is in its conductive form (Scheme 3.1). This oxidation of the polypyrrole chain is produced together with a partial reduction of Pt ions to metallic Pt (Fig. 3.8b).

Safety is very important from a green standpoint. Sodium borohydride has been recognized to be safe and stable at room temperature if stored in a closed vessel and anhydrous medium, but decomposes at 565 °C [26]. Green chemistry is also engaged in sustainability. It intensely supports the utilization of renewable feedstocks, and boron sources are not renewable, although sodium borohydride is recyclable. From this point of view, sodium borohydride should be regarded to be only relatively green. In this study,

plasma reduction with Ar has been proposed as a greener alternative to reduction processes involving the use of chemicals.

Plasmas have an abundance of high energy electrons which may serve as reducing agents. Therefore, plasma reduction is based on a direct transfer of electrons from the plasma to the metal ions. In this work, ability of reduction of the catalyst precursor (PPy/Pt) with Ar plasma has been considered. Plasma RF power, as well the influence of experimental conditions, have been studied. The reduction time was set to 60 min, but also single 60 min reduction treatment with Ar plasma (100 W) was compared to a repetitive 10 min reduction treatment carried out for 6 times and always PPy/Pt samples were manual mixing between treatments to assure an even exposure to the plasma.

Table 3.2 shows that it is preferable to carry out a repetitive plasma treatment of PPy/Pt (10 min x 6 times), because a more efficient reduction of platinum ions is achieved as compared to a single 60 min treatment. Thus, the Pt^{o}/Pt^{n+} ratio is 0.69 for a single plasma treatment *versus* 1.08 when a discontinuous treatment is performed, using the same RF power (100 W). Furthermore, there is also a decrease of N^{+} moieties (Fig. 3.7d, Table 3.2), which is in agreement with the abundance of high energy electrons in the plasma that act as reducing agents. These electrons are implicated in the reduction of both Pt ions and N^{+} species. It has to be noted that chemical treatment with borohydride, although effective in partially reducing Pt ions, produced an increase of N^{+} (Fig. 3.7c, Table 3.2). Thus, it can be concluded that electrons in the plasma are responsible for the reduction of N^{+} species and a more efficient reduction of platinum ions to the metallic state than reduction with borohydride.

On the other hand, the single plasma reduction treatment (60 min x 1 time) introduces carboxylate moieties (RO-C=O), as revealed in the XPS spectra of the C 1s level (Fig. 3.5d, Table 3.2), which are not present when repetitive treatments are performed. Previous studies [27] have shown that Ar plasma activated polymeric surfaces in such a way that ulterior exposure to air leads to the creation of oxygen moieties (Fig. 3.6d). Besides, it must be taken into account that plasma can also lead to an indirect process involving the water molecules within the polymer network to generate active species and radicals that may favor polymer degradation, as schemed in Scheme 3.2. This is favored either by performing a continuous treatment during 60 min, or by increasing

discontinuous plasma treatments power. Thus, Table 3.2 shows that the increase of the plasma power from 100 W to 150 and 200 W results in an increase of carboxylate groups (13.4 % at 150 W, 15.1 % at 200 W) and also a considerable increase of the Pt^{o}/Pt^{n+} ratio from 1.08 % (100 W) to 2.68 % (150 W) and to 3.50 % (200 W).

Another effect usually produced by plasma treatment of polymers is the surface ablation, that is, the removal of the outermost polymer surface layers [28]. Table 3.1 shows that there is an increase of the surface Pt percentage obtained from XPS analysis from 0.1 at. % in the impregnated PPy/Pt to 1.1 at. % in the plasma treated PPy/Pt for 1 h at 100 W. This effect is more obvious when the plasma power is increased in the repetitive plasma treatments. Thus, surface Pt percentage increases from 0.2 at. % at 100 W to 1.3 at. % at 150 W and 1.8 at. % at 200 W. Ar plasma is able to ablate the polypyrrole surface [28] and to remove an oxidized layer of the degraded polypyrrole material [16], leaving platinum from the inner polymer network exposed to XPS analysis (detection depth of XPS is approximately 5 nm). A decrease in the O percentage and an increase in the N, Pt and Cl percentages when the plasma power is increased from 100 to 200 W can also be observed (Table 3.1). Besides, effectiveness of platinum ion reduction is enhanced with the increase of the plasma treatment power (Fig. 3.9). Consequently, it is expected that catalytic performance would be improved due to the increase of Pt^{0} atoms exposed at the surface.

X-ray diffraction was used to analyze the structural characteristics of the catalyst. The XRD pattern of PPy/Pt (Fig. 3.1) shows a broad band of mainly amorphous polypyrrole, but also a strong peak at 32.62 º and some other less intense peaks at 2θ = 27.37 º, 26.52 º, 22.96 º and 21.42 º, which are assigned to the 2θ values of the platinum precursor after impregnation. Diffraction data base [29] showed that those values are found in compounds where platinum is anchored onto organic amines and halogens, as in $PtCl_2(C_5H_4N)_2$, which shows peaks at 2θ = 33.00 º, 26.42 º and 22.83 º, or as in $[Pt^{II}(C_2H_5NH_2)_4][Pt^{IV}I_2(C_2H_5NH_2)_4]I_4$, which shows peaks at 2θ = 32.91 º, 27.28 º, 23.15 º and 21.44 º. This evidence is in agreement with XPS results, which showed binding energies of 72.9 eV (Pt $4f_{7/2}$) after impregnation of polypyrrole with H_2PtCl_6, which correspond to Pt(II) species. These results support the existence of an interaction between Pt and N^{+} species in the support structure, and that the incorporation of platinum anions

affects the ordering of the polymer backbone.

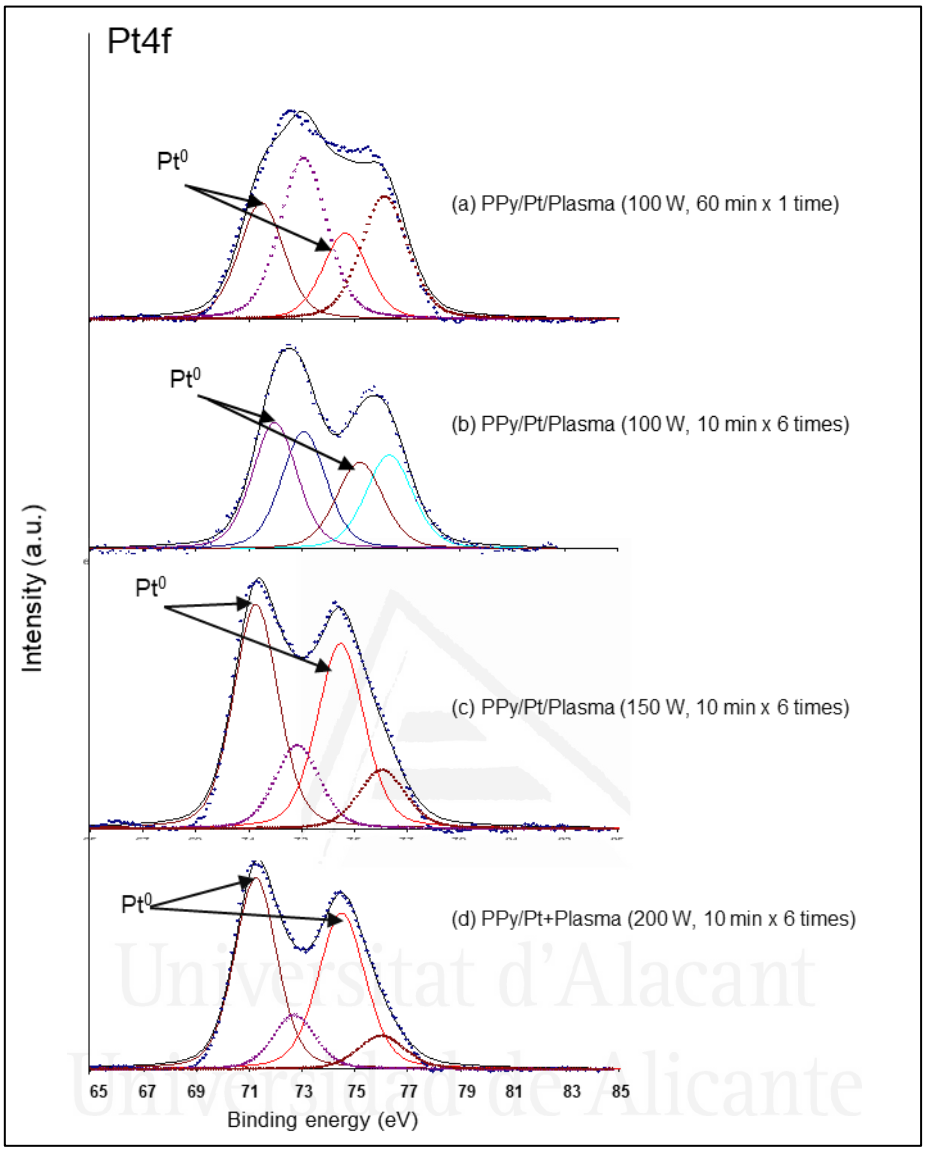

Figure 3.9. XPS Pt 4f spectra of polypyrrole impregnated with H_2PtCl_6 and treated with Ar plasma under different conditions.

The XRD profiles of the PPy/Pt systems after reduction with Ar plasma and with sodium borohydride are reported in Figure 3.1c-f. In contrast with the non-reduced sample (Fig. 3.1b), no diffraction peaks corresponding to Pt species, typically located at 2θ = 39.8 º and 46.2 º [30,31], can be observed, although Pt(0) was effectively detected by XPS (Fig. 3.9).

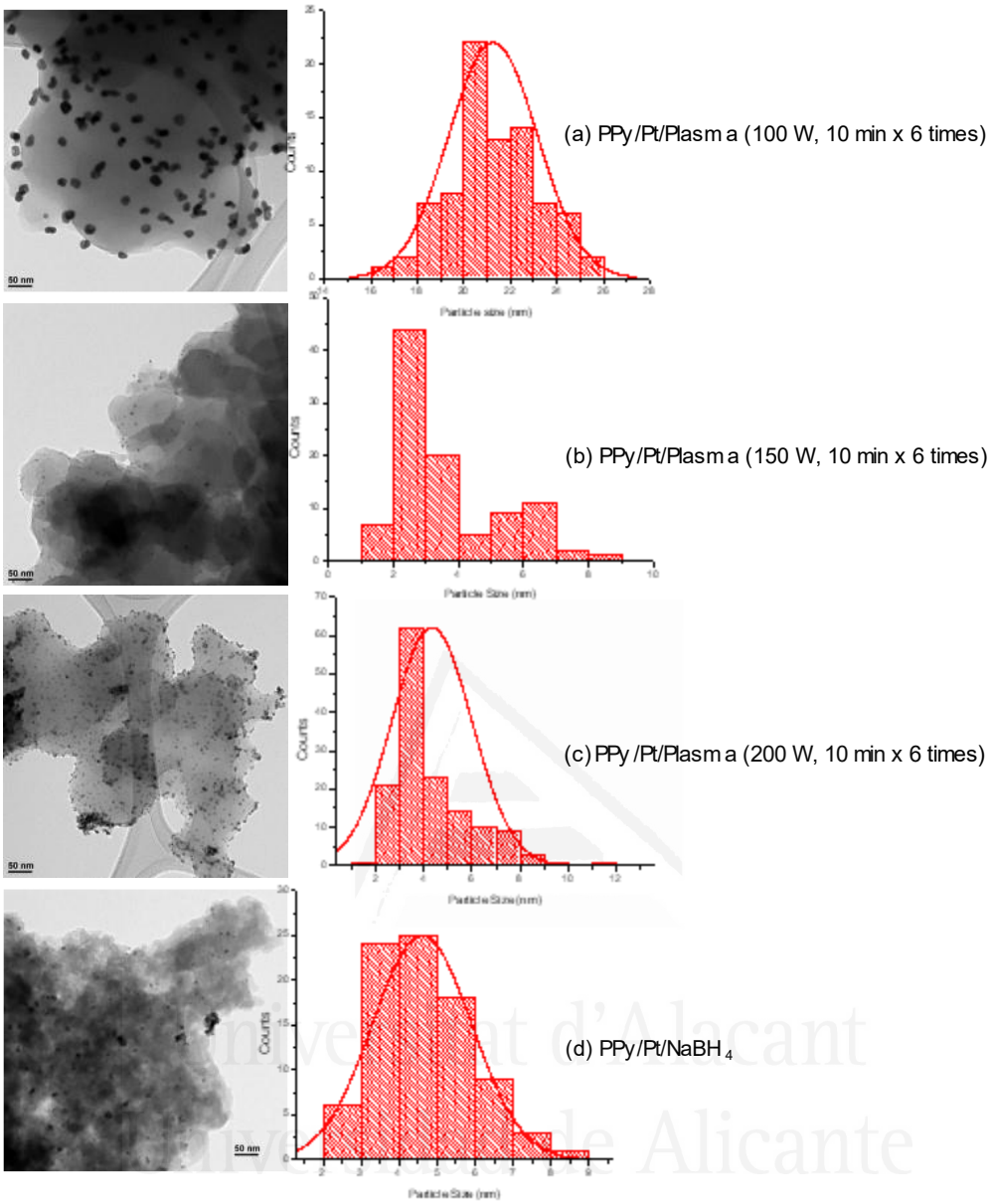

Figure 3.10. TEM images and particle size distributions of PPy/Pt after different reduction treatments.

TEM images of PPy/Pt after the different reduction treatments (Fig. 3.10) show that aggregation of Pt nanoparticles is produced mainly when Ar plasma treatment is carried out at 100 W. However, the mean particle size determined from the particle size distributions in samples reduced in Ar plasma at 150 and 200 W was between 2.5 and 4.5 nm, respectively, and it was 4.5 nm for the sample reduced with borohydride. The EDX analysis confirmed that these nanoparticles corresponded to Pt [10,16,32,33].

X. Zhu *et al.* [4] reported that Pt nanoparticles obtained after reduction in plasma treatment could retain some static electric charge and repel each other, resulting in a uniform distribution of Pt on γ-Al_2O_3. The more uniform distribution in samples treated in Ar plasma at 150 and 200 W might be related to the more effective plasma treatment.

3.3. Catalytic behavior

Preliminary results on the catalytic behavior of platinum nanoparticles supported on polypyrrole, obtained after treatment in Ar plasma at 200 W, in the reduction of aqueous nitrate to N_2 with H_2 have been obtained. It is known that at pH > 8 ammonium is formed preferentially *versus* molecular nitrogen. Thus, a CO_2 flow was used as a buffer to keep a constant value of pH ≈ 5 during the reaction tests [34]. Figure 3.11 shows that nitrate reduction is rapidly achieved and, after 120 min, the nitrate concentration is below the maximum acceptable level of 50 $mg \cdot L^{-1}$ regulated by the European legislation. Furthermore, considerable low concentrations of nitrite (the maximum acceptable level by European legislation is 0.5 $mg \cdot L^{-1}$) and ammonium are obtained. Consequently, further studies have been carried out to elucidate the role of the polymer support in this reaction and these results are shown in the following chapters of this work.

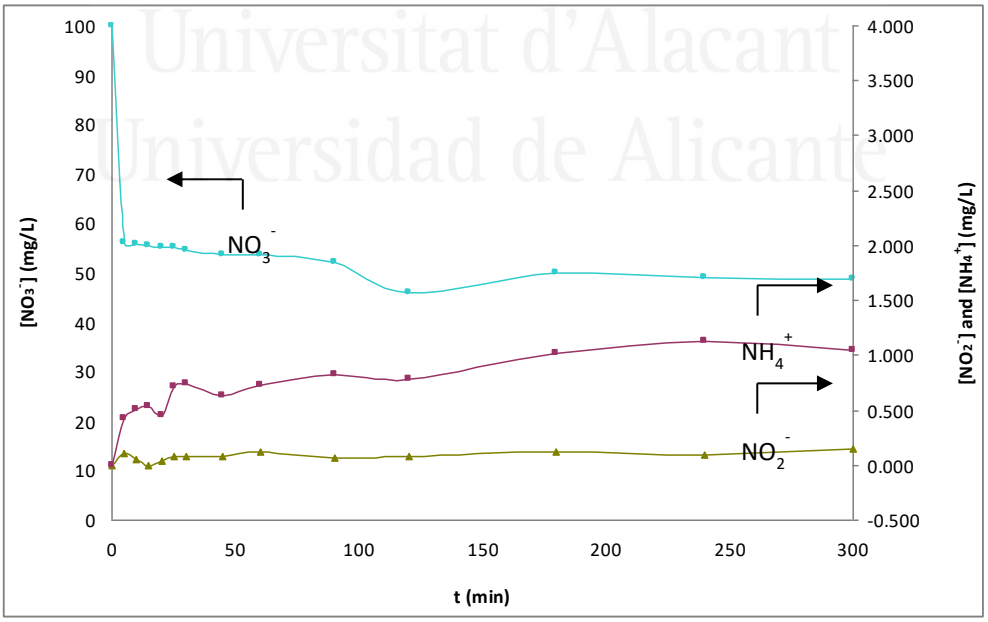

Figure 3.11. Nitrate, nitrite and ammonium concentrations ($mg \cdot L^{-1}$) as a function of time (min) during aqueous nitrate reduction with H_2 in the presence of platinum supported on polypyrrole (PPy/Pt/Plasma/200 W).

4. CONCLUSIONS

Ar plasma reduction at room temperature provides a simple, low time-consuming, green and effective process for the synthesis of polypyrrole-supported Pt catalysts, compared to the wet chemical reduction with borohydride. It has been shown that platinum in the metal precursor (H_2PtCl_6) is partially reduced to Pt(II) species upon the impregnation of polypyrrole, with -NH- groups being subsequently oxidized to N^+. This provides anchoring sites for the metal precursor which results in a high dispersion of the active metal. Ar plasma leads to a more effective reduction of platinum ions in the chloroplatinum complex to metallic platinum compared to reduction with borohydride, due to direct transfer of the abundant electrons in the plasma to platinum ions. Furthermore, reduction of N^+ groups to -NH- in the polymer support is also performed. Another effect of the plasma reduction is the activation of the polypyrrole surface, in such a way that the ulterior exposure to air leads to the creation of carboxylated moieties.

The increase of the Ar plasma power from 100 to 150 and 200 W results in an increase of carboxylate groups as well as in a more effective reduction of platinum ions into its zero-valent metallic state. The platinum nanoparticles supported on polypyrrole, obtained after treatment with argon plasma at 200 W, effectively catalyzed the reaction of reduction of nitrates in water with H_2 up to N_2, producing very low amounts of nitrite and ammonium ions.

5. REFERENCES

[1] M. Králik, A. Biffis. *J. Mol. Catal. A: Chem*. **2001**, *177(1)*, 113-138.

[2] J.J. Zou, Y.P. Zhang, C.J. Liu. *Langmuir*. **2006**, *22(26)*, 11388-11394.

[3] T.K. Vishnuvardhan, V.R. Kulkarni, C. Basavaraja, S.C. Raghavendra. *Bull. Mater. Sci*. **2006**, *29(1)*, 77-83.

[4] X. Zhu, P.P. Huo, Y.P. Zhang, C.J. Liu. *Ind. Eng. Chem. Res*. **2006**, *45(25)*, 8604–8609.

[5] T.A. Skotheim, J.R. Reynolds. *Recent advances in polypyrrole* in *Handbook of conducting polymers. Conjugated polymers: theory, synthesis, properties, and characterization*. 3rd ed. CRC Press: Boca Raton, FL, USA. **2007**, Chap. 8.

[6] B.K. Moss, R.P. Burford. *Polym. Int*. **1991**, *26(4)*, 225-231.

[7] R. Ansari. *E-J. Chem*. **2006**, *3(4)*, 186-201.

[8] I. Dodouche, F. Epron. *Appl. Catal., B: Env*. **2007**, *76(3-4)*, 291-299.

[9] P. Mavinakuli, S. Wei. Q. Wang, A.B. Karki, S. Dhage, Z. Wang, D.P. Young, Z. Guo. *J. Phys. Chem. C*. **2010**, *114*, 3874-3882.

[10] I. Dodouche, D.P. Barbosa, M.C. Rangel, F. Epron. *Appl. Catal., B: Env*. **2009**, *93(1-2)*, 50-55.

[11] J. Sá, J.A. Anderson. *Appl. Catal., B : Env*. **2008**, *77(3-4)*, 409-417.

[12] X. Liang, C.J. Liu, P. Kuai. *Green Chem.* **2008**, *10*, 1318-1322.

[13] J.C. Serrano-Ruiz, A. López-Escudero, J. Solla-Gullón, A. Sepúlveda-Escribano, A. Aldaz, F. Rodríguez-Reinoso. *J. Catal*. **2008**, *253(1)*, 159-166.

[14] J. Ouyang, Y. Li. *Polymer*. **1997**, *38(15)*, 3997-3999.

[15] J. Wang, K.G. Neoh, E.T. Kang. *Thin Solid Films*. **2004**, *446(2)*, 205-217.

[16] S.V. Vasilyeva, M.A. Vorotyntsev, I. Bezverkhyy, E. Lesniewska, O. Heintz, R. Chassagnon. *J. Phys. Chem. C*. **2008**, *112(50)*, 19878-19885.

[17] B. Tian, G. Zerbi. *J. Chem. Phys*. **1990**, *92*, 3886.

[18] T. Fernández-Otero. *Rev. Iberoamericana de Polímeros*. **2003**, *4(4)*, 1-37.

[19] D. Briggs. *Surface analysis of polymers by XPS and static SIMS*. Cambridge University Press. **1998**, p. 186.

[20] Z. Wang, R.T. Yang. *J. Phys. Chem. C*. **2010**, *114(13)*, 5956-5963.

[21] F. Coloma, A. Sepúlveda-Escribano. J.L.G. Fierro, F. Rodríguez-Reinoso. *Langmuir*. **1994**, *10(3)*, 750-755.

[22] S.R. de Miguel, O.A. Scelza, M.C. Román-Martínez, C. Salinas-Martínez de Lecea, D. Cazorla-Amorós, A. Linares-Solano. *Appl. Catal., A: Gen*. **1998**, *170(1)*, 93-103.

[23] F. Alonso, R. Buitrago, Y. Moglie, A. Sepúlveda-Escribano, M. Yus. *Organometallics*. **2012**, *31*, 2336-2342.

[24] J. Lu, D.B. Dreisinger, W.C. Cooper. *Hydrometallurgy*. **1997**, *45(3)*, 305-322.

[25] V.S. Khan. *Russ. J. Inorg. Chem.* **1983**, *28*, 1410-1413.

[26] U.B. Demirci, P. Miele. *Energy Environ. Sci*. **2009**, *2(6)*, 627-637.

[27] A.B. Ortíz-Magán, M.M. Pastor-Blas, J.M. Martín-Martínez. *J. Adhes*. **2004**, *80(7)*, 613-634.

[28] A.B. Ortíz-Magán, M.M. Pastor-Blas. *Plasma Chem. Plasma Process*. **2008**, *28(3)*, 391-404.

[29] Diffrac Plus Evaluation Software, Bruker.

[30] A. Drelinkiewicz, A. Zieba, J.W. Sobczak, M. Bonarowska, Z. Karpiński, A. Waksmundzka-Góra, J. Stejskal. *React. Funct. Polym.* **2009**, *69(8)*, 630-642.

[31] A. Nyczyk, A. Sniechota, A. Adamczyk, A. Bernasik, W. Turek, M. Hasik. *Eur. Polym. J.* **2008**, *44(6)*, 1594-1602.

[32] H.J. Salavagione, C. Sanchís, E. Morallón. *J. Phys. Chem. C.* **2007**, *111(33)*, 12454-12460.

[33] M. Harada, H. Einaga. *J. Colloid Interface Sci.* **2007**, *308(2)*, 568-572.

[34] O.S.G.P. Soares, E.O. Jardim, A. Reyes-Carmona, J. Ruiz-Martínez, J. Silvestre-Albero, E. Rodríguez-Castellón, J.J.M. Órfão, A. Sepúlveda-Escribano, M.F.R. Pereira. *J. Colloid Interface Sci.* **2012**, *369(1)*, 294-301.

Chapter IV. Optimization of the platinum loading and the argon plasma treatment

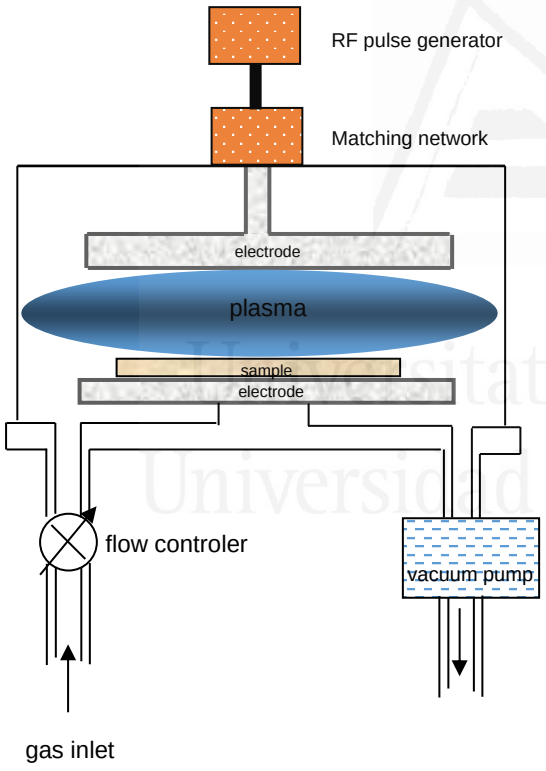

1. INTRODUCTION

The size and distribution of the metal nanoparticles on the support depend on the nature and concentration of the reducing agent, the reduction procedure and the metal loading. In the previous chapter, a metal loading of 1 wt. % Pt was selected and reduction using sodium borohydride ($NaBH_4$) as a mild chemical reducing agent has been compared with Ar cold plasma reduction. It was concluded that electrons in the plasma are responsible for the more effective reduction of platinum ions to the metallic state than reduction with borohydride. Different RF powers (100 W, 150 W and 200 W) and also a repetitive plasma treatment were studied [1]. The experimental results showed that the increase of the Ar plasma power results in a more effective reduction of platinum ions into is zero-valent metallic state and that the manual mixing between repetitive treatments assure an even exposure to the plasma.

In this chapter, the RF power has been set to 200 W, and the influence of the platinum loading and the length of the plasma treatment will be analysed.

2. EXPERIMENTAL

2.1. Materials preparation

Polypyrrole was prepared by chemical oxidative polymerization of pyrrole (C_4H_5N) with ferric chloride ($FeCl_3 \cdot 6H_2O$). The experimental procedure was described in Chapter II, Section 1.1.1 [2].

The influence of the platinum loading was considered. Thus, the samples were wet impregnated with the proper amount of $H_2PtCl_6 \cdot 6H_2O$ to obtain increasing platinum loadings (0.16 wt. %, 0.62 wt. %, 1 wt. %, 2 wt. % and 5 wt. % platinum) (Chapter II, Section 1.2.1).

Several lengths of Ar plasma treatment (0.5 h, 1 h, 1.5 h, 2 h, 2.5 h and 3 h) were carried out on samples loaded with 1 wt. % platinum to produce the reduction of the supported platinum ions (chapter II, section 1.3). Each sample was treated in Ar plasma (200 W) in cycles of 5 min each. The number of cycles was varied to achieve the desired total treatment time. A manual mixing of the powder samples was carried out between

cycles and the temperature of the sample surfaces was controlled by a non-contact infrared thermometer (PCE Instruments, model PCE-888), which showed that the surface temperature was below 50 ºC in all cases.

2.2. Materials characterization

The samples were characterized by infrared spectroscopy (FTIR), X-ray diffraction (XRD), transmission electron microscopy (TEM) and X-ray photoelectron spectroscopy (XPS), as described in Chapter II, Section 2.

3. RESULTS AND DISCUSSION

3.1. Influence of the metal loading

Different nominal metal loadings were studied: 0.16 wt. %, 0.62 wt. %, 1 wt. %, 2 wt. % and 5 wt. %.

No differences are observed in the FTIR (Fig. 4.1) spectra of the samples impregnated with different amounts of the platinum precursor. All of them show the typical bands of the polymer (discussed in Chapter III, Section 3.1).

However, XPS analysis shows (Table 4.1) a considerable increase of the percentage of Pt detected on the samples as the percentage of the platinum precursor increases up to 2 wt. % and then remains constant.

Table 4.1. XPS surface chemical composition (atomic %) of the different samples.

Binding energy *(eV)*	284.5	531.5	398.1	198.5	71.2	710.9	531.5/284.5
Element	**C 1s**	**O 1s**	**N 1s**	**Cl 2p**	**Pt 4f**	**Fe 2p**	O/C
PPy	87.2	7.2	4.6	1.0	-	0.0	0.08
PPy/0.16%Pt	74.1	12.1	10.4	3.0	0.4	0.0	0.16
PPy/0.62%Pt	71.8	13.1	11.1	3.5	0.5	0.0	0.18
PPy/1%Pt	74.5	10.7	11.0	3.1	0.7	0.0	0.14
PPy/2%Pt	66.5	12.0	10.4	7.9	3.2	0.0	0.18
PPy/5%Pt	65.7	12.0	11.0	8.1	3.2	0.0	0.18

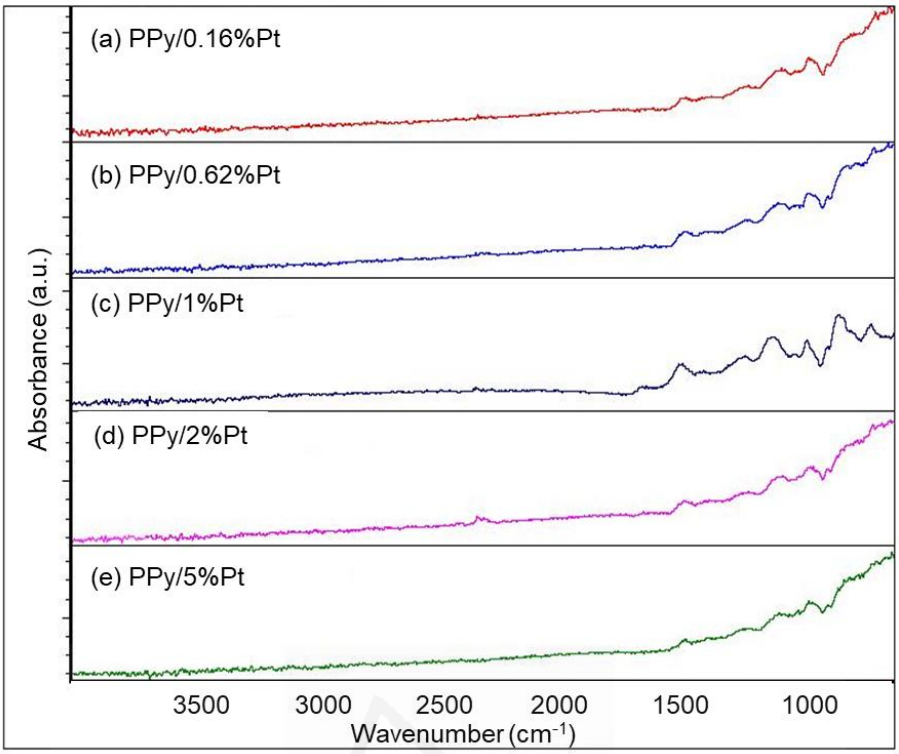

Figure 4.1. FTIR-ATR spectra of polypyrrole synthesized with $FeCl_3$ and impregnated with different amounts of H_2PtCl_6.

3.2. Influence of the length of Ar plasma treatment

Figure 4.2 shows the FTIR spectrum of polypyrrole impregnated with the platinum salt (H_2PtCl_6) at a nominal platinum loading of 1 wt. % (PPy/1%Pt) and also the spectra corresponding to the samples impregnated with the platinum precursor and treated in Ar plasma for different times in order to obtain metal platinum nanoparticles dispersed on the PPy. All the spectra are similar and all of them show the typical bands of PPy (Fig. 3.4, Chapter III, Section 3.1) [2-5]: C=N in-plane bending (1563 cm^{-1}), =C-H out of plane bending (1047 cm^{-1}) [3,4], C-N^+ stretching (1206 cm^{-1}) and C=N^+-C stretching (931 cm^{-1}).

The X-ray diffraction patterns of all the samples (Fig. 4.3) show a broad peak centered at $2\theta \approx 26.0$ º, which is characteristic of amorphous polypyrrole and is due to the scattering from PPy chains at the interplanar spacing [6]. Peaks due to diffraction from (111), (200), (220) and (311) planes of the face-centered cubic (*fcc*) Pt at $2\theta \approx 40.0$ º, 47.0 º, 68.0 º and 81.5 º are present only in the XRD profiles of the samples treated in Ar plasma for at least 2 h (Fig. 4.3c-h). The samples treated for shorted times do not show

those diffraction peaks due to the high dispersion of the platinum nanoparticles [7-9], although they were detected by XPS.

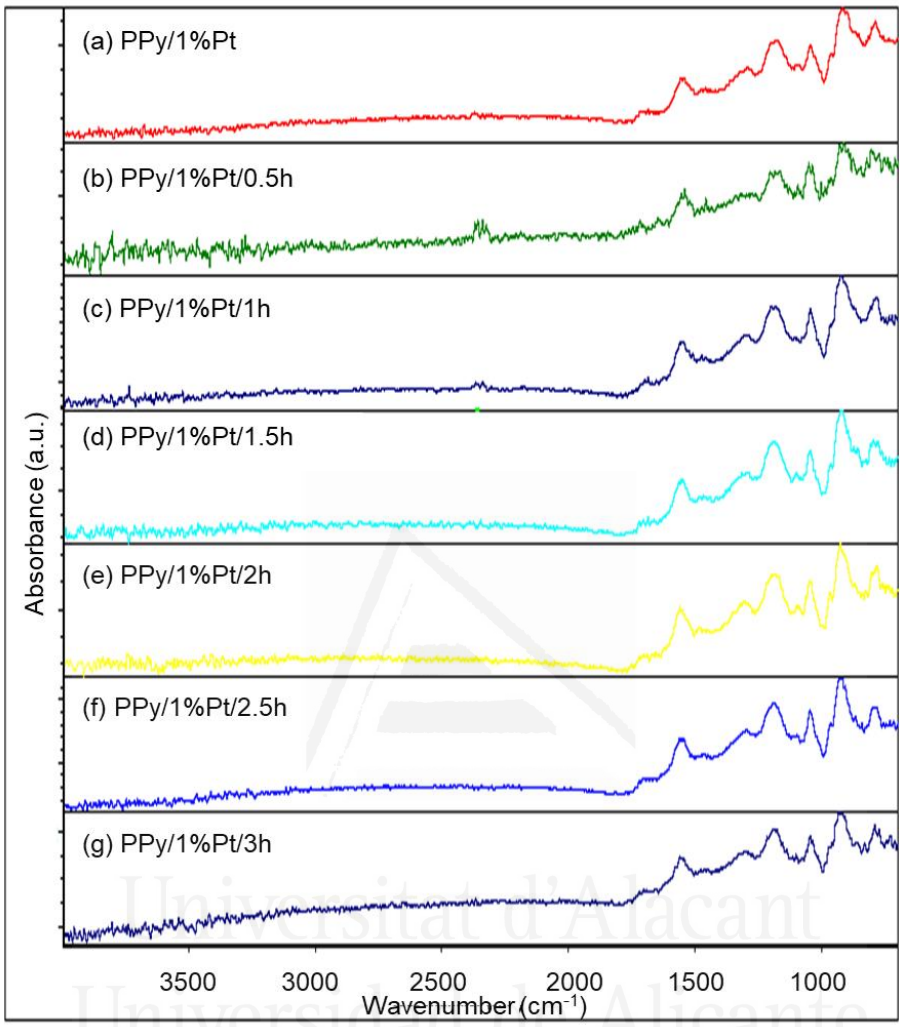

Figure 4.2. FTIR-ATR spectra of (a) polypyrrole synthesized with $FeCl_3$ and impregnated with H_2PtCl_6 (PPy/1%Pt) and (b-g) PPy/1%Pt treated in Ar plasma for several lengths of time.

As discussed in the previous chapter, XPS analysis of chemically synthesized polypyrrole (PPy) (Table 4.2) shows the presence of C and N from the polymer, Cl from the doping with $FeCl_3$ and also a certain degree of surface oxidation (O/C = 0.08).

Impregnation of polypyrrole with the platinum salt results in the anchoring of a platinum chlorocomplex to the N^+ moieties of the semioxidized polymeric chain. Consequently, ionic platinum (Pt^{n+}) at 72.9 eV is detected in PPy/1%Pt (Fig. 4.4, Table 4.3). Plasma treatment produces the reduction of platinum ion in the platinum chlorocomplex to metal platinum, being this reduction more effective as the time of

plasma treatment increases: Pt^{o}/Pt^{n+} ratio increases from 2.15 to 5.90. The increase of metal platinum is therefore acompanied by the decrease in Cl percentage (Table 4.2). The abundance of energetic electrons in plasma also contribute to the reduction of the nitrogen moieties in the polymeric chain, consequently, the ratio N^{+}/-NH- is decreased from 18.23 to 1.24 with the increase of the plasma treatment time.

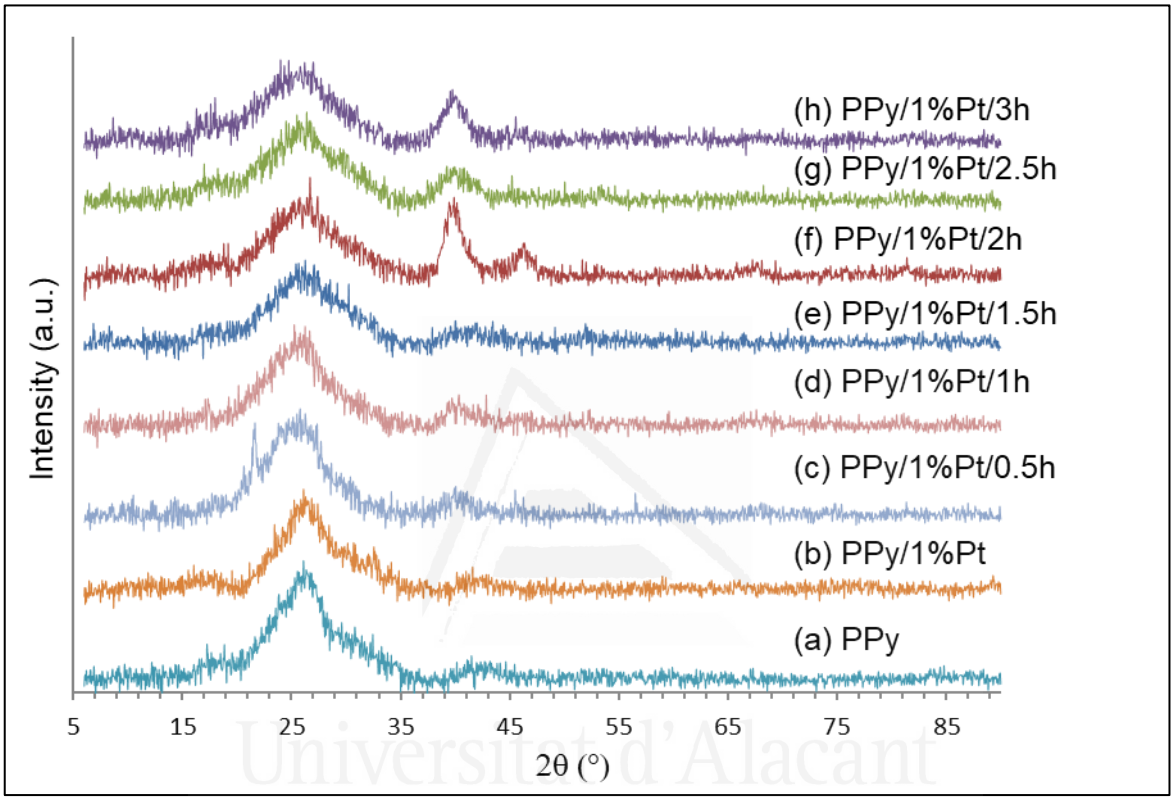

Figure 4.3. XRD patterns of polypyrrole (a) synthesized with $FeCl_3$ (PPy), (b) synthesized with $FeCl_3$ and impregnated with H_2PtCl_6 (PPy/1%Pt) and (c-h) PPy/1%Pt treated in Ar plasma for several lengths of time.

Table 4.2. XPS surface chemical composition (atomic %) of the different samples.

Binding energy *(eV)*	284.5	531.5	398.1	198.5	71.2	710.9	531.5/284.5
Element	**C 1s**	**O 1s**	**N 1s**	**Cl 2p**	**Pt 4f**	**Fe 2p**	O/C
PPy	87.2	7.2	4.6	1.0	-	0.0	0.08
PPy/1%Pt	74.5	10.7	11.0	3.1	0.7	0.0	0.14
PPy/1%Pt/0.5h	67.7	16.2	12.5	2.4	1.2	0.0	0.24
PPy/1%Pt/1h	68.7	15.4	12.8	1.8	1.3	0.0	0.22
PPy/1%Pt/1.5h	69.9	18.2	9.4	1.3	1.2	0.0	0.26
PPy/1%Pt/2h	68.0	17.0	11.9	1.5	1.6	0.0	0.25
PPy/1%Pt/2.5h	69.7	16.7	10.9	1.1	1.6	0.0	0.24
PPy/1%Pt/3h	70.3	16.7	10.3	1.1	1.6	0.0	0.24

Table 4.3. Percentages (%) of the different surface species estimated from the areas of the contributions to the XPS spectra corresponding to the C 1s, O 1s, N 1s and Pt $4f_{7/2}$ levels.

Binding energy (eV)	Species	PPy	PPy/ 1%Pt	PPy/1%Pt/Plasma200W – time (h)					
				0.5	1	1.5	2	2.5	3
C 1s									
284.5	C-C, C-H, C-N	52.8	68.7	64.9	66.6	67.8	66.2	70.0	72.1
286.2	C-O	30.6	21.6	16.4	14.5	14.5	15.1	14.3	12.8
288.1	C=O	16.6	9.7	18.7	18.9	17.7	18.7	15.7	15.1
O 1s									
531.5	O=C, O-H	38.3	48.8	4.5	55.4	64.3	73.5	8.6	25.2
533.0	O-C	41.6	40.4	70.3	32.2	35.7	26.5	69.4	54.2
534.0	O-C	20.1	10.8	25.2	12.4	-	-	22.0	20.6
N 1s									
399.8	-NH-	76.7	50.5	5.2	10.8	12.3	8.8	12.1	44.7
401.2	N^+	23.3	49.5	94.8	89.2	87.7	91.2	87.9	55.3
	N^+/-NH-	0.30	0.98	18.23	8.26	7.13	10.36	7.26	1.24
Pt $4f_{7/2}$									
71.2	Pt^o	-	0	68.3	69.7	75.8	82.1	81.9	85.5
72.9	Pt^{n+}	-	100	31.7	30.3	24.2	17.9	18.1	14.5
	Pt^o/Pt^{n+}	-	0	2.15	2.30	3.13	4.59	4.52	5.90

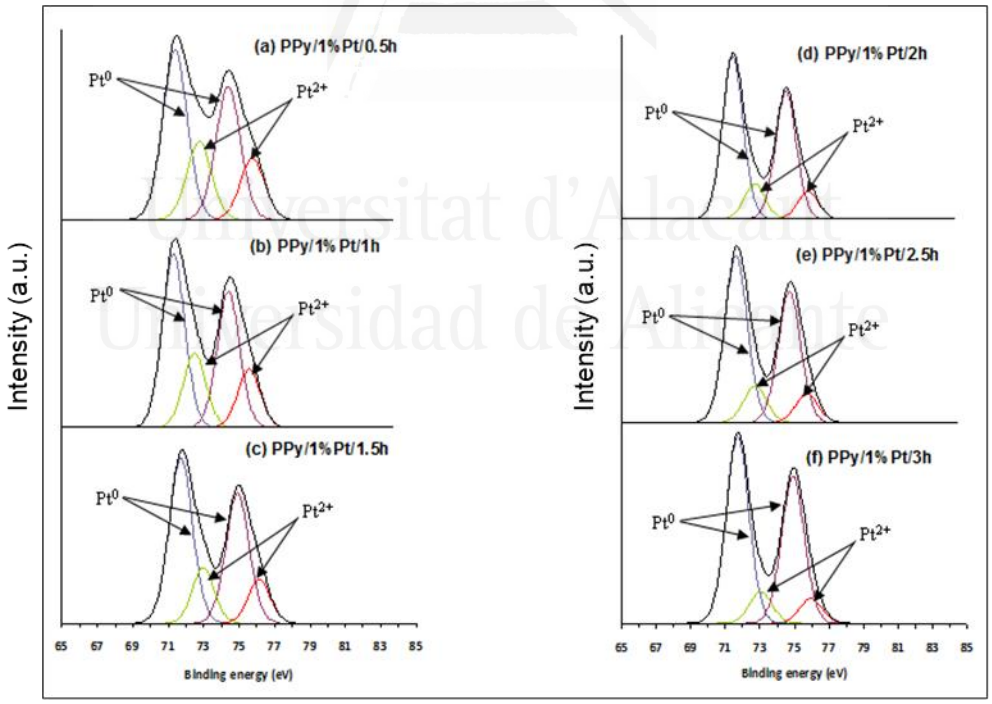

Figure 4.4. XPS Pt 4f spectra of polypyrrole synthesized with $FeCl_3$, impregnated with H_2PtCl_6 (PPy/1%Pt) and treated in Ar plasma for several lengths of time.

4. CONCLUSIONS

Ar plasma reduction treatment at room temperature provides an effective process for the synthesis of metal platinum nanoparticles dispersed on the surface of polypyrrole. From the above results it is concluded that the best performance of the plasma treatment is achieved using a RF power of 200 W and when the treatment is carried out in cycles of 5 min during a total time of 3 h (5 min x 36 times) with a manual mixing of the samples between cycles.

5. REFERENCES

[1] R. Buitrago-Sierra, M.J. García-Fernández, M.M. Pastor-Blas, A. Sepúlveda-Escribano. *Green Chem.* **2013**, *15*, 1981-1990.

[2] I. Dodouche, F. Epron. *Appl. Catal., B.* **2007**, *76(3-4)*, 291-299.

[3] X. Zhu, P.P. Huo, Y.P. Zhang, C.J. Liu. *Ind. Eng. Chem. Res*. **2006**, *45(25)*, 8604–8609.

[4] J. Wang, K.G. Neoh, E.T. Kang. *Thin Solid Films*. **2004**, *446(2)*, 205-217.

[5] B. Tian, G. Zerbi. *J. Chem. Phys*. **1990**, *92*, 3886.

[6] J. Ouyang, Y. Li. *Polymer*. **1997**, *38(15)*, 3997-3999.

[7] Y. Liu, N. Lu, S. Poyraz, X. Wang, Y. Yu, J. Scott, J. Smith, M.J. Kim, X. Zhang. *Nanoscale*. **2013**, *5*, 3872-3879.

[8] A. Drelinkiewicz, A. Zieba, J.W. Sobczak, M. Bonarowska, Z. Karpiński, A. Waksmundzka-Góra, J. Stejskal. *React. Funct. Polym.* **2009**, *69(8)*, 630-642.

[9] A. Nyczyk, A. Sniechota, A. Adamczyk, A. Bernasik, W. Turek, M. Hasik. *Eur. Polym. J.* **2008**, *44(6)*, 1594-1602.

Chapter V. Comparative study of the nitrate removal in water using monometallic and bimetallic catalysts supported on polypyrrole

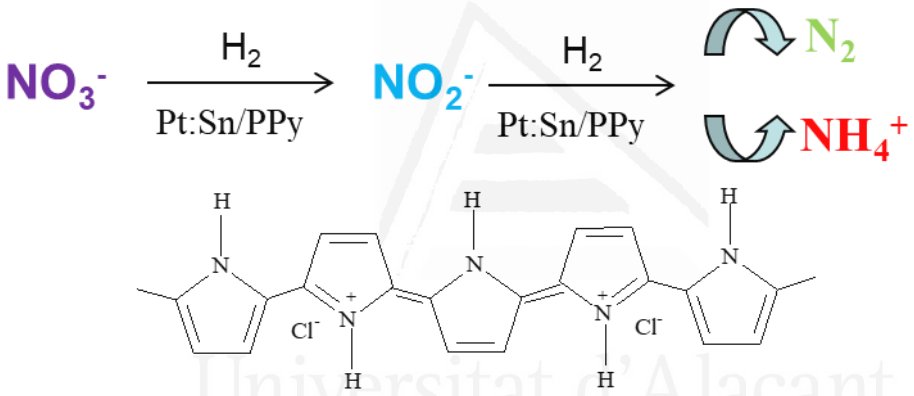

M.J. García-Fernández, R. Buitrago-Sierra, M.M. Pastor-Blas, O.S.G.P. Soares, M.F.R. Pereira, A. Sepúlveda-Escribano, "Green Synthesis of polypyrrole-supported metal catalysts: application to nitrate removal in water", *RSC Advances.* **2015**, *5*, 32706-32713.

1. INTRODUCTION

Nitrate (NO_3^-) is a naturally occurring form of nitrogen found in soil which is formed as a part of the nitrogen cycle. Plants use nitrates from the soil to satisfy nutrient requirements and may accumulate nitrate in their leaves and stems. Due to its high mobility, nitrate also can leach into groundwater. In moderate amounts, nitrate is a harmless constituent of food and water. However, if people or animals drink water with a high content of nitrate, it may cause methemoglobinemia, or blue baby syndrome, an illness found especially in infants [1], and even cancer. Nitrate values are commonly reported as either nitrate (NO_3^-) or as nitrate-nitrogen (NO_3^--N). The maximum contaminant level (MCL) in drinking water as nitrate (NO_3^-) is 50 $mg \cdot L^{-1}$, whereas as nitrate-nitrogen (NO_3^--N), which relates to the actual nitrogen in nitrate, is 11.3 $mg \cdot L^{-1}$ [2,3].

Although the term "nitrate toxicity" is commonly used, the toxic principle is actually nitrite. Nitrate is converted to nitrite in the stomach. Nitrite is absorbed from the stomach and converts blood hemoglobin to methemoglobin, which cannot transport oxygen to body tissues, thus causing death.

While it is technically possible to treat contaminated groundwater, it can be difficult, expensive and not totally effective. Charcoal filters and water softeners do not adequately remove nitrates from water. Boiling nitrate-contaminated water does not make it safe to drink and, actually, this treatment increases the concentration of nitrates. Other water treatments include distillation, reverse osmosis and ion exchange. These technologies transfer nitrates from water to a concentrate phase that requires further treatment or disposal. In this way, catalytic reduction of nitrates with H_2 using supported metal catalysts has been proposed as an alternative.

Nitrate reduction progresses through nitrite (NO_2^-) and daughter intermediates (*e.g.* nitric oxide (NO) and nitrous oxide (N_2O)), which are then reduced to dinitrogen (N_2) and ammonium (NH_4^+). Considering the toxicity of ammonium, a catalyst which is highly selective to nitrogen must be developed. It has been reported [4-6] that initial reduction of NO_3^- to NO_2^- requires a bimetallic catalyst (a noble metal as Pd, combined with a secondary promoter metal as Cu, In, Sn, Co). The intermediate NO_2^- can then be

further reduced on monometallic sites. It is also known that the catalytic behavior is affected by the support [7]. Carbonaceous supports (activated carbon, carbon nanotubes) [8], metal oxides such as TiO_2 [9,10], SiO_2 [11], Nb_2O_5 [12], SnO_2 [13], ZrO_2 [14], Al_2O_3 [15], CeO_2 [16], zeolites [17] and hydrotalcites [18] have been proposed as supports for the catalyzed reduction of nitrate [17,19-21]. In this thesis, the properties of a conducting polymer (polypyrrole) as the catalytic support have been assessed.

Polypyrrole can easily change between its reduced (non-conducting) and oxidized (conducting) forms. This feature makes it interesting to prepare supported catalysts by impregnation of a metal salt, as electrons from the polymeric chain may be transferred to the metallic ion promoting its reduction [22]. Considering their limited thermal stability, applications of polymer-supported catalysts are restricted to low temperature reactions. In this chapter, activity and selectivity of monometallic (Pt) and bimetallic (Pt:Sn) catalysts supported on polypyrrole have been determined in the reduction of nitrate in water with H_2 as the reducing agent. The use of plasma is a powerful method to synthesize nanoparticles. Hydrogen atmospheric dielectric-barrier plasma has been used to reduce supported Pt and co-catalysts [23]. Since reduction is an electron transfer process, and plasma reduction treatment is based in a direct transfer of high energy electrons from the plasma to the metal ions, it should be possible to use other gases such as helium and argon as reducing agents instead of hydrogen. These is the reason why in this thesis, the activation of the catalysts to obtain metal nanoparticles has been carried out by the environmentally friendly cold argon plasma treatment [22].

2. EXPERIMENTAL

2.1. Materials preparation

Polypyrrole was prepared by chemical polymerization of pyrrole (C_4H_5N) with ferric chloride ($FeCl_3 \cdot 6H_2O$) as an oxidant. The experimental procedure was described in in Chapter II, Section 1.1.1 [5,6]. The monometallic PPy-supported platinum catalyst was prepared by wet impregnation in excess of solvent, using $H_2PtCl_6 \cdot 6H_2O$ as the metal precursor. Thus, the proper amount of this salt to obtain 2 wt. % Pt loading was dissolved in ultrapure water, and then it was contacted with polypyrrole (25 mL solution$\cdot g_{PPy}^{-1}$) (Chapter II, Section 1.2.1). Bimetallic catalysts were prepared by co-impregnation with $H_2PtCl_6 \cdot 6H_2O$ (2 wt. % Pt) and $SnCl_2 \cdot 2H_2O$ aqueous solutions in Pt:Sn atomic ratios 3:1

and 1:1 (Chapter II, Section 1.2.2). In all cases, the obtained material was splitted in two portions, one of them to be characterized and the other one to be treated by Ar plasma.

The polypyrrole-supported catalyst precursors (PPy/Pt or PPy/Pt:Sn) were submitted to an Ar plasma treatment as detailed in Chapter II, Section 1.3. The discharge power was set to 200 W and 36 cycles of 5 min each were applied to each sample (180 min treatment in total) with manual mixing of the sample between treatments to assure an even exposure to the plasma. The temperature of the sample after the plasma treatment was below 50 °C in all cases.

2.2. Materials characterization

The polypyrrole support (PPy) and the catalysts (PPy/Pt) and (PPy/Pt:Sn) were characterized, before and after the plasma treatment by N_2 adsorption at -196 °C, thermogravimetric analysis (TGA), X-ray diffraction (XRD), electrical conductivity, infrared spectroscopy (FTIR), X-ray photoelectron spectroscopy (XPS) and transmission electron microscopy (TEM). The specifications of the corresponding equipments are detailed in Chapter II, Section 2.

2.3. Catalyst evaluation

The catalytic activity of the polypyrrole-supported catalysts obtained after treatment in Ar plasma at 200 W was evaluated in the aqueous reduction of nitrate with H_2 at room temperature. The reaction took place in a semi-batch reactor equipped with a magnetic stirrer (700 rpm) following the experimental procedure detailed in Chapter II, Section 1.4. Aliquots (1 mL) were withdrawn at different times from the reactor and immediately filtered for determination of nitrate, nitrite and ammonium concentrations by ion chromatography. Nitrate conversion $\left(X_{NO_3^-}\right)$ and selectivities to NO_2^- $\left(S_{NO_2^-}\right)$ and NH_4^+ $\left(S_{NH_4^+}\right)$ were calculated using the equations 2.8, 2.9 and 2.10 as described in Chapter II, Section 2.9.

The absence of metal leaching was checked by Inducted Coupled Plasma Mass Spectrometry (ICP-MS) in aliquots withdrawn from the reactor once the nitrate reduction reaction was completed (Chapter II, Section 2.10).

3. RESULTS AND DISCUSSION

3.1. Characterization of polypyrrole and the monometallic and bimetallic catalysts

The porous texture of the polypyrrole synthesized with ferric chloride (PPy) was determined by physical adsorption of nitrogen at -196 °C. A type II - adsorption isotherm (according to the classification of the IUPAC) was obtained, which is characteristic of non porous materials (Fig. 5.1). The calculated BET surface area was 4 $m^2 \cdot g^{-1}$ (calculated as it is described in Chapter II, Section 2.2, equations 2.4 and 2.5).

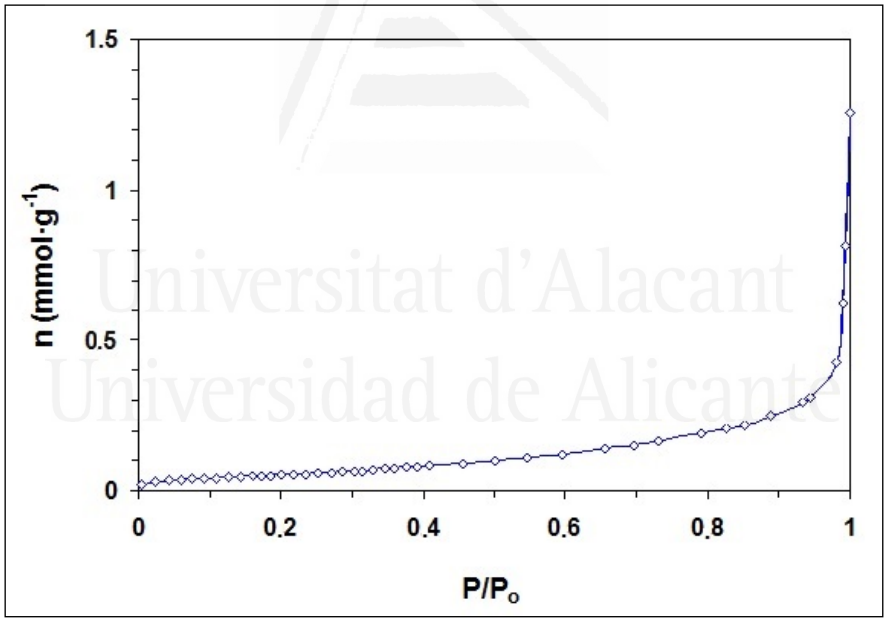

Figure 5.1. Nitrogen adsorption isotherm at - 196 °C of polypyrrole synthesized with $FeCl_3$.

The thermal stability of polypyrrole in nitrogen and in air was evaluated by TGA. Figure 5.2 shows the TGA profiles in nitrogen for the different studied materials. In all cases there is a first weight loss of less than 10 wt. % between 25 and 210 °C (centered at 100 °C), which corresponds to removal of water or non-incorporated monomer (pyrrole). The second weight loss, between 210 and 700 °C (centered at 430 °C), corresponds to the thermal degradation of ramifications of the polypyrrole chain.

Afterwards, there is a more pronounced slope (at about 900 °C) which may correspond to the degradation of the linear part of the polymer chains, and at 1200 °C, a residue of approximately 20 wt. % is obtained. Impregnation with Pt and Pt-Sn produces a shift of TGA curves to higher weight loss at the same temperature, but the subsequent reduction treatments with Ar plasma do not significantly modify the TGA curves.

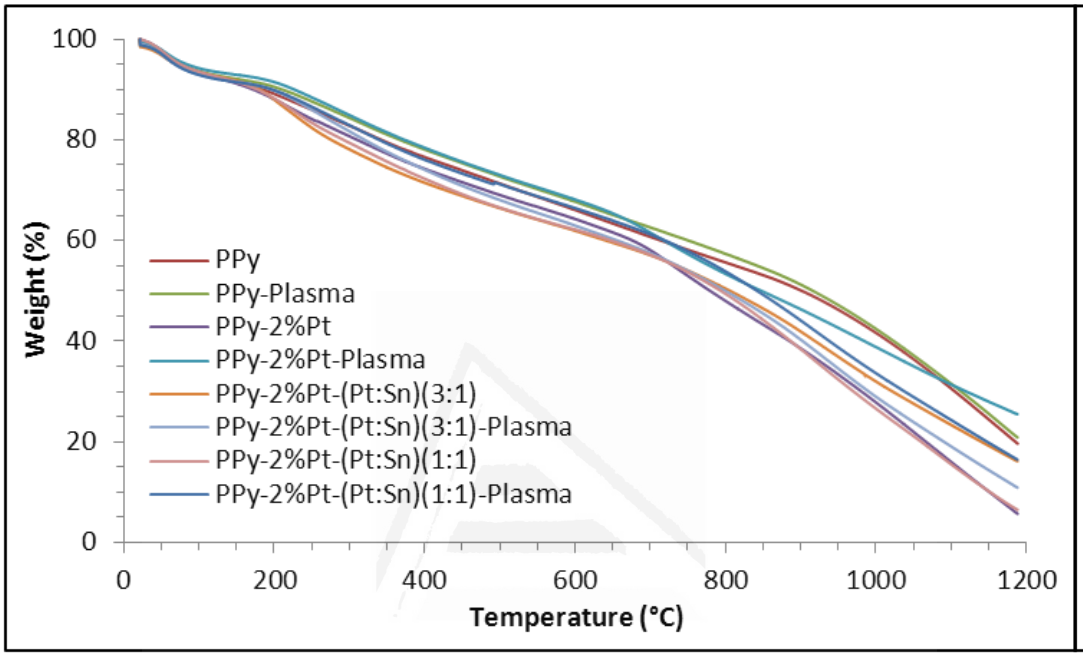

Figure 5.2. TGA profile in N_2 atmosphere of the different samples.

When the TGA analysis is carried out in air atmosphere (Fig. 5.3) the thermal degradation of polypyrrole is complete at 500 °C and there is no residue. It can be seen that the presence of metals catalyzes the degradation of polypyrrole, mainly in oxidizing atmosphere. From the TGA analysis it can be concluded that the application of polypyrrole as catalyst support would be restricted to reactions performed at temperatures below 200 °C.

The X-ray diffraction patterns (Fig. 5.4) show that synthesized polypyrrole and also the prepared catalysts are mainly amorphous. All studied samples have a broad peak centered at 2θ = 25.95 º, and a shoulder at 2θ = 16.45 º due to the scattering from PPy chains at the interplanar spacing between pyrrole groups [24]. Additionally, polypyrrole impregnated with Pt and Sn precursors shows a sharp peak at 2θ = 33.00 º, which is more evident when the Pt:Sn ratio is 1:1, and corresponds to the scattering of platinum ions

anchored to N in polypyrrole [22]. Therefore, this platinum chlorocomplex induces a more ordered arrangement of the polypyrrole chains. The *d*-spacing calculated from the Bragg's equation (2.6) (Chapter II, Section 2.5) is 0.36 nm, and the average crystallite size has been estimated from the full width at half maximum (FWHM) using the Scherrer's equation (2.7) (Chapter II, Section 2.5), and it results 1.7 nm.

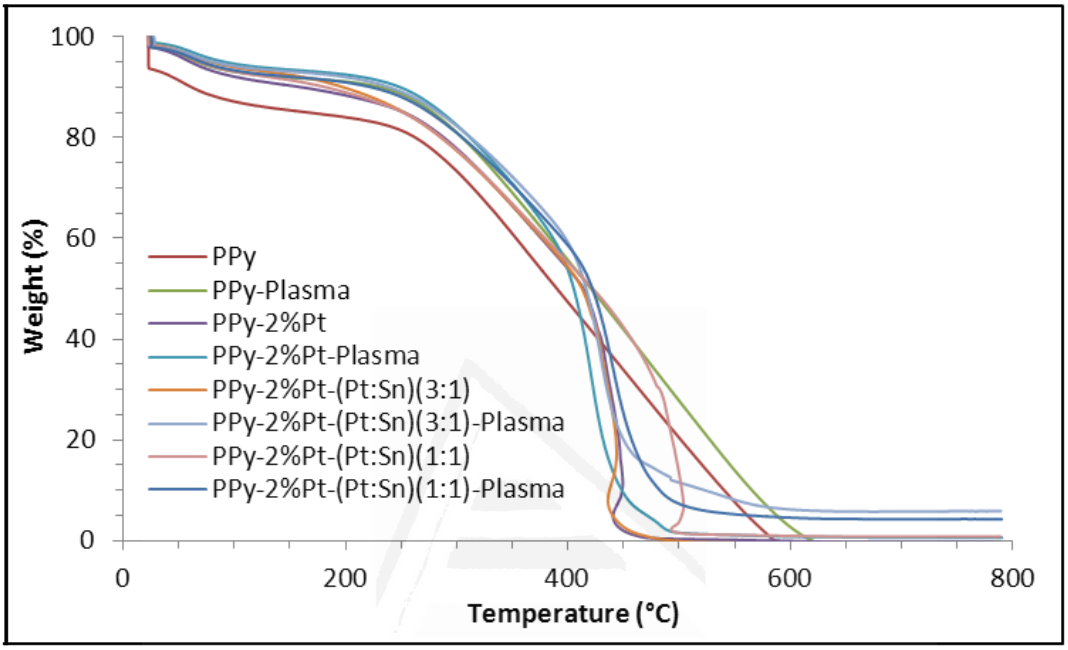

Figure 5.3. TGA profile in air atmosphere of the different samples.

Conductivity of polypyrrole depends on the counterion, the doping level and the polymer synthesis conditions; so, different conductivity values are reported in the literature: $4.9 \cdot 10^{-4}$ S·cm^{-1} [25], $3.6 \cdot 10^{-2}$ S·cm^{-1} [26] and 8 S·cm^{-1} [27]. In this thesis, synthesized polypyrrole with $FeCl_3$ shows a conductivity of $4.5 \cdot 10^{-2}$ S·cm^{-1}. All polypyrrole-supported monometallic and bimetallic catalysts show conductivities between 10^{-3} and 10^{-4} S·cm^{-1}.

The FTIR spectrum of PPy (Fig. 5.5a) shows the typical bands of this material [28] (Table 5.1). Insolubility of the chemically synthesized polypyrrole indicates that reticulation of polymeric chains has been produced during chemical oxidative polymerization, due to a high concentration of cationic polymeric radicals. Some degree of surface oxidation is detected (band at 1694 cm^{-1} of C=O stretching) which may be due to polypyrrole backbone oxidation through free radical oxygen insertion, and may

also be produced by exposure of the polymer to air. IR spectrum of polypyrrole after impregnation with $H_2PtCl_6 \cdot 6H_2O$ (Fig. 5.5b) shows differences in bands of C=N-C at 1530, 1174 and 898 cm^{-1} and N-H stretching at 779 cm^{-1}. This suggests that platinum may interact with the polypyrrole chain through the nitrogen atom, which is consistent with previous results [22].

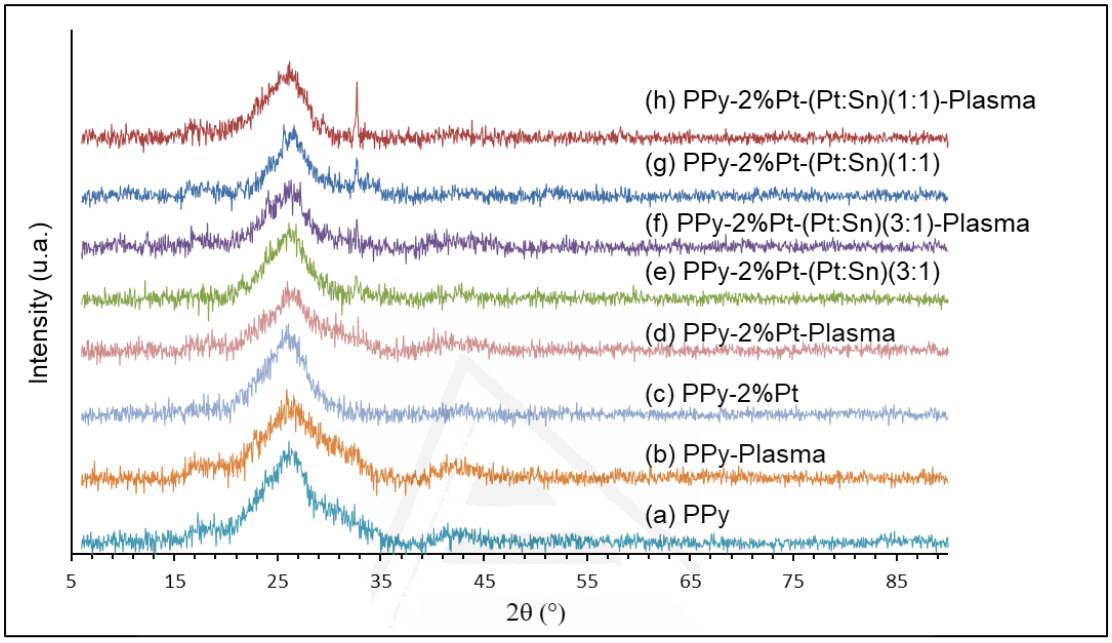

Figure 5.4. XRD patterns of (a) polypyrrole synthesized with $FeCl_3$ (PPy), (b) polypyrrole synthesized with $FeCl_3$ and treated in plasma (PPy/Plasma) and (c-h) mono and bimetallic catalysts with and without Ar plasma reduction treatment.

Table 5.1. IR-bands assignment.

PPy (cm^{-1})	PPy/2%Pt (cm^{-1})	Assignment[a]
1694	1699	C=O st
1542	1530	C=N st
1450	1421	C=C st
1285	1269	C-C st
1180	1174	C-N st
1044	1024	=C-H δ_{oop}
911	898	C=N-C δ
787	779	N-H δ

[a] Stretching (st), in-plane bending (δ) and out-of-plane bending (δ_{oop}).

XPS analysis of chemically synthesized polypyrrole (Table 5.2) shows C and N from the polymeric chain, as well as Cl from the $FeCl_3$ oxidant used for the chemical polymerization of polypyrrole. The analysis of the C 1s (Fig. 5.6a) and O 1s (Fig. 5.6b)

level shows the presence of C=O and C-O moieties (Tables 5.3 and 5.4), which supports PPy degradation and/or surface oxidation [22]. On the other hand, the N 1s spectra (Fig. 5.7, Table 5.5) shows the presence of =N- (399.7 eV) and -NH- (400.3 eV) species in polypyrrole.

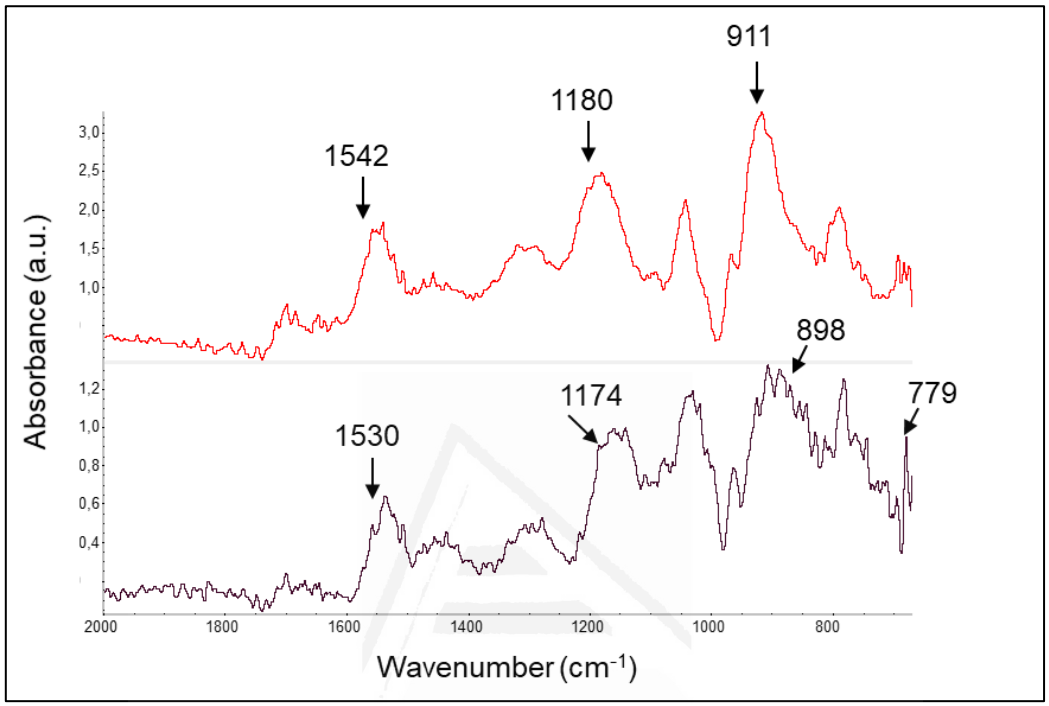

Figure 5.5. FTIR-ATR spectra of (a) polypyrrole synthesized with $FeCl_3$ (PPy) and (b) polypyrrole synthesized with $FeCl_3$ and impregnated with H_2PtCl_6 (PPy/2%Pt).

Table 5.2. XPS surface chemical composition (atomic %) of the different samples.

Binding energy (*eV*)	284.5	531.5	398.1	198.5	71.2	487.6	710.9
Element	**C 1s**	**O 1s**	**N 1s**	**Cl 2p**	**Pt 4f**	**Sn 3d**	**Fe 2p**
PPy/2%Pt/(Pt:Sn)(1:1)	74.2	14.0	4.5	3.7	1.1	2.5	0.0
PPy/2%Pt/(Pt:Sn)(1:1)/Plasma	65.1	19.1	6.1	4.3	2.1	3.3	0.0
PPy/2%Pt/(Pt:Sn)(1:1)/Plasma-R[a]	69.2	20.6	6.3	0.5	0.7	2.7	0.0
PPy/2%Pt/(Pt:Sn)(3:1)	71.7	4.4	12.1	11.4	0.2	0.2	0.0
PPy/2%Pt/(Pt:Sn)(3:1)/Plasma	68.6	15.4	6.7	3.3	4.2	1.8	0.0
PPy/2%Pt/(Pt:Sn)(3:1)/Plasma-R[a]	72.4	16.2	7.8	0.6	1.4	1.6	0.0
PPy/2%Pt	84.1	5.7	5.0	3.5	1.7	-	0.0
PPy/2%Pt/Plasma	70.3	14.9	8.0	3.0	3.7	-	0.1
PPy/2%Pt/Plasma-R[a]	78.3	12.4	7.7	0.6	1.0	-	0.0
PPy	77.9	6.5	13.2	2.4	-	-	0.0
PPy-R[a]	77.8	10.3	11.5	0.4	-	-	0.0
PPy/Plasma	71.8	14.1	12.4	1.7	-	-	0.0
PPy/Plasma-R[a]	73.6	13.7	12.2	0.5	-	-	0.0

[a] R = recovered catalyst after 300 min of nitrate reduction with hydrogen.

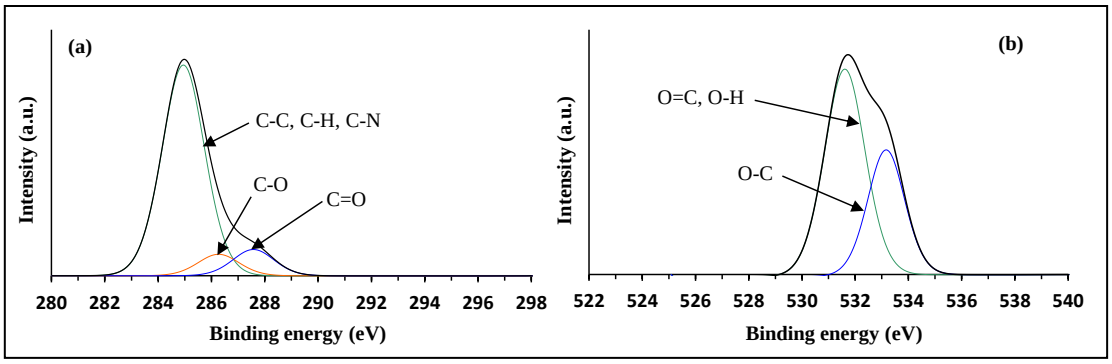

Figure 5.6. XPS (a) C 1s and (b) O 1s spectra of polypyrrole synthesized with $FeCl_3$.

Table 5.3. Atomic percentages of the different surface species estimated from the areas of the contributions to the XPS spectra corresponding to the C 1s level.

Sample	Biding energy (eV)	Species	Composition (at. %)		
			No Plasma	Plasma	Plasma-R[a]
PPy/2%Pt/(Pt:Sn)(1:1)	284.9	C-C, C-H, C-N	63.9	50.6	56.9
	286.6	C-O	6.9	8.0	5.4
	288.4	C=O	3.4	6.5	6.9
PPy/2%Pt/(Pt:Sn)(3:1)	285.1	C-C, C-H, C-N	63.7	51.5	61.4
	287.2	C-O	5.8	10.1	6.3
	289.1	C=O	2.2	7.0	4.7
PPy/2%Pt	285.1	C-C, C-H, C-N	73.0	52.8	65.6
	286.7	C-O	6.9	10.2	9.1
	288.3	C=O	4.2	7.3	3.6
PPy	285.0	C-C, C-H, C-N	63.8	57.7	59.7
	286.3	C-O	6.3	5.3	7.3
	287.6	C=O	7.8	8.8	6.6

[a] R = recovered catalyst after 300 min of nitrate reduction with hydrogen.

Table 5.4. Atomic percentages of the different surface species estimated from the areas of the contributions to the XPS spectra corresponding to the O 1s level.

Sample	Binding energy (eV)	Species	Composition (at. %)		
			No Plasma	Plasma	Plasma-R[a]
PPy/2%Pt/(Pt:Sn)(1:1)	531.7	O=C, O-H	8.4	10.7	13.3
	533.1	O-C	5.6	8.4	7.3
PPy/2%Pt/(Pt:Sn)(3:1)	531.8	O=C, O-H	2.4	9.0	9.4
	533.1	O-C	2.0	6.4	6.8
PPy/2%Pt	532.0	O=C, O-H	3.5	8.9	8.6
	533.6	O-C	2.2	6.0	3.8
PPy	531.6	O=C, O-H	4.2	9.9	9.9
	533.2	O-C	2.3	4.2	3.8

[a] R = recovered catalyst after 300 min of nitrate reduction with hydrogen.

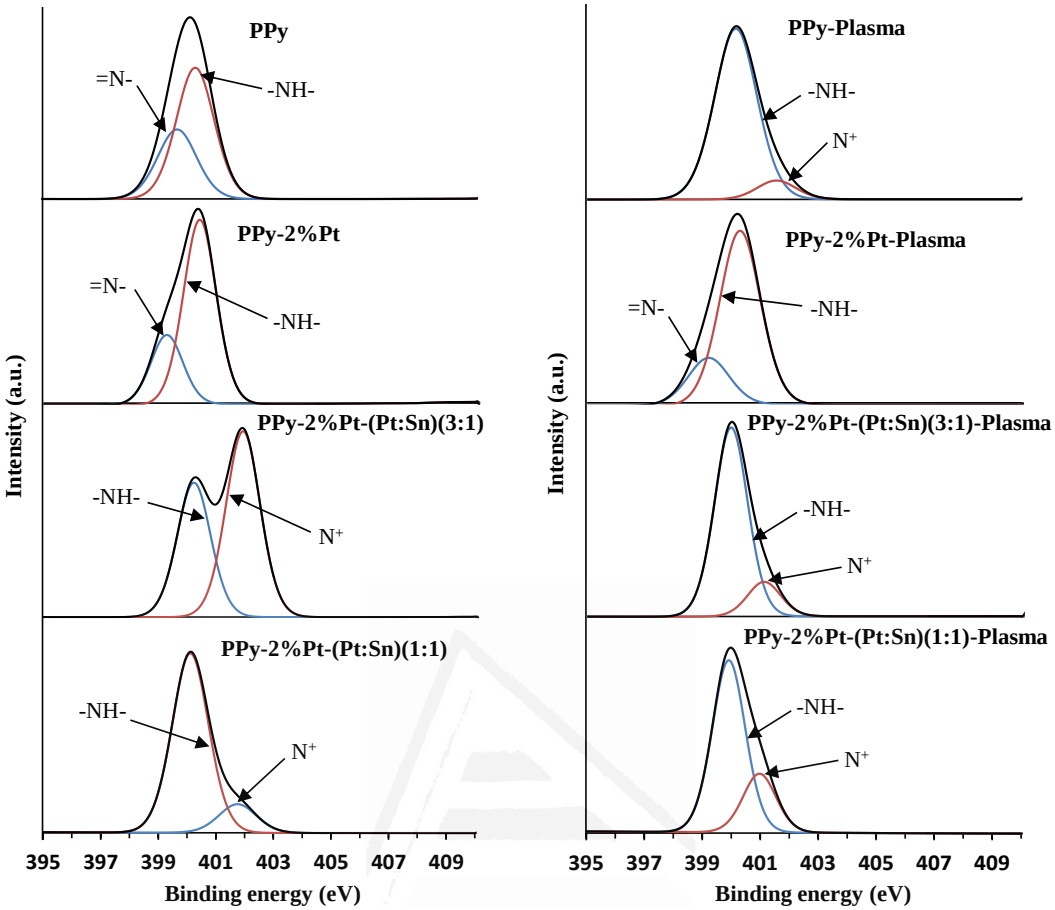

Figure 5.7. Curve fit of N 1s level in XPS spectra of different samples.

Table 5.5. Atomic percentages of the different surface species estimated from the areas of the contributions to the XPS spectra corresponding to the N 1s level.

Sample	Binding energy (eV)	Species	Composition (at. %)		
			No Plasma	Plasma	Plasma-R[a]
PPy/2%Pt/(Pt:Sn)(1:1)	400.1	-NH-	3.9	4.6	2.0
	401.8	N^+	0.6	1.5	4.3
PPy/2%Pt/(Pt:Sn)(3:1)	400.2	-NH-	5.0	5.7	1.8
	401.9	N^+	7.1	1.0	6.0
PPy/2%Pt	399.3	=N-	1.4	1.8	2.2
	400.4	-NH-	3.6	6.2	5.5
PPy	399.7	=N-	4.7	0.0	3.1
	400.3	-NH-	8.5	11.3	9.1
	401.5	N^+	0.0	1.1	0.0

[a] R = recovered catalyst after 300 min of nitrate reduction with hydrogen.

Previous studies [22] (Chapter III, Section 3.2) have shown that impregnation of polypyrrole with H_2PtCl_6 produces the anchoring of the platinum chlorocomplex on the polypyrrole by interaction with the N moieties in the polymer structure, together with a partial reduction of Pt(IV) to Pt(II) and the oxidation of the polypyrrole polymeric chain. Table 5.6 shows an increase of the -NH- contribution respective to =N- in PPy/2%Pt, when compared with PPy. The XPS spectra corresponding to the Pt 4f level of polypyrrole impregnated with H_2PtCl_6 can be deconvoluted into two bands (Fig. 5.8, Table 5.7) at 74.0 eV ($Pt4f_{7/2}$) and 77.4 eV ($Pt4f_{5/2}$), which correspond to Pt(IV), and two other at 72.9 eV ($Pt4f_{7/2}$) and 76.1 eV ($Pt4f_{5/2}$), which correspond to Pt(II), which is the predominant specie. The absence of metallic platinum, which should appear at lower binding energies, is confirmed. XPS spectra of polypyrrole co-impregnated with H_2PtCl_6 and $SnCl_2$ show the presence of Pt ions, as Pt(IV) and Pt(II), and tin ions (it is not possible to discern between both oxidation stated by XPS analysis) (Fig. 5.8, Table 5.7). There is also a shift of the N 1s band to higher binding energies, and N^+ at 401.9 eV is detected (Fig. 5.7). When the Sn content increases, Pt(IV) becomes dominant compared to the Pt(II) contribution, and the N^+/-NH- ratio is also affected, *i.e.* 1.41 for Pt:Sn (3:1) and 0.16 for Pt:Sn (1:1) (Fig. 5.7, Table 5.6). This suggests that the reduction of Pt(IV) to Pt(II) becomes hindered as the amount of tin increases, and, consequently, the polymeric chain also results in a lower oxidation degree (evaluated from the N^+/-NH- ratio). Therefore, it may be concluded that the presence of ionic tin species modifies the extent of electron transfer from the nitrogen atoms in the polymeric chain to platinum ions anchored as platinum chlorocomplex.

Table 5.6. Atomic ratios (XPS) of the different surface species.

Sample	C / O	-NH- /=N-	N^+/-NH-	Pt^o / Pt^{n+}
PPy/2%Pt/(Pt:Sn)(1:1)	5.31	-	0.16	-
PPy/2%Pt/(Pt:Sn)(1:1)/Plasma	3.41	-	0.34	0.70
PPy/2%Pt/(Pt:Sn)(1:1)/Plasma-R[a]	3.35	-	2.21	0.49
PPy/2%Pt/(Pt:Sn)(3:1)	16.14	-	1.41	-
PPy/2%Pt/(Pt:Sn)(3:1)/Plasma	4.46	-	0.18	2.81
PPy/2%Pt/(Pt:Sn)(3:1)/Plasma-R[a]	4.48	-	3.25	1.50
PPy/2%Pt	14.81	2.68	-	-
PPy/2%Pt/Plasma	4.73	3.57	-	1.57
PPy/2%Pt/Plasma-R[a]	6.33	2.44	-	-
PPy	11.96	1.83	-	-
PPy-R[a]	7.56	3.87	-	-
PPy/Plasma	5.07	-	0.10	-
PPy/Plasma-R[a]	5.37	2.92	-	-

[a] R = recovered catalyst after 300 min of nitrate reduction with hydrogen.

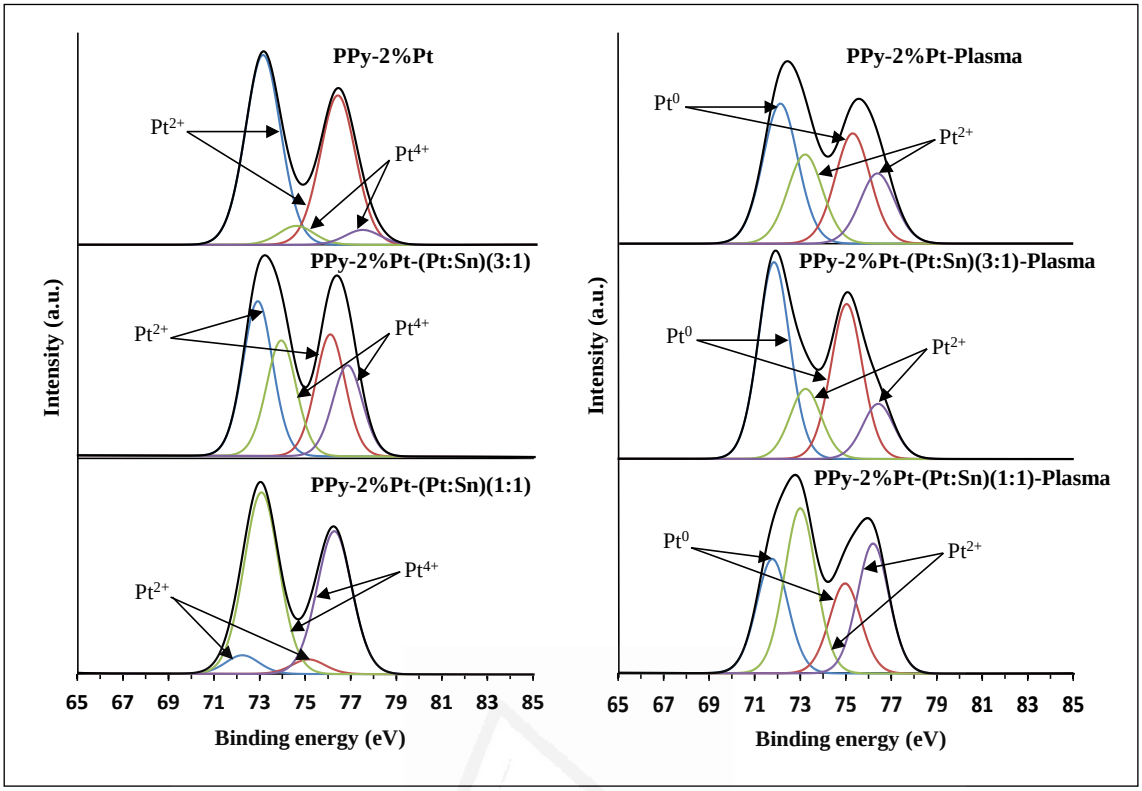

Figure 5.8. Curve fit of Pt 4f level in XPS spectra of different samples.

Table 5.7. Atomic percentages of the different surface species estimated from the areas of the contributions to the XPS spectra corresponding to the Pt 4f level.

Sample	Species	Composition (at. %)
PPy/2%Pt/(Pt:Sn)(1:1)	Pt^{2+}	0.1
	Pt^{4+}	1.0
PPy/2%Pt/(Pt:Sn)(1:1)/Plasma	Pt^{o}	0.9
	Pt^{2+}	1.2
PPy/2%Pt/(Pt:Sn)(1:1)/Plasma-R[a]	Pt^{o}	0.2
	Pt^{2+}	0.5
PPy/2%Pt/(Pt:Sn)(3:1)	Pt^{2+}	0.1
	Pt^{4+}	0.1
PPy/2%Pt/(Pt:Sn)(3:1)/Plasma	Pt^{o}	3.1
	Pt^{2+}	1.1
PPy/2%Pt/(Pt:Sn)(3:1)/Plasma-R[a]	Pt^{o}	0.8
	Pt^{2+}	0.6
PPy/2%Pt	Pt^{2+}	1.5
	Pt^{4+}	0.2
PPy/2%Pt/Plasma	Pt^{o}	2.3
	Pt^{2+}	1.4
PPy/2%Pt/Plasma-R[a]	Pt^{2+}	0.4
	Pt^{4+}	0.6

[a] R = recovered catalyst after 300 min of nitrate reduction with hydrogen.

For most platinum-catalyzed reactions, the presence of platinum in its zero-state is required. Thus, the reducing capability of Ar plasma treatment was analyzed by XPS. In the previous chapters it has been shown the capability of Ar plasma to partially reduce platinum ions in monometallic polypyrrole-supported catalysts [22] (Chapter III, Section 3.2). Pt 4f curve fit (Fig. 5.8, Table 5.7) shows that argon plasma produces partial reduction of platinum ions into metallic platinum and Pt(IV) is not further present. However, no metallic tin is detected, although it has to be taken into account that it could be produced upon the plasma treatment but re-oxidized during the subsequent air exposure. Besides, Ar plasma treatment activates polypyrrole surface in such a way that ulterior contact with air favors the creation of oxygenated moieties. Accordingly, the C/O ratio decreased after argon plasma treatment (Table 5.6). Ar plasma treatment also produces ablation of the polypyrrole surface and, as a result of this, platinum and tin located within the polymer network were exposed to the outermost polypyrrole surface and were detected by XPS, with the consequent increase of surface Pt and Sn percentages (Table 5.2). Consequently, an improvement of efficiency of these catalysts after plasma treatment is expected.

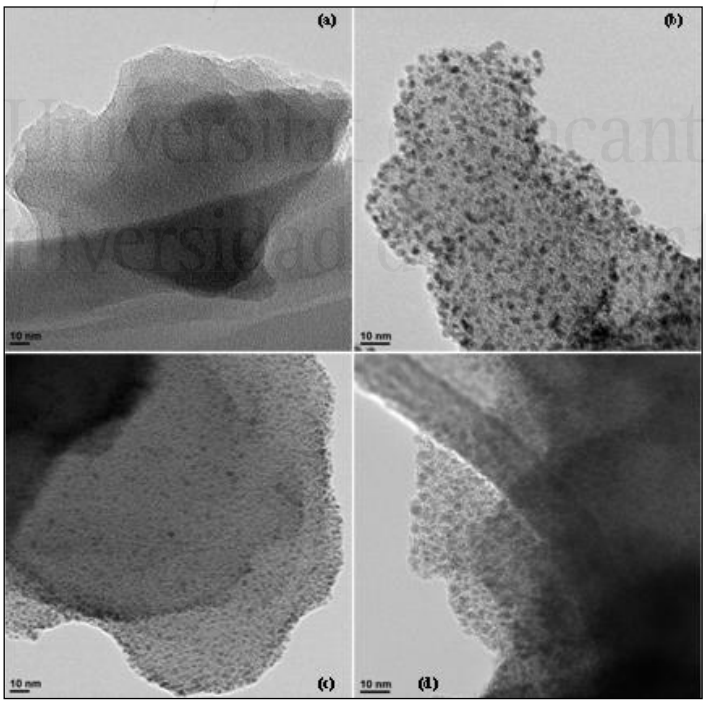

Figure 5.9. TEM images of (a) PPy/Plasma, (b) PPy/2%Pt/Plasma, (c) PPy/2%Pt/(Pt:Sn)(3:1)/Plasma and (d) PPy/2%Pt/(Pt:Sn)(1:1)/Plasma.

TEM images of platinum and platinum-tin impregnated-polypyrrole (Fig. 5.9) show a good dispersion of metal nanoparticles. Plasma treatment produced only a slight aggregation of nanoparticles, although in all cases the particle sizes were smaller than 5 nm. As a consequence of high dispersion, no metallic platinum is detected by X-ray diffraction (Fig. 5.4), although Pt(0) was detected by XPS on plasma treated samples.

3.2. Catalytic behavior

A control reaction was carried out flowing H_2 (reducing agent) and CO_2 (buffer) through the aqueous nitrate solution. Aliquots were periodically extracted and analyzed by ion chromatography. After 300 min, nitrate concentration remained unmodified and neither nitrite nor ammonium was detected. This indicates that the reaction did not run in the absence of a catalyst. In order to elucidate the role of the polymeric support in the removal of nitrates from water, the polymer was put into contact with the aqueous nitrate solution in the presence of CO_2 (buffer) flow. No metal catalyst or reducing agent was added. A considerable decrease of nitrate concentration was observed, but no nitrite was detected and only a very small ammonium concentration was detected after 300 min (Fig. 5.10).

The mechanism of nitrate abatement on these systems could at first be explained by ion exchange between Cl^- (as doped polypyrrole counterion) and NO_3^-. However, if a simple ion exchange occurred, nitrate would be present at the polymeric support after the reaction. But recovered PPy after 300 min in contact with nitrate solution did not show NO_3^- contribution to N 1s (XPS) at 406 eV. Considering the redox potentials for the implied species (PPy^+/PPy, E° = 0.1520 V; NO_3^-/NH_4^+, E° = 0.875 V; NO_3^-/N_2, E° = 1.246 V) reduction of nitrate is expected to be produced by electrons coming from the polypyrrole chain (Scheme 5.1). Thus, nitrate is reduced to nitrite as a stepwise reaction and then rapidly reduced to nitrogen and only a small part would be reduced to ammonium. It has been assumed that the amount of other nitrogen species eventually produced is negligible [4]. Consequently, PPy which is initially in a semioxidized state as assessed by XPS (4.7 at. % of =N- at 399.7 and 8.5 at. % of -NH- at 400.3 eV in Table 5.5) shows oxidation of its nitrogen species when is recovered after being in contact with a nitrate solution in a CO_2 flow for 300 min (9.31 at. % of -NH- at 400.05 eV and 0.52 at. % of N^+ at 401.27 eV).

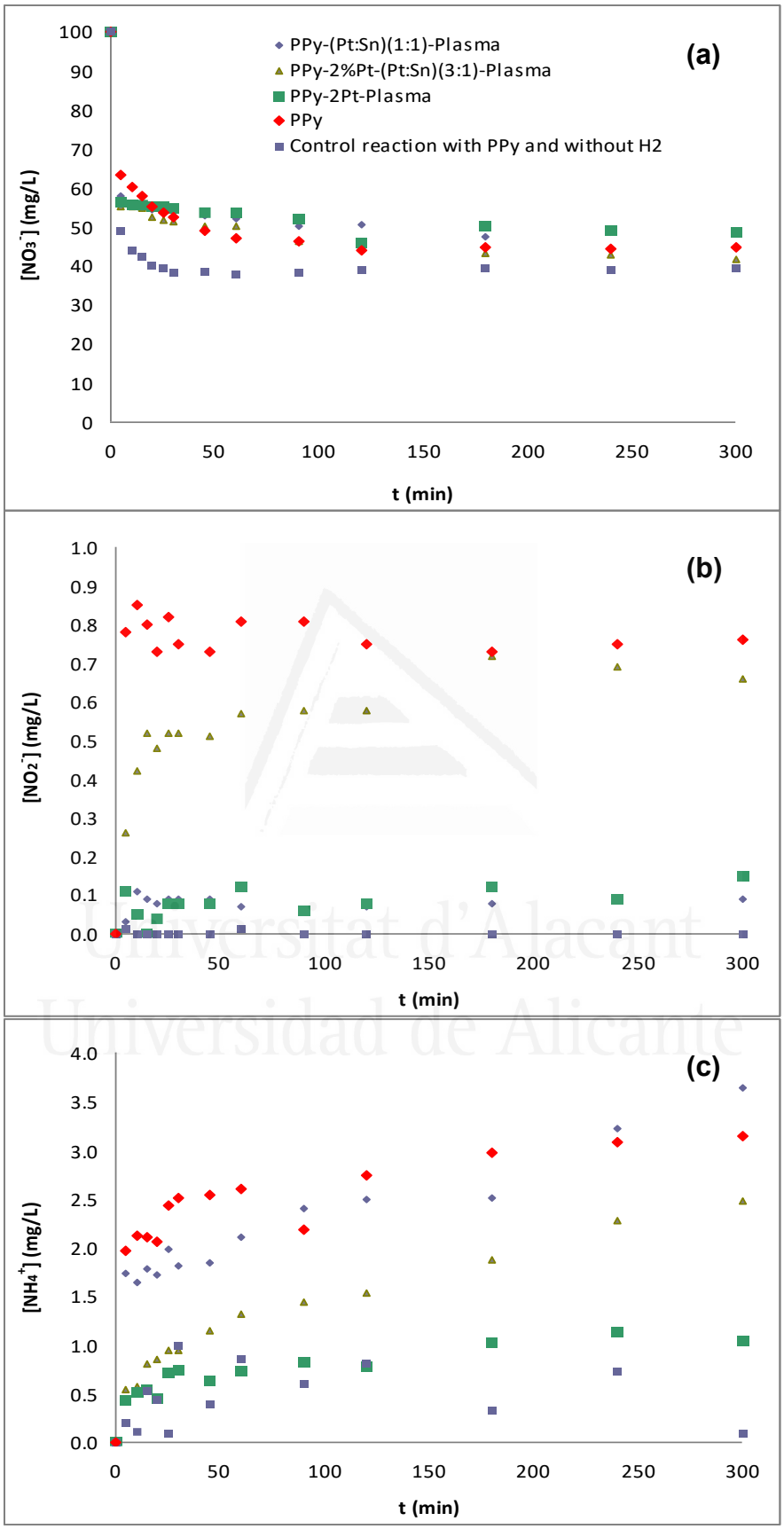

Figure 5.10. (a) Nitrate, (b) nitrite and (c) ammonium concentrations (mg·L^{-1}) as a function of time (min) during aqueous nitrate reduction with hydrogen in the presence of three different catalysts.

$$NO_3^- + 2\,H^+ + 2\,e^- \rightarrow NO_2^- + H_2O \quad (NO_3^-/NO_2^-) \quad E^o = 0.930\ V\ (pH = 0)$$

$$2\,NO_2^- + 8\,H^+ + 6\,e^- \rightarrow N_2 + 4\,H_2O \quad (NO_2^-/N_2) \quad E^o = 1.520\ V\ (pH = 0)$$

$$NO_2^- + 8\,H^+ + 6\,e^- \rightarrow NH_4^+ + 2\,H_2O \quad (NO_2^-/NH_4^+) \quad E^o = 0.897\ V\ (pH = 0)$$

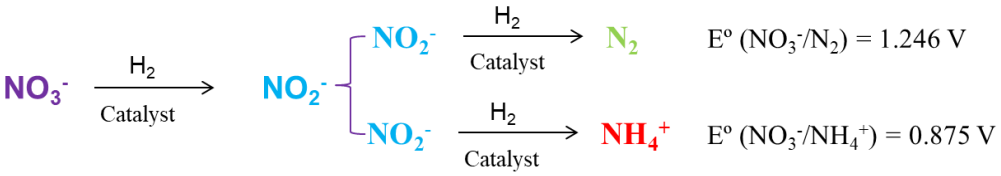

Scheme 5.1. Reaction pathways and redox potentials for aqueous nitrate reduction by hydrogen.

A similar experiment was performed, but in the presence of hydrogen as reductor. Thus, PPy was put into contact with the aqueous nitrate solution in the presence of CO_2 and H_2. Nitrate abatement from solution in the presence of hydrogen acting as reductor is not as effective as nitrate removal by the polymer in the absence of hydrogen. Nevertheless, measured nitrate concentration is below 50 $mg \cdot L^{-1}$ (Fig. 5.10). Nitrogen species in recovered PPy are in a similar oxidation state (3.1 at. % of =N- and 9.1 at. % of -NH-) than in the pristine PPy (4.7 at. % of =N- and 8.5 at. % of -NH-), this suggesting that the main reductor in this case has been hydrogen. However, considerable amounts of nitrite and ammonium are detected. Consequently, in order to minimize NO_2^- and NH_4^+ production, it is necessary to catalyze the selective reduction of NO_3^- to N_2. Therefore, the activity and selectivity of the polypyrrole-supported platinum and platinum-tin catalysts was evaluated.

Previous studies [6,29] stated that Pd or Pt monometallic catalysts catalyze reduction of nitrite (NO_2^-), but a promoter is necessary for the reduction of nitrate (NO_3^-) when carbon materials are used as support. However, in this thesis, nitrate concentration in water below the maximum acceptable level of 50 $mg \cdot L^{-1}$ (91/676/CEE European legislation) is achieved with all studied monometallic and bimetallic catalysts (Fig. 5.10, Table 5.8).

Table 5.8. Nitrate, nitrite and ammonium concentrations, nitrate conversion and selectivities to nitrite and ammonium after 300 min of nitrate reduction with hydrogen.

Sample	(mg·L^{-1})			(%)		
	[NO_3^-]	[NO_2^-]	[NH_4^+]	$X_{NO_3^-}$	$S_{NO_2^-}$	$S_{NH_4^+}$
PPy/2%Pt/(Pt:Sn)(1:1)/Plasma	48.9	0.1	3.7	51	0.2	24.3
PPy/2%Pt/(Pt:Sn)(3:1)/Plasma	41.8	0.7	2.5	58	1.5	14.6
PPy/2%Pt/Plasma	48.8	0.2	1.0	51	0.4	7.0
PPy	44.7	0.8	3.1	55	1.9	19.4
PPy control without H_2	39.7	0	0.1	61	0	0.6

The most important decrease of nitrate concentration in water was achieved with PPy/2%Pt/(Pt:Sn)(3:1)/Plasma bimetallic catalyst, which was the one with the highest metallic platinum content, as estimated by XPS analysis (Pt^o/Pt^{2+} = 2.81; Table 5.6). However, with this catalyst, nitrate reduction progresses through the non-desired nitrite intermediate (maximum acceptable nitrite level in water is 0.5 mg·L^{-1}). On the other hand, ammonium concentration is higher with the PPy/2%Pt/(Pt:Sn)(1:1)/Plasma catalyst (Pt^o/Pt^{2+} = 0.70; Table 5.6). However, considering not only the efficiency in nitrate reduction, but also the minimized concentrations of the undesired intermediate (nitrite) and byproduct (ammonium), the monometallic PPy/2%Pt/Plasma catalyst seems to be the most promising one. At this point, it is interesting to note that ICP-MS results (Table 5.9) show that neither platinum nor tin leaching was produced, as lixiviated metal (platinum or tin) is less than 0.1 %.

Table 5.9. Concentration of lixiviated (l) and theorical (T) metals detected by ICP-MS in solution after 300 min of reaction of nitrate reduction with hydrogen.

Sample	(ppb)		% Pt_l	(ppb)		% Sn_l
	$[Pt]_l$	$[Pt]_T$		$[Sn]_l$	$[Sn]_T$	
PPy/2%Pt/(Pt:Sn)(3:1)/Plasma	3.630	$1.031 \cdot 10^4$	0.035	0.816	$2.138 \cdot 10^3$	0.038
PPy/2%Pt/Plasma	2.061	$1.129 \cdot 10^4$	0.018	-	-	-

Recovered catalysts after 300 min reaction have been analyzed by XPS. A decrease of Cl and Pt contents was observed in all cases (Table 5.2). The XPS spectra for the N 1s level of the recovered bimetallic catalysts (Table 5.6) show that there is an increase of the N^+/-NH- ratio in polypyrrole, which supports the hypothesis that the polymeric support participates in the reduction reaction. As suggested before, a possible mechanism would be an ion exchange between the Cl^- counterion present in polypyrrole doped with $FeCl_3$ by NO_3^- from solution. This is supported by the fact that the Cl content estimated from XPS analysis is lower in recovered catalysts. Then, polypyrrole in its

reduced state might donate electrons to nitrate, which reduces to nitrogen and/or ammonium. The electron donation degree is influenced by the presence of ionic tin species. XPS spectra of the Sn 3d level show that no metallic tin is detected, but it is not possible to discern between Sn(II) and Sn(IV) species. Besides, there is a decrease of the metallic platinum/ionic platinum ratio in the recovered bimetallic catalysts, and no metallic Pt is detected on the surface of the recovered monometallic catalyst (Table 5.6). These findings suggest that during the nitrate reduction reaction, a given amount of metallic platinum supported on polypyrrole is oxidized to ionic platinum (as polypyrrole chain is reduced). Polypyrrole chain can act as a source and drain of electrons, donating electrons to nitrate, which become reduced, and accepting electrons from metallic platinum, which oxidizes to different extent depending on ionic tin being present or not. Ionic tin affects in some way the electron transfer from and towards the polymeric chain; this explains that the XPS N 1s band is shifted to higher binding energies in the bimetallic catalysts, compared to monometallic one. Thus, the balance between two processes, Cl^-/NO_3^- exchange and electron transfer between hydrogen, polypyrrole, platinum and nitrate, may be modified depending on the presence of the platinum catalyst and the tin promoter.

4. CONCLUSIONS

Pt and Pt:Sn catalysts supported on polypyrrole have been prepared using environmentally-friendly argon plasma treatment, which produces a partial reduction of platinum ions, anchored as a platinum chlorocomplex to the polypyrrole chain, into metallic platinum, but it did not reduce ionic tin to its metallic state. Furthermore, this treatment activated the polypyrrole surface and subsequent exposure to air produced C=O moieties. An indirect process involving the water molecules within the polymer network led to the creation of C=O and RO-C=O moieties under plasma treatment.

The polymeric support suffered ion exchange of Cl^- counterions by NO_3^- from reaction solution, and also participated in the redox process of nitrate reduction. A balance between two processes, Cl^-/NO_3^- exchange and electron transfer between polypyrrole, platinum and nitrate, can be modified depending on the presence of the platinum catalyst and the tin promoter.

All the supported metal catalysts were effective in the reduction of aqueous nitrate with H_2 at room temperature, and nitrate concentrations in water below the maximum acceptable level of 50 $mg \cdot L^{-1}$ were achieved in all cases. However, considering not only the efficiency in nitrate reduction, but also minimized concentrations of the undesired intermediate (nitrite) and by-product (ammonium), the monometallic Pt catalyst seems to be most effective one.

Nevertheless, nitrate abatement produced by the metal catalysts supported on PPy is less effective than the nitrate removal produced by the metal-free polymer (although high ammonium concentrations are obtained). Platinum nanoparticles anchor to the polypyrrole chain through nitrogen positions. Therefore, electron transfer from polypyrrole to nitrate is direct in absence of platinum but is platinum-mediated in the platinum catalyst, which shows lower efficiency in the removal of nitrates from water.

Besides, the polypyrrole chain seems to be a more effective reductor than dihydrogen. Consequently, reduction of nitrate is more effectively produced by electrons provided by polypyrrole chain than by dihydrogen presumably chemisorbed on platinum nanoparticles.

The mechanisms which govern these processes will be analyzed and discussed in the following chapters.

5. REFERENCES

[1] T. E. Arbuckle, G. J. Sherman, P. N. Corey, D. Walters, B. Lo. *Arch. Environ. Health*. **1988**, *43(2)*, 162-167.

[2] ECETOC (European Centre for Ecotoxicology and Toxicology Of Chemicals), Technical Report No. 27, *Nitrate and Drinking Water*, Brussels. **1988**.

[3] USEPA (United State Environmental Protection Agency), *National Primary Drinking Water Regulations*, Washington, DC, **2008**, Title 40, Part 141.

[4] R. Zhang, D. Shuai, K.A. Guy, J.R. Shapley, T.J. Strathmann, C.J. Werth. *ChemCatChem*. **2013**, *5(1)*, 313-321.

[5] I. Dodouche, F. Epron. *Appl. Catal., B*. **2007**, *76(3-4)*, 291-299.

[6] I. Dodouche, D.P. Barbosa, M.C. Rangel, F. Epron. *Appl. Catal., B.* **2009**, *93(1-2)*, 50-55.

[7] O.S.G.P. Soares, J.J.M. Órfão, M.F.R. Pereira. *Desalination*. **2011**, *279(1-3)*, 367-374.

[8] O.S.G.P. Soares, J.J.M. Órfão, M.F.R. Pereira. *Ind. Eng. Chem. Res.* **2010**, *49(16)*, 7183-7192.

[9] J. Sá, J.A. Anderson. *Appl. Catal., B.* **2008**, *77(3-4)*, 409-417.

[10] J. Sá, C.A. Agüera, S. Gross, J.A. Anderson. *Appl. Catal., B.* **2009**, *85(3-4)*, 192-200.

[11] A. Garron, K. Lázár, F. Epron. *Appl. Catal., B.* **2005**, *59(1-2)*, 57-69.

[12] M.P. Maia, M.A. Rodrigues, F.B. Passos. *Catal. Today*. **2007**, *123(1-4)*, 171-176.

[13] M. D'Arino, F. Pinna, G. Strukul. *Appl. Catal., B.* **2004**, *53(3)*, 161-168.

[14] Z. Xu, L. Chen, Y. Shao, D. Yin, S. Zheng. *Ind. Eng. Chem. Res*. **2009**, *48(18)*, 8356-8363.

[15] F. Epron, F. Gauthard, C. Pinéda, J. Barbier. *J. Catal.* **2001**, *198(2)*, 309-318.

[16] F. Epron, F. Gauthard, J. Barbier. *J. Catal*. **2002**, *206(2)*, 363-367.

[17] K. Nakamura, Y. Yoshida, I. Mikami, T. Okuhara. *Appl. Catal., B.* **2006**, *65(1-2)*, 31-36.

[18] A.E. Palomares, J.G. Prato, F. Rey, A. Corma. *J. Catal*. **2004**, *221(1)*, 62-66.

[19] O.S.G.P. Soares, J.J.M. Órfão, M.F.R. Pereira. *Appl. Catal., B.* **2011**, *102(3-4)*, 424-432.

[20] U. Prüsse, K.D. Vorlop. *J. Mol. Catal. A: Chem*. **2001**, *173(1-2)*, 313-328.

[21] K. Wada, T. Hirata, S. Hosokawa, S. Iwamoto, M. Inoue. *Catal. Today*. **2012**, *185(1)*, 81-87.

[22] R. Buitrago-Sierra, M.J. García-Fernández, M.M. Pastor-Blas, A. Sepúlveda-Escribano. *Green Chem.* **2013**, *15*, 1981-1990.

[23] S.S. Kim, H. Lee, B.K. Na, H.K. Song. *Catal. Today*. **2004**, *89(1-2)*, 193-200.

[24] K. Cheah, M. Forsyth, V.T. Truong. *Synth. Met.* **1999**, *101(1-3)*, 19.

[25] P. Mavinakuli, S. Wei. Q. Wang, A.B. Karki, S. Dhage, Z. Wang, D.P. Young, Z. Guo. *J. Phys. Chem. C*. **2010**, *114*, 3874-3882.

[26] T.A. Skotheim, J.R. Reynolds. *Recent advances in polypyrrole* in *Handbook of conducting polymers. Conjugated polymers: theory, synthesis, properties, and characterization*. 3rd ed. CRC Press: Boca Raton, FL, USA. **2007**, Chap. 8.

[27] N. Dubey, M. Leclerc. *J. Polym. Sci., Part B: Polym. Phys*. **2011**, *49(7)*, 467-475.

[28] B. Sari, M. Talu. *Synth. Met*. **1998**, *94(2)*, 221-227.

[29] O.S.G.P. Soares, E.O. Jardim, A. Reyes-Carmona, J. Ruiz-Martínez, J. Silvestre-Albero, E. Rodríguez-Castellón, J.J.M. Órfão, A. Sepúlveda-Escribano, M.F.R. Pereira. *J. Colloid Interface Sci*. **2012**, *369(1)*, 294-301.

Chapter VI. Metal-free procedure for the removal of nitrates in water: effect of the oxidant used in the synthesis of polypyrrole

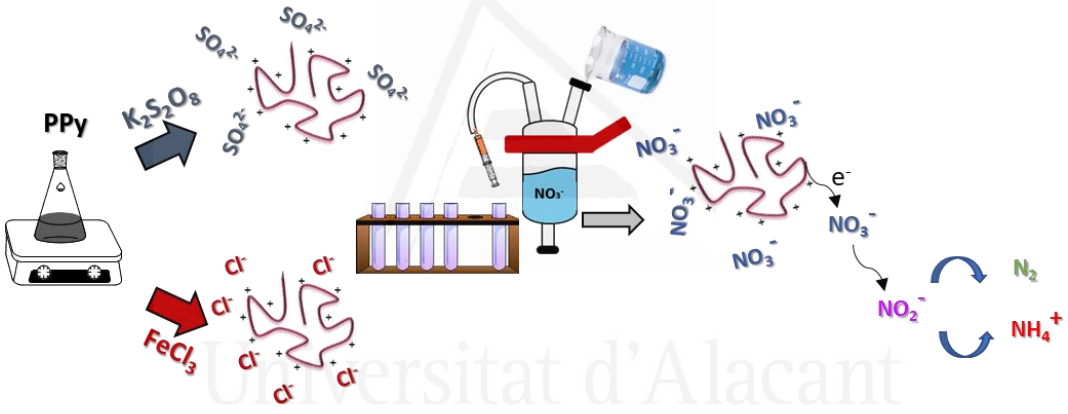

1. INTRODUCTION

In the previous chapter, it has been showed that nitrate abatement produced by the hydrogenation of nitrate using monometallic and bimetallic catalysts supported on PPy is less effective than the nitrate removal produced by the metal-free polymer (either in the presence or not of hydrogen). As the metal nanoparticles are anchored to the PPy chain at the nitrogen positions, the electron transfer from PPy to nitrate is considerably reduced. Thus, electron transfer between PPy and nitrate is direct in the absence of the metal catalyst, which results in a more effective nitrate reduction. In this chapter, PPy will be synthesized using two different oxidants and the mechanisms which govern the abatement of nitrate in the presence of the metal-free conducting polypyrrole will be analyzed.

PPy is cheap, easy to prepare, and has a very good environmental stability. It is a conjugated polymer that has switchable oxidation states. Its synthesis can be carried out by electro-polymerization on a conductive substrate (electrode) through the application of an external potential, or by chemical polymerization in solution with the use of a chemical oxidant. The polymerization reaction of pyrrole is shown in Scheme 6.1. In a first step, a neutral pyrrole monomer (Scheme 6.1a) oxidizes and yields a cation radical (Scheme 6.1b), which can recombine to form a bypyrrole (dication) (Scheme 6.1c). Then, the bypyrrole suffers deprotonation producing a neutral molecule (Scheme 6.1d) which undergoes further oxidation (Scheme 6.1e), recombination and deprotonation steps until neutral polypyrrole (Scheme 6.1f) is obtained as the final product [1,2]. Chemical polymerization is carried out with relatively strong chemical oxidants, such as potassium peroxydisulfate ($K_2S_2O_8$) and iron (III) chloride ($FeCl_3$), which are able to oxidize the pyrrole monomer. The oxidant also provides a counterion (the dopant), which is the oxidant's anion or its reduced product [1,3]. Chemical polymerization occurs in the bulk of the solution, and the resulting polypyrrole precipitates as an insoluble solid.

It has been determined [4] that there is one anion for every 3 – 4 pyrrole units, depending on the type and charge of the anion that is incorporated to provide electroneutrality. This represents a level of oxidation of 0.25 – 0.33 per pyrrole unit Scheme 6.2.

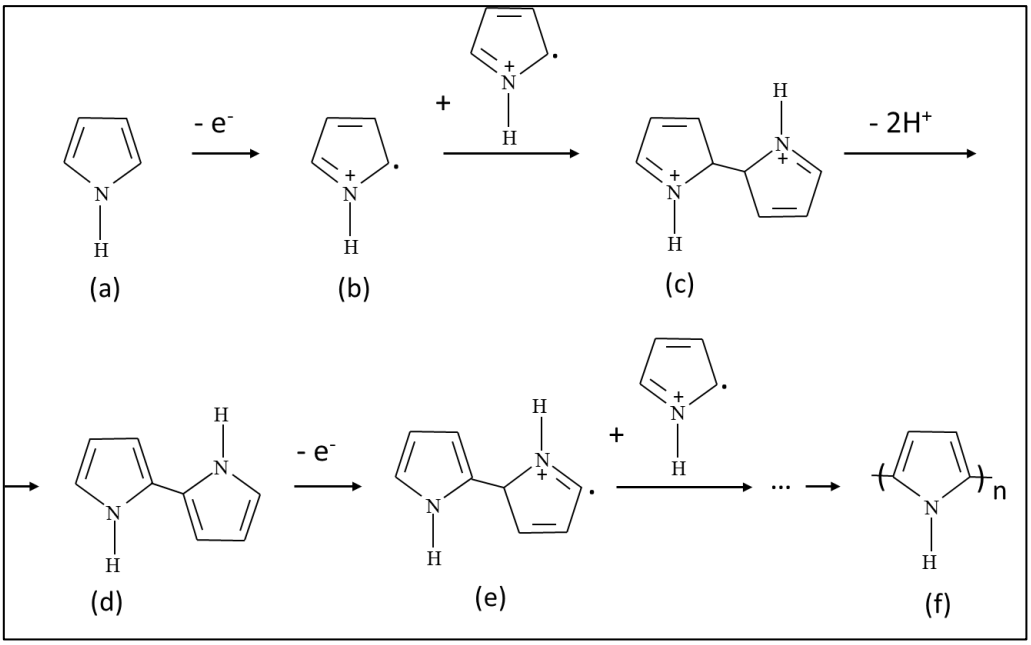

Scheme 6.1. Schematic representation of polypyrrole synthesis.

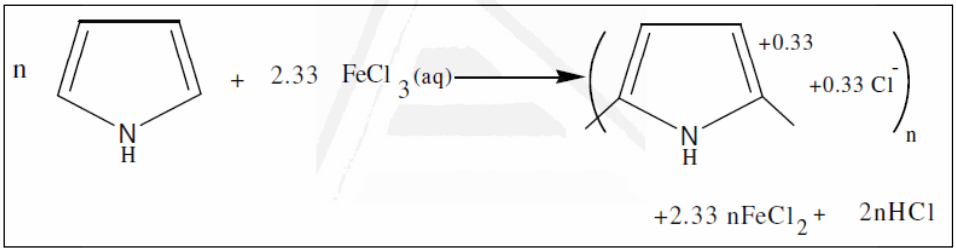

Scheme 6.2. Schematic representation of the oxidative chemical polymerization of pyrrole with $FeCl_3$, showing 0.33 oxidation level per pyrrole unit (figure adapted from [5]).

As a result of the simultaneous oxidation and polymerization of the pyrrole monomer, a delocalized positive charge on the π-electron system is produced. The mechanism of conduction in these polymers is based on the motion of charged carriers called "polarons" and "bipolarons" (biradical cations) within the conjugated framework. Neutral PPy behaves as an insulator with a band gap of 3.16 eV. Upon extraction of a negative charge from a neutral segment of a PPy chain a polaron is formed [1,3] (Fig. 1.2 in Chapter I, Section 1.1), and as a result, new intermediate states are introduced within the band gap [1] (Fig. 1.1 in Chapter I, Section 1.1). As oxidation continues further, another electron is removed from the PPy chain that already contains a polaron, this resulting in the formation of a bipolaron, which is energetically preferred to the formation of two polarons. The bipolaron is known to extend over about four pyrrole units. As the degree of oxidation increases, the bipolaronic energy states overlap, resulting in the

formation of narrow intermediate band structures. Formation of polarons and bipolarons as charge carriers are responsible for the increase of electrical conductivity of PPy and, also, for the capability of PPy of alternating between different switching oxidation states. Like most of the conducting polymers, polypyrrole is doped/undoped by redox reactions. Delocalized electronic states combined with the restriction on the extent of delocalization make most of the conductive polymers to behave like p-type semiconductors.

The dopant (A^-) is not necessarily the supporting electrolyte anion (if polypyrrole is prepared by electropolymerization) or the counteranion from the oxidant (if chemical oxidative polymerization is carried out). Other negatively charged molecules (surfactants or polyelectrolites) can be incorporated to the polypyrrole matrix as dopants [6]. When small dopants are used, the counterion (A^-) is able to freely leave the polymer matrix when the redox process takes place. This is the case for Cl^- and $S_2O_8^{2-}$. If large anion dopants as polyelectrolytes or surfactants are used [2,4], they will remain immobilized within the polymer matrix and, in this case, cation movement towards the counterion will predominate to provide electroneutrality (Scheme 6.3).

Therefore, oxidation of pyrrole produces a charged polymer with incorporated anions. During a following reduction process (e.g. by electrochemically applying a sufficiently negative potential) these anions (A^-) are released (undoping) in such a way that electroneutrality is maintained. It is also possible [2,4] that cations from the electrolyte solution (C^+) are incorporated (Scheme 6.3b). On the other hand, if a positive potential is applied to oxidize the neutral polypyrrole, either the anions are incorporated (doping) or the cations are expelled. However, the basic structure of the polymer is not modified by the ion-exchange process and, then, its morphology is altered [2,3].

It has been reported [7] that when a conducting polymer such as PPy is exposed to some gases or liquids, electron transfer from or to the analyte takes place. Gases as NO_2 or vapors as I_2, which are electron acceptors, can remove electrons from the aromatic ring of polypyrrole. In this case, the doping level of this p-type conductive polymer, as well as its electrical conductance, is enhanced. Conversely, when an electron donating gas such as ammonium is brought into contact with PPy, the polymer conductance falls down sharply.

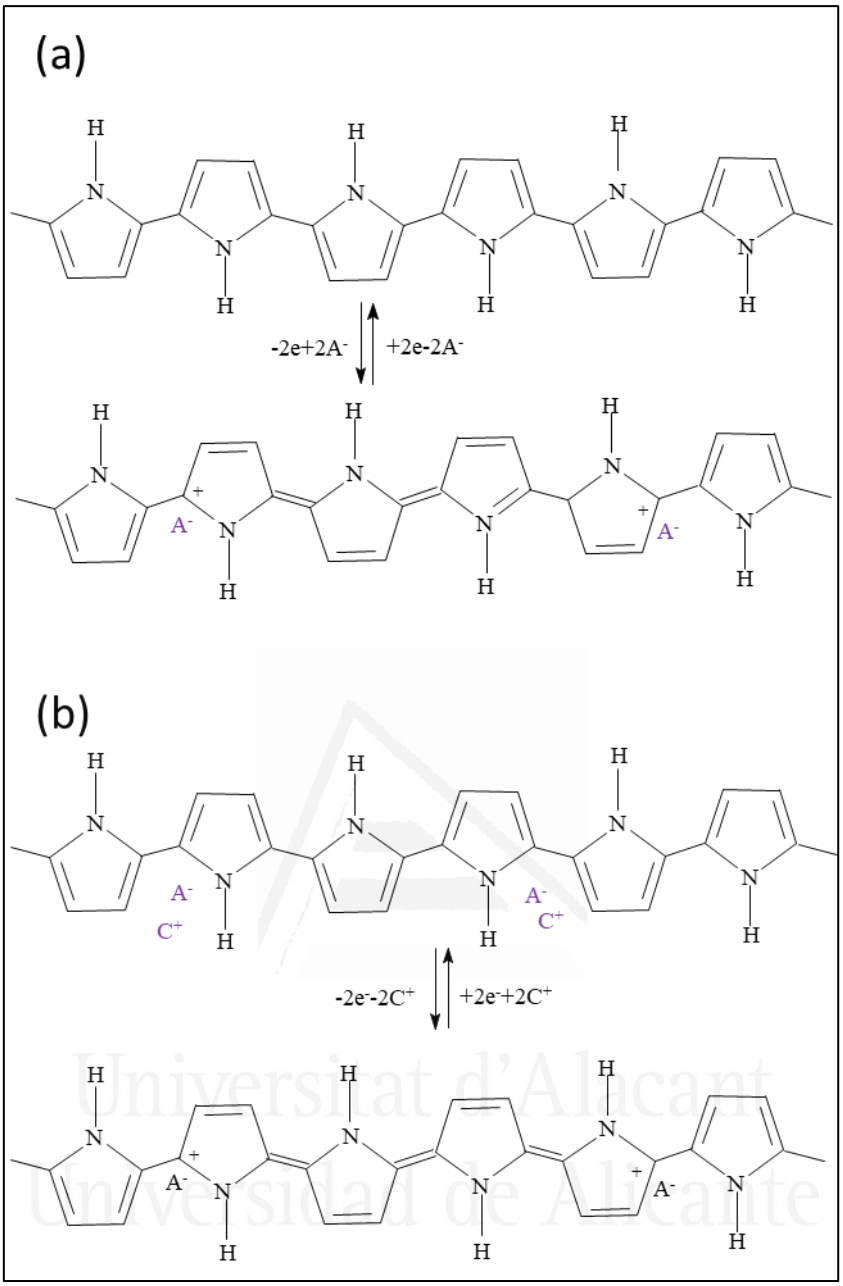

Scheme 6.3. Schematic representation of polypyrrole when a (a) small or (b) large anion dopant is used during its synthesis.

The ion-exchange and the redox properties of PPy make this polymer suitable for removal of toxic contaminants from aqueous solutions. In this chapter, the effect of the counterion acting as dopant on the mechanism of removal of nitrates from water has been considered. Polypyrrole has been synthesized by chemical polymerization of pyrrole (C_4H_5N) using ferric chloride ($FeCl_3$) or potassium peroxydisulfate ($K_2S_2O_8$) as oxidants and dopants. Ferric chloride provides chloride ions as counterion to the oxidized polypyrrole chain to maintain charge neutrality. Potassium peroxydisulfate acts as a

dopant providing either $S_2O_8^{2-}$ anions, or SO_4^{2-} anions resulting from the redox reaction with the pyrrole monomer. Ion exchange and redox properties of PPy are likely affected by the oxidant used in the synthesis. The ability of PPy for removing nitrate by ion-exchange with the counterion and/or by reduction by electrons provided by the pyrrolic chain has been evaluated (Scheme 6.4).

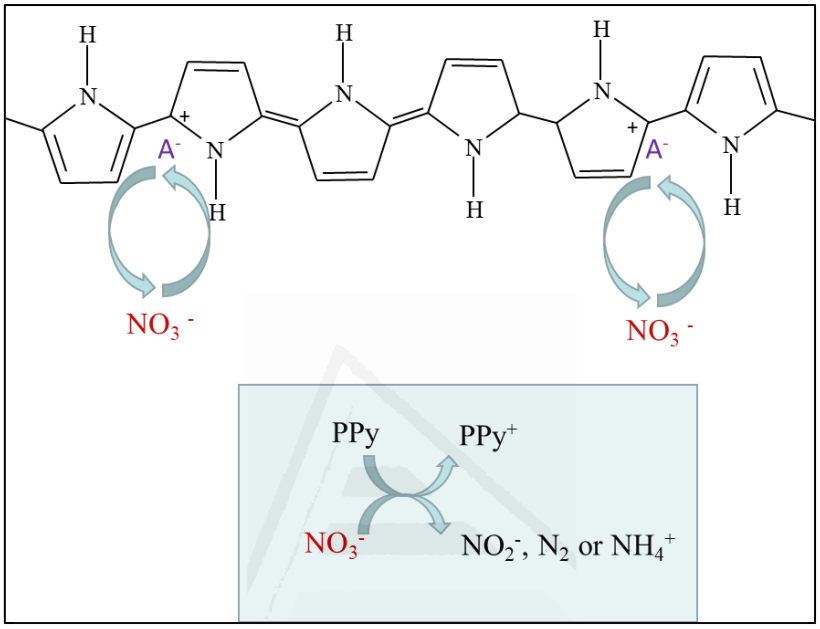

Scheme 6.4. Schematic representation of ion exchange between counterion in doped polypyrrole and nitrate from water and further nitrate reduction by electrons from polypyrrole chain.

2. EXPERIMENTAL

2.1. Materials preparation

Potassium peroxydisulfate ($K_2S_2O_8$) or ferric (III) chloride hexahydrate ($FeCl_3 \cdot 6H_2O$) were used as oxidants and dopants in the chemical polymerization of pyrrole (C_4H_5N) [8]. The experimental procedure was described in Chapter II, Section 1.1.1.

2.2. Materials characterization

The different samples were characterized, before and after being put into contact with the aqueous nitrate solution, by different techniques: electrical conductivity, N_2 adsorption at -196 °C, X-ray diffraction (XRD), thermogravimetric analysis (TGA),

infrared spectroscopy (FTIR) and X-ray photoelectron spectroscopy (XPS). The specifications of the equipments used in the different characterization techniques are detailed in Chapter II, Section 2.

2.3. Nitrate abatement evaluation

The ability of polypyrrole samples synthesized with both oxidants to abate nitrate from water was tested using a semi-batch reactor equipped with a magnetic stirrer (700 rpm) as detailed in Chapter II, Section 1.4. No external reductant as H_2 was used, however, a CO_2 flow was passed for 15 min through the reactor with a flow rate of 75 $mL \cdot min^{-1}$ to assure removal of oxygen and buffer the solution to keep a constant value of pH ≈ 5. Aliquots (1 mL) were withdrawn at different times from the reactor and immediately filtered for determination of nitrate, nitrite and ammonium concentrations by ion chromatography as indicated in Chapter II, Section 2.9.

3. RESULTS AND DISCUSSION

3.1. Characterization of the polymers

Polypyrrole chemically synthesized with $K_2S_2O_8$ and $FeCl_3$ showed electrical conductivity values of 25 and 4.5 $S \cdot m^{-1}$, respectively. PPy/$FeCl_3$ and PPy/$K_2S_2O_8$ showed low BET surface areas of of 4 and 11 $m^2 \cdot g^{-1}$, respectively. Figure 5.1 (Chapter V, Section 3.1) and Figure 6.1 show the corresponding isotherms characteristic of non-porous materials.

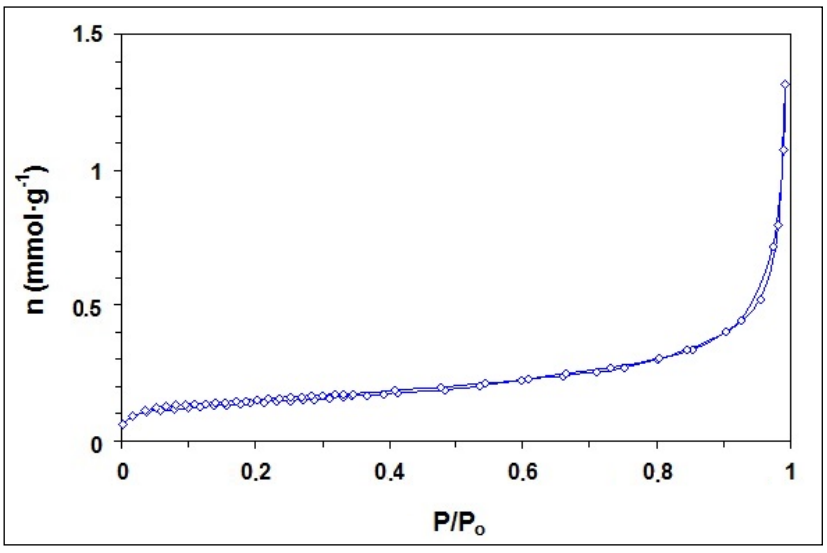

Figure 6.1. Nitrogen adsorption isotherm at - 196 °C of PPy/$K_2S_2O_8$.

The X-ray diffraction patterns of both materials (Fig. 6.2) are similar and characteristic of amorphous polymers, with a broad peak centered at 2θ = 25.0 º due to the scattering from PPy chains at the interplanar spacing.

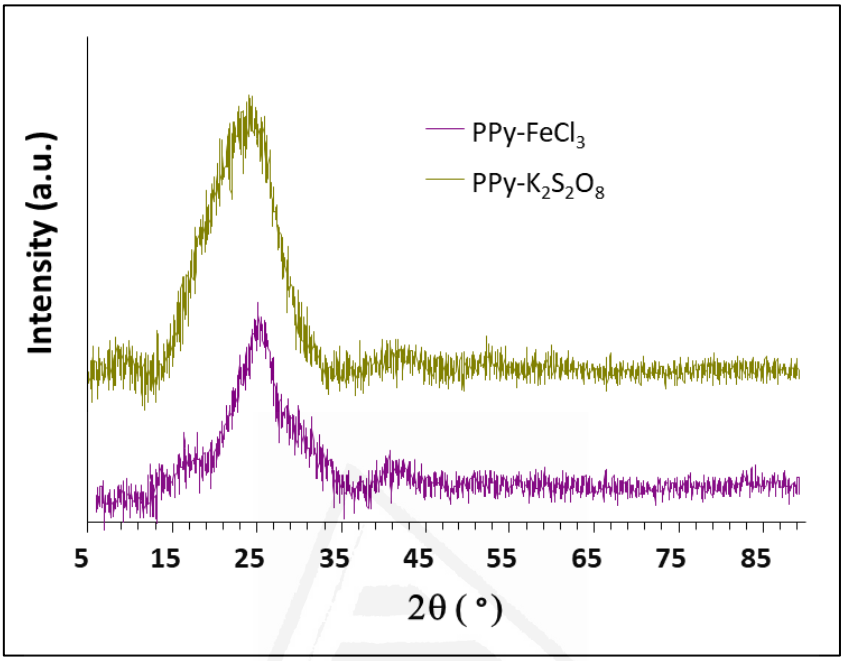

Figure 6.2. XRD patterns of polypyrrole synthesized with (a) $FeCl_3$ (PPy/$FeCl_3$) and (b) $K_2S_2O_8$ (PPy/$K_2S_2O_8$).

DSC analysis of polypyrrole is characteristic of an amorphous polymer, what is in agreement with the XRD profile. The glass transition temperature is located between 50 and 100 °C, and degradation of the polymer occurs around 700 °C in all cases, irrespective of the oxidant and of the pre-treatment (Fig. 6.3). The thermal stability of polypyrrole was also analyzed by TGA (Fig. 6.4). There is a first mass loss (about 8 – 9 %) between 30 and 100 °C due to the loss of non-reacted monomer and water. At 200 °C, only 15 % of the mass is lost. Degradation of the polymer is accelerated from 700 °C and almost complete for polypyrrole synthesized with $K_2S_2O_8$ (10 % mass remains). However, around 20 % mass of the polymer is retained when polypyrrole is synthesized with $FeCl_3$.

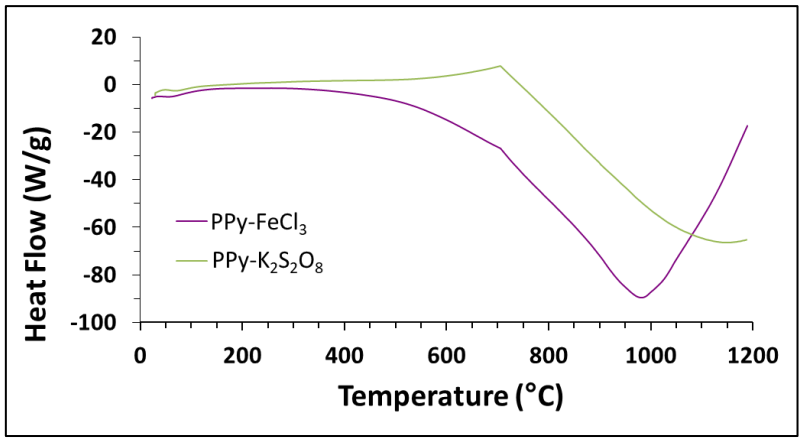

Figure 6.3. DSC profile in N_2 atmosphere of chemically synthesized polypyrrole with $FeCl_3$ (PPy/$FeCl_3$) and $K_2S_2O_8$ (PPy/$K_2S_2O_8$).

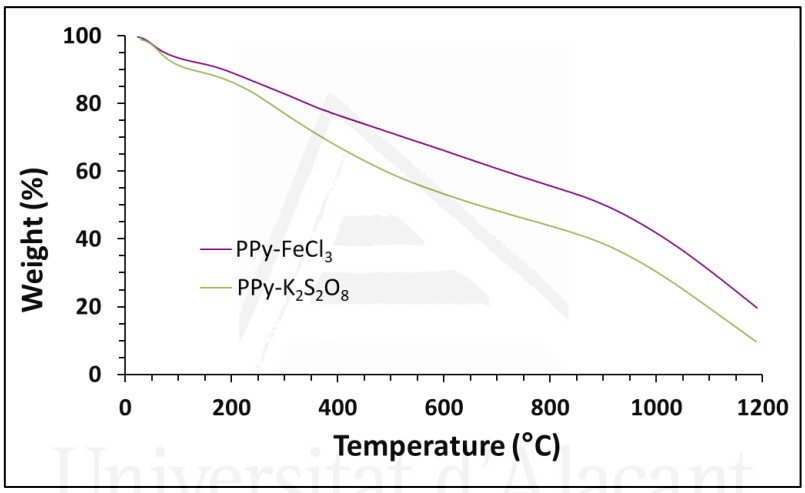

Figure 6.4. TGA profile in N_2 atmosphere of chemically synthesized polypyrrole with $FeCl_3$ (PPy/$FeCl_3$) and $K_2S_2O_8$ (PPy/ $K_2S_2O_8$).

FTIR spectra of PPy synthesized with both oxidants show typical absorption bands (Fig. 6.5): C=C stretching (1485 cm^{-1}), C-C stretching (1298 and 1102 cm^{-1}), =C-H out of plane bending (1046 cm^{-1}) and N-H bending (801 cm^{-1}). Characteristic bands of C=N-C are slightly shifted towards higher wavenumbers in PPy/$K_2S_2O_8$ compared to PPy/$FeCl_3$: C=N stretching (1565 vs. 1540 cm^{-1}), C-N stretching (1202 vs. 1183 cm^{-1}) and C=N-C bending (922 vs. 915 cm^{-1}). These bands are attributed in the literature to the bipolaron bands characteristics of the doping [9]. Besides, stretching C=O absorption at 1700 - 1710 cm^{-1} in both spectra suggests the formation of oxygenated moieties as a consequence of the reaction of the polymeric chain with the aqueous medium during polymerization, and also by surface oxygenation upon contact with air.

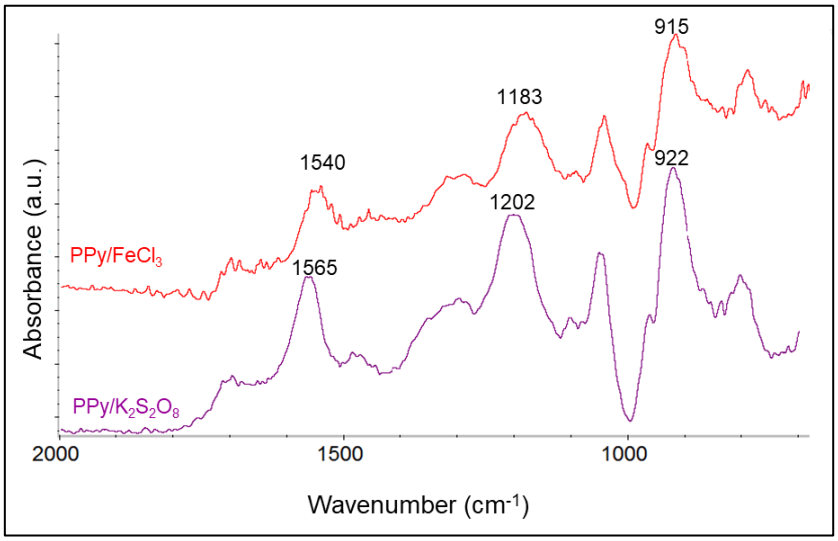

Figure 6.5. FTIR-ATR spectra of polypyrrole synthesized with $FeCl_3$ and $K_2S_2O_8$.

3.2. Nitrate removal ability of polypyrrole

Polypyrrole samples synthesized with both oxidants, $K_2S_2O_8$ and $FeCl_3$, were put into contact with an aqueous nitrate solution to evaluate their ability to remove nitrate from water. Figure 6.6 shows a considerable abatement of nitrate in solution produced by PPy in the absence of any other reductant. In less than 10 min, nitrate concentration falls down the maximum allowed concentration in drinking water (50 $mg \cdot L^{-1}$). This nitrate removal produced by PPy is considerably more efficient that the catalytic hydrogenation using platinum supported on PPy [10]. As discussed in the previous chapter, the electron transfer from PPy to nitrate is considerably reduced because of Pt nanoparticles are anchored to the PPy chain at the nitrogen positions. However, electron transfer between PPy and nitrate is direct in the absence of the metal catalyst, what result in a more effective nitrate reduction.

Nevertheless, depending on the oxidant used to polymerize pyrrole, there is a significant difference not only in the decrease of nitrate concentration, which is more significant with $PPy/FeCl_3$, but also in the by-products detected by ion chromatography. Thus, the oxidant used in the preparation of PPy greatly affects the selectivity in nitrate reduction.

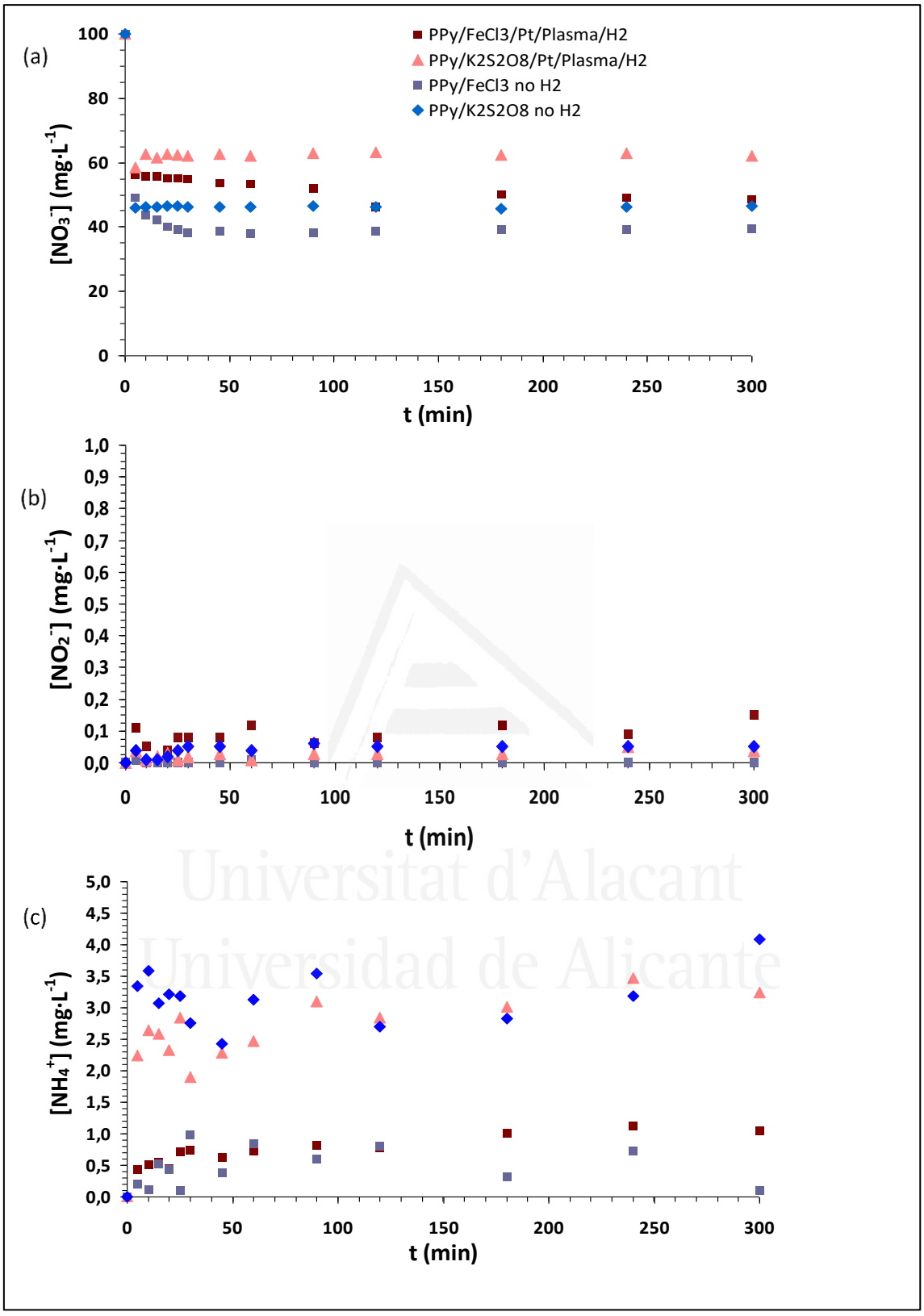

Figure 6.6. (a) Nitrate, (b) nitrite and (c) ammonium concentrations ($mg \cdot L^{-1}$) as a function of time (min), determined by ion chromatography during aqueous nitrate reduction with and without hydrogen in the presence of polypyrrole synthesized with $FeCl_3$ and $K_2S_2O_8$.

XPS characterization results can add some light to understand this different behavior. Oxygen is present in both polymers, but in a considerable higher percentage in PPy/$K_2S_2O_8$ compared to PPy/$FeCl_3$ (18.0 at. % vs 6.5 at. %) (Table 6.1). Oxygenated moieties are detected in the curve fit of the C 1s level (Fig. 6.7) as C-O (286.2 eV) or C=O (287.6 eV). This is in agreement with the stretching band of C=O at 1700 - 1710 cm^{-1} detected by FTIR, which is more intense in PPy/$K_2S_2O_8$. Depending on the oxidant used $K_2S_2O_8$ or $FeCl_3$, S or Cl are detected by XPS. The binding energy of S 2p peak (168.3 eV) in PPy/$K_2S_2O_8$ corresponds to sulfate ion, this evidencing reduction of $S_2O_8^{2-}$ to SO_4^{2-} when incorporates as a counterion to the polymeric chain during the oxidative polymerization of pyrrole with potassium peroxydisulfate. When ferric chloride is used, chlorine ion is detected in PPy/$FeCl_3$ (Cl $2p_{3/2}$ at 198.5 eV). These results support the ability of the oxidants to provide counterions to neutralize the positively charged polymeric chain. Some chlorine is also detected in PPy/$K_2S_2O_8$ (Table 6.1), which may come from water contamination, and this evidences the ion-exchange ability (some SO_4^{2-} anions replaced by some Cl^- anions) of counterions in the oxidized PPy chain [11]. Cations from the oxidants are not anchored to the positively charged polymeric chain and, in this way, neither potassium is detected in PPy/$K_2S_2O_8$ nor is iron detected in PPy/$FeCl_3$.

Table 6.1. XPS surface chemical composition (atomic %) of the different samples.

Binding energy (*eV*)	284.5	531.5	398.1	198.5	168.3
Element	**C 1s**	**O 1s**	**N 1s**	**Cl 2p**	**S 2p**
PPy/$K_2S_2O_8$	69.2	18.0	12.2	0.2	0.4
PPy/$K_2S_2O_8$-R[a]	69.5	17.8	12.4	0.1	0.2
PPy/$FeCl_3$	78.0	6.5	13.1	2.4	-
PPy/$FeCl_3$-R[a]	75.2	14.4	9.8	0.6	-

[a] R = recovered catalyst after 300 min of reaction.

The oxidation degree of the polymeric chains can be evaluated from the XPS analysis of the N 1s level. The N 1s experimental band can be deconvoluted into four contributions, each of them corresponding to a different nitrogen species: neutral imine nitrogen atom (-N=), neutral amine (-NH-), positively charged nitrogen ($-N^+$) and protonated imine ($=N^+$), with increasing binding energy values as the oxidation degree increases. Polypyrrole synthesized with $K_2S_2O_8$ shows 93 % of positively charged nitrogen at 400.3 eV (Fig. 6.8, Table 6.2), whereas PPy/$FeCl_3$ results to be in a less oxidized form (65 % of positively charged nitrogen). These results can be correlated with

the differences in electrical conductivities found for PPy/$K_2S_2O_8$ and PPy/$FeCl_3$, respectively.

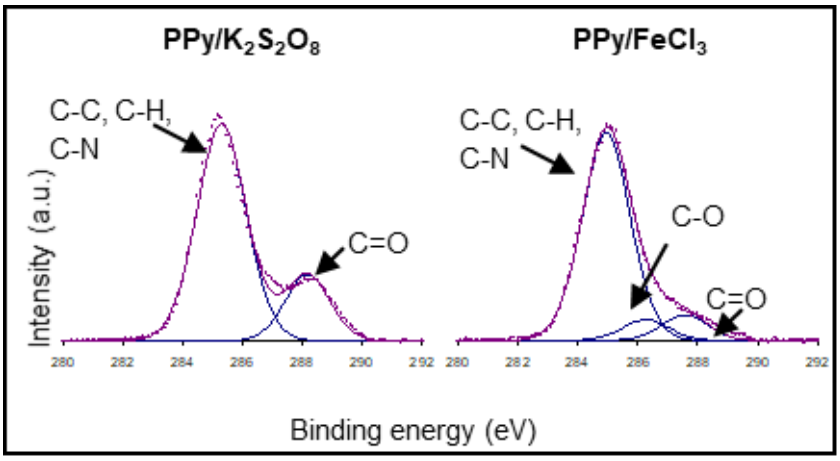

Figure 6.7. XPS C 1s spectra of polypyrrole synthesized with (a) $K_2S_2O_8$ and with (b) $FeCl_3$.

Table 6.2. Percentages of the different surface species estimated from the areas of the contribution to the XPS corresponding to the N 1s level.

Sample	Binding energy (*eV*)	Species	Composition (%)
PPy/$K_2S_2O_8$	398.8	-N=	7
	400.3	$-N^+$	93
PPy/$K_2S_2O_8$-R[a]	399.8	-NH-	33
	400.6	$-N^+$	67
PPy/$FeCl_3$	399.7	-NH-	35
	400.3	$-N^+$	65
PPy/$FeCl_3$-R[a]	400.1	$-N^+$	95
	401.3	$=N^+$	5

[a] R = recovered catalyst after 300 min of reaction.

When the polymers are put into contact with the aqueous nitrate solution, ion exchange between the polypyrrole counterions and NO_3^- may occur. However, reduction of nitrate might also be produced by electrons transferred from the PPy chain, what is consistent with the reduction potential of nitrate (NO_3^-/NH_4^+, E° = 0.875 V; NO_3^-/N_2, E° = 1.246 V) and polypyrrole (PPy^+/PPy, E° = 0.150 V). The extension of ion exchange and reduction mechanisms seems to be affected by the oxidant used in the polymerization of pyrrole.

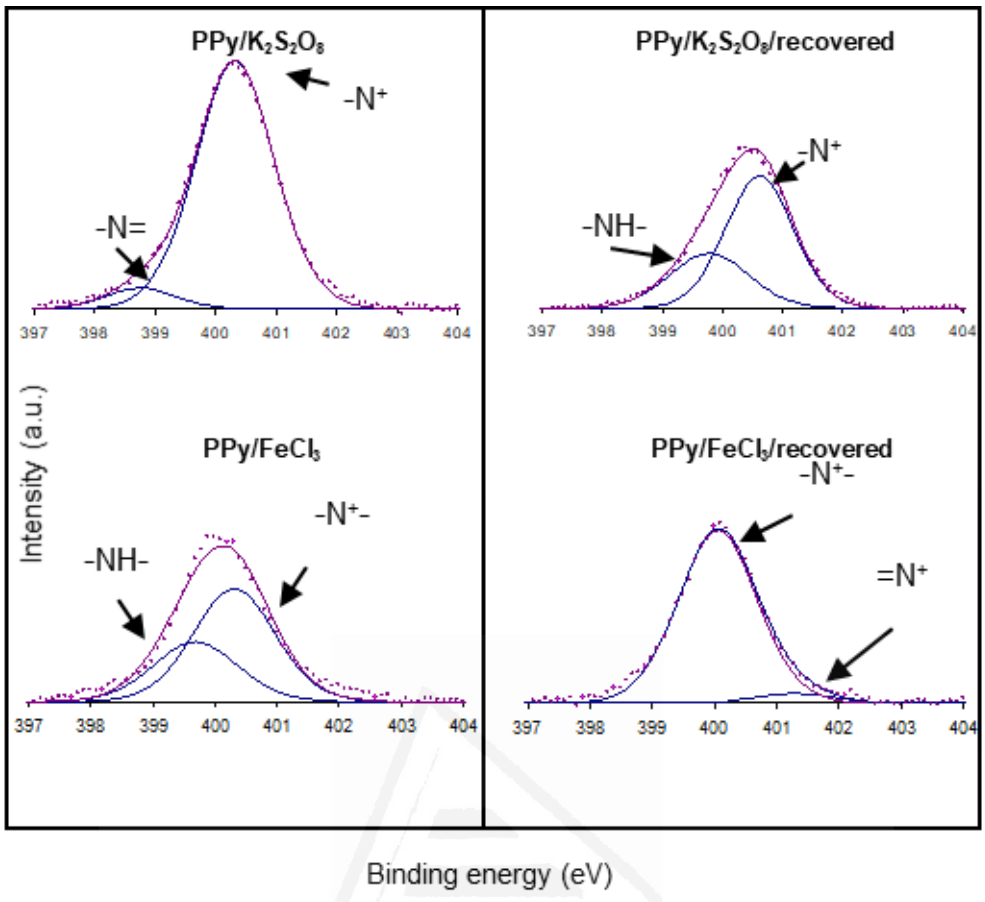

Figure 6.8. Curve fit of N 1s level in XPS spectra of PPy synthesized with $K_2S_2O_8$ and $FeCl_3$, pristine and recovered after contact with nitrate solution for 300 min.

Nitrate is reduced to nitrogen and ammonium through intermediate nitrite by the polypyrrole chain of PPy/$K_2S_2O_8$. Nitrogen can not be detected in solution, but nitrite and ammonium ions are indeed detected by ion chromatography (Table 6.3), which reveals that nitrate is being reduced by polypyrrole. In the case of PPy/$FeCl_3$, neither nitrite nor ammonium ions are detected.

Table 6.3. Nitrate, nitrite and ammonium concentrations, nitrate conversion and selectivities to nitrite and ammonium after 300 min of nitrate reduction without hydrogen.

Sample	(mg·L^{-1})			(%)			
	[NO_3^-]	[NO_2^-]	[NH_4^+]	$X_{NO_3^-}$	$S_{NO_2^-}$	$S_{NH_4^+}$	S_{N_2}
PPy/$K_2S_2O_8$ without H_2	46.6	0.05	4.1	53	0.1	26.1	73.8
PPy/$FeCl_3$ without H_2	39.7	0	0.1	61	0	0.6	100

Nitrate conversion $\left(X_{NO_3^-}\right)$ and selectivities to nitrite $\left(S_{NO_2^-}\right)$, ammonium $\left(S_{NH_4^+}\right)$ and nitrogen (S_{N_2}) after 300 min reaction, which are shown in Table 6.3, were calculated using the equations 2.8, 2.9, 2.10 and 2.11 (Chapter II, Section 2.9).

The oxidant used in the polymerization of pyrrole affects the selectivity of nitrate reduction by electrons coming from the polymer. Thus, PPy/$FeCl_3$ is highly selective to nitrogen, whereas selectivity to nitrogen is considerably decreased in PPy/$K_2S_2O_8$ due to the higher production of ammonium ($S_{NH_4^+}$ = 26.1 %).

Polymers were recovered from solution after 300 min reaction and analyzed by XPS. The surface composition of the recovered PPy/$K_2S_2O_8$ after being in contact with the nitrate solution for 300 min is quite similar to that of the pristine polymer, except for a decrease of the amount of sulfur species (from 0.4 to 0.2 at. %) (Table 6.1). PPy/$FeCl_3$/recovered shows a more important decrease of the amount of chlorine species (from 2.4 to 0.6 at. %), together with a considerable increase of the surface oxygen concentration (from 6.5 to 14.4 at. %). The relative size of the chloride ionic radius (181 pm) and the thermochemical radii of NO_3^- (179 pm) and SO_4^{2-} (258 pm) [12] determines that exchanging of nitrate ion with chloride ion is easier than with sulfate ion [13].

Although nitrate is exchanged with chloride or sulfate counterions it is not detected by XPS in the recovered polymers, as no contribution to the N 1s peak at 406 eV is observed (Fig. 6.8). This suggests that after ion exchange between chloride or sulfate in PPy and nitrate in the aqueous solution, reduction of nitrate by electrons from the polymer is produced. A stepwise reaction which implies reduction of nitrate to nitrite could take place. However, XPS analysis of recovered PPy did not show any nitrite contribution (XPS peak at 403.6 eV, Fig. 6.8). Some nitrite is detected in solution (0.05 $mg \cdot L^{-1}$) when PPy/$K_2S_2O_8$ is used, although most of it is reduced to ammonium (4.1 $mg \cdot L^{-1}$, Table 6.3) or to N_2 (not measured). As a consequence of the reduction of nitrate ions in solution with electrons from the polypyrrole chain, an important oxidation is observed in PPy/$FeCl_3$/recovered (Fig. 6.8, Table 6.2). Thus, positively charged nitrogen ($-N^+$) and protonated imine ($=N^+$) species are detected.

XPS results support that the initial oxidation degree of the polymer imparted by the oxidant ($K_2S_2O_8$ or $FeCl_3$) is determinant in the ability of the polymer to produce the reduction of nitrate by electron transfer from the PPy chain to the nitrate ions. The more reduced the pristine polymeric chain, the more important the reduction transfer to nitrate. PPy/$FeCl_3$ is initially in a more reduced state than PPy/$K_2S_2O_8$ and, in this way, abatement of nitrate in the aqueous solution is more effective with the former (Fig. 6.6). Besides, neither nitrite nor ammonium are produced in the presence of PPy/$FeCl_3$ (Fig. 6.6, Table 6.3).

The oxidized nitrogen moieties found in the recovered PPy/$FeCl_3$ after 300 min in contact with the nitrate solution suggest that PPy has taken part in the redox process. Although the amount of nitrogen gas produced can not be determined, the absence of ammonium and nitrite suggest that nitrate has been mainly reduced to nitrogen in the presence of PPy/$FeCl_3$. The maximum allowed levels of nitrite and ammonium in drinking water are 0.5 $mg \cdot L^{-1}$ for both [14]. Considering the final concentrations of nitrate, nitrite and ammonium in solution, and also the selectivities to nitrite and ammonium of the reduction reaction (Table 6.3), it can be concluded that PPy/$FeCl_3$ is appropriate to effectively remove nitrate from drinking water following the European regulations. On the other hand, ammonium levels exceeding the maximum allowed ammonium concentrations are obtained with PPy/$K_2S_2O_8$.

4. CONCLUSIONS

The oxidant used in the chemical polymerization of pyrrole plays a definitive role in the ability of this polymer to remove nitrate from water. From the results obtained in this chapter, it can be concluded that:

a) Ion exchange and redox properties of PPy are affected by the oxidant used in the synthesis, $K_2S_2O_8$ or $FeCl_3$, as they provide different counterions and produce a different degree of oxidation of the pyrrolic chain.

b) The initial oxidation degree of the polymer, imparted by the oxidant, is determinant in the ability of the polymer to produce the reduction of nitrate in aqueous solution by electron transfer from the polypyrrole chain to the nitrate anion. The more

reduced the pristine polymeric chain, the more important the electron transfer to nitrate. Consequently, nitrate reduction is more effectively produced by PPy/$FeCl_3$, which is in a more reduced state than PPy/$K_2S_2O_8$.

c) The selectivity of nitrate reduction to nitrogen is also affected by the oxidant. Nitrate is selectively reduced to N_2 in the presence of PPy/$FeCl_3$, whereas the reaction is highly selective to ammonium with PPy/$K_2S_2O_8$. Considering the final concentration of nitrate, nitrite and ammonium, and also the selectivities to nitrite and to ammonium, it can be concluded that PPy/$FeCl_3$ is appropriate to effectively remove nitrates from drinking water in agreement with the European regulations.

5. REFERENCES

[1] T.A. Skotheim, J.R. Reynolds. *Recent advances in polypyrrole* in *Handbook of conducting polymers. Conjugated polymers: theory, synthesis, properties, and characterization*. 3rd ed. CRC Press: Boca Raton, FL, USA. **2007**, Chap. 8.

[2] A. Malinauskas. *Polymer*. **2001**, *42(9)*, 3957-3972.

[3] R. Ansari. *Russ. J. Electrochem*. **2005**, *41(9)*, 950-955.

[4] R. Ansari, N. Khoshbakht-Fahim, A. Fallah-Delavar. *The Open Proc. Chem.* J. **2009**, *2*, 1-5.

[5] U. Prüsse, M. Hähnlein, J. Daum, K.D. Vorlop. *Catal. Today*. **2000**, *55(1-2)*, 79-90.

[6] M.H. Ansari, J.B. Parsa. *Separation Purification Technol*. **2016**, *169(1)*, 158-170.

[7] H.K. Chitte, N.V. Bhat, V.E. Walunj, G.N. Shinde. *J. Sensor Technol*. **2011**, *1(2)*, 47-56.

[8] M.J. García-Fernández, S. Sancho-Querol, M.M. Pastor-Blas and A. Sepúlveda-Escribano. *J. Coll.Interf. Sci*. **2017**, *494*, 98-106.

[9] I. Dodouche, F. Epron. *Appl. Catal., B*. **2007**, *76(3-4)*, 291-299.

[10] M.J. García-Fernández, R. Buitrago-Sierra, M.M. Pastor-Blas, O.S.G.P. Soares, M.F.R. Pereira, A. Sepúlveda-Escribano. *RSC Adv*. **2015**, *5*, 32706-32713.

[11] J. Karuppiah, Y.S. Mok. *Int. J. Hydrogen Energy*. **2014**, *39(29)*, 16329-16338.

[12] M. Weller, T.L- Overton, J.P. Rourke, F.A. Armstrong. *Inorganic Chemistry*. 6 th ed. Oxford University Press, UK. **2014**.

[13] H. Ge, G.G. Wallace. *Reactive Polymers*. **1992**, *18(2)*, 133-140.

[14] EC (European Community), Official Journal of the European Communities, Council Directive 98/83/EC on the quality of water intended for human consumption, *The Drinking Water Directive (DWD)*, Brussels. **1998**, Annex 1, Part B, 42-44.

Chapter VII. Proposed mechanisms for the hydrogenation of nitrate catalyzed by platinum nanoparticles supported on polypyrrole and polyaniline

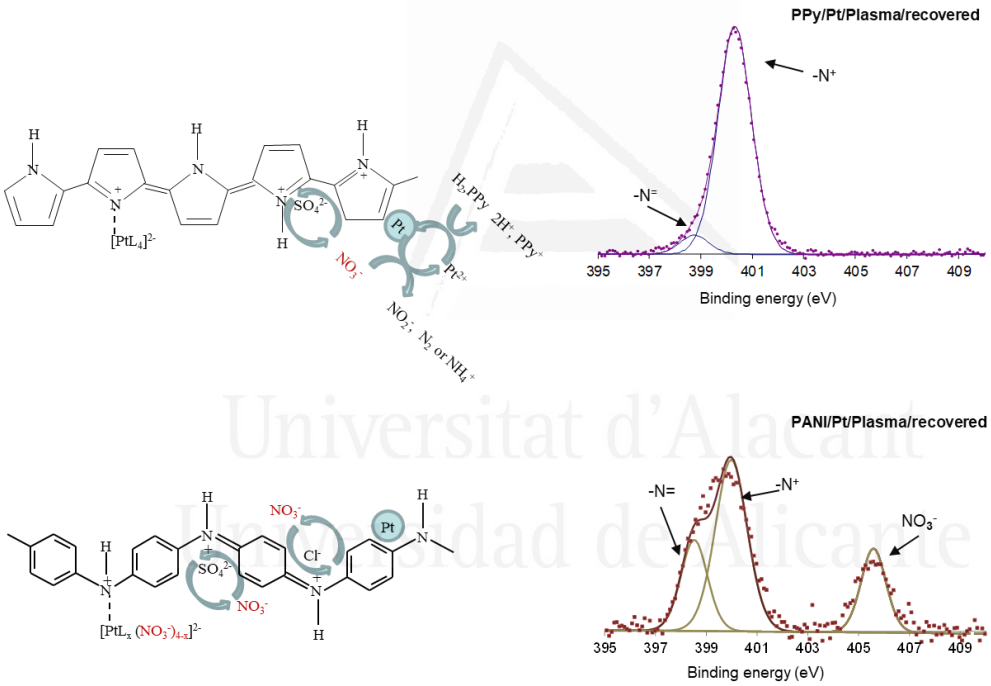

M.J. García-Fernández, M.M. Pastor-Blas, F. Epron, A. Sepúlveda-Escribano, "Proposed mechanisms for the removal of nitrate from water by platinum catalysts supported on polyaniline and polypyrrole", *Applied Catalysis B: Environmental*. **2018**, *225*, 162-171.

1. INTRODUCTION

Since the discovery of electrical conducting properties of conjugated polymers promoted by doping, they have been studied for a great variety of applications such as lightweight battery electrodes, electromagnetic shielding devices, anticorrosion coatings, etc. The feature that makes them useful for most applications is not the metal-like electrical conductivity itself, but the combination of electrical conductivity and polymeric properties such as flexibility, low density and ease of structural modification that suffice for many commercial applications [1]. However, their use in catalysis had not been extensively studied. In chapter V it has been demonstrated that nitrate can be abated from water by catalytic hydrogenation in the presence of platinum supported on polypyrrole. In this chapter, the study will be extended to other conducting polymer, polyaniline (PANI), used as support of the metal catalyst.

Among conducting polymers, polypyrrole (PPy) and polyaniline (PANI) have attracted great attention. Their hetero-aromatic and extended π-conjugated backbone structure provides them with chemical stability and electrical conductivity, respectively. However, the π-conjugated structure is not enough to produce appreciable conductivity on its own; a doping process, which can be achieved chemically or electrochemically, is necessary. This produces a partial charge extraction from the polymer chain and, depending on the doping degree, polypyrrole and polyaniline can exhibit multiple inherent oxidation states. Charge carriers are located in the main chain and compensated by counterions.

The process of chemical oxidative polymerization of PPy and PANI is usually followed by visible changes in the color of the polymerization solution. PPy appears yellow-green and dark blue-grey in its neutral (non-conducting) and oxidized (conducting) forms, respectively. When the pyrrole monomer is put into contact with an oxidant (Scheme 7.1), an initially colorless solution turns blue and dark blue after a while, indicating the formation of oligomers. Some time later, the precipitation of a dark blue or black solid polymer is observed, thus corresponding to the conducting PPy [2].

On the other hand, PANI shows the greatest number of characterized forms among the conducting polymers [3]. The polymer is composed of reduced (B-NH-B-NH) and

oxidized (B-N=Q=N-B) units where B and Q are benzenoid and quinoid rings, respectively. The variation of the amine and imine ratio in its structure gives rise to several forms: leucoemeraldine, which contains only benzenoid rings and is the completely reduced form, emeraldine containing half benzenoid rings and half quinoids and pernigraniline that only shows quinoid rings. In turn, each of these forms can be found protonated or deprotonated, producing a total of six forms, which can be transformed into one another by reactions of oxidation, reduction, protonation and deprotonation. Scheme 7.2 shows the different reactions that take place between the different states of PANI. Protonated forms of PANI are known by the term "salt", while non-protonated forms are called "base". They show different colors depending on their oxidation state and their protonation. The leucoemeraldine base is clear yellow, emeraldine base is blue and pernigraniline base is violet. The corresponding protonated forms are leucoemeraldine salt (colorless), emeradine salt (green) and pernigraniline salt (blue but in a different shade than that of emeraldine base).

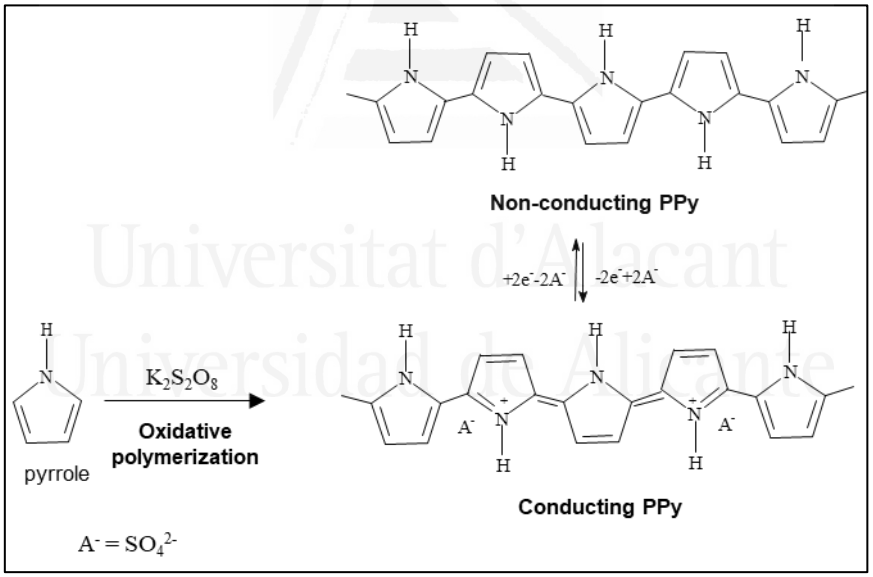

Scheme 7. 1. Scheme showing the oxidative polymerization of pyrrole with potassium peroxydisulfate producing conducting PPy.

The oxidation of aniline in acidic aqueous media using ammonium peroxydisulfate as oxidant has become the most widely synthetic route to produce conducting PANI [3], which is obtained in the form of protonated emeraldine salt, named after its green colour. Emeraldine salt is the one that shows greater electrical conductivity

than the rest of states and is highly stable in environmental conditions (presence of air, humidity).

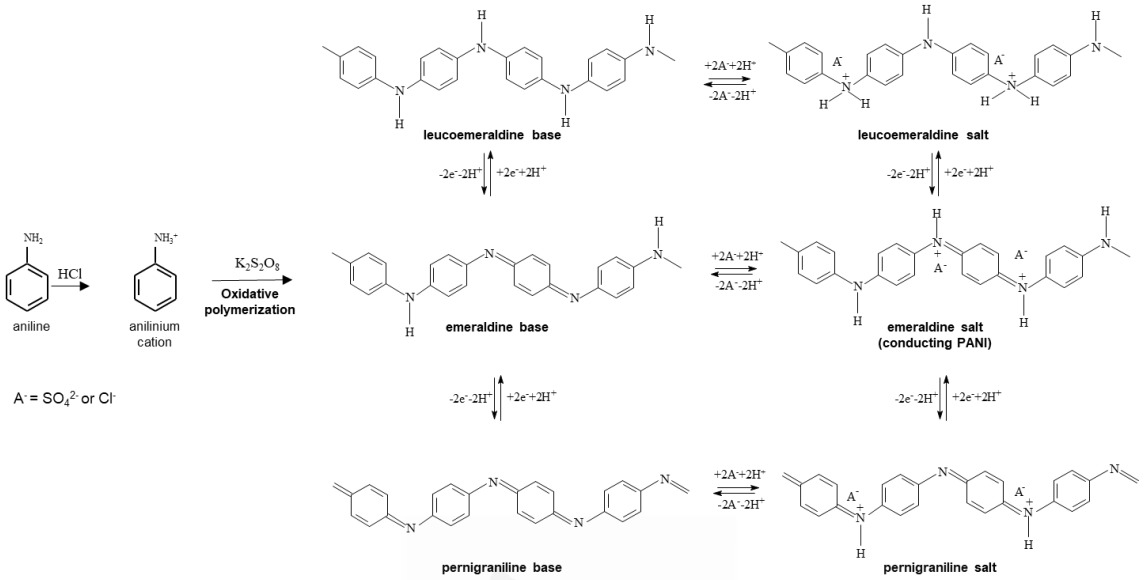

Scheme 7. 2. Scheme showing the oxidative polymerization of aniline with potassium peroxydisulfate in acidic aqueous medium producing conducting PANI.

Metal particles (e.g. Au, Ag, Pt, Pd) can be readily deposited on these polymers by direct chemical or electrochemical redox reactions between the polymer and the oxidative metal cations [4,5]. However, it is not easy to control the size and distribution of the metal particles across the polymer matrix. Many catalyzed reactions require small monodispersed metal particles to achieve a high catalytic activity, so reduction of metal precursors is necessary. The catalytic properties of metal species are closely related to their morphology and particle size, which are normally determined by the reduction conditions. In many cases, catalysts are reduced by flowing hydrogen at elevated temperatures or by chemical reductants, such as formaldehyde, hydrazine or sodium borohydride. In this thesis dissertation, non-thermal Ar plasma has been proposed as an alternative reduction technology operating at room temperature, which complies with the requirements of green chemistry, and is easy to perform [6-8]. The reducibility of metal ions by plasma can be determined by the value of their standard electrode potential; thus, those metal ions with positive standard electrode potential, such as Pd, Pt, Au, Ag, Rh and Ir can easily be reduced by non-hydrogen plasma at room temperature. It is well known that these metals have very interesting applications in catalysis [9].

In this chapter, polypyrrole and polyaniline have been used as support for platinum catalysts, using H_2PtCl_6 as the metal precursor and Ar plasma to reduce it to metallic platinum. The synthesis and characterization of the polymer-supported catalysts, and their catalytic performance in the reduction of nitrates in water have been discussed. As previously described, nitrates are found in excess in water due to the use of fertilizers and waste effluents from industry. Nitrate pollution can cause water reservoirs eutrophication and it is also harmful for humans as it produces cancer and the commonly known blue-baby disease. The European legislation [10] has established a maximum permitted level of nitrate, nitrite and ammonium in water of 50, 0.5 and 0.5 $mg \cdot L^{-1}$, respectively. Recommendations by the World Health Organization (WHO) [11] are similar. Catalytic nitrate reduction at room temperature is a promising process, based on the use of bimetallic catalysts, generally associating a noble metal to a reducible promotor (Cu, Fe, Sn, In, etc.) on a classical support, or of monometallic catalysts where the noble metal is deposited on a reducible support [12]. In many cases, the efficiency of the studied catalysts is not satisfactory as high concentrations of toxic nitrite or ammonium by-products instead of the desired nitrogen are produced. In this sense, it is of great interest to develop catalytic systems that are active in the reduction of nitrates in water, with a high selectivity to nitrogen instead of nitrites or ammonium. The aim of the research described in this chapter is to compare the performance of the platinum catalysts supported on polypyrrole and polyaniline and discern the mechanisms that govern the nitrate abatement form water [13].

2. EXPERIMENTAL

2.1. Materials preparation

An extremely low yield is obtained when PANI is synthesized by oxidative chemical polymerization with $FeCl_3$. Therefore, for comparison purposes, the same oxidant, potassium peroxydisulfate ($K_2S_2O_8$), was used for the synthesis of both, polypyrrole (PPy) and polyaniline (PANI) (Schemes 7.1 and 7.2). In this study, the oxidant/pyrrole molar ratio was 2.33 and the oxidant/aniline molar ratio was 1.25 [13].

PPy was synthesized using potassium peroxydisulfate ($K_2S_2O_8$, *Sigma-Aldrich*, 99 %) as oxidant and dopant in the chemical polymerization of pyrrole (C_4H_5N, *Sigma-*

Aldrich, reagent grade, 98 %). The experimental procedure was described in chapter VI, section 2.1.

For the synthesis of PANI, 3.7 g of $K_2S_2O_8$ (M_m = 270.30 g·mol^{-1}, *Sigma-Aldrich*) were dissolved in 75 mL of HCl (0.2 mol·L^{-1}), 1 mL of aniline ($C_6H_5NH_2$, M_m = 93.13 g·mol^{-1}, *Sigma-Aldrich*) was added drop wise and the solution was stirred for 20 h at room temperature. As soon as the aniline mixed with the oxidant solution, it turned to dark green color, characteristic of the emeraldine salt form of PANI. The precipitated polyaniline powder was filtered, washed with a solution of HCl (0.2 mol·L^{-1}) until yellowish washing waters turned uncolored, and dried at 80 °C for 12 h.

The monometallic catalysts supported on polypyrrole and on polyaniline were prepared by impregnating the polymers with an aqueous solution of H_2PtCl_6, used as the metal precursor. Thus, the proper amount of this salt to obtain 2 wt. % Pt loading was dissolved in ultrapure water, and then PPy or PANI were added to the solution (25 mL solution·$g_{polymer}^{-1}$), following the experimental procedure described in chapter II, section 1.2.1. In all cases, the obtained material was splitted in two portions, one of them to be characterized and the other one to be treated by Ar plasma in order to produce the metal catalyst.

To produce the reduction with Ar plasma [14], the precursors of the polymer-supported catalysts were loaded on an aluminum boat, which was placed into the plasma system (as described in chapter II, section 1.3). The discharge power was set to 200 W and 36 cycles of 5 min each were applied to each sample (180 min treatment in total) with manual mixing of the sample between treatments to assure an even exposure to the plasma. The temperature of the sample after the plasma treatment was measured by a non-contact infrared thermometer (PCE Instruments, model PCE-888). It could be determined that the surface temperature was below 50 °C in all cases.

2.2. Materials characterization

The different samples were characterized, before and after the plasma treatment and the reaction of removal of nitrates from water by different techniques described in chapter II, section 2: electrical conductivity, N_2 adsorption at -196 °C, infrared

spectroscopy (FTIR), X-ray photoelectron spectroscopy (XPS), X-ray diffraction (XRD) and transmission electron microscopy (TEM).

2.3. Catalyst evaluation

The catalytic behavior of the polymer-supported catalysts obtained after treatment in Ar plasma at 200 W was evaluated in the reduction of aqueous nitrate under H_2 at room temperature. The reaction took place in a semi-batch reactor equipped with a magnetic stirrer (700 rpm) as it is detailed in chapter II, section 1.4. The reduction of nitrate leads to the formation of hydroxide ions, which cause the increase of pH value up to 10 [15]. To avoid it, the system was buffered with a CO_2 flow to keep a constant value of pH ≈ 5. Aliquots (1 mL) were withdrawn at different times from the reactor and immediately filtered for determination of nitrate, nitrite and ammonium concentrations by ion chromatography as described in chapter II, section 2.9.

The absence of metal leaching was checked by Inducted Coupled Plasma Mass Spectrometry (ICP-MS) in aliquots withdrawn from the reactor once the nitrate reduction reaction was completed as indicated in chapter II, section 2.10.

3. RESULTS AND DISCUSSION

3.1. Characterization of materials

Polypyrrole and polyaniline chemically synthesized with $K_2S_2O_8$ showed electrical conductivities values of 25 and 478 $S \cdot m^{-1}$, respectively. Nitrogen adsorption isotherms of both PPy/$K_2S_2O_8$ (Fig. 6.1 in chapter VI, section 3.1) and PANI/$K_2S_2O_8$ (Fig. 7.1) are characteristic of not porous materials, with low BET surface areas of 11 and 40 $m^2 \cdot g^{-1}$, respectively.

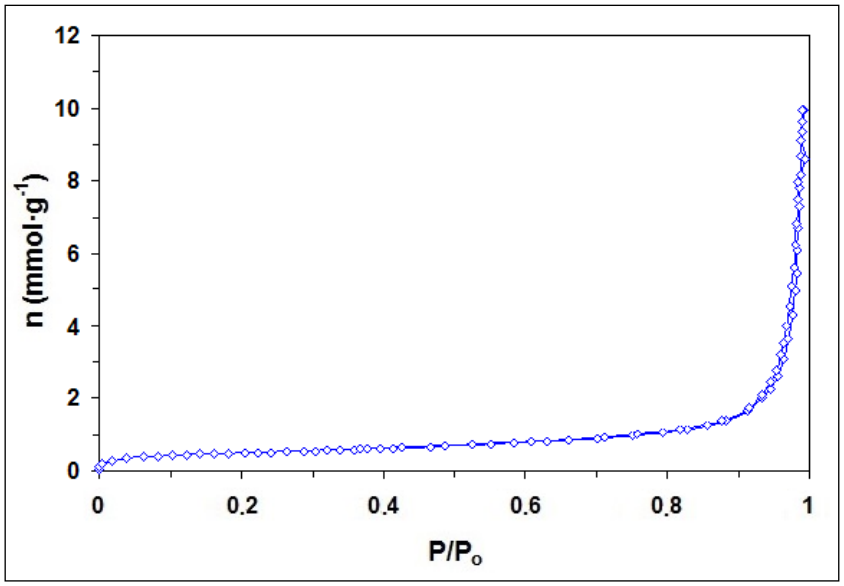

Figure 7. 1. Nitrogen adsorption isotherm at – 196 °C of PANI/$K_2S_2O_8$.

The FTIR spectrum of polypyrrole synthesized with $K_2S_2O_8$ (PPy) shows IR absorption bands characteristic of C=N-C species: C-N stretching at 1197 cm^{-1}, C=N stretching at 1562 cm^{-1} and C=N-C bending at 920 cm^{-1} (Fig. 7.2a, Table 7.1). The band at 1095 cm^{-1} corresponds [16] to the in-plane deformation vibration of NH^+ present in PPy after protonation (Scheme 7.1). Besides, the band at 1714 cm^{-1} (C=O stretching) is due to surface oxygenated groups created as a consequence of the reaction of the polymeric chain with water within the polymer network, as polypyrrole is hygroscopic. Spectrum of polypyrrole impregnated with H_2PtCl_6 (PPy/Pt) (Fig. 7.2c) shows asymmetric and symmetric stretching bands of C-H at 2920 and 2854 cm^{-1}, which indicates the existence of alkyl groups which may be originated by the breaking of some pyrrole rings [17]. Bands of C=N-C species are modified in shape when compared to pristine PPy in Fig. 7.2a, due to the interaction of platinum with nitrogen of the polypyrrole chain [14]. Besides there is an increase of the intensity of the C=O stretching band (1714 cm^{-1}) due to the degradation of the PPy surface by the aqueous H_2PtCl_6 solution, which creates more surface oxygen functionalities of the carbonyl type.

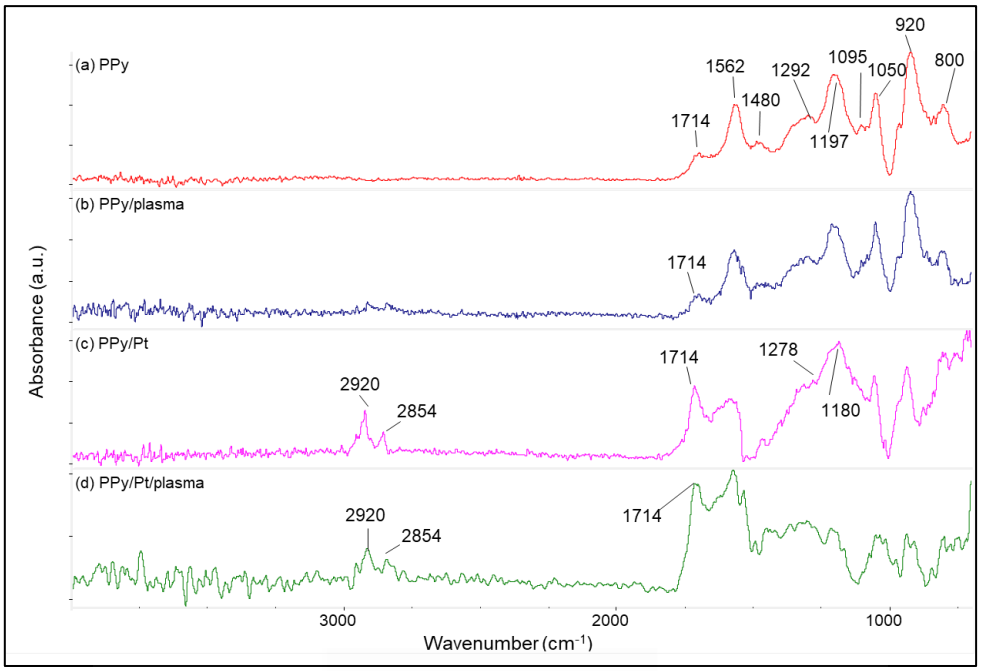

Figure 7. 2. FTIR-ATR spectra of PPy synthesized with $K_2S_2O_8$ after different treatments: (a) pristine polypyrrole (PPy), (b) polypyrrole treated in plasma (PPy/plasma), (c) polypyrrole impregnated with 2% H_2PtCl_6 (PPy/Pt) and (d) polypyrrole impregnated with 2% H_2PtCl_6 and treated in plasma (PPy/Pt/plasma).

Table 7. 1. IR-bands assignment in pristine PPy/$K_2S_2O_8$ and PANI/$K_2S_2O_8$.

PPy/$K_2S_2O_8$ (cm^{-1})	Assignment[a]	PANI/ $K_2S_2O_8$ (cm^{-1})	Assignment[a]
1714	C=O st		
1562	C=N st	1598	C=N st, Q
1480	C=C st	1484	C=C st, B
1292	C-C st	1296	C-C st
1197	C-N st	1245	C-N^+ st
1095	NH^+ δ_{ip}	1145 1140	-NH^+= C-C δ_{ip}
1050	=C-H δ_{oop}	1048	=C-H δ_{oop}
920	C=N-C δ	820	N-H δ
800	N-H δ		

[a] Stretching (st), bending (δ), in-plane bending (δ_{ip}) and out-of-plane bending (δ_{oop}).

On the other hand, the spectra of polyaniline doped with $K_2S_2O_8$ shows typical bands of the polymeric chain [18,19] (Fig. 7.3a, Table 7.1). The absorption bands at 1598 and 1484 cm^{-1} correspond to the absorption of quinoid (Q) and benzenoid (B) ring-stretching deformations, respectively, characteristic of emeraldine [1,20]. The absorption band at 1296 cm^{-1} corresponds to π-electron delocalization induced in the polymer by protonation and the absorption band at 1245 cm^{-1} is characteristic of the conducting protonated form and it has been ascribed to the C-N^+ stretching vibration in the polaron structure [16] (Scheme 7.2). The intense band at 1145 cm^{-1} has been ascribed [16] to a

vibration mode of the -NH^+= structure formed during protonation (Scheme 7.2). Impregnation of PANI with H_2PtCl_6 (PANI/Pt) (Fig. 7.3c) results in the presence of several bands between 1600 and 1800 cm^{-1} similar to overtones in benzene derivatives due to ring substitution. This suggests that conjugation in the polymeric chain is affected by the interaction of the platinum ion with nitrogen atoms. There is also a shift to lower wavenumbers of the quinoid band (1598 cm^{-1} in PANI to 1540 cm^{-1} in PANI/Pt), similar to those reported in the literature [18,21]. However, contrary to what was observed with PPy, bands corresponding to C-H stretching at 2920 and 2854 cm^{-1} are not evidenced in PANI.

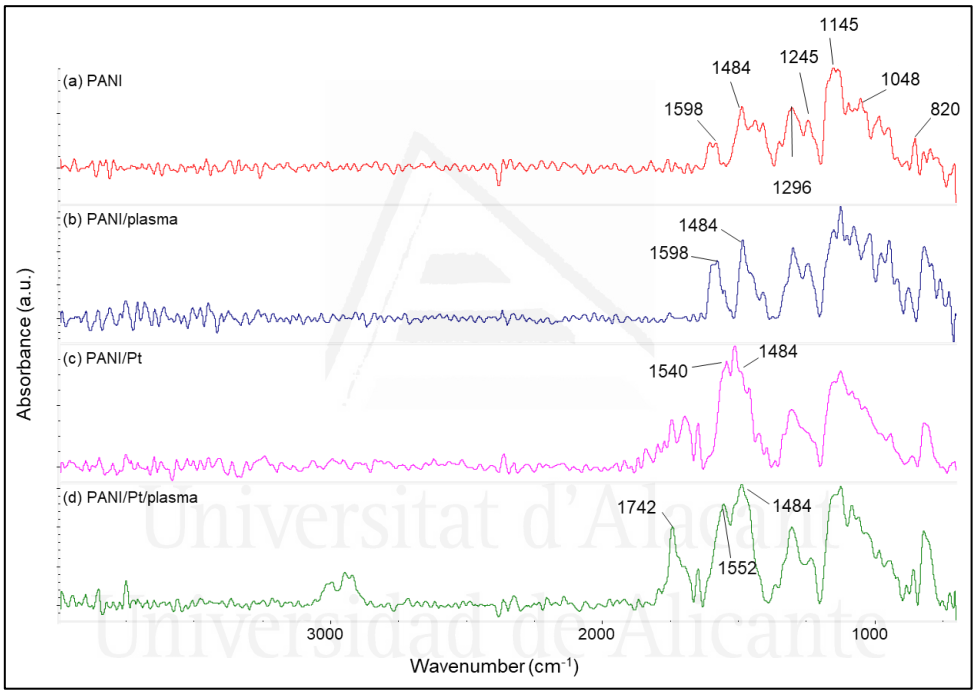

Figure 7. 3. FTIR-ATR spectra of PANI synthesized with $K_2S_2O_8$ after different treatments: (a) pristine polyaniline (PANI), (b) polyaniline treated in plasma (PANI/plasma), (c) polyaniline impregnated with 2% H_2PtCl_6 (PANI/Pt) and (d) polyaniline impregnated with 2% H_2PtCl_6 and treated in plasma (PANI/Pt/plasma).

The plasma treatment does not produce significant modifications in the IR spectra of PPy (Fig. 7.2b) and PANI (Fig. 7.3b), but it does affect the platinum-impregnated polymers. The spectrum of the plasma-treated impregnated polypyrrole (PPy/Pt/Plasma) (Fig. 7.2d) shows a decrease of the intensity of bands assigned to asymmetric and symmetric stretching of carbon-hydrogen bonds (C-H sy st and C-H as st) at 2920 and 2854 cm^{-1}, and an increase of the C=O stretching band (1714 cm^{-1}). Plasma treatment also creates oxygenated moieties on platinum-impregnated polyaniline (PANI/Pt/Plasma)

(C=O stretching band at 1742 cm^{-1}). These C=O moieties are created when the plasma-activated polymer surface is put in contact with air (Fig. 7.3d).

XPS surface analysis is useful to determine the degree of oxidation of the polymeric chains and the oxidation state of platinum species. Surface analysis of both polymers show carbon and nitrogen species from the polymeric chain, and also sulfur from the oxidant (Table 7.2). Potassium peroxydisulfate may incorporate into the oxidized polymeric chains as a counterion, acting as a dopant, but it also might be introduced as sulfate as a result of the redox reaction with the pyrrole or aniline monomers. The binding energy of the S 2p level peak, 168.3 eV, corresponds to SO_4^{2-}, what evidences the reduction of $S_2O_8^{2-}$ upon anchoring to the polymers. The presence of chlorine as chloride (there is a doublet corresponding to Cl $2p_{1/2}$ at 198.6 eV and Cl $2p_{3/2}$ at 197.1 eV) reveals the ability of Cl^- (from HCl in PANI synthesis) to produce the doping of the polymer in competition with SO_4^{2-} from peroxydisulfate. There is also a contribution of chlorine at a higher binding energy (Cl $2p_{1/2}$ at 201.9 eV and Cl $2p_{3/2}$ at 200.2 eV), which has been ascribed [18,22,23] to chlorine atoms covalently bound to aromatic rings in PPy and PANI. Analysis of the XPS spectra of the C 1 s level (Table 7.3) shows oxygenated moieties (C=O on the pristine PPy and C-O on pristine PANI), produced as a result of the contact of the polymer surface with water present in the reaction medium. This is consistent with FTIR data (Figs. 7.2 and 7.3). On the other hand, the oxidation degree of the polymeric chain, evaluated from the N 1 s curve fit (Fig. 7.4, Table 7.4), is different for both polymers. Thus, the pristine polypyrrole (PPy) chain shows a considerable higher percentage of oxidized nitrogen (-N^+-) (93 %) than the pristine polyaniline (PANI) (17 %).

Table 7. 2. XPS surface chemical composition (atomic %) of the different samples.

Binding energy (*eV*)	284.5	531.5	398.1	198.5	71.2	168.3
Element	**C 1s**	**O 1s**	**N 1s**	**Cl 2p**	**Pt 4f**	**S 2p**
PPy	69.2	18.0	12.2	0.2	-	0.4
PPy/Pt	70.9	16.8	11.0	0.7	0.3	0.3
PPy/Pt/Plasma	62.3	23.2	13.0	0.6	0.3	0.6
PPy/Pt/Plasma-R[a]	69.1	17.5	12.6	0.2	0.4	0.2
PANI	77.7	7.8	9.6	3.9	-	1.0
PANI/Pt	77.2	6.2	10.4	5.1	0.3	0.8
PANI/Pt/Plasma	64.3	17.9	9.8	2.4	3.9	1.7
PANI/Pt/Plasma-R[a]	69.9	11.4	12.0	1.7	4.6	0.4

[a] R = recovered catalyst after 300 min of reaction.

Table 7. 3. XPS analysis of the C 1s level. Contribution (%) of different carbon species.

Average binding energy (*eV*)	284.6	286.3	288.3
Carbon species	C-C, C-H, C-N	C-O	C=O
PPy	78	-	22
PPy/Pt	75	15	10
PPy/Pt/Plasma	73	10	17
PPy/Pt/Plasma-R[a]	70	15	15
PANI	84	16	-
PANI/Pt	67	29	4
PANI/Pt/Plasma	63	31	6
PANI/Pt/Plasma-R[a]	66	28	6

[a] R = recovered catalyst after 300 min of reaction.

Table 7. 4. XPS analysis of the N 1s level. Contribution (%) of different nitrogen species.

Average binding energy (*eV*)	397.9	399.2	400.5	401.0	406.0
Nitrogen species	=N-	-NH-	$-N^{+}-$	$=N^{+}$	NO_3^-
PPy	7	-	93	-	-
PPy/Pt	-	-	100	-	-
PPy/Pt/Plasma	-	-	83	17	-
PPy/Pt/Plasma-R[a]	9	-	91	-	-
PANI	-	83	17	-	-
PANI/Pt	-	90	10	-	-
PANI/Pt/Plasma	-	62	38	-	-
PANI/Pt/Plasma-R[a]	24	55	-	-	21

[a] R = recovered catalyst after 300 min of reaction.

H_2PtCl_6 is a strong acid and anions formed during its dissociation are hydrolyzed in aqueous medium [24] to give a variety of chloro-aqua complexes such as $[PtCl_6]^{2-}$, $[PtCl_5(H_2O)]^-$ and $[PtCl_3(H_2O)]^+$. These complexes may anchor to nitrogen species of the polymeric chain [18,23,25]. XPS analysis detects platinum on the polymers surfaces. Analysis of the Pt 4f level in polypyrrole and polyaniline impregnated with H_2PtCl_6 (Fig. 7.5) shows two predominant bands at 72.9 eV (Pt $4f_{7/2}$) and 76.3 eV (Pt $4f_{5/2}$), which correspond to Pt^{2+}, and represent 86 % (in PPy) and 91 % (in PANI) (Table 7.5). Pt^{4+} is also detected in both polymers (bands at 74.0 eV (Pt $4f_{7/2}$) and 77.4 eV (Pt $4f_{5/2}$)). This suggests that Pt^{4+} suffers spontaneous reduction to Pt^{2+} by electrons provided by the polymeric chain. The absence of metallic platinum is confirmed by the absence of bands that should appear at lower binding energies, typically at 71.1 eV (Pt $4f_{7/2}$) and 74.4 eV (Pt $4f_{5/2}$). Redox potentials shown in Table 7.6 confirm that the reduction of $[PtCl_6]^{2-}$ to $[PtCl_4]^{2-}$ during the impregnation process is possible, and it should be accompanied by oxidation of the polymeric chain. The oxidation of the PPy chain upon impregnation with hexachloroplatinic acid is evidenced by the disappearance of the reduced imine moieties (=N- at 397.9 eV) shown in pristine PPy, which are not present in the platinum-

impregnated PPy, where only oxidized amine groups are depicted (-N^+- at 400.5 eV) (Fig. 7.4, Table 7.4). It can be assumed that Pt(IV) species from H_2PtCl_6 are initially introduced as $[PtCl_6]^{2-}$ counterions of PPy and PANI (synthesized as the conductive emeraldine salt form), but they are easily reduced to Pt(II) species which coordinatively bond to the polymeric chain as a platinum chloro complex. Sulfate ions from the dopant ($K_2S_2O_8$) used in the synthesis of both PPy and PANI, and also chlorine coming from the acid medium (HCl) used in the synthesis of PANI, could act as counterions of the oxidized nitrogen moieties (N^+) of the polymeric chain, as well as ligands of the platinum complex (Scheme 7.3b). The reductive ability of the polymers is responsible for the observed reduction of Pt(IV) to Pt(II) in this platinum complex, but no metallic platinum is observed.

XPS analysis shows that treatment with non-thermal argon plasma is able to partially reduce platinum ions into Pt(II) and metallic platinum in the polymer-supported catalyst. Consequently, Pt(IV) is not further present on any polymer after treatment in argon plasma. However, the effectiveness of reduction treatment with Ar plasma depends on the polymer nature. This was already demonstrated for Pt deposited onto PPy [14,26]. The reduction mechanism produced by plasma treatment is quite different from widely used redox processes involving reductive chemicals as sodium borohydride. This one is an inner sphere mechanism of re-emplacement of chlorine and/or sulfate ligands by BH_4^-, followed by a redox reaction where electron transfer in the intermediate complex is produced [27]. Otherwise, when a cold plasma treatment is performed, the energetic electrons present in the plasma serve as reducing agents for the platinum ions (Schemes 7.3b and 7.3c). In the case of PANI support, platinum ions anchored to N^+ moieties located out of the aromatic ring in PANI (Scheme 7.4b) are more easily reduced than platinum ions anchored to N^+ located inside the ring in PPy (Scheme 7.3c). Therefore, considerably higher amount of metallic platinum is detected on PANI surface (83 %) compared to PPy (47 %) after plasma treatment (Table 7.5). Formation of platinum nanoparticles implies dissociation of the platinum complexes anchored to the polymeric chain through the nitrogen functionality (-N^+-$[PtL_4]^{2-}$) (Scheme 7.4b). As a result, there is a change in the oxidation state of the polymeric chain, which becomes oxidized, as assessed by N 1 s contributions: 62 % of amine -NH- groups and 38 % of oxidized amine N^+ groups are detected in the plasma treated PANI. PPy oxidation is even more important with the presence of 83 % of -N^+- (at 400.5 eV) and 17 % of N^+= moieties (at 401.0 eV).

The ligands released from the dissociated platinum complex (L^{n-}) (Scheme 7.3c) could act as counteranions to stabilize the oxidized polymeric chain.

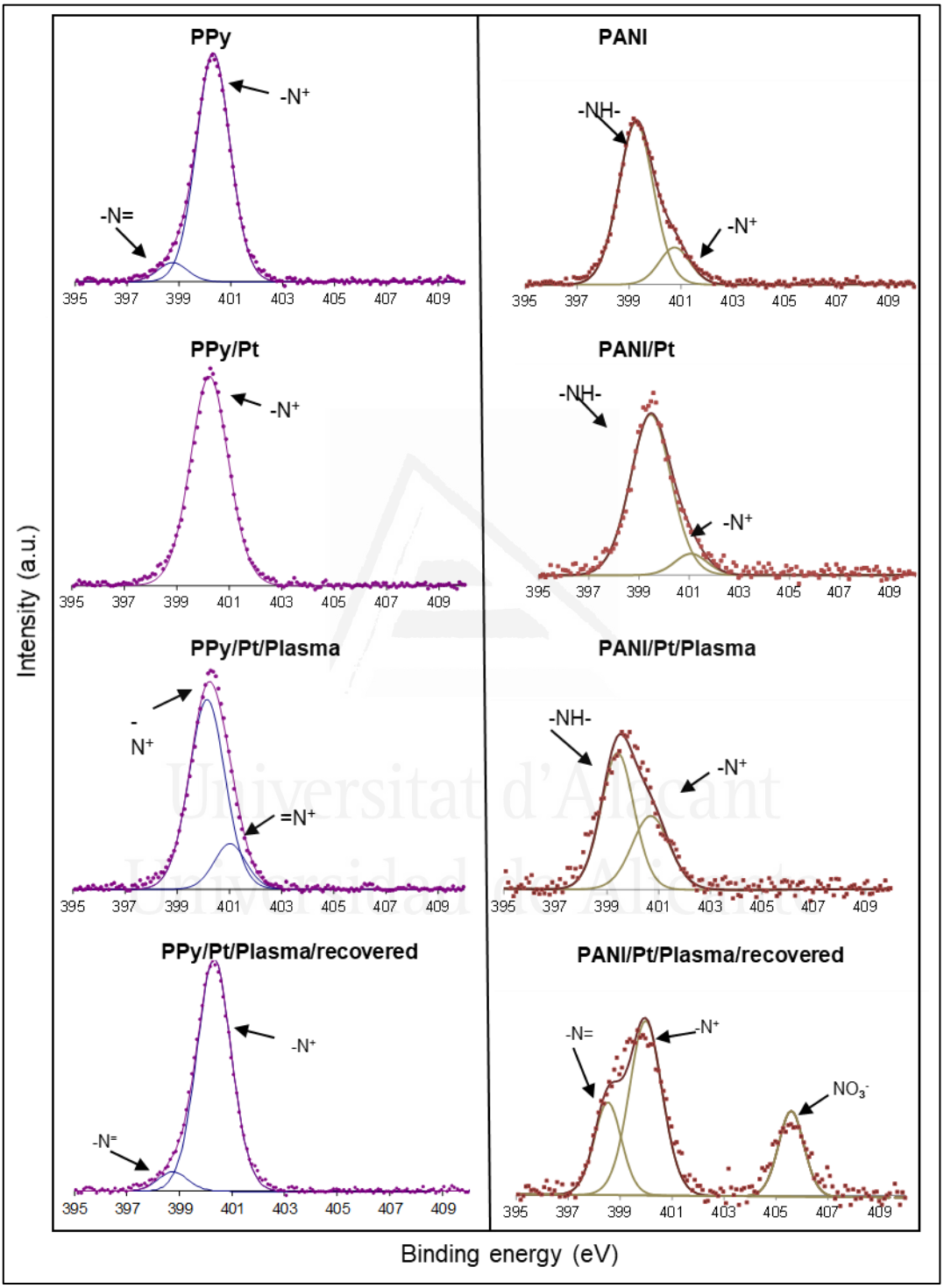

Figure 7. 4. Curve fit of N 1s level (XPS) of PPy and PANI synthesized with $K_2S_2O_8$: pristine, platinum impregnated, treated in plasma and recovered catalysts after contact with the nitrate solution for 300 min.

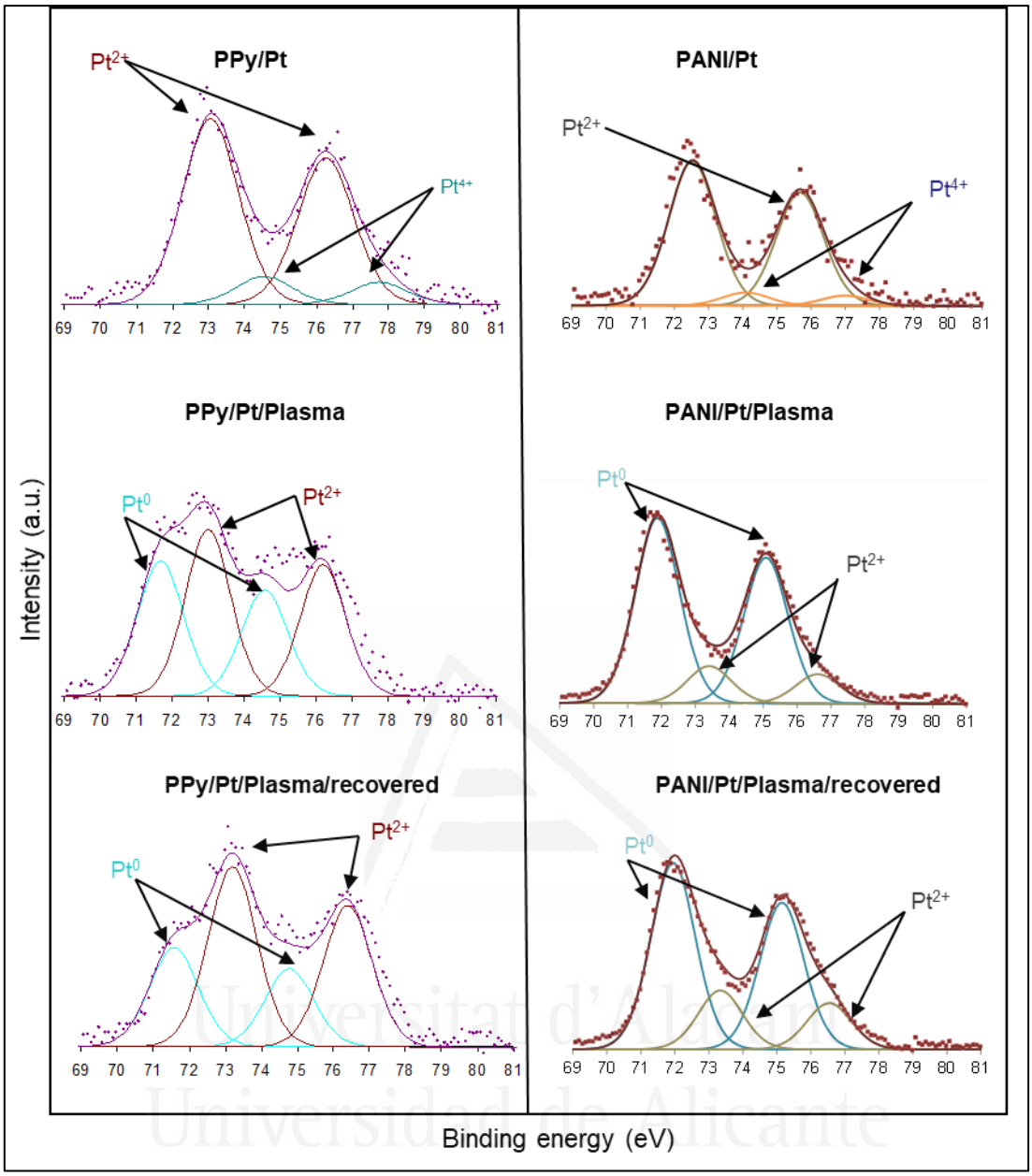

Figure 7. 5. Curve fit of Pt 4f level (XPS) of PPy and PANI synthesized with $K_2S_2O_8$: pristine, platinum impregnated, treated in plasma and recovered catalysts after contact with the nitrate solution for 300 min.

Table 7. 5. XPS analysis of the Pt $4f_{7/2}$ level. Contribution (%) of different platinum species.

Average binding energy (*eV*)	71.1	72.9	74.0
Species	Pt^o	Pt^{2+}	Pt^{4+}
PPy	-	-	-
PPy/Pt	-	86	14
PPy/Pt/Plasma	47	53	-
PPy/Pt/Plasma-R[a]	37	63	-
PANI	-	-	-
PANI/Pt	-	91	9
PANI/Pt/Plasma	83	17	-
PANI/Pt/Plasma-R[a]	76	24	-

[a] R = recovered catalyst after 300 min of reaction.

Table 7. 6. Redox potentials of different systems.

System	E^o (volts)
PPy^+/PPy	+ 0.15
Emeraldine/leucoemeraldine	+ 0.342
Pernigraniline/emeraldine	+ 0.942
$[PtCl_6]^{2-}/[PtCl_4]^{2-}$	+ 0.68
$[PtCl_4]^{2-}/Pt$	+ 0.73
Pt^{2+}/Pt	+ 1.20
NO_3^-/NH_4^+	+ 0.875
NO_3^-/N_2	+ 1.246
$2H^+/H_2$	0

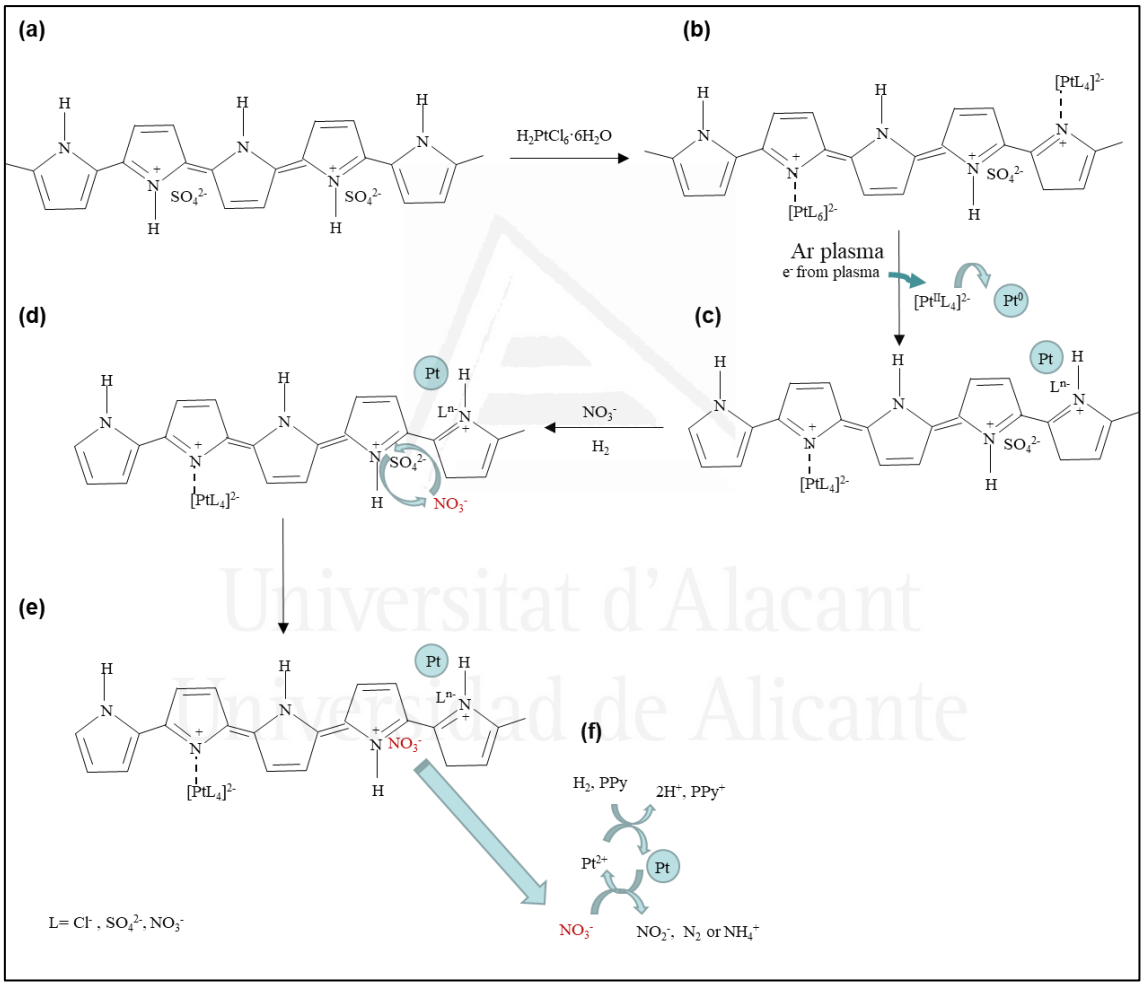

Scheme 7. 3. Proposed mechanisms for nitrate abatement from water in the presence of platinum nanoparticles supported on PPy.

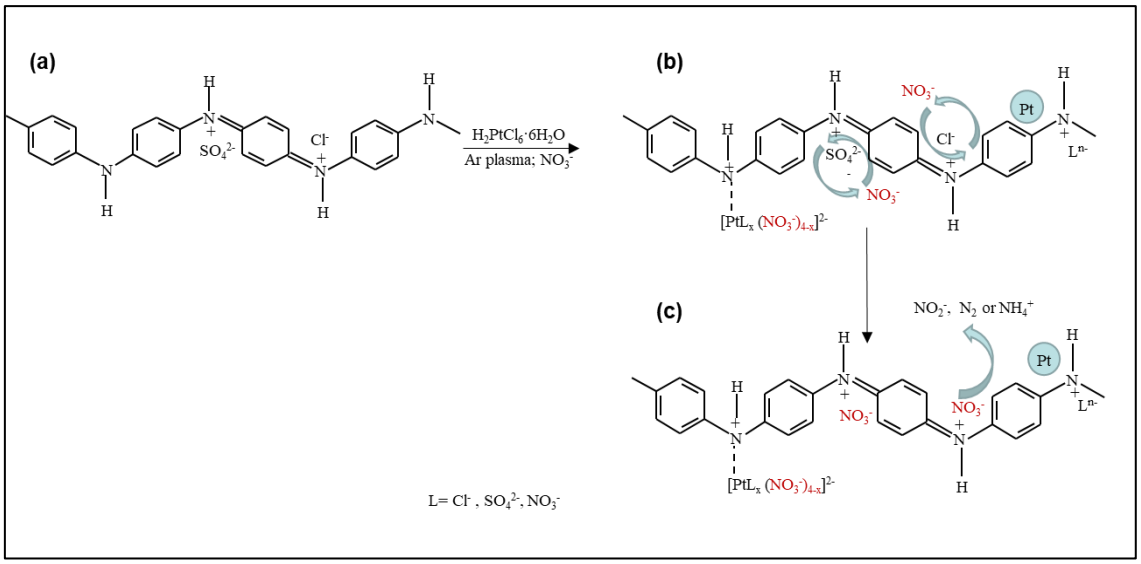

Scheme 7. 4. Proposed mechanisms for nitrate abatement from water in the presence of platinum nanoparticles supported on PANI.

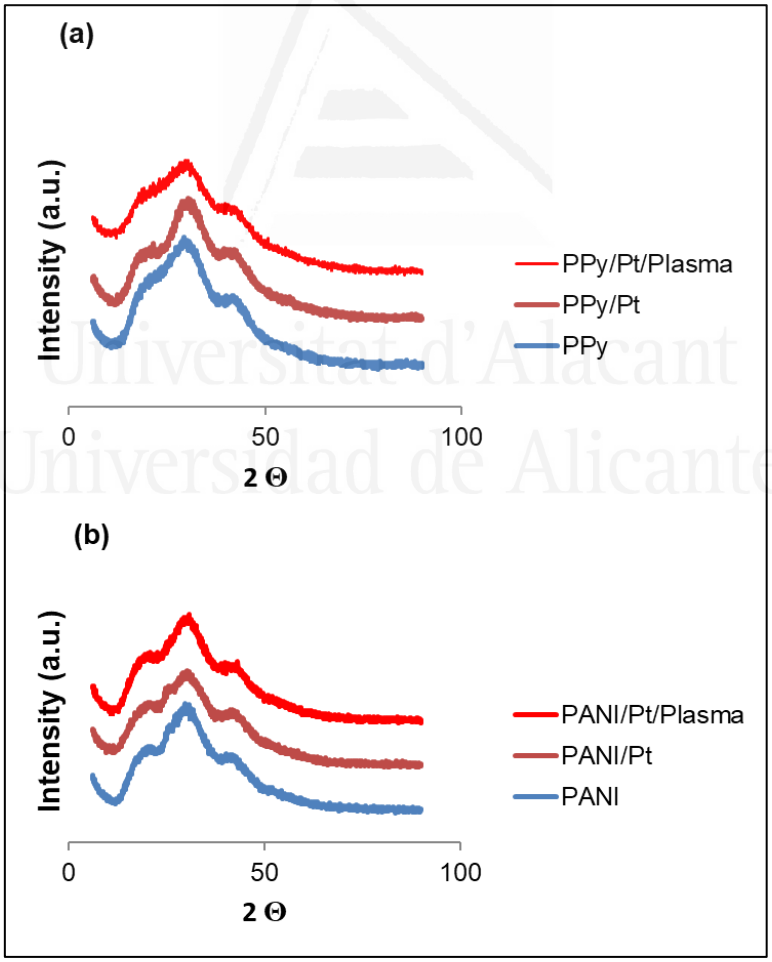

Figure 7. 6. XRD patterns of (a) polypyrrole (PPy) and (b) polyaniline (PANI) synthesized with $K_2S_2O_8$ and their respective supported catalysts.

The X-ray diffraction patterns of PPy and PANI (Fig. 7.6) are characteristic of amorphous polymers, showing three broad bands. One band centered at $2\theta = 17 - 18$ º for PPy and $2\theta = 18 - 20$ º for PANI corresponds to the periodicity along the polymeric chain, another band centered at $2\theta = 25$ º for PPy and $2\theta = 27 - 28$ º for PANI corresponds to the periodicity perpendicular to the polymer chain [18]. The third band at $2\theta = 42$ º in both polymers is also typical of the polymer phase [19].

X-ray diffraction patterns of polymers impregnated with Pt and treated with Ar plasma do not show reflexions due to crystalline metallic platinum, which should be located at $2\theta = 39.8$ º for Pt(100) and 46.2 º for Pt(200) [18,28], indicating a high metallic dispersion.

TEM micrographs (Fig. 7.7a) show the PPy and PANI polymeric supports alone and after deposition of Pt before and after plasma treatment. After deposition of platinum on the supports, platinum nanoparticles are only visible after treatment with Ar plasma. The average size of the nanoparticles is 4.5 nm when supported on PPy and 5.0 nm when supported on PANI (Fig. 7.7b).

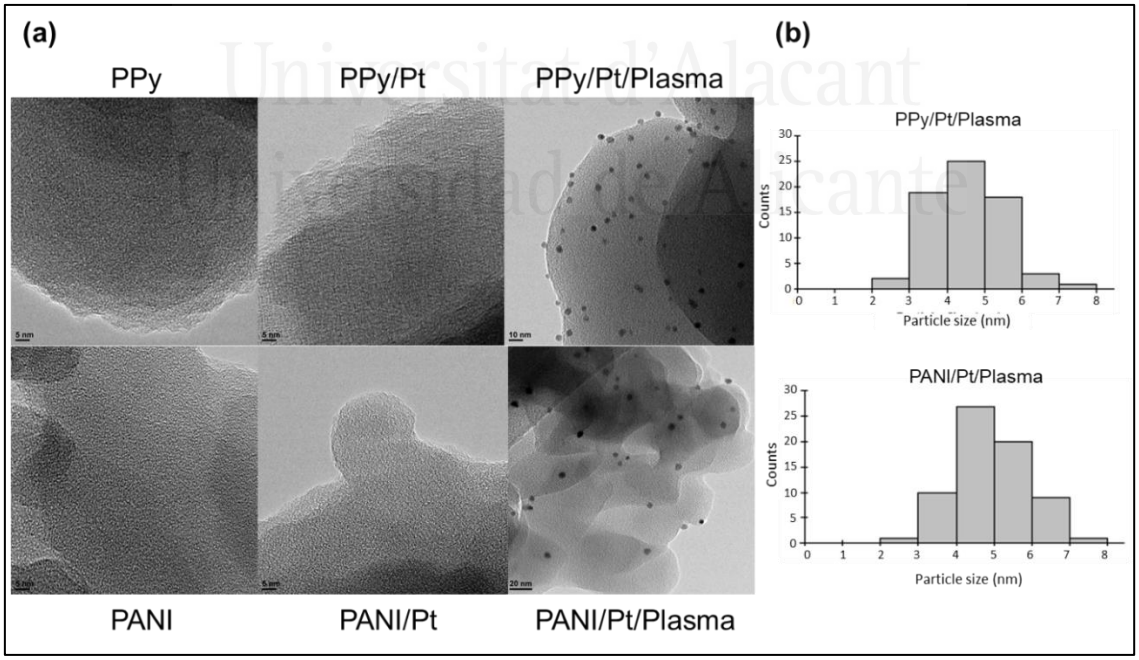

Figure 7. 7. (a) TEM micrographs and (b) particle size distributions of PPy and PANI (synthesized with $K_2S_2O_8$) and their respective supported catalysts.

3.2. Catalytic behavior

The redox mechanism of nitrates removal involves a first step in which nitrates are reduced to nitrites, followed by the reduction of nitrites to N_2 and/or ammonium [13,15,29-31]. Table 7.6 shows the redox potentials of nitrate reduction to the desired N_2 and to the undesired ammonium. Although this reaction is thermodynamically favored, a catalyst is needed for the reaction to proceed at a measurable rate. A blank experiment, which consisted on flowing the reducing agent (H_2) and the buffer (CO_2) through the aqueous nitrate solution in the absence of any catalyst, and analyzing by ion chromatography aliquots periodically extracted from the solution, revealed that nitrate concentration was unaltered after 300 min and that neither nitrite nor ammonium were detected. Therefore, in this chapter, the catalytic activity of platinum nanoparticles synthesized by argon plasma treatment onto polypyrrole and polyaniline has been tested in the catalytic reduction of nitrates in water with hydrogen.

A decrease of nitrate concentration below 50 $mg \cdot L^{-1}$ is produced within the first 5 min of reaction with the platinum catalysts supported on both polymers, with 51 % and 57 % conversion achieved with PPy and PANI, respectively (Table 7.7). These measured concentrations remained constant with time up to 300 min (Fig. 7.8). Besides, selectivity of the reaction to nitrite is extremely low, in such a way that measured nitrite concentrations are much smaller than the maximum permitted levels of nitrite in drinking water (0.5 $mg \cdot L^{-1}$) [10,11]. Although a very low ammonium concentration is detected when the platinum catalyst is supported on PANI (0.13 $mg \cdot L^{-1}$) (Table 7.7), contrary to what is observed when platinum is supported on PPy, (2.25 $mg \cdot L^{-1}$), this amount exceeding the maximum allowed ammonium concentration (0.5 $mg \cdot L^{-1}$). It is not possible to measure nitrogen production, but the ammonium concentration detected in the reactor reveals that a redox process is taking place. These data suggest that the removal of nitrate on the polymer-supported Pt catalysts is not a simple adsorption process that may occur at the catalyst surface. Nitrate anions can be exchanged with the dopant counterions [32], but they can also be retained by interaction with the chloro-platinum complex [33]. Thus, it has to be considered that dopant anions are inserted in the polymer matrix, bigger dopants occupying a larger space. Taking into account the relative ionic radius of dopants (258 pm for sulfate anion, 181 pm for chloride anion) and nitrate anion (179 pm for NO_3^-), ion exchange between nitrate and counterions resulting from polymer doping (SO_4^{2-} in

both PPy and PANI, and Cl^- from HCl in PANI) is possible. XPS characterization of the catalyst before and after reaction evidences the exchange between the dopants and nitrate (Table 7.2), with considerable lower Cl and S concentrations and increased N amounts in the polyaniline-supported catalyst recovered from the reactor after being in contact with the nitrate aqueous solution, compared to the pristine polymer. Furthermore, the XPS spectra of the N 1s level of PANI/Pt/Plasma/recovered (Fig. 7.4) also shows an important contribution of nitrate (406.0 eV), which suggests that nitrate was retained by PANI. However, no nitrate contribution is observed in PPy/Pt/Plasma/recovered. Considering that not all the platinum ions in the chloro-complexes have been reduced to the metallic state by the plasma treatment, and that a considerable amount of Pt(II) was still present, as assessed by XPS, nitrate could form an adduct with the platinum complex or even enter in its coordination sphere as a ligand ($[PtL_x(NO_3^-)_{4-x}]^{2-}$) (Scheme 7.4b). The minimized steric hindrance provided by the location of the nitrogen atom external to the ring in PANI, compared to PPy, favors the removal of nitrate from water by this mechanism in the presence of PANI, which could explain the lower formation of ammonium ions on PANI/Pt/Plasma compared to its PPy counterpart (Table 7.7). If a large amount of nitrate just remained anchored to the polymeric chain as NO_3^- by ion exchange, with no further reduction, further treatment or disposal of nitrate containing polymers would be necessary, which is also an environmental concern. It is not possible to measure N_2 production, but there is some ammonium production (Table 7.7), which suggests that at least some of the nitrate initially retained by PANI is reduced by a catalytic way. In this case, nitrate is firstly exchanged with SO_4^{2-} and Cl^- counteranions present in doped PANI (Scheme 7.4b) and, in a second step, it suffers reduction by the electrons provided by the polymeric chain through the nitrogen functionality (Scheme 7.4c).

Table 7. 7. Nitrate, nitrite and ammonium concentrations, nitrate conversion and selectivities to nitrite and ammonium after 5 min of reaction.

Sample	(mg·L^{-1})			(%)		
	$[NO_3^-]$	$[NO_2^-]$	$[NH_4^+]$	$X_{NO_3^-}$	$S_{NO_2^-}$	$S_{NH_4^+}$
PPy/Pt/Plasma 1st cycle	48.6	0.04	2.3	51	0.10	15.0
PANI/Pt/Plasma 1st cycle	42.4	0.01	0.1	57	0.02	0.8
PPy/Pt/Plasma 2nd cycle	50.0	0.03	2.0	50	0.08	13.0
PANI/Pt/Plasma 2nd cycle	46.4	0.01	0.1	53	0.05	0.6

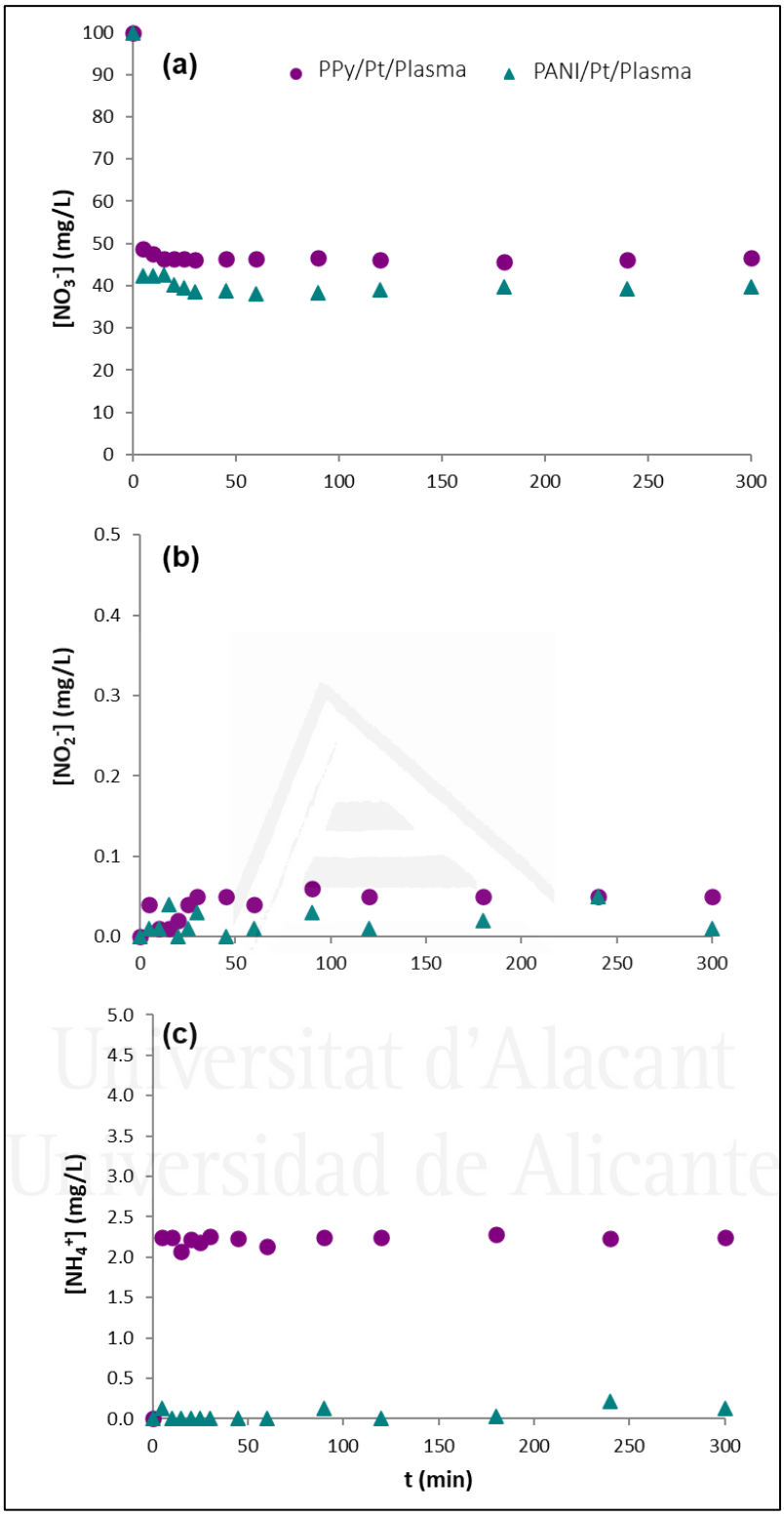

Figure 7. 8. (a) Nitrate, (b) nitrite and (c) ammonium concentrations ($mg \cdot L^{-1}$) as a function of time (min) during aqueous nitrate reduction with hydrogen in the presence of platinum (2%) supported on PPy and PANI synthesized with $K_2S_2O_8$.

In polypyrrole (Scheme 7.3a), the nitrogen atom located within the aromatic ring minimizes the possibility of formation of an adduct or enter as a ligand into the platinum complex. Thus, in polypyrrole, ion exchange between counterions present in the doped polymer and NO_3^- from the nitrate aqueous solution is produced in a first step (Scheme 7.3d), followed by reduction of nitrate by electrons from the polymer (Scheme 7.3f). As a result, no nitrate is retained, as evidenced by XPS.

Recyclability of the catalysts was tested. Thus, the catalysts recovered after one reaction cycle were put into contact with a 1 $mol \cdot L^{-1}$ solution of NaCl during 30 min under stirring with the purpose of regenerate them by exchanging adsorbed nitrate anions with chloride ions. Both catalysts, irrespective of their ability in adsorbing nitrate during the course of the reaction were treated in the same way, for comparison purposes. Table 7.7 shows that the nitrate conversions achieved with both regenerated catalysts are only slightly lower than those obtained during the first run. Similar ammonium selectivities were obtained and nitrite was not detected in any case.

The inherent ability of conducting polymers such as PPy and PANI of switching between different oxidation states imparts them the capability of acting as a source and or a drain of electrons, depending on the redox process in which they are involved [33,34]. Upon reduction of nitrate, some of the metallic platinum is oxidized to Pt^{2+} (Fig. 7.5, Table 7.5), what is accompanied by a reduction of the oxidation state of the polymeric nitrogen, as evidenced in the recovered polymers (Fig. 7.4, Table 7.5). Evidence of donation of electron density from platinum nanoparticles to polypyrrole has been previously reported [35]. These results show that the polymeric matrix participates in the redox process by switching between different oxidation states as a response to the electron transfer from platinum to nitrate (Scheme 7.3f).

The hydrogen flow into the reactor avoids any contact with air of the plasma-reduced Pt catalyst before and during the course of the reaction [29], and it could also contribute to the regeneration of oxidized Pt^{2+} to Pt^{o}. Lixiviated platinum measured by ICP-MS was always less than 0.05 % (Table 7.8).

Table 7. 8. Concentration of lixiviated (l) and theorical (T) platinum detected by ICP-MS in solution after 300 min of reaction of nitrate reduction with hydrogen.

Sample	(ppb)		(%)
	$[Pt]_l$	$[Pt]_T$	$[Pt]_l/[Pt]_T$
PPy/Pt/Plasma	2.040	$1.129 \cdot 10^4$	0.018
PANI/Pt/Plasma	5.110	$1.088 \cdot 10^4$	0.047

On both catalysts, both platinum ions in form of a platinum complex and metallic platinum nanoparticles are detected by XPS. The presence of platinum in both oxidation states significantly alters the redox properties of the polymers. Metallic platinum may promote reduction of nitrate [33,36] and oxidized platinum species may promote oxidation of the polymer. Therefore, continuous electron transfer between the polymer and nitrate is being produced.

4. CONCLUSIONS

Platinum nanoparticles have been synthesized on polyaniline and polypyrrole from a platinum salt precursor using a reducing treatment with cold Ar plasma. These catalysts produce an important abatement of nitrate from water in only 5 min. However, nitrate abatement proceeds by two different mechanisms, depending on the nature of the conducting polymer:

Mechanism A: Nitrate is adsorbed on the platinum complex either forming an adduct or entering the complex as a ligand. This mechanism is favored in PANI, where the nitrogen atom is external to the ring system and steric hindering is minimized.

Mechanism B: There is an ion exchange between Cl^- and/or SO_4^{2-} present in the doped polymers as counterions and NO_3^- from the nitrate aqueous solution. This mechanism is favored in PPy.

In both cases, the adsorption or ion exchange of nitrate is followed by a redox process in which metallic platinum nanoparticles synthesized by argon plasma have a role in the reduction of nitrate to either ammonium (measured) and nitrogen (not measured). Ammonium production was more important when platinum was supported on PPy compared to PANI, but it was maintained constant with reaction time. The location of the nitrogen atom within the aromatic ring in PPy restricts the extension of mechanism A,

and favors mechanism B, which involves the reduction of nitrate located next to platinum nanoparticles.

As a result of any of the redox process involving platinum, that is, platinum ions being reduced by electrons coming from plasma and, on the other hand, metal platinum nanoparticles being oxidized as nitrate is reduced, the oxidation state of the polymeric chain changes. This evidence an active participation of the polymer matrix in the redox process.

Regeneration of the catalysts data showed that the removal of nitrate ability was maintained after two cycles.

5. REFERENCES

[1] T.A. Skotheim, J.R. Reynolds. *Recent advances in polypyrrole* in *Handbook of conducting polymers. Conjugated polymers: theory, synthesis, properties, and characterization*. 3rd ed. CRC Press: Boca Raton, FL, USA. **2007**, Chap. 8.

[2] A. Malinauskas. *Polymer*. **2001**, *42(9)*, 3957-3972.

[3] J. Stejskal, R.G. Gilbert. *Pure Appl. Chem*. **2002**, *74(5)*, 857-867.

[4] M.D. Bedre, S. Basavaraja, B.D. Salwe, V. Shivakumar, L. Arunkumar, A. Venkataraman. *Polym. Compos*. **2009**, *30(11)*, 1668-1677.

[5] D.W. Hatchett, N.M. Millick, J.M. Kinyanjui, S. Pookpanratana, M. Bär, T. Hofmann, A. Luinetti, C. Heske. *Electrochim. Acta*. **2011**, *56(17)*, 6060-6070.

[6] J.J. Zou, Y.P. Zhang, C.J. Liu. *Langmuir*. **2006**, *22(26)*, 11388-11394.

[7] X. Zhu, P.P. Huo, Y.P. Zhang, C.J. Liu. *Ind. Eng. Chem. Res*. **2006**, *45(25)*, 8604–8609.

[8] P. Slepička, N. Slepičková-Kasalková, E. Stránská, L. Bačáková, V. Švorčik. *Biotechnol. Adv*. **2015**, *33(6)*, 1120-1129.

[9] X. Liang, C.J. Liu, P. Kuai. *Green Chem.* **2008**, *10*, 1318-1322.

[10] EC (European Community), Official Journal of the European Communities, Council Directive 98/83/EC on the quality of water intended for human consumption, *The Drinking Water Directive (DWD)*, Brussels. **1998**, Annex 1, Part B, 42-44.

[11] USEPA (United State Environmental Protection Agency), *National Primary Drinking Water Regulations*, Washington, DC, **2008**, Title 40, Part 141.

[12] N. Barrabés, J. Sá. *Appl. Catal., B.* **2011**, *104(1-2)*, 1-5.

[13] I. Dodouche, F. Epron. *Appl. Catal., B.* **2007**, *76(3-4)*, 291-299.

[14] R. Buitrago-Sierra, M.J. García-Fernández, M.M. Pastor-Blas, A. Sepúlveda-Escribano. *Green Chem.* **2013**, *15*, 1981-1990.

[15] A. Garron, K. Lázár, F. Epron. *Appl. Catal., B.* **2005**, *59(1-2)*, 57-69.

[16] N.V. Blinova, J. Stejskal, M. Trchová, J. Prokeš, M. Omastová. *Eur. Polym. J.* **2007**, *43(6)*, 2331-2341.

[17] J. Morales, M.G. Olayo, G.J. Cruz, R. Olayo. *J. Appl. Polym. Sci*. **2002**, *85(2)*, 263-270.

[18] A. Drelinkiewicz, A. Zieba, J.W. Sobczak, M. Bonarowska, Z. Karpiński, A. Waksmundzka-Góra, J. Stejskal. *React. Funct. Polym.* **2009**, *69(8)*, 630-642.

[19] A. Nyczyk, A. Sniechota, A. Adamczyk, A. Bernasik, W. Turek, M. Hasik. *Eur. Polym. J.* **2008**, *44(6)*, 1594-1602.

[20] J. Tang, X. Jing, B. Wang, F. Wang. *Synth. Met.* **1988**, *24(3)*, 231-238.

[21] A. Drelinkiewicz, M. Hasik, M. Choczyński. *Mater. Res. Bull*. **1998**, *33(5)*, 739-762.

[22] J.F. Moulder, W.F. Stickle, P.E. Sobol, K.D. Bomben. J. Chastain, R.C. King Jr (Eds.). *Handbook of X-ray photoelectron spectroscopy: a reference book of standard spectra for identification and interpretation of XPS data*. Perin-Elmer Corporation Physical Electronics Division: Inc Minnesota, USA. **1995**.

[23] M. Hasik, A. Bernasik, A. Adamczyk, G. Malata, K. Kowalski, J. Camra. *Eur. Polym. J.* **2003**, *39(8)*, 1669-1678.

[24] D. Nachtigall, S. Artelt, G. Wünsch. *J. Chromatogr. A.* **1997**, *775(1-2)*, 197-210.

[25] R. Jamal, F. Xu, W. Shao, T. Abdiryim. *Nanoscale Res. Lett.* **2013**, *8(1)*, 117-124.

[26] M.J. García-Fernández, R. Buitrago-Sierra, M.M. Pastor-Blas, O.S.G.P. Soares, M.F.R. Pereira, A. Sepúlveda-Escribano. *RSC Adv.* **2015**, *5*, 32706-32713.

[27] V.S. Khan. *Russ. J. Inorg. Chem.* **1983**, *28*, 1410-1413.

[28] Diffrac Plus Evaluation Software, Bruker, 2017.

[29] E. Gautron, A. Garron, E. Bost, F. Epron. *Catal. Commun*. **2003**, *4*(8), 435-439.

[30] I. Dodouche, D.P. Barbosa, M.C. Rangel, F. Epron. *Appl. Catal., B.* **2009**, *93(1-2)*, 50-55.

[31] M. Pera-Titus, M. Fridmann, N. Guilhaume, K. Fiaty. *J. Membr. Sci*. **2012**, *401-402*, 204-216.

[32] M.H. Ansari, J.B. Parsa. *Separation Purification Technol.* **2016**, *169(1)*, 158-170.

[33] W. Dhaoui, M. Hasik, D. Djurado, A. Bernasik, A. Pron. *Synth. Met*. **2010**, *160(23-24)*, 2546-2551.

[34] A. Nyczyk, M. Hasik, W. Turek, A. Sniechota. *Synth. Met*. **2009**, *159(7-8)*, 561-567.

[35] R.B. Moghaddam, O.Y. Ali, M. Javashi, P.L. Warburton, P.G. Pickup. *Electrochim. Acta*. **2015**, *162*, 230-236.

[36] O.S.G.P. Soares, E.O. Jardim, A. Reyes-Carmona, J. Ruiz-Martínez, J. Silvestre-Albero, E. Rodríguez-Castellón, J.J.M. Órfão, A. Sepúlveda-Escribano, M.F.R. Pereira. *J. Colloid Interface Sci*. **2012**, *369(1)*, 294-301.

Chapter VIII. Surfactant-assisted synthesis of conducting polymers and their application to the removal of nitrates from water

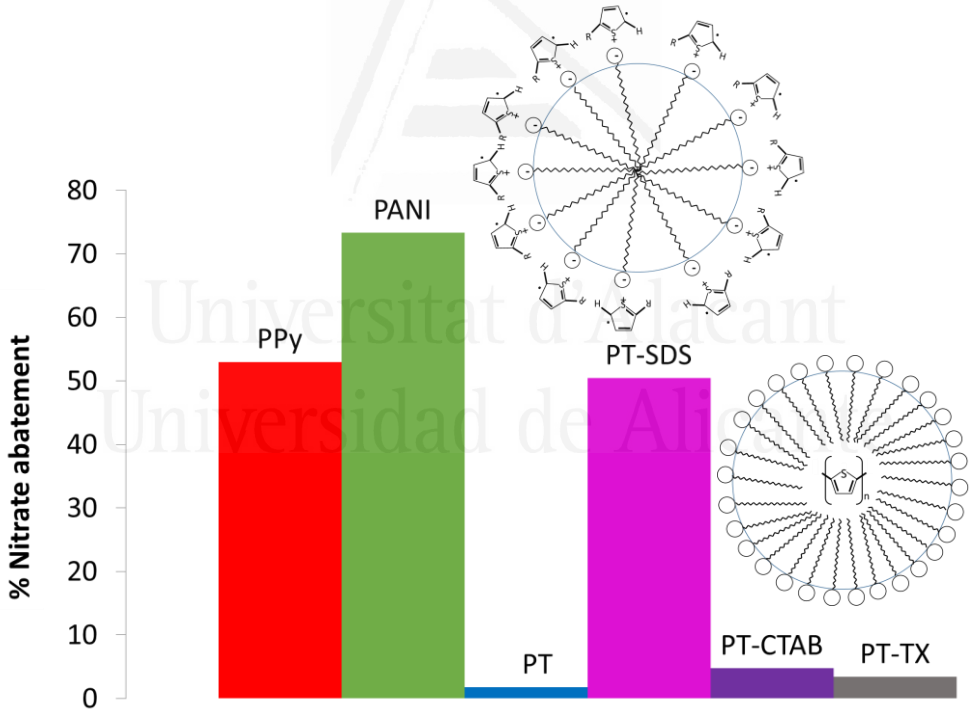

M.J. García-Fernández, S. Sancho-Querol, M.M. Pastor-Blas, A. Sepúlveda-Escribano, "Surfactant-assisted synthesis of conducting polymers. Application to the removal of nitrates from water", *Journal of Colloid and Interface Science*. **2017**, *494*, 98-106.

1. INTRODUCTION

Conducting polymers as polypyrrole (PPy), polyaniline (PANI) and polythiophene (PT) have a heteroaromatic and extended π-conjugated backbone structure that provides them with chemical stability and electrical conductivity, respectively. However, the π-conjugated structure is not enough to produce appreciable conductivity by its own. A doping process, which produces a partial charge extraction from the polymer chain, is mandatory [1].

Conducting polymers are prepared by chemical or electrochemical oxidation of the corresponding monomers. As a result, they have positive charges along the polymeric backbone, which become charge carriers. Counteranions called dopants are introduced during the synthesis of the conducting polymers to neutralize the positive charges of the backbones. The intrinsic conducting polymers in a doped or oxidized state become insulating when they are reduced. Upon reduction, the cationic charge carriers are lost and the small-sized dopant molecules are extracted from the polymer [2]. Schemes 8.1 and 8.2 show the reduced and oxidized forms of PT and PPy, respectively, where A^- is the counteranion of the oxidized polymer backbone.

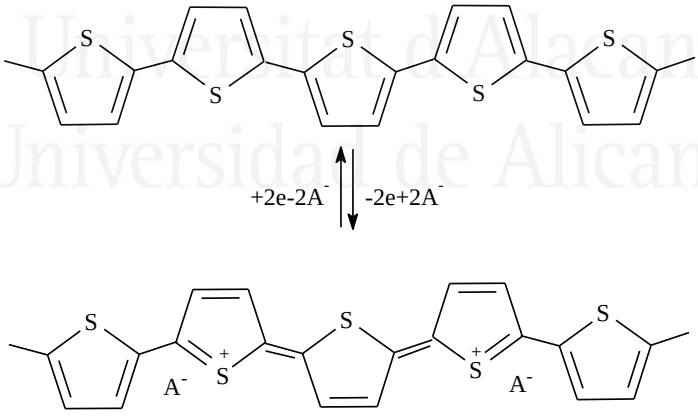

Scheme 8. 1. (a) Reduced and (b) oxidized (conducting) forms of PT.

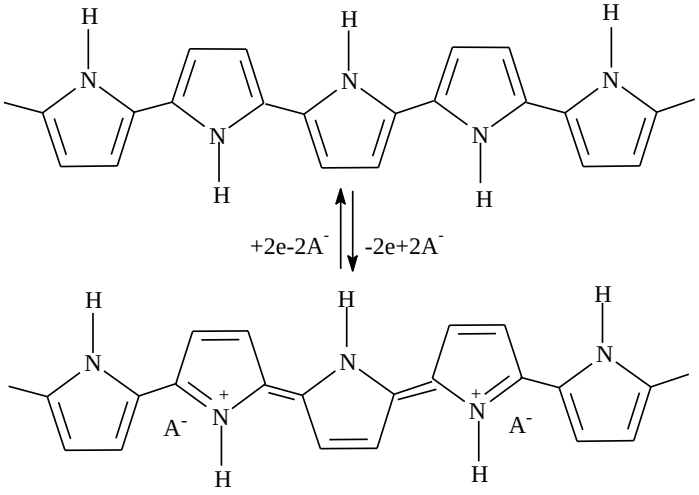

Scheme 8. 2. (a) Reduced and (b) oxidized (conducting) forms of PPy.

PANI can exist in many interconvertible oxidation states (Scheme 8.3). Leucoemeraldine is the fully reduced one; it shows only benzenoid rings with amine (-NH-) links and it is white/clear or colorless; pernigraniline is the fully oxidized state with imine (=N-) links instead of amine links, and it is blue/violet in color. Emeraldine base, the half oxidized form, has half benzenoid half quinoid rings, with an equal amount of amine and imine sites. Imine sites are subjected to protonation to form bipolarons, *i.e.* dications (emeraldine salt form). PANI in the form of emeraldine base (blue) can be doped (protonated) to the conductive form of emeraldine salt (green). Emeraldine base is regarded as the most useful form of polyaniline due to its high stability at room temperature and the fact that, upon doping with an acid, the resulting emeraldine salt form is highly electrical conducting. Leucoemeraldine and pernigraniline are poor conductors, even when doped with an acid. Thus, PANI is electrically conductive in its emeraldine oxidation state when doped with an acid that protonates the imine nitrogens on the polymer backbone. Dopants can be added in any desired quantity until all imine nitrogens (half of total nitrogens) are doped, simply by controlling the pH of the dopant acid solution. PANI's conductivity increases with doping from the un-doped insulated base form ($\sigma \leq 10^{-8}$ S·m^{-1}) to the fully doped, conducting acid form ($\sigma \geq 10^{2}$ S·m^{-1}). Doping and un-doping processes can be carried out electrochemically or chemically. The synthesis of PANI by chemical oxidative polymerization involves the aniline monomer, an acid and an oxidant (*e.g.* hydrogen peroxide, ferric chloride, ammonium or potassium peroxydisulfate). Different oxidants provide different dopants, which act as counterions which compensate the positively charged

(semioxidized) polymer chain in the conductive form (emeraldine salt). Doping can be produced with common acids such as hydrochloric acid and de-doping with bases such as ammonium hydroxide. The doping process can drastically change the electronic, optical, magnetic and/or structural properties of the polymer and increases its conductivity significantly [1].

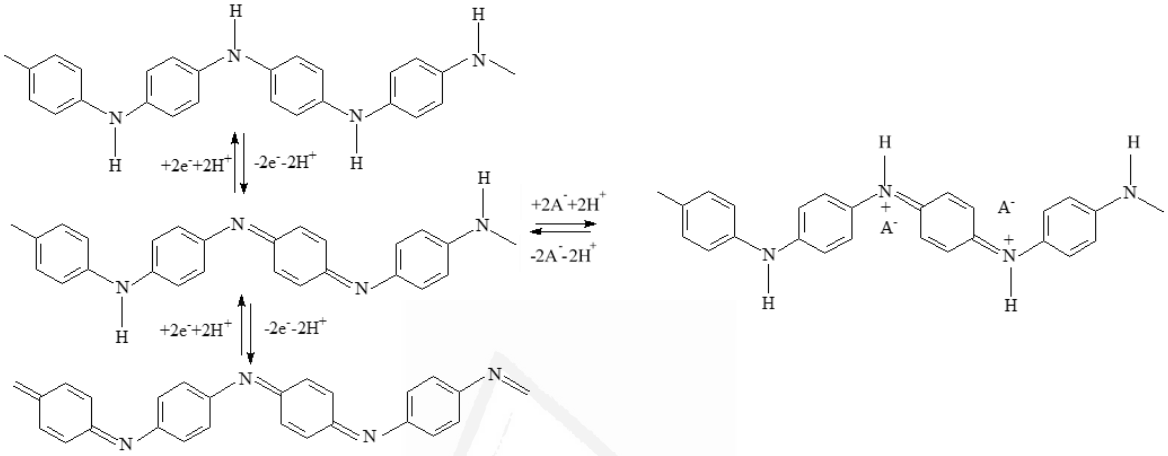

Scheme 8. 3. Different forms of PANI: (a) leucoemeraldine, (b) emeraldine base, (c) pernigraniline and (d) emeraldine salt.

As described in previous chapters, these intrinsic conducting polymers have been used in a great variety of applications such as lightweight battery electrodes, electromagnetic shielding devices, anticorrosion coatings, electrochromic displays, chemical/gas sensors, photo-electrochemical cells, actuators and artificial muscles. The combination of electrical conductivity and polymeric properties such as flexibility, low density and ease of structural modification make them very interesting for many processes, such as abatement of contaminants.

In the previous chapter, the mechanisms involved in the abatement of nitrate by platinum nanoparticles supported on PPy and PANI, and the extension of each mechanism depending on the polymer nature were discussed. Nevertheless, as showed in chapter V, nitrate abatement produced by the metal-free PPy is more effective than the hydrogenation of nitrate catalyzed by the mono or bimetallic catalysts. As platinum nanoparticles anchor to the polypyrrole chain through nitrogen positions, the electron transfer from polypyrrole to nitrate is direct in absence of platinum, but is platinum-mediated in the platinum catalyst,

which shows lower efficiency in the removal of nitrates from water. Therefore, the polypyrrole chain seems to be a more effective reductor than dihydrogen.

In this chapter, three different conducting polymers, polypyrrole (PPy), polyaniline (PANI) and polythiophene (PT) have been considered for the abatement of nitrate from water. No metal catalyst and no external reductant such as hydrogen have been used. The intrinsic conducting nature of these polymers, with switchable oxidation states, determines that the polymeric chain may act either as a source or a drain of electrons depending on the redox process in which it is involved. However, the different functionalities of the polymeric chain, *i.e.* nitrogen in the pyrrolic ring of PPy; nitrogen external to the ring in PANI and sulfur in PT, may play a definitive role in the performance and selectivity of nitrate adsorption and reduction processes.

On the other hand, the aqueous synthesis of polythiophene is especially complicated due to its low solubility in water, so it is generally synthesized using $FeCl_3$ in non-polar solvents such as chloroform [3]. However, it is the main goal of this work to develop environmentally friendly processes. Therefore, new synthesis routes involving the use of surfactants need to be developed.

2. EXPERIMENTAL

2.1. Materials preparation

The synthesis conditions as pH, temperature and doping level affect the morphology and also the conducting properties of the polymer. Therefore, optimized polymerization procedures have been carried out in this chapter.

PPy and PANI were synthesized by chemical oxidative polymerization. $K_2S_2O_8$ was used in PANI synthesis due to the low aniline conversion with other oxidants (as for instance ferric chloride). For the sake of simplicity and comparison purposes, the same oxidant was used in polypyrrole synthesis.

PANI was synthesized using potassium peroxydisulfate ($K_2S_2O_8$, *Sigma-Aldrich*, 99 %) as oxidant and dopant in the chemical polymerization of aniline ($C_6H_5NH_2$, *Sigma-Aldrich*). The experimental procedure was described in chapter VII, section 2.1.

PPy was synthesized using potassium peroxydisulfate ($K_2S_2O_8$, *Sigma-Aldrich*, 99 %) as oxidant and dopant in the chemical polymerization of pyrrole (C_4H_5N, *Sigma-Aldrich*, reagent grade, 98 %). The experimental procedure was described in chapter VI, section 2.1.

The oxidative chemical polymerization of thiophene in aqueous media is complicated due to the poor solubility of PT in water, the low oxidizing activity of the catalysts and an extremely low conversion. In this chapter, a combination of anhydrous ferric chloride ($FeCl_3$) as catalyst and hydrogen peroxide (H_2O_2) as oxidant was used to guarantee high conversion (*ca.* 99 %) of thiophene monomers with only trace amounts of $FeCl_3$ ($FeCl_3/H_2O_2$ ratio was 0.00422). In this way, continuous regeneration of the Fe^{3+} catalyst through Fe^{2+} oxidation by H_2O_2 is assured [4] (Scheme 8.4). The experimental procedure was as follows: 1.9 mL of thiophene monomer (C_4H_4S, M_m = 84.14 g·mol^{-1}) was dissolved in 60 mL of ultrapure water and added to a three necked glass reactor fitted with a reflux condenser, a nitrogen gas inlet, an ingredient inlet and a mechanical stirrer. Hydrogen peroxide (7.5 mL, 50 % aq. solution) was added to the reactant mixture solution. $FeCl_3$ (16.0 mg) was dissolved in 5 mL of ultrapure water and slowly added to the reactant mixture solution with a syringe. This mixture was then stirred at 300 rpm for 12 h at 50 °C. The initial colorless solution turned to yellowish and finally brown, indicating the polymerization process. The dark brown PT precipitate was washed with ultrapure water, filtered and dried at 50 °C for 24 h.

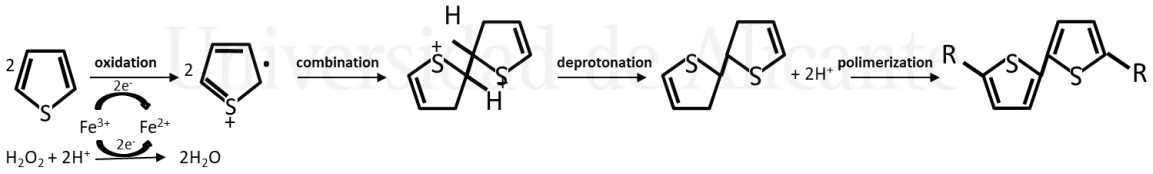

Scheme 8. 4. Polymerization of conducting PT with $FeCl_3/H_2O_2$.

PT was also synthesized using surfactants of different nature: sodium dodecyl sulfate (SDS) as anionic surfactant, cetyltrimethylammonium bromide (CTAB) as cationic surfactant and polyethylene glycol terc-octyphenil ether (Triton X; TX) as non-ionic surfactant (Scheme 8.5). In these syntheses, the same experimental procedure was used but 0.1 g of surfactant were dissolved in 60 mL of ultrapure water and added to the glass reactor before the addition of the thiophene monomer.

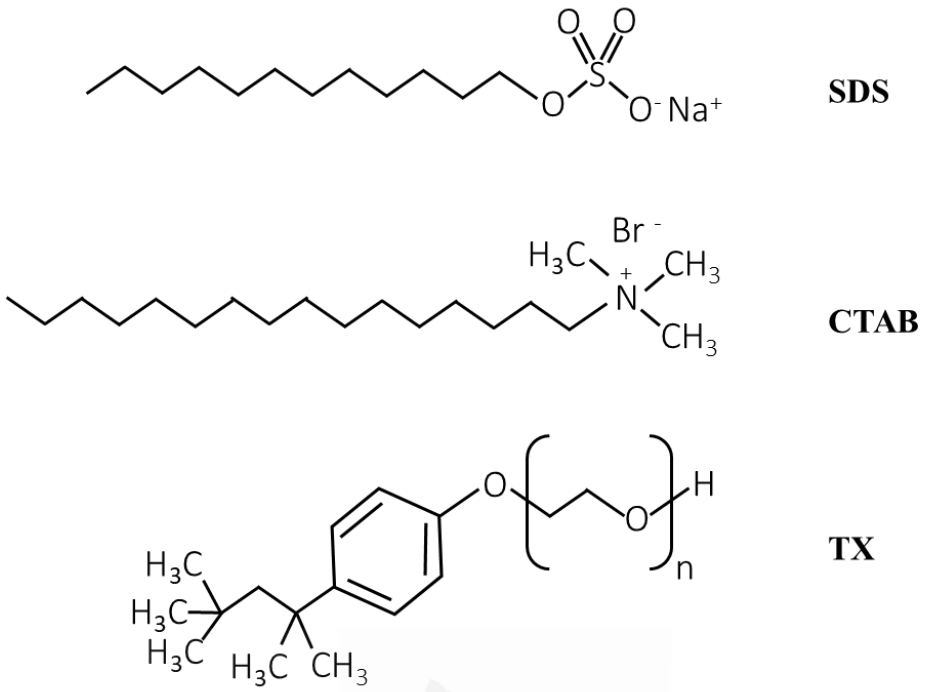

Scheme 8. 5. Chemical structure of surfactants SDS, CTAB and TX.

2.2. Materials characterization

Electrical conductivity, N_2 adsorption at -196 °C, infrared spectroscopy (FTIR), X-ray photoelectron spectroscopy (XPS), X-ray diffraction (XRD), transmission electron microscopy (TEM), thermogravimetric analysis (TGA) and differential scanning calorimetry (DSC) were used to characterize the samples. The experimental details are described in chapter II, section 2.

2.3. Catalyst evaluation

The nitrate removal ability of the three synthesized polymers was evaluated in the reduction of an aqueous solution of sodium nitrate at room temperature. The reaction took place in a semi-batch reactor equipped with a magnetic stirrer (700 rpm) as it is detailed in chapter II, section 1.4. Aliquots (1 mL) were withdrawn at different times from the reactor and immediately filtered for determination of nitrate, nitrite and ammonium concentrations by ion chromatography as it is indicated in chapter II, section 2.9.

3. RESULTS AND DISCUSSION

3.1. Characterization of polymers

Synthesized polymers were characterized by FTIR. PPy (Fig. 8.1a, Table 8.1) shows absorption bands at 1562, 1197 and 920 cm^{-1} which are characteristic of C=N-C moieties. Besides, the band at 1714 cm^{-1} (C=O stretching) is assigned to surface oxygenated groups created as a consequence of the reaction of the polymeric chain with water within the polymer network, as polypyrrole is hygroscopic. Spectrum of PANI (Fig. 8.1b) shows typical bands of the polymeric chain [5,6] (Table 8.1). The absorption bands at 1580 and 1484 cm^{-1} correspond to the absorption of quinoid and benzenoid rings, respectively, characteristic of emeraldine (Scheme 8.3). The relative intensities of these bands provide an indication of the PANI oxidation states [1,6]. Spectrum of PT shows adsorbed water at 3073 cm^{-1}. The bands at 1668 and 1400 cm^{-1} correspond to the asymmetric and symmetric stretching vibration modes of the thiophene ring. The bands at 874 and 704 cm^{-1} are assigned to C-S bending.

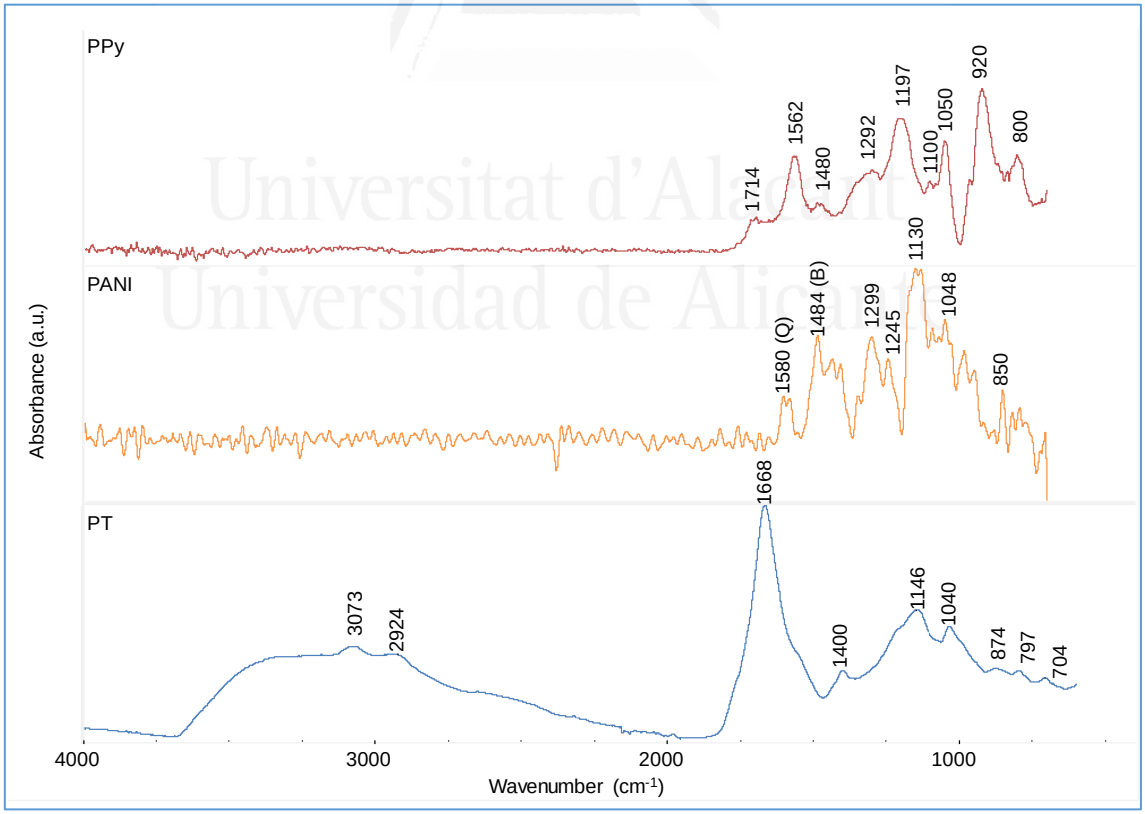

Figure 8. 1. FTIR-ATR spectra of PPy, PANI and PT.

Table 8. 1. IR-bands assignment in PPy, PANI and PT.

PPy (cm^{-1})	Assignment[a]	PANI (cm^{-1})	Assignment[a]	PT (cm^{-1})	Assignment[a]
1714	C=O st	1580	C=N st, Q	3073	O-H st
1562	C=N st	1484	C=C st, B	2924	C-H st
1480	C=C st	1296	C-C st	1668	C=C as st
1292	C-C st	1245	C-N st	1400	C=C sy st
1197	C-N st	1145	$-NH^{+}=$	1146	C-H δ
1050	=C-H δ_{oop}	1140	C-C δ_{ip}	1040	C-H δ_{ip}
920	C=N-C δ	1048	=C-H δ_{oop}	874	C-S δ
800	N-H δ	820	N-H δ	797	C-H δ_{oop}
				704	C-S δ

[a] Stretching (st), bending (δ), in-plane bending (δ_{ip}), out-of-plane bending (δ_{oop}), symmetric (sy), asymmetric (as), quinoid (Q) and benzenoid (B).

Synthesized PPy, PANI and PT showed electrical conductivities of 25, 478 and $2.71 \cdot 10^{-2}$ $S \cdot m^{-1}$, respectively.

The N_2 adsorption isotherms at - 196 °C were type II in all cases, which are characteristic of non-porous solids. The BET surface areas obtained from the adsorption isotherms were 11 $m^2 \cdot g^{-1}$ for PPy, 40 $m^2 \cdot g^{-1}$ for PANI and 20 $m^2 \cdot g^{-1}$ for PT.

The thermal stability of the polymers in air was assessed by TGA experiments (Fig. 8.2). PANI and PPy showed a first weight loss (around 8 – 9 % of its initial mass) between 30 and 100 °C, which corresponds to the loss of water trapped in the polymers and non-reacted monomers. PPy showed a second weight loss which can be assigned to the degradation of the polymer. In PANI, degradation proceeded in two steps: the first one, with a 10 % weight loss and centered at around 250 °C, could be assigned to the thermal degradation of the cross-linked chains and the second one, centered at 500 °C, can be assigned to the decomposition of the lineal part of the chains. Total burning of the polymers was produced at 730 °C for PPy and 630 °C for PANI. In PT there was a first weight loss at around 100 °C, which corresponds to the loss of water and nonreacted monomers. Then, degradation of PT occurred above 200 °C.

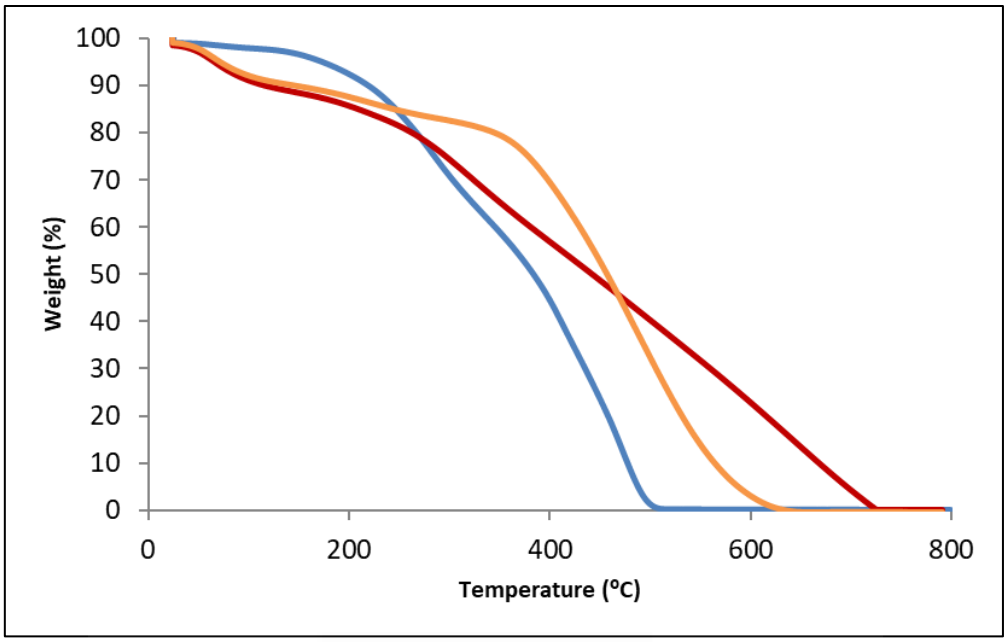

Figure 8. 2. TGA profile in air atmosphere of PPy; PANI and PT.

XRD diffraction patterns of PPy, PANI and PT (Fig. 8.3) are characteristic of amorphous polymers. The bands centered at 2θ = 17 − 18 º for PPy and 2θ = 18 − 20 º for PANI correspond to the periodicity along the polymeric chain. Another band centered at 2θ = 25 º for PPy and 2θ = 27 − 28 º for PANI corresponds to the periodicity perpendicular to the polymer chain [5]. The third band situated at 2θ = 42 º in both polymers is also typical of the polymer phase [6]. PT shows only a broad band around 2θ = 23 º due to its molecular π-π stacking structure [7].

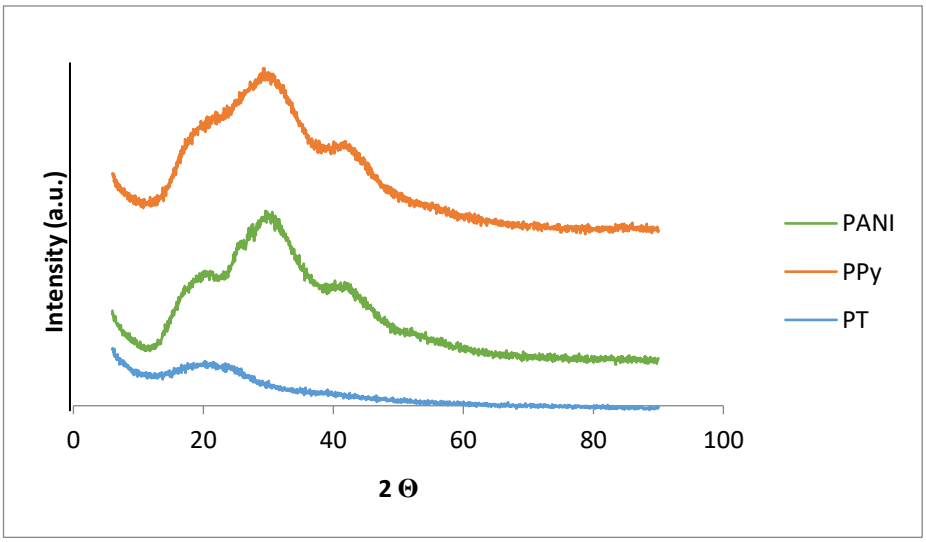

Figure 8. 3. XRD patterns of synthesized polymers.

3.2. Nitrate removal by conducting polymers

The capability of PPy, PANI and PT conducting polymers of removing of nitrate from water was evaluated. The mechanism for nitrate removal may proceed by (i) ion exchange between the counteranion of the oxidized polymeric chain and nitrate, and/or (ii) reduction of nitrate anchored to the polymeric chain by electrons donated by the conducting polymer [8]. The chemical nature of the conducting polymer plays a definitive role. Whereas electron transfer is produced through the nitrogen atom (located within the ring in PPy or outside the ring in PANI), PT possesses an S atom in its chemical structure within the thiophene ring. This seems to definitively affect the ability of the polymers to produce the abatement of nitrate.

Legislation establishes that the maximum permitted levels of nitrate, nitrite and ammonium in drinking water are 50, 0.5 and 0.5 $mg \cdot L^{-1}$ respectively [9,10]. Figure 8.4 shows that only PPy and PANI were able to produce a decrease of nitrate concentration below 50 $mg \cdot L^{-1}$. This decrease of nitrate concentration measured in the aqueous solution in contact with the polymers was produced within the first 5 min, and then it was maintained with time. Table 8.2 shows that a considerably high nitrate concentration is remaining in water after 300 min in the presence of PT.

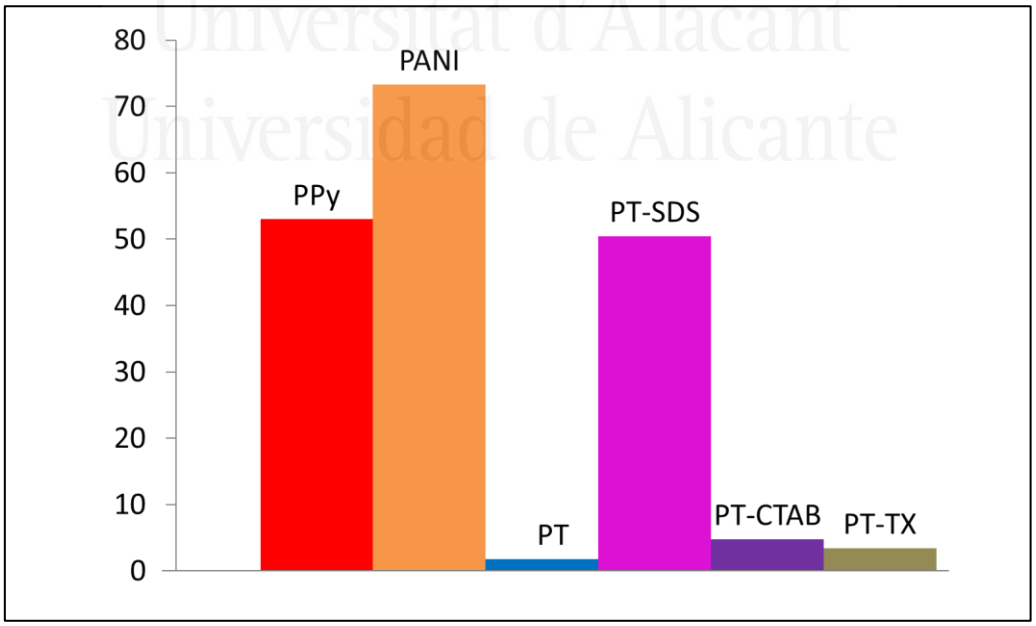

Figure 8. 4. Nitrate abatement produced by the different synthesized conducting polymers.

Table 8. 2. Nitrate, nitrite and ammonium concentrations ($mg \cdot L^{-1}$) after 300 min in contact with the polymers.

($mg \cdot L^{-1}$)	**PPy**	**PANI**	**PT**	**PT-SDS**	**PT-CTAB**	**PT-TX**
$[NO_3^-]$	47.00	26.70	98.22	49.54	95.23	96.57
$[NO_2^-]$	0.05	0.01	0.65	0.67	0.61	0.60
$[NH_4^+]$	4.09	0	1.39	6.06	2.28	1.75
$[Cl^-]$	1.66	12.41	1.43	12.41	5.48	1.59

When comparing the N-containing polymers, it could be observed that the decrease of nitrate concentration was much more important with PANI than with PPy. It was not possible to measure N_2 production; however, a considerable ammonium production was detected with PPy, which supports the idea of nitrate being reduced by electrons provided by the polymer. It must be taken into account that ion exchange between Cl^- and/or SO_4^{2-} present in these doped polymers and NO_3^- may be taking place. However, if nitrate would remain anchored to the polymeric chain as NO_3^- by a simple electrostatic interaction, with no further reduction process, it would be necessary to treat or to disposal the nitrate saturated polymers, which is also an environmental concern. In the case of PPy there was ammonium production; so at least some of the initially retained nitrate was suffering reduction by the electrons provided by the polymeric chain. However, neither nitrite nor ammonium was measured in the aqueous solution in contact with PANI, which may be due to nitrate being only exchanged by sulfate anions in PANI with no further redox process.

On the other hand, the S-containing PT was not effective in successfully removing nitrate from the solution, although the redox process was taking place to some extent as there was some nitrite and ammonium production (Table 8.2).

XPS was helpful to elucidate the mechanism of nitrate abatement produced by PPy and PANI. Surface composition from XPS analysis (Table 8.3) showed C from the polymeric chain and O from surface oxidation due to the contact of the polymers with the aqueous media during the polymerization reaction. Nitrogen was obviously detected in PPy and PANI and sulfur in PT.

Table 8. 3. XPS surface chemical composition (atomic %) of the different samples.

Binding energy (*eV*)	284.5	531.5	398.1	198.5	168.3
Element	**C 1s**	**O 1s**	**N 1s**	**Cl 2p**	**S 2p**
PPy	69.2	18.0	12.2	0.2	0.4
PPy-R[a]	69.6	17.8	12.3	0.1	0.2
PANI	77.7	7.8	9.6	3.9	1.0
PANI-R[a]	77.4	9.6	10.9	1.9	0.2
PT	65.0	22.7	-	-	12.3
PT-R[a]	62.4	20.8	-	-	16.8
PT-SDS	76.3	19.0	-	0.1	4.6
PT-SDS-R[a]	72.4	19.0	-	-	8.6
PT-CTAB	61.2	24.4	-	-	14.4
PT-CTAB-R[a]	67.0	19.5	-	-	13.5
PT-TX	61.4	23.3	-	-	15.3
PT-TX-R[a]	69.1	22.4	-	-	8.5

[a] R = recovered catalyst after 300 min of reaction.

Sulfur was also detected in N-containing polymers (PPy and PANI) but in a considerably lower amount compared to PT. This sulfur comes from the oxidant added in excess (potassium peroxydisulfate). K was not detected, but S 2p doublets at 168.6 (S $2p_{3/2}$) and 169.9 eV (S $2p_{1/2}$) in PPy, and at 168.3 (S $2p_{3/2}$) and 169.6 eV (S $2p_{1/2}$) in PANI can be assigned to sulfate (SO_4^{2-}) produced as a result of reduction of peroxydisulfate ($S_2O_8^{2-}$) when it is anchored to the polymeric chain of PPy and PANI as a counteranion, during the course of the polymerization. This results in an oxidized polymeric chain with oxidized nitrogen groups (-N^+-) as assessed by the deconvolution of the N 1s level band (Fig. 8.5, Table 8.4). However, the degree of oxidation was different in PPy and PANI. The polypyrrole chain showed a considerable higher percentage of oxidized nitrogen (-N^+-) compared to PANI, where mainly amine groups (-NH-) are present.

Table 8. 4. XPS analysis of the N 1s level. Contribution (%) of different nitrogen species.

Sample	**Nitrogen species**	**Energy (eV)**		**Composition (%)**	
		Pristine	**Recovered[a]**	**Pristine**	**Recovered[a]**
PPy	-N=	398.8	-	7	-
	-NH-	-	399.8	-	33
	$-N^{\cdot+}$	400.3	400.6	93	67
PANI	=N-	-	398.6	-	28
	-NH-	399.3	399.3	83	64
	$-N^{\cdot+}$	400.8	-	17	-
	NO_3^-	-	406.2	-	8

[a] recovered catalyst after 300 min of reaction.

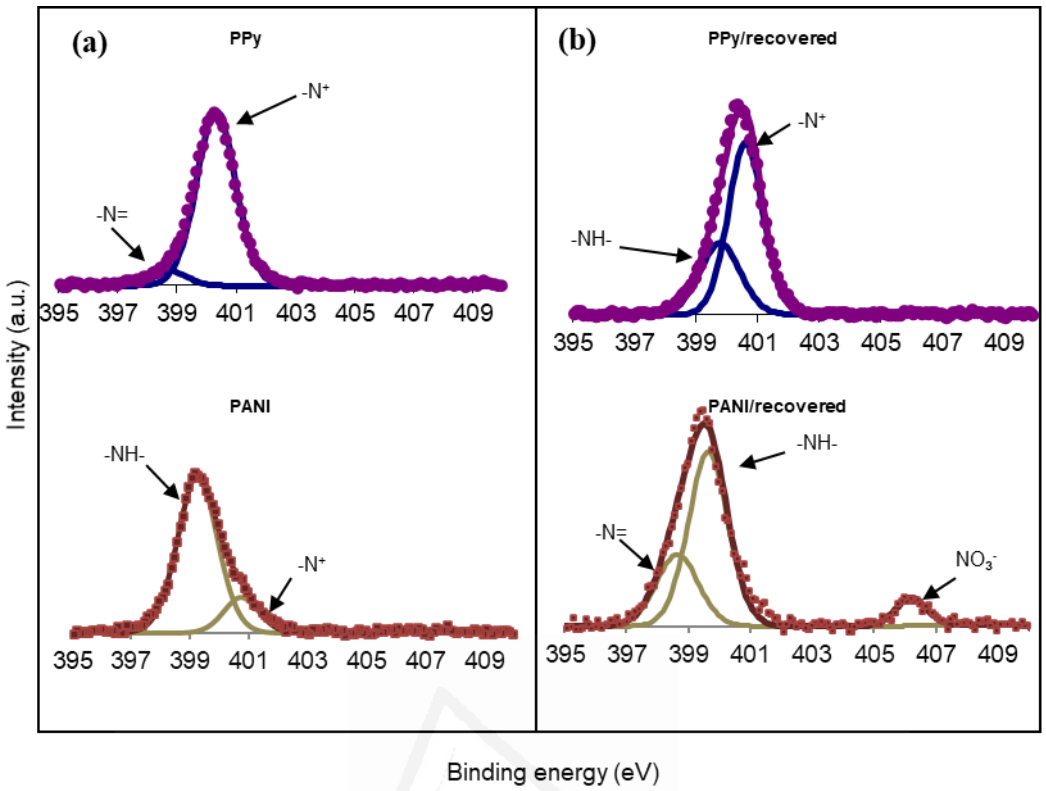

Figure 8. 5. XPS N 1s spectra of PPy and PANI: (a) pristine and (b) recovered after 300 min in contact with the aqueous nitrate solution.

A noticeable percentage of chlorine as chloride anion (Cl $2p_{3/2}$ at 197.1 and Cl $2p_{1/2}$ at 198.6 eV) was detected in PANI, as polymerization was carried out in aqueous HCl medium. This chloride incorporates to the polymer as a counterion together with SO_4^{2-}. In PPy, some chlorine was also detected by XPS. As polymerization of polypyrrole was carried out in water and HCl was not added, the small amount of Cl^- detected has to come from water contamination.

The oxidation degree of the pristine PT can be evaluated from the analysis of the XPS S 2p curve fit (Fig. 8.6a), which shows the contribution of the reduced S-C moieties at 163.6 eV (S $2p_{3/2}$) and 164.8 eV (S $2p_{1/2}$). Only 12 % (Table 8.5) of the detected sulfur was oxidized as S^+-C, as shown by the presence of the doublet at 166.4 eV (S $2p_{3/2}$) and 167.7 eV (S $2p_{1/2}$). This positive oxidation state exists in water as hydrated cations, and then undergo reactions between the cations and water to neutralize their positive charges. PT synthesis in aqueous medium requires the use of a catalyst/oxidant combination to assure an appropriate yield. In this system, thiophene monomers are oxidized to cationic radicals, which react among them to produce PT. As only a trace of anhydrous $FeCl_3$ was used, neither

Fe nor Cl is detected by XPS. Consequently, due to the low percentage of oxidized S^+-C moieties in PT (compared to the percentage of oxidized N^+ moieties in PPy and PANI, which are charge-compensated by Cl^- or SO_4^{2-} counterions), nitrate abatement from water is very poorly produced by PT. Nevertheless, the measured concentrations of nitrite and ammonium anions suggest that electron transfer from the PT chain to nitrate was indeed produced to some extent.

Table 8. 5. XPS analysis of the S $2p_{3/2}$ level. Contribution (%) of different sulfur species[a].

Sample	Sulfur species	Energy (eV)		Composition (%)	
		Pristine	Recovered[a]	Pristine	Recovered[a]
PPy	SO_4^{2-}	168.6	168.6	100	100
PANI	SO_4^{2-}	168.4	168.1	100	100
PT	S-C	163.6	163.5	88	90
	S^+-C	166.4	166.9	12	10
PT-SDS	S-C	163.5	163.5	79	52
	RSOR	-	165.2	-	34
	S=O	167.1	-	21	-
	S^+-C	-	168.4	-	14
	SO_4^{2-}	-	-	-	-
PT-CTAB	S-C	163.3	163.6	92	92
	S^+-C	167.0	167.2	8	8
PT-TX	S-C	163.3	163.4	94	93
	S^+-C	167.6	166.2	6	7

[a] recovered catalyst after 300 min of reaction.

The capability of the conducting polymers of switching between different oxidation states imparts these polymers the capability of acting as a source or a drain of electrons, depending on the redox process in which they are involved. Therefore, it is possible that nitrate is reduced by these conducting polymers to nitrogen (desired) or ammonium (non desired), what is confirmed by the redox potentials of polymers and nitrogen-containing species involved in the nitrate reduction process: polypyrrole (PPy^+/PPy, E° = 0.15 V); polyaniline (emeraldine/leucoemeraldine, E° = 0.342 V; pernigraniline/ emeraldine, E° = 0.942 V) [11]; polythiophene (PT^+/PT, E° = 0.7 V) [2] and nitrate (NO_3^-/N_2, E° = 1.246 V; NO_3^-/NH_4^+, E° = 0.875 V).

Upon reduction of nitrate, the polymeric chain is expected to become oxidized during the course of the reaction. In this way, PPy and PANI which were recovered after 300 min in contact with nitrate solution were analyzed by XPS.

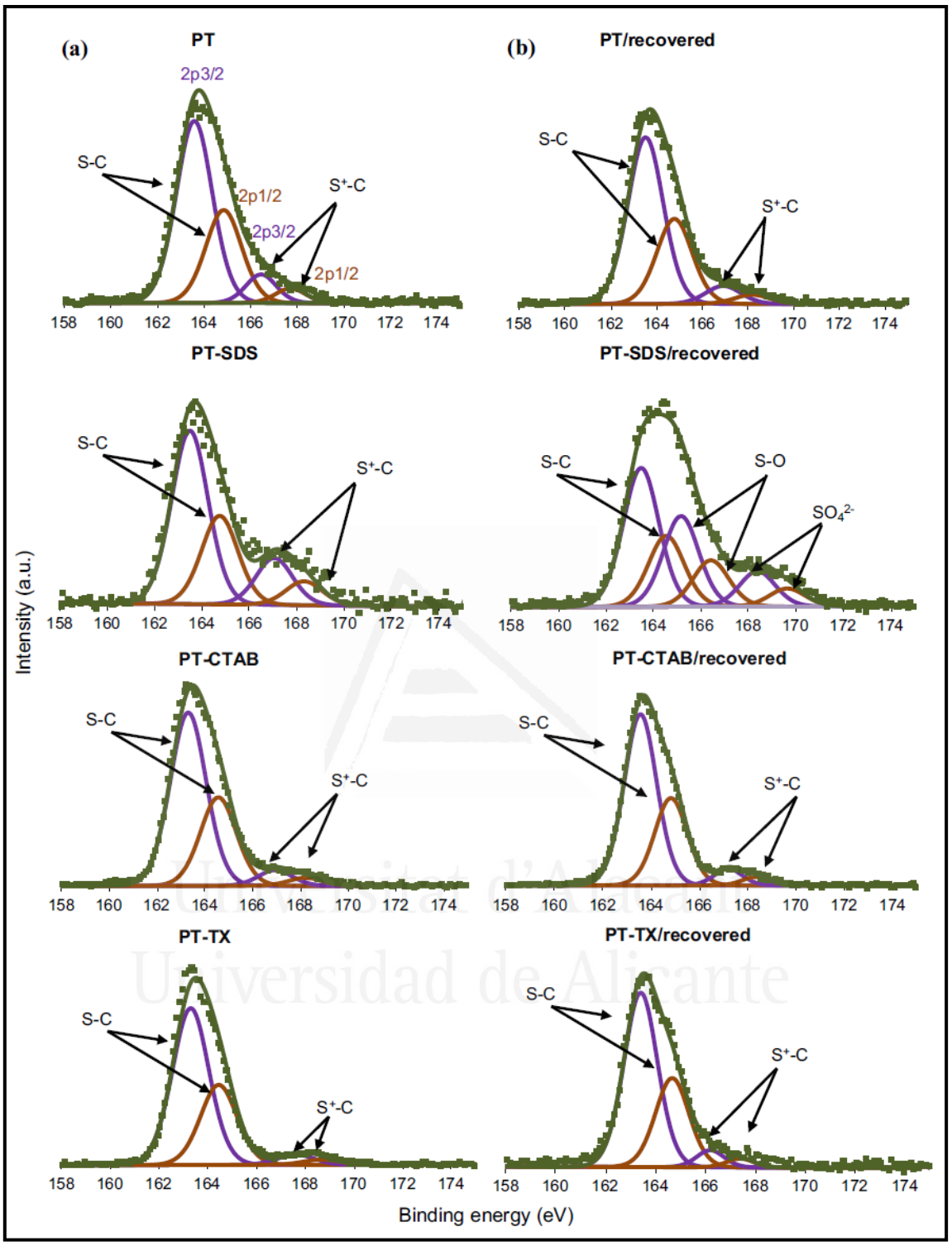

Figure 8. 6. XPS S 2p spectra of PT: (a) pristine and (b) recovered after 300 min in contact with the aqueous nitrate solution.

Table 8.3 shows an important decrease of Cl and S contents and an increase of N content in recovered PANI. Whereas pristine PANI showed -NH- and $-N^+$ contributions of emeraldine salt, recovered PANI showed amine (-NH-) and imine (-N=) contributions of

emeraldine base, as well as an important contribution at 406 eV of nitrate (NO_3^-) (Table 8.4, Fig. 8.5). A considerable amount of chlorine (12.41 $mg \cdot L^{-1}$) was detected by ion chromatography in the aliquots extracted from the aqueous nitrate solution in contact with PANI (Table 8.2). These findings evidence the occurrence of ion exchange between NO_3^- and counteranions present in the doped PANI (Cl^- and SO_4^{2-}).

However, no nitrate contribution was observed in the N 1s spectra of PPy, and the oxidation of the polypyrrole chain in contact with the nitrate aqueous solution was evidenced. Imine contribution (=N-) at 398.8 eV in pristine PPy was not present in recovered PPy, as imine groups have been oxidized to -NH- amine groups (Fig. 8.5).

Therefore, it can be concluded that removal of NO_3^- from water proceeds by ion exchange in a first step, which may be followed by a redox process. The ion exchange is predominant in PANI, but nitrate is completely reduced by PPy after been exchanged by sulfate anion. The different location of nitrogen outside the aromatic cycle in PANI and inside the cycle in PPy could have some influence in the extension of each mechanism, ion exchange and redox process. On the other hand, PT does not show any relevant change in the oxidation state of its polymeric chain, as it is evidenced by the contribution of reduced S-C and oxidized S^+-C moieties (Fig. 8.6, Table 8.5). Consequently, no satisfactory nitrate removal is obtained with PT.

3.3. Use of surfactants in polythiophene synthesis

The oxidative polymerization of thiophene in aqueous media is complicated due to poor water solubility of PT, the low oxidizing activity of the catalysts and an extremely low conversion [12]. A synthesis route which includes a $FeCl_3/H_2O_2$ catalyst/oxidant combination system has been used to assure a good yield [4]. However, this synthesized PT, which is mainly in a reduced state, did not provide good results in the abatement of nitrate from water.

The preparation of PT in colloidal form using surfactants is an attractive alternative to overcome its poor water solubility. The surfactant molecules form micelles in the reactant solution which affect the molecular and supramolecular structure of PT by altering the locus of polymerization [7]. In the presence of surfactants, the polymerization mechanism of

thiophene with $H_2O_2/FeCl_3$ has been reported [4,13] to be determined by several steps: (i) stabilization step: the formation of stable thiophene monomer swollen micelles; (ii) diffusion step: the metal cations (Fe^{3+}) diffuse from the aqueous phase into the micelles; (iii) initiation step: thiophene monomers are oxidized by the Fe^{3+} cations followed by the formation of cationic thiophene monomeric radicals; (iv) propagation step: thiophene cationic radicals are coupled to form dimers, the dimers are further oxidized to form cationic radicals and the coupling reaction continue to gradually form polymer chains and, (v) regeneration step: oxidation of Fe^{2+} by H_2O_2. The oxidant anions (Cl^-) may interfere with the diffusion process of the Fe^{3+} metal cations from aqueous phase to micelles by electrostatic attraction or may interact with cationic radicals affecting their propagation reaction.

The effect of surfactants of different nature on the capability of PT of abating nitrate from water was evaluated. Therefore, PT was synthesized using an anionic surfactant (sodium dodecyl sulfate, SDS), a cationic surfactant (cetyltrimethylammonium bromide, CTAB) and a non-ionic surfactant (polyethylene glycol terc-octyphenil ether, Triton X).

Synthesized polythiophenes were analyzed by ATR-IR. Figure 8.7 shows bands at 2925 and 2854 cm^{-1} due to C-H stretching from the surfactants, which are more important in PT-SDS. This reveals that a certain amount of the surfactants is retained by PT after washing.

SEM micrographs (Fig. 8.8) also show a change in the morphology of PT by the presence of the anionic SDS surfactant. PT-SDS shows a spherical morphology instead of the colliflower-like structure exhibited by its counterparts. In aqueous medium, the molecules of surfactant form micelles spontaneously due to its amphiphilic nature, with the hydrophilic parts extending and the hydrophobic segments aggregating inside. These micelles become loci of polymerization of thiophene monomers, usually accommodated inside. As the polymerization proceeds, the hydrophobic segments of surfactants adsorb onto the PT chains to form colloid particles which stabilize themselves through electrostatic repulsion (ionic surfactants) or steric repulsion between the adsorbed layers of the non-ionic surfactant. When a critical polymeric chain length is achieved, precipitation of the polymer is produced [13].

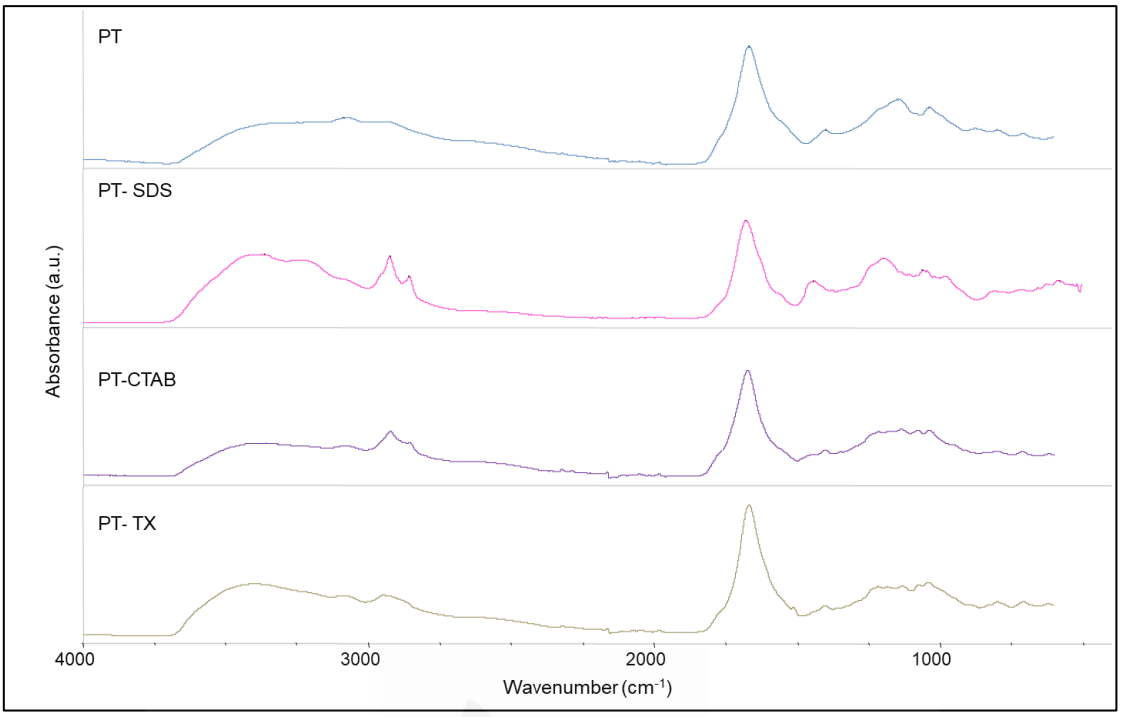

Figure 8. 7. FTIR-ATR spectra of — PT; PT synthesized with: — SDS; — CTAB and — TX.

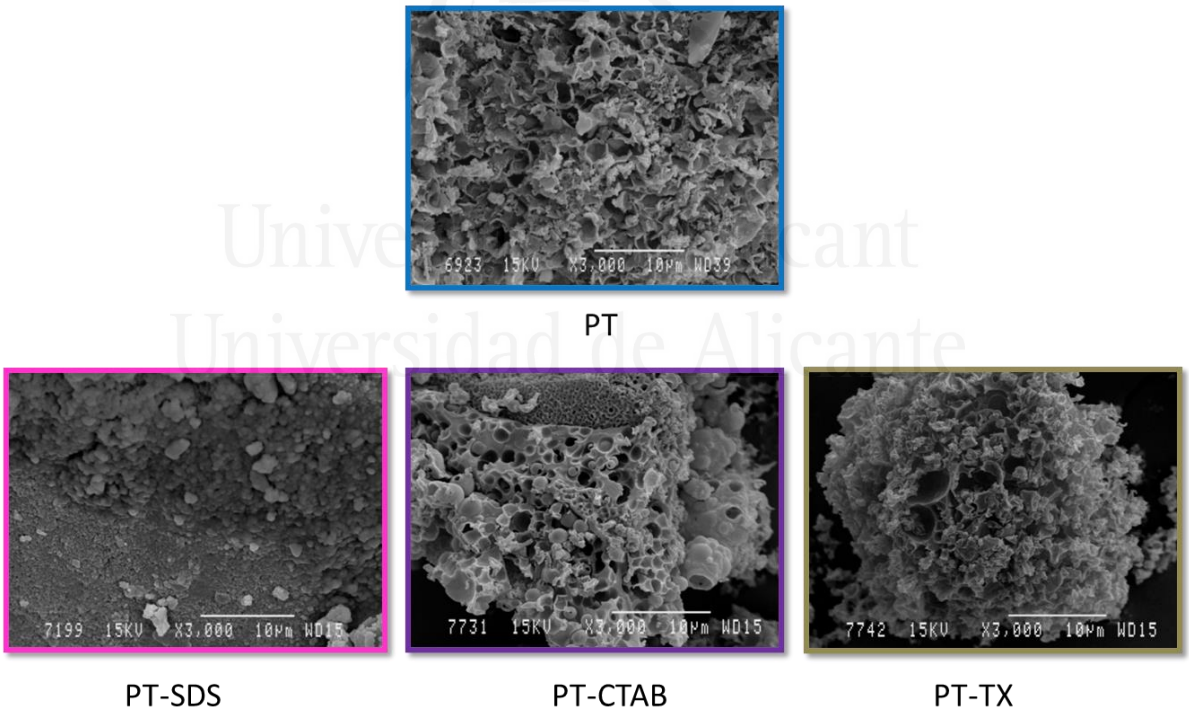

Figure 8. 8. SEM micrographs of — PT and PT synthesized with — SDS; — CTAB; — TX.

Lee et al. [4] established that the mechanism of micelle formation depends on the nature of the surfactant. Thus, when thiophene polymerization with $FeCl_3/H_2O_2$ (Scheme 8.4) is carried out in the presence of a cationic surfactant (CTAB), an electrostatic repulsion

between the $(CH_3)_3N^+$ groups of the CTAB surfactant and Fe^{3+} cations is produced. Thus, Fe^{3+} ions are drawn into the micelle where they catalyze the polymerization of thiophene (Scheme 8.6a) which had previously diffused into the inner part of the micelle due to hydrophobic-hydrophobic interactions.

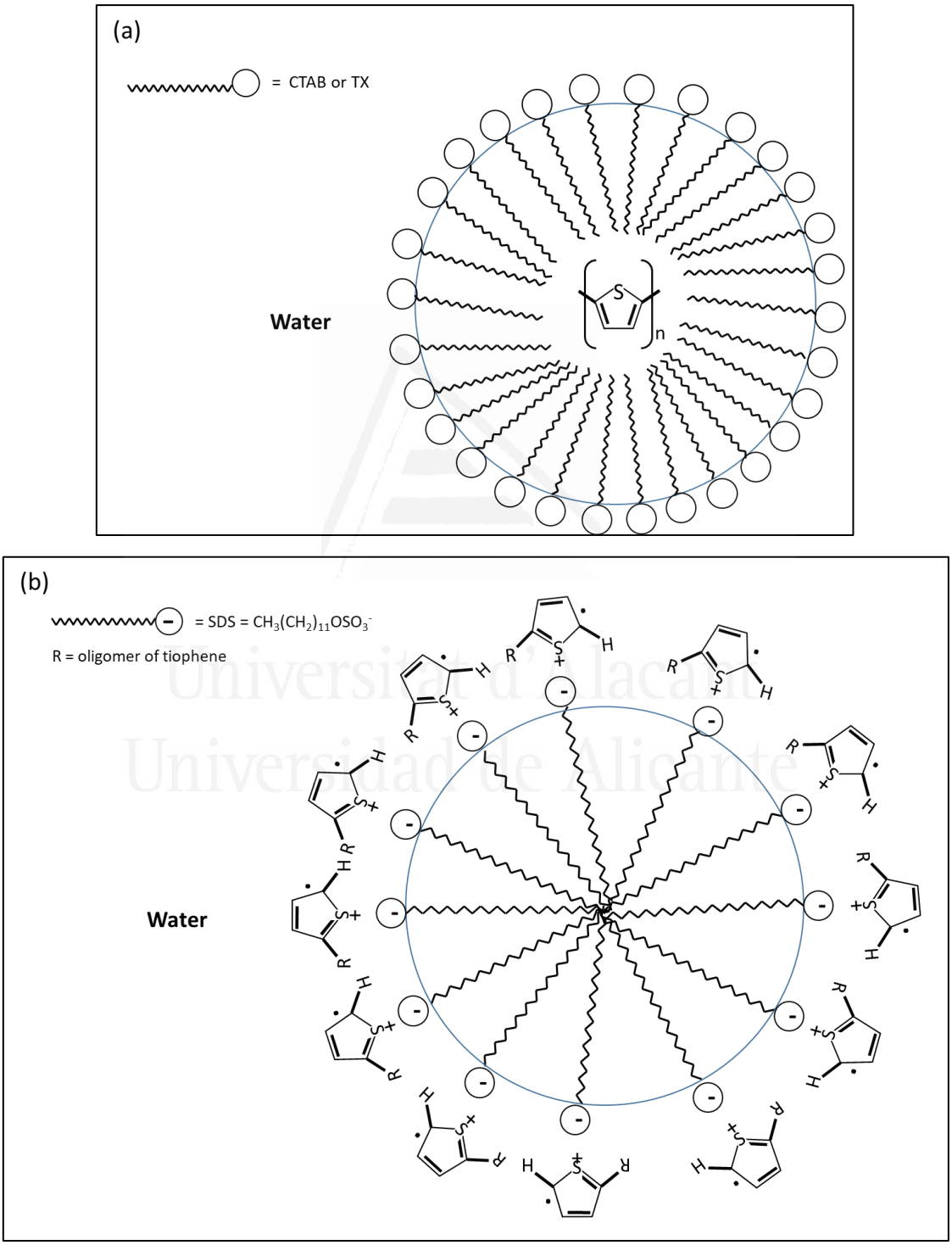

Scheme 8. 6. Scheme showing polymerization of thiophene in the presence of (a) CTAB or TX and (b) sodium dodecyl sulfate (SDS).

In the case of the non-ionic surfactant (TX), polymerization of thiophene also proceeds inside the micelle (Scheme 8.6a), as Fe^{3+} ions can be attracted to the lone pair electrons of oxygen atoms present in the polyethylene glycol chain of the non-ionic TX surfactant and be drawn into the micelle to get into contact with the thiophene monomer [14]. Thus, with both CTAB and TX surfactants, Fe^{3+} ions dissolved in the aqueous medium are drawn into the droplet, where they catalyze oxidative polymerization of thiophene.

However, in the case of the anionic surfactant SDS, electrostatic interactions between the OSO_3^- groups from the surfactant and the Fe^{3+} cations are produced. In this case, polymerization of thiophene (Scheme 8.4) would proceed preferentially at the surface of the micelle [4,15] (Scheme 8.6b). In this case, OSO_3^- groups from SDS and Cl^- from $FeCl_3$ may also act as dopants of polythiophene. Consequently, both SDS and $FeCl_3$ should be detected on polythiophene synthesized with SDS (PT-SDS).

Actually, TEM micrographs (Fig. 8.9) show black spots of $FeCl_3$ only when thiophene was polymerized in the presence of SDS. In the presence of CTAB and TX, Fe^{3+} ions dissolved in the aqueous medium are drawn into the micelle to come into contact with the swollen thiophene monomers and there, Fe^{3+} ions catalyze thiophene polymerization. In these cases, the micelle acts as a microreactor and the polymerization reaction is produced within the micelle.

The incorporation of SDS surfactant into the conducting polymer affects its thermal stability and conductivity. Thus, TGA analysis (Fig. 8.10) shows that there is an increase of thermal stability of PT in PT-SDS. With the addition of CTAB and TX there is a slight decrease of thermal stability probably due to the lower molecular weight of the PT synthesized inside the micelles.

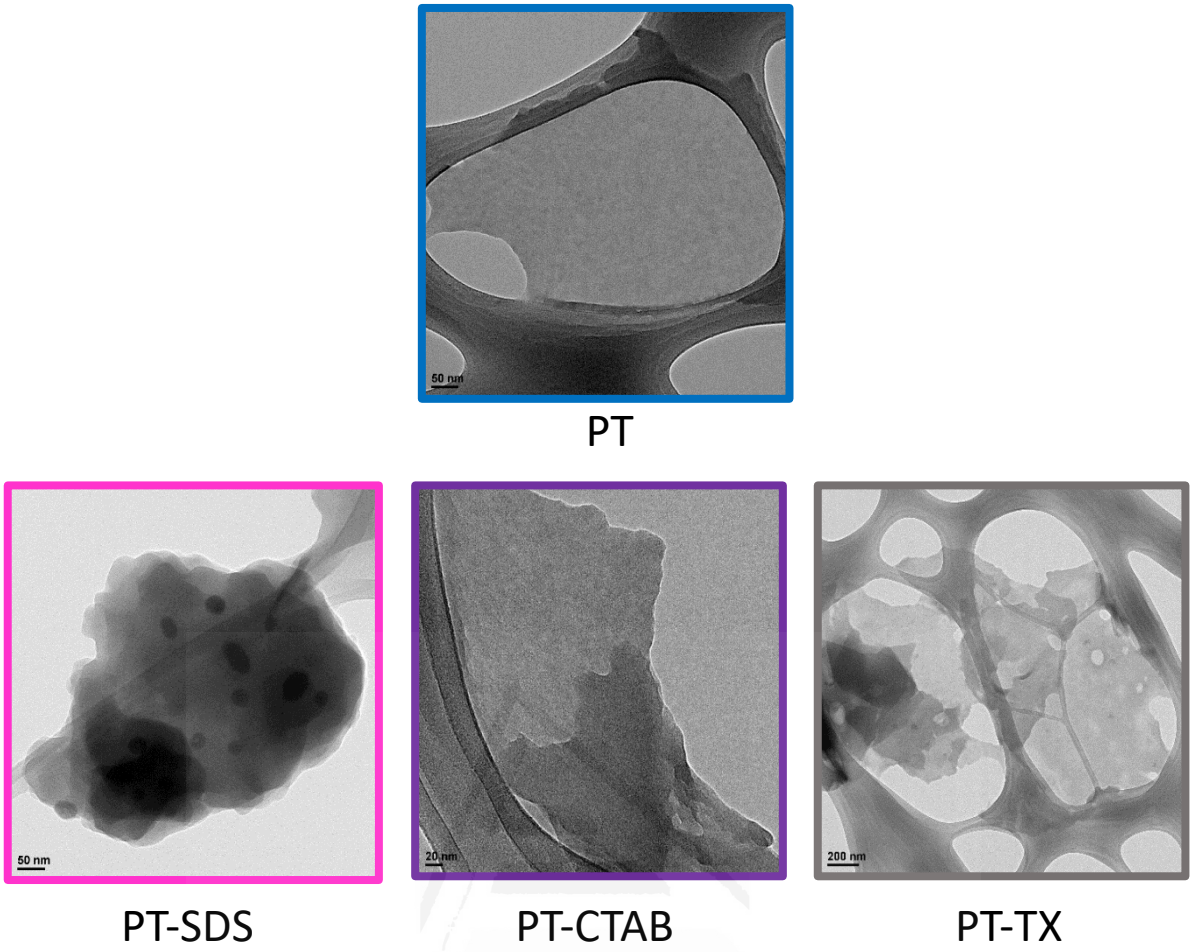

Figure 8. 9. TEM micrographs of — PT and PT synthesized with — SDS; — CTAB; — TX.

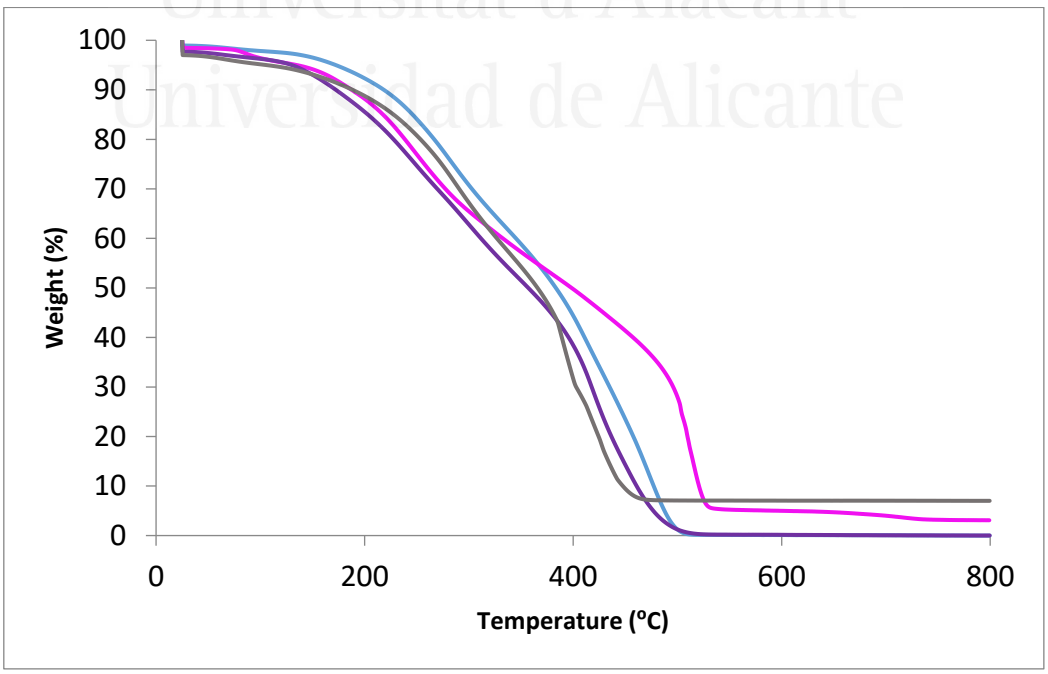

Figure 8. 10. TGA profile in air atmosphere of — PT and PT synthesized with — SDS; — CTAB; — TX.

The electrical conductivity of polythiophene was not affected by the introduction of the anionic surfactant ($3.46 \cdot 10^{-2}$ S·m^{-1} in PT-SDS *vs.* $2.71 \cdot 10^{-2}$ S·m^{-1} in PT) but it was significantly decreased with the cationic ($1.0 \cdot 10^{-4}$ S·m^{-1} in PT-CTAB) and the non-ionic surfactants ($7.7 \cdot 10^{-3}$ S·m^{-1} in PT-TX). This may be due to the different mechanism of micelle formations. When polymerization of thiophene takes place at the surface of SDS conductivity is not affected, but when polymerization proceeds at the core of the microreactor there is no space enough for the chains of polythiophene (PT-CTAB and PT-TX) to expand, so there will be in a shorter conjugation length which results in a decrease of conductivity [15,16].

The presence of $FeCl_3$ on PT-SDS particles, which was detected by TEM, was also confirmed by XRD. The diffraction pattern of PT-SDS shows several peaks (Fig. 8.11). The peak at $2\theta = 41$ º corresponds to the SDS surfactant, and the rest of them correspond to $FeCl_3$ [17].

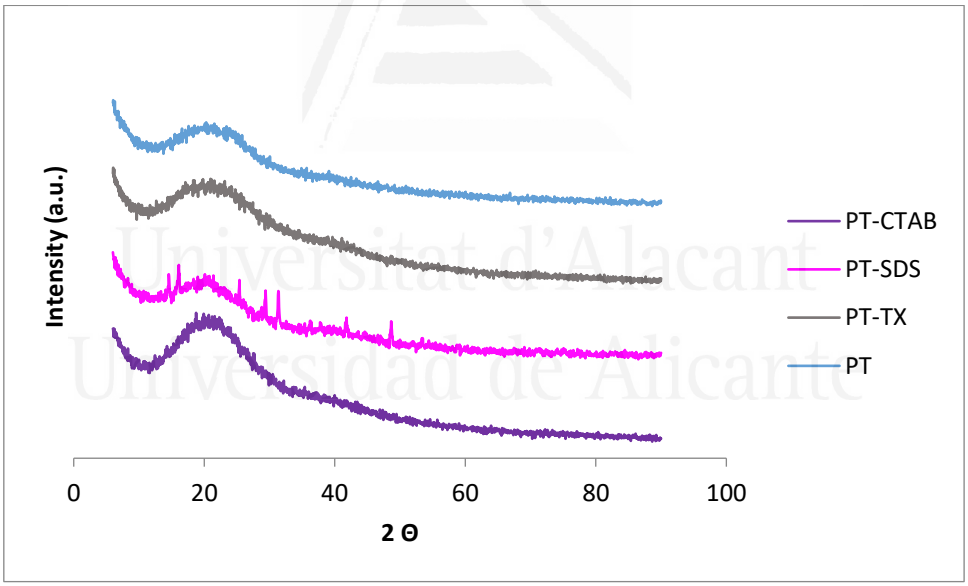

Figure 8. 11. XRD patterns of — polythiophene and polythiophene synthesized with — SDS; — CTAB; — Triton-X.

The chlorine anion from the oxidant ($FeCl_3$) was also detected by XPS (Table 8.3). Chlorine, as Cl^-, was identified by the Cl 2p doublet at 199.1 eV (Cl $2p_{3/2}$) and 200.7 eV (Cl $2p_{1/2}$). This chloride anion may also act as a dopant in the final synthesized polythiophene. Thus, as in PT-SDS $FeCl_3$ is located at the surface of polythiophene particles; Cl^- anion is more accessible and easily exchanged by the nitrate anion (NO_3^-) from water. In a second

step, reduction of nitrate by electrons coming from conducting polythiophene might take place. Table 8.2 shows a considerably high concentration of Cl^- anion in the solution at the reactor, similar to that of PANI, when aqueous solution was in contact with PT-SDS. This confirms exchange between nitrates and chlorides. As a result, PT-SDS greatly increases its effectivity in removing nitrate from water (Fig. 8.4). Nitrate concentration falls down the maximum required levels (50 $mg \cdot L^{-1}$). However, there is a production of nitrite and ammonium, which are determined by ion chromatography, in concentrations above the maximum permitted levels established by European legislation (0.5 $mg \cdot L^{-1}$, Table 8.2). Analysis of the S 2p XPS level (Fig. 8.6) shows the presence of S-O and SO_4^{2-} moieties from the surfactant. No nitrogen was detected by XPS (Table 8.3), which indicates that nitrate is not being retained by PT. However, reduction of nitrate is in fact being produced (nitrite and ammonium are detected) by electrons coming from PT.

4. CONCLUSIONS

Redox and ion exchange properties of PPy and PANI doped with $K_2S_2O_8$ have a determinant role in the removal of nitrates from water. However, the nature of each polymer greatly influences the reaction mechanism. Whereas ion exchange between Cl^- and SO_4^{2-} counterions and NO_3^- from water is the main responsible for the effective nitrate removal in PANI, as assessed by FTIR and XPS, the mechanism for nitrate removal is based in an electron transfer from PPy to nitrate through N located in the pyrrolic ring.

On the other hand, PT is not able to exchange nitrate unless it is synthesized using an anionic surfactant (sodium dodecyl sulfate, SDS). In this case, the electrostatic attraction between ($-OSO_3^-$) groups from the SDS surfactant and Fe^{3+} ions from $FeCl_3$ results in the doping of the oxidized PT growing chain with chloride and sulfate anions. As a result, ion exchange between counteranions and nitrate is enhanced, and ulterior reduction of nitrate by electrons of thiophene is produced.

5. REFERENCES

[1] T.A. Skotheim, J.R. Reynolds. *Recent advances in polypyrrole* in *Handbook of conducting polymers. Conjugated polymers: theory, synthesis, properties, and characterization*. 3rd ed. CRC Press: Boca Raton, FL, USA. **2007**, Chap. 8.

[2] H.S. Park, S.J. Ko, J.S. Park, J.Y. Kim, H.K. Song. *Sci. Rep*. **2013**, *3*, 2454-2459.

[3] G. Inzelt. *Conducting polymers: a new era in electrochemistry*. Springer, Berlin, Germany. **2008**, Chap. 1.

[4] S.J. Lee, J.M. Lee, I.W. Cheong, H. Lee, J.H. Kim. *J. Polym. Sci., Part A: Polym. Chem*. **2008**, *46(6)*, 2097-2107.

[5] A. Drelinkiewicz, A. Zieba, J.W. Sobczak, M. Bonarowska, Z. Karpiński, A. Waksmundzka-Góra, J. Stejskal. *React. Funct. Polym.* **2009**, *69(8)*, 630-642.

[6] A. Nyczyk, A. Sniechota, A. Adamczyk, A. Bernasik, W. Turek, M. Hasik. *Eur. Polym. J.* **2008**, *44(6)*, 1594-1602.

[7] B. Senthilkumar, P. Thenamirtham, R.K. Selvan. *Appl. Surf. Sci*. **2011**, *257(21)*, 9063-9067.

[8] M.J. García-Fernández, R. Buitrago-Sierra, M.M. Pastor-Blas, O.S.G.P. Soares, M.F.R. Pereira, A. Sepúlveda-Escribano. *RSC Adv*. **2015**, *5*, 32706-32713.

[9] EC (European Community), Official Journal of the European Communities, Council Directive 98/83/EC on the quality of water intended for human consumption, *The Drinking Water Directive (DWD)*, Brussels. **1998**, Annex 1, Part B, 42-44.

[10] USEPA (United State Environmental Protection Agency), *National Primary Drinking Water Regulations*, Washington, DC, **2008**, Title 40, Part 141.

[11] I. Dodouche, F. Epron. *Appl. Catal., B*. **2007**, *76(3-4)*, 291-299.

[12] H.W. Ryu, Y.S. Kim, J.H. Kim, I.W. Cheong. *Polymer*. **2014**, *55(3)*, 806-812.

[13] Z. Wang, Y. Wang, D. Xu, E.S.W. Kong, Y. Zhang. *Synth. Met*. **2010**, *160(9-10)*, 921-926.

[14] R.C. Liu, Z.P. Liu. *Chin. Sci. Bull*. **2009**, *54(12)*, 2028-2032.

[15] Deepshikha, T. Basu. *J. Exp. Nanosci*. **2013**, *8(1)*, 84-102.

[16] J. Stejskal, M. Omastová, S. Fedorova, J. Prokeš, M. Trchová. *Polymer*. **2003**, *44(5)*, 1353-1358.

[17] Diffrac Plus Evaluation Software, Bruker, 2017.

Chapter IX. Synthesis of conducting polymer-TiO_2 hybrid materials for their application in the removal of nitrate from water

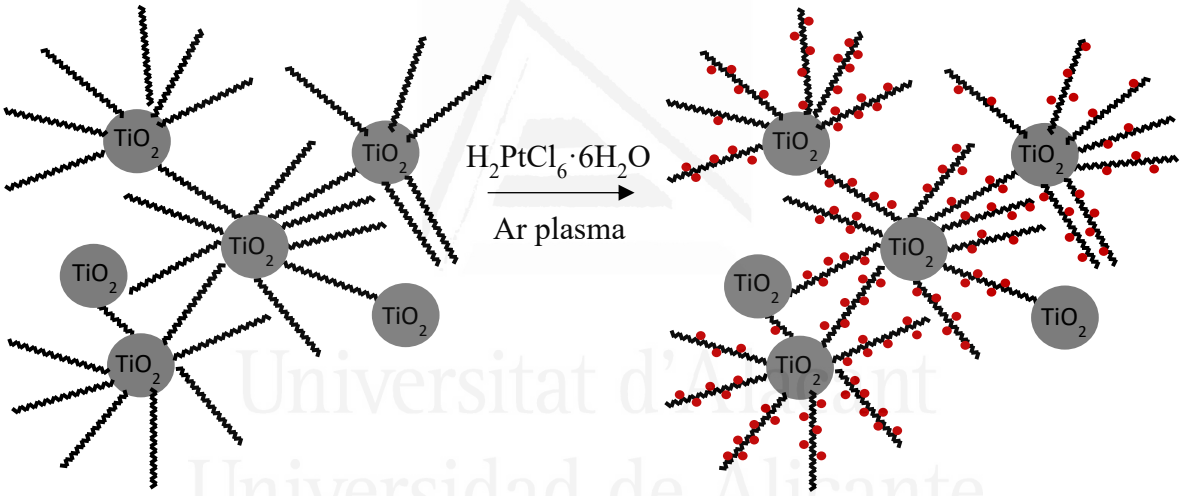

J.J. Villora-Picó, V. Belda-Alcázar, **M.J. García-Fernández**, E. Serrano, A. Sepúlveda-Escribano, M.M. Pastor-Blas, "Conducting polymer-TiO_2 hybrid materials: application in the removal of nitrates from water", *Langmuir*. **2019**, *35*, 6089-6105.

1. INTRODUCTION

In previous chapters nitrate abatement has been accomplished using a metal catalyst supported on conducting polymers with a very low surface area as polypyrrole. It was demonstrated that –NH- groups in polypyrrole are anchoring sites for the metal precursor, which results in a high dispersion of the active metal. The platinum nanoparticles supported on polypyrrole, obtained after treatment with an argon plasma, selectively catalyzed the reaction of reduction of nitrates in water with dyhydrogen towards nitrogen. However, the use of gaseous hydrogen [1] as a reactive agent to reduce nitrates represents a safety hazard. Besides, the polymeric support has a limited thermal stability, which limits its application for other reactions at temperatures above 150 ºC.

It had also been widely accepted that the reduction of nitrate requires the promotion of the noble metal by addition of a second metal [2,3]. The role of the noble metal is to activate hydrogen, which reduces the promoter metal, completing the catalytic cycle. This is the accepted mechanism for non-reducible supports. However, nitrate reduction has been successfully achieved with monometallic catalysts on partially reduced supports as TiO_2. In this case, the reduction of nitrates is promoted by sites of the partially reduced support [4-6]. The most likely mechanism for nitrate uptake in the presence of water is via displacement of surface hydroxyl groups in TiO_2 [7]. The nitrate anions are adsorbed on exposed Lewis acid sites of TiO_2 (unsaturated surface Ti^{3+} sites) produced as a consequence of the removal of surface oxygen during the reduction process. The reduction of the coordination number of titanium cations leads to the presence of oxygen vacancies and a consequent positive charging of the surface, which results in the creation of favorable sites for the adsorption of anionic species as nitrate anions. These sites are expected to be located at the vicinity of the noble metal (usually Pd or Pt). The electrons, associated with the reduction process, may be located on the Ti^{3+} sites. In the literature there is evidence that the electrons are transferred from the support to the metal; however, it has also been reported that nitrate can be reduced by electron enriched titania species (probably Ti_4O_7 formed by hydrogen spillover), producing nitrites as a stepwise reaction, which are subsequently hydrogenated leading to molecular nitrogen or ammonium [8]. Evidence of the existence of Ti_4O_7 species have been provided in TiO_2 after reduction at ~ 500 °C. The presence of the noble metal influences the state of the titania support prior to nitrate adsorption, so reduction of nitrates relies on a strong metal-support interaction and it is also dependent on the metal supported on TiO_2.

The goal of this investigation is to develop materials that are able to produce the green and safe reduction of nitrate from water without the need of a metal catalyst and avoiding the risks associated with the use of gaseous hydrogen. For that purpose, ceramic/polymeric hybrid materials have been synthesized by the oxidative chemical polymerization of aniline or pyrrole onto TiO_2 to produce hybrid materials with synergistic properties.

It is well known the tendency of TiO_2 to oxygen deficiency [9-16], which is evidenced by the creation of oxygen vacancies and the reduction of some Ti^{4+} to Ti^{3+}, which imparts its capability of electron donor; consequently, it is widely considered to be a strongly n-type semiconductor [17]. However, some studies have demonstrated the ability of TiO_2 to act either as n-type or p-type semiconductor. The latter occurs under strongly oxidizing conditions, as a result of formation of titanium vacancies [18-20] or by doping TiO_2 with a suitable acceptor [21-23].

The polymeric part of the hybrid material prepared in this work is a conducting polymer (polypyrrole or polyaniline) synthesized onto the TiO_2 particles by oxidative chemical oxidation of their monomers. If the fully oxidized form is obtained, the conducting polymer would behave as a p-type semiconductor. However, conducting polymers can switch between different redox states. Therefore, depending on the degree of oxidation achieved during the oxidative polymerization, the conducting polymer may act either as a source or a drain of electrons, depending on the process in which it is involved [24]. Consequently, upon polymerization of pyrrole or aniline onto titanium dioxide, electron transfer would be possible in both directions due to the capability of both materials to accept and donate electrons.

It must also be taken into consideration that during the oxidative chemical polymerization of aniline or pyrrole, the polymer is simultaneously doped with the anions provided by the oxidant. These counterions in the reaction medium are incorporated into the growing polymeric chains to maintain the electrical neutrality of the polymer system [25] and might be easily exchanged by nitrate ions (NO_3^-) present in contaminated water. Therefore, different dopants introduced by different oxidants, as $FeCl_3$ or $K_2S_2O_8$, are expected to have different performances in the adsorption of nitrates.

A synergistic behavior between the conductive polymers and the titania is expected. The ion exchange properties of the polymer in these hybrid materials and the redox properties of both the polymer and the titanium dioxide, would make these materials suitable for application in the abatement of nitrate from water, not as support of the active metal catalyst, but participating themselves in the reaction of nitrate reduction. This would lead to a metal-free method of abatement of nitrates from water without the risks associated with the use of gaseous hydrogen. The mechanism of nitrate abatement and the role of both, titania and polymer counterparts, in the hybrid materials will be discussed.

2. EXPERIMENTAL

2.1. Hybrid materials preparation

TiO_2/PANI and TiO_2/PPy hybrid materials were prepared by oxidative chemical polymerization of aniline and pyrrole on commercial TiO_2 (*Degussa P*-25, 80 % anatase, 20 % rutile) [26], previously calcined at 500 °C for 5 h in order to obtain mainly the anatase phase. Different TiO_2:monomer ratios (60:40, 50:50 and 40:20) were used.

For the synthesis of TiO_2/PPy two different oxidants, $FeCl_3 \cdot 6H_2O$ and $K_2S_2O_8$, were used. The oxidant was added in excess, so the oxidant/pyrrole molar ratio was 2.33 [27]. 2 mL of pyrrole (C_4H_5N, *Sigma-Aldrich*, reagent grade, 98 %) were added dropwise to calcined TiO_2. The oxidant solution was prepared by dissolving 18 g of oxidant ($FeCl_3 \cdot 6H_2O$ or $K_2S_2O_8$) in 400 mL of ultrapure water. This ferric chloride solution showed an orange color whereas the potassium peroxydisulfate solution was colorless. However, as soon as the pyrrole mixed with the oxidant solution it turned to its characteristic black color, this indicating the formation of polypyrrole (PPy) in its doped form onto TiO_2. The solution was stirred for 6 h at room temperature. Then, the precipitated TiO_2/PPy powder was filtered, washed with distilled water and dried at 80 °C for 12 h.

For the synthesis of TiO_2/PANI, only potassium peroxydisulfate ($K_2S_2O_8$, *Sigma-Aldrich*, 99 %) was used as oxidant, as a very low yield was obtained with iron chloride. The oxidant/aniline molar ratio was 1.25 [28]. 2 mL of aniline ($C_6H_5NH_2$, *Sigma-Aldrich*) were added dropwise under magnetic stirring to the required quantity of calcined TiO_2. Synthesis of polyaniline (PANI) requires an acidic medium so 7.4 g of $K_2S_2O_8$ were dissolved in 150

mL of HCl (0.2 mol·L^{-1}), and this solution was added to the TiO_2/aniline suspension. Polymerization of aniline took place as soon as the oxidant was in contact with aniline. Solution showed a blue color, characteristic of emeraldine base, which turned within seconds into dark green, characteristic of the emeraldine salt form of polyaniline. The solution was stirred for 20 h at room temperature. The precipitated TiO_2/PANI powder was filtered, washed with a solution of HCl (0.2 mol·L^{-1}) until yellowish washing waters turned uncolored and dried at 80 °C for 12 h.

2.1.1. Platinum nanoparticles synthesis

Platinum monometallic catalysts were supported on TiO_2/PANI and TiO_2/PPy. They were prepared by wet impregnation in excess of solvent, using $H_2PtCl_6 \cdot 6H_2O$ as the metal precursor. The proper amount of this salt to obtain 1 wt. % Pt loading was dissolved in ultrapure water, then the hybrid support (TiO_2/PANI/$K_2S_2O_8$, TiO_2/PPy/$K_2S_2O_8$ or TiO_2/PPy/$FeCl_3$) was added (25 mL solution·$g_{support}^{-1}$). The suspension was stirred for 12 h at room temperature and then the solvent was evaporated under reduced pressure in a rotary evaporator. The supported catalyst precursor was dried in an oven at 80 °C for 12 h and then the obtained material was treated with Ar plasma to decompose the platinum precursor and obtain reduced platinum nanoparticles.

The supported catalysts were submitted to an Ar plasma treatment [29], (chapter II, section 1.3) at 200 W. 36 cycles of 5 min each were run to each sample (180 min treatment in total) with manual mixing of the powdered sample between treatments to assure an even exposure to the plasma. The surface temperature was below 50 °C in all cases.

2.2. Materials characterization

Full characterization of the samples was conducted by thermogravimetric analysis (TGA), N_2 adsorption at -196 °C, X-ray diffraction (XRD), transmission electron microscopy (TEM) and X-ray photoelectron spectroscopy (XPS). The experimental details are described in chapter II, section 2.

2.3. Nitrate removal evaluation

The ability of removing nitrate from the aqueous solution by the titania/polymer hybrid materials was evaluated and compared with the hydrogenation of nitrate catalyzed by the platinum nanoparticles supported on these materials. The reaction took place in a semi-batch reactor equipped with a magnetic stirrer (700 rpm) as it is detailed in chapter II, section 1.4. The course of reaction was monitored by ion chromatography (chapter II, section 2.9).

When the reaction was performed in the presence of the platinum catalysts, a possible metal leaching was evaluated by Inducted Coupled Plasma Mass Spectrometry (ICP-MS) in aliquots withdrawn from the reactor once the nitrate reduction reaction was completed as indicated in chapter II, section 2.10.

3. RESULTS AND DISCUSSION

3.1. Materials characterization

The synthesized titania/polymer hybrid materials have been fully characterized and their properties compared to those of the pristine materials. Their thermal stability was evaluated by TGA in inert (Fig. 9.1) and oxidizing (Fig. 9.2) atmospheres. Whereas TiO_2 does not suffer thermal degradation between 0 and 1200 °C, both polymers show a first mass loss (around 8 – 9 % of its initial mass) between 30 and 100 °C which corresponds to the loss of water trapped in the polymers and the loss of non-reacted monomer. In PANI, thermal degradation in nitrogen atmosphere (Fig. 9.1a) proceeds in several steps: there is a first step with a 10 % mass loss between 100 and 300 °C which may correspond to the thermal dedoping of HCl and $K_2S_2O_8$ [30]. Another 10 % mass loss is produced between 300 and 420 °C where the polymer starts to decompose. The more pronounced thermal degradation between 420 and 600 °C can be assigned to thermal degradation of the cross-linked chains; and the 40 % mass loss registered between 600 and 1200 °C is due to the decomposition of the lineal part of the chains. In PPy (Fig. 9.1b and 9.1c), after the initial loss of water and unreacted polymer, there is a second mass loss between 100 and 250 °C which is due to the loss of the dopant bound to the polymeric chains. At 250 °C, degradation of the polymer starts, which proceeds in two steps, from 250 to 800 °C which corresponds to the thermal degradation of the cross-linked chains and from 850 to 1200 °C where degradation of the lineal part of the polymeric chains. The most important degradation in nitrogen atmosphere

is produced for PPy synthesized with $K_2S_2O_8$ (10 % mass remains) (Fig. 9.1b); however, around 20 % mass of PPy is retained when synthesized with $FeCl_3$ (Fig. 9.1c). On the other hand, 28 % of PANI is not degraded (Fig. 9.1a). In air atmosphere (Fig. 9.2), total burning of PPy/$FeCl_3$ and PANI/$K_2S_2O_8$ is produced around 600 °C, but it is produced at 730 °C for PPy/$K_2S_2O_8$.

These results show that the polymer nature and the oxidant used in the oxidative polymerization influence their final thermal properties. The thermal behavior of the hybrid materials is in between that of the polymer and that of TiO_2. The TGA curves show the mass loss steps corresponding to water and monomer loss, thermal dedoping and polymer degradation, but the increase of TiO_2 content decreases thermal degradation and increases the residual mass at 1200 °C in nitrogen (Fig. 9.1) and at 800 °C in air (Fig. 9.2). Impregnation with platinum produces only a slight shift of the TGA curves of all the materials. Treatment with plasma does not significantly modify TGA curves (Fig. 9.3). From thermogravimetric analysis it can be concluded that application of the pristine polymeric materials may be restricted to temperatures below 250 °C for PPy and 300 °C for PANI, but hybrid polymeric/TiO_2 materials have enhanced thermal properties.

The porous texture of the hybrid materials was evaluated by N_2 adsorption at - 196 °C. In all cases type II isotherms, typical of non-porous materials, were obtained (Fig. 9.4). Table 9.1 shows that BET surface areas of the hybrid materials prepared in a 50:50 TiO_2/polymer ratio are very similar (between 30 and 37 $m^2 \cdot g^{-1}$), irrespective of the polymer, and they are slightly lower than that of TiO_2 (53 $m^2 \cdot g^{-1}$) due to the polymer presence.

Table 9. 1. BET surface evaluated from N_2 adsorption isotherms at - 196 °C.

Sample	S_{BET} ($m^2 \cdot g^{-1}$)
TiO_2	53
PANI/$K_2S_2O_8$	40
TiO_2/PANI/$K_2S_2O_8$/50:50	37
PPy/$K_2S_2O_8$	11
TiO_2/PPy/$K_2S_2O_8$/50:50	30
PPy/$FeCl_3$	4
TiO_2/PPy/$FeCl_3$/50:50	36

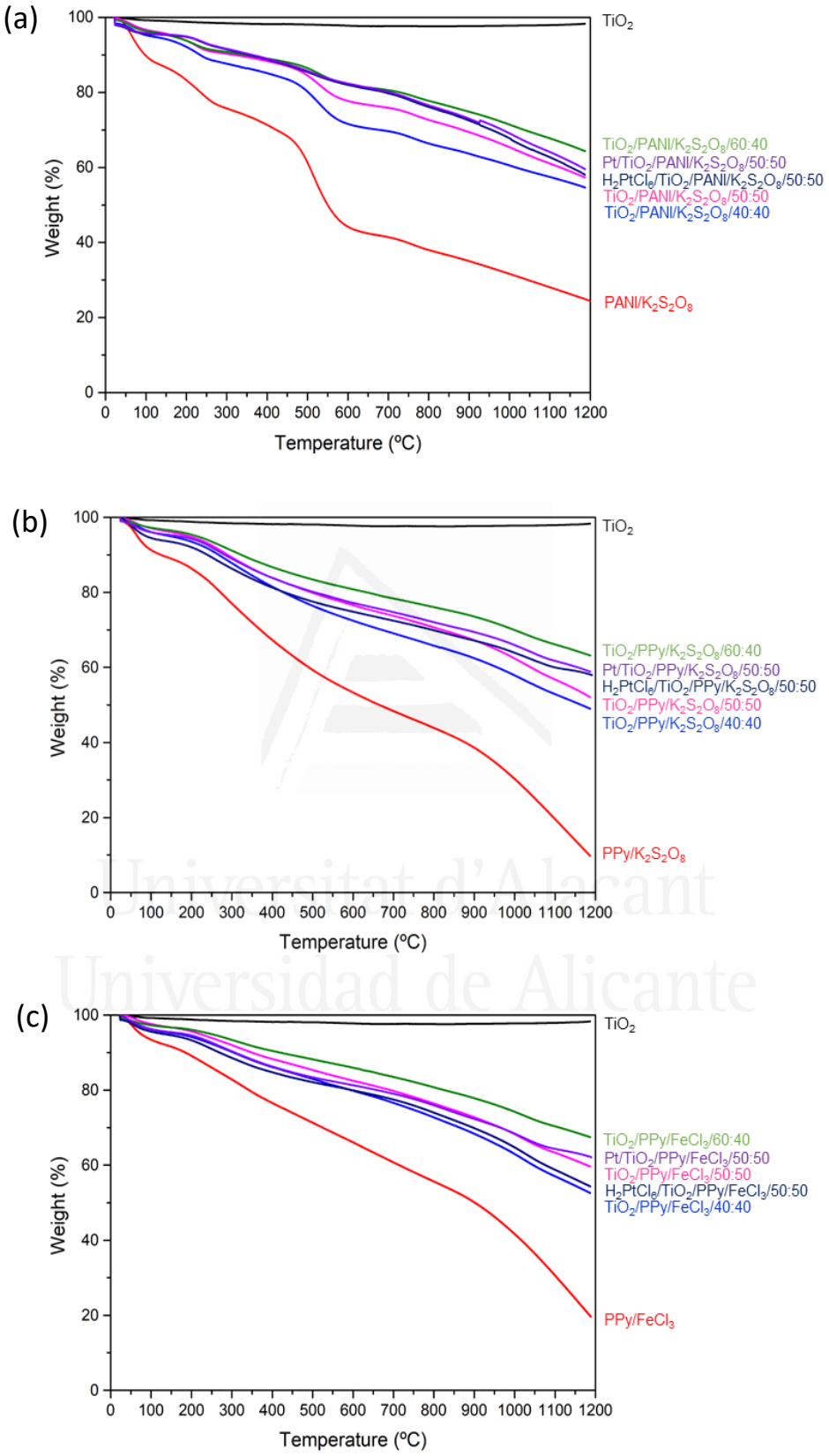

Figure 9. 1. TGA profile in N_2 atmosphere of (a) $TiO_2/PANI/K_2S_2O_8$; (b) $TiO_2/PPy/K_2S_2O_8$ and (c) $TiO_2/PPy/FeCl_3$.

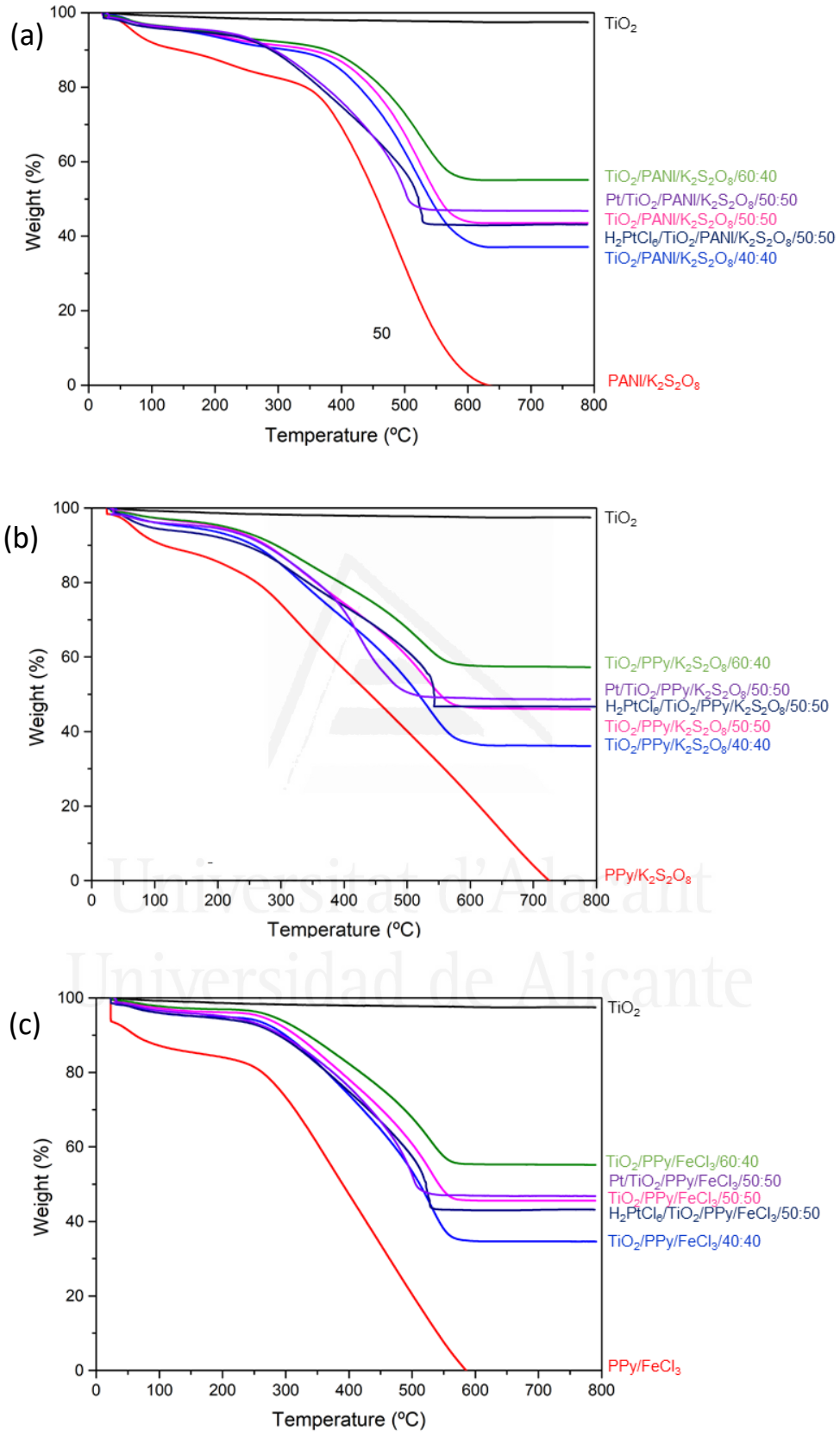

Figure 9. 2. TGA profile in air atmosphere of (a) $TiO_2/PANI/K_2S_2O_8$; (b) $TiO_2/PPy/K_2S_2O_8$ and (c) $TiO_2/PPy/FeCl_3$.

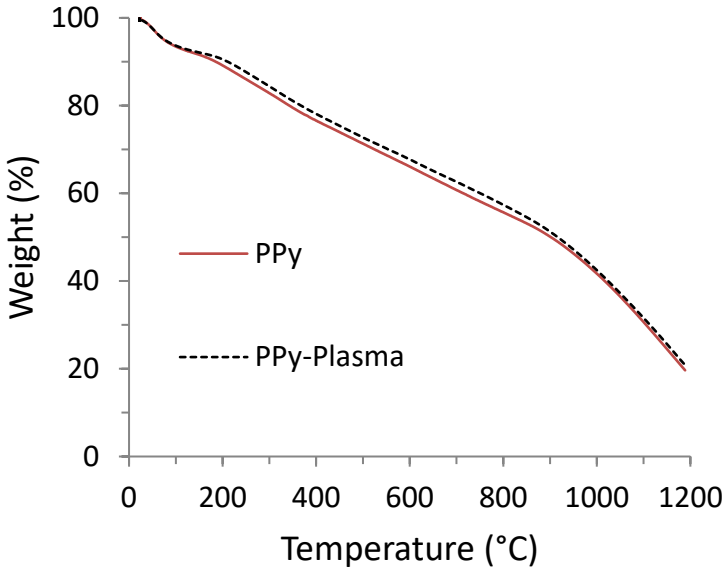

Figure 9. 3. TGA profile in N_2 atmosphere of as synthesized and plasma treated PPy/$FeCl_3$.

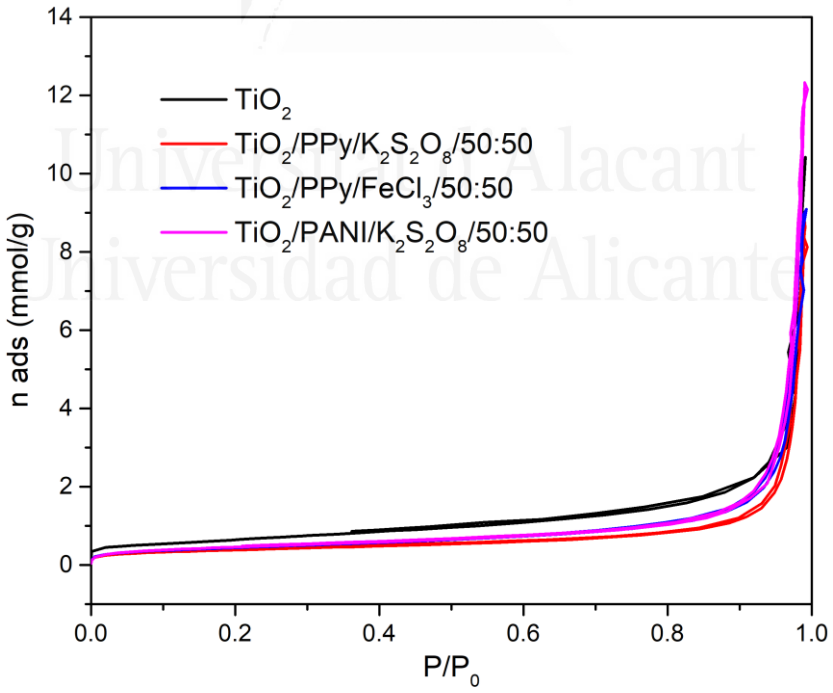

Figure 9. 4. Nitrogen adsorption isotherm at - 196 °C of hybrid materials.

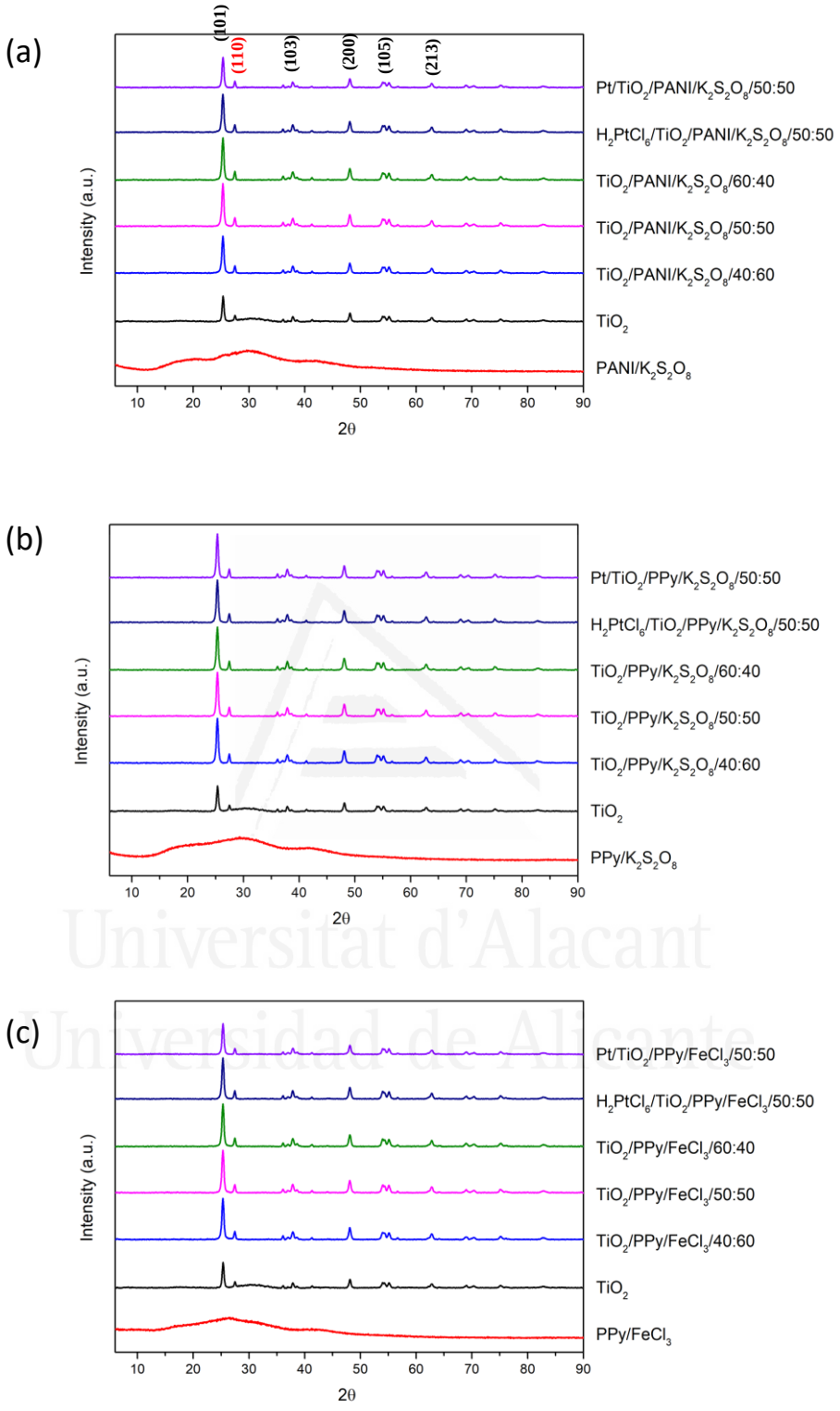

Figure 9. 5. XRD patterns of hybrid materials: (a) $TiO_2/PANI/K_2S_2O_8$; (b) $TiO_2/PPy/K_2S_2O_8$ and (c) $TiO_2/PPy/FeCl_3$.

The XRD patterns of PANI and PPy (Fig. 9.5) are typical of amorphous materials with a certain degree of crystallinity, which is shown by the band corresponding to the periodicity perpendicular to the polymer chain centered at $2\theta = 30$ º for PANI; $2\theta = 29.1$ º for PPy/$K_2S_2O_8$ and $2\theta = 26.1$ º for PPy/$FeCl_3$ [31,32]. In the XRD pattern of PANI there is also a band centered at $2\theta = 18 - 20$ º that corresponds to the periodicity along the polymeric chain, and a third band situated at $2\theta = 42$ º also typical of the polymer phase [33]. All the hybrid materials became strongly oriented, revealing a strong effect of the TiO_2, thus no amorphous bands from the polymer are shown. The XRD patterns of TiO_2/PANI and TiO_2/PPy show sharp and well-defined peaks, indicating the crystallinity of all the synthesized hybrid materials, irrespective of the monomer ratio. The more intense peak at $2\theta = 25.3$ º corresponds to the (101) plane of anatase [34], whereas the peaks at 37.8 º, 48 º, 54 º and 63 º correspond to (103), (200), (105) and (213) planes of this phase [35]. There is also a small reflexion from the (110) plane of rutile at $2\theta = 28$ º [36]. In the platinum impregnated samples treated in plasma, reflexions from platinum (typically at $2\theta = 39.8$ º and 46.2 º) are not present [37]. This may be due to a low percentage of metallic platinum or a high dispersion of the platinum nanoparticles [29].

TEM images (Fig. 9.6) show that TiO_2 particles with diameters in the range between 10 and 50 nm are embedded in the polymer matrix, which leads to an oriented morphology. These results reveal that the improvement in crystallinity of hybrid materials is due to the addition of TiO_2 nanoparticles. During the synthesis of the nanocomposites, aniline or pyrrole monomers are adsorbed on the TiO_2 particles (Schemes 9.1a and 9.1b). With the addition of the oxidant polymerization starts and growing polymer chains of different length surround and connect TiO_2 particles [38] as shown in Scheme 9.1c. Similar morphologies are obtained irrespective of the polymer (PANI or PPy) and the oxidant ($K_2S_2O_8$ or $FeCl_3$) (Fig. 9.7, 9.8 and 9.9). As a result of the addition of the oxidant, the conducting protonated form of both polymers are obtained: protonated emeraldine salt in PANI (Scheme 9.1a) and conducting PPy (Scheme 9.1b). As nanoparticles usually tend to agglomerate due to the driving force to reduce their surface energy, it is crucial to assure the interaction of the conducting polymer with the TiO_2 nanoparticles at the nanometer scale as the uniform dispersion of TiO_2 nanoparticles into the polymeric matrix is a key factor. TiO_2 agglomeration is avoided by the repulsion between the positive charges of the conducting forms of the polymers [39].

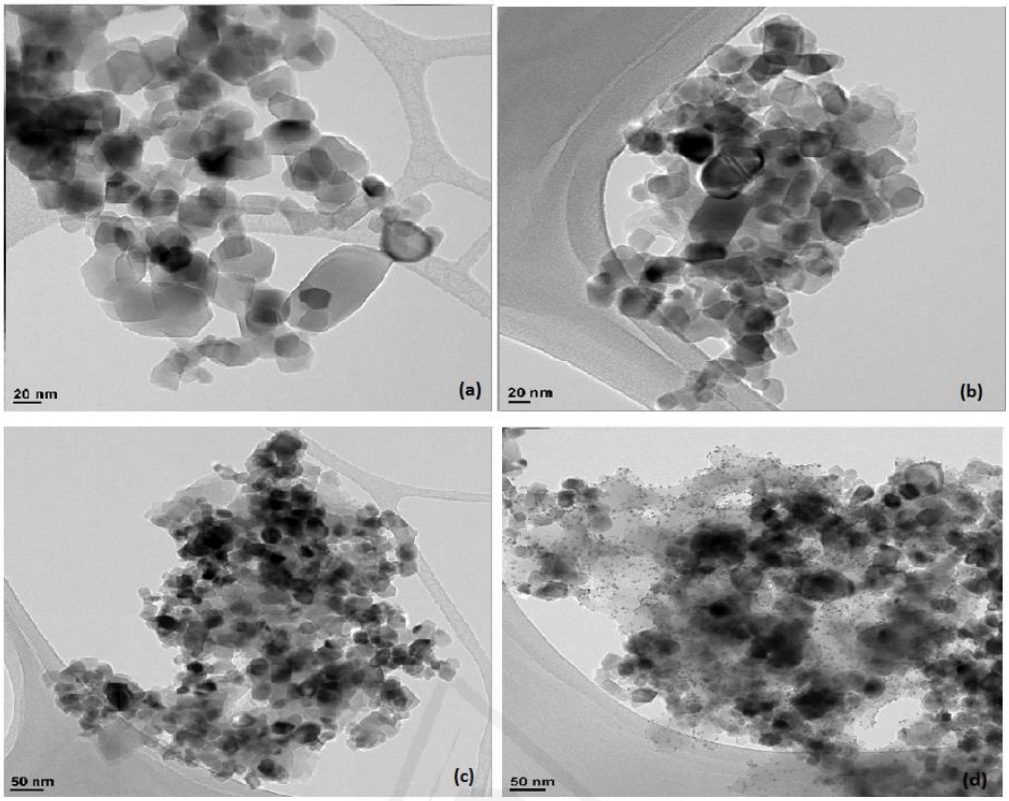

Figure 9. 6. TEM images of (a) TiO_2, (b) TiO_2/PANI/50:50; (c) H_2PtCl_6/TiO_2/PANI and (d) Pt/TiO_2/PANI.

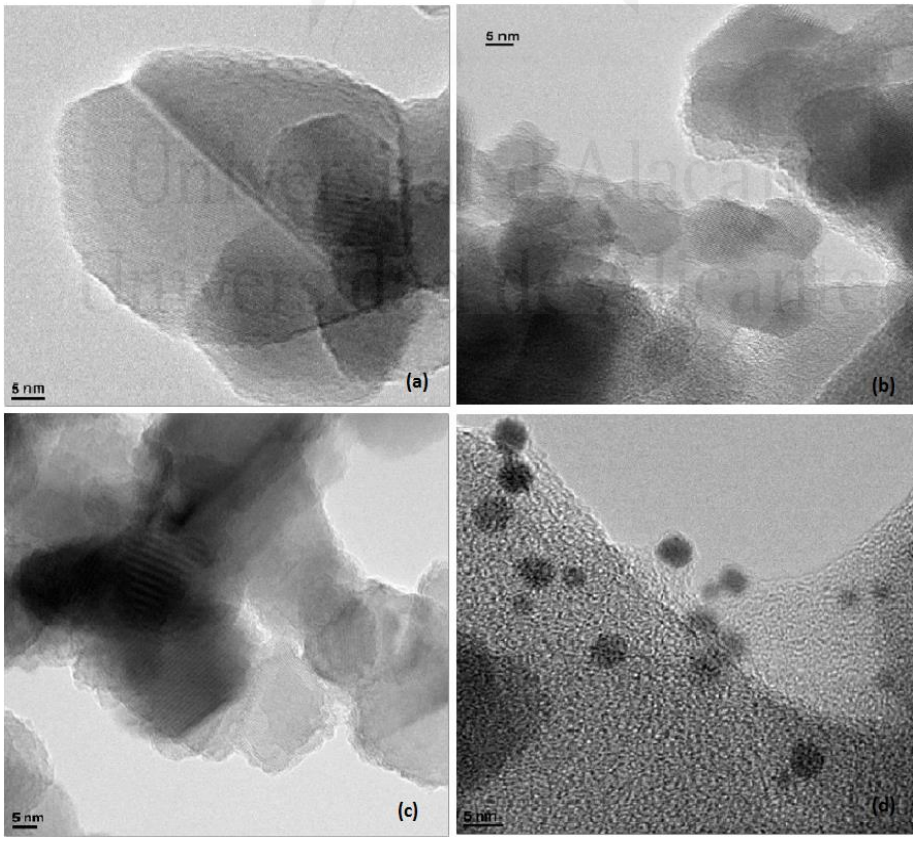

Figure 9. 7. TEM images of (a) TiO_2, (b) TiO_2/PANI/50:50; (c) H_2PtCl_6/TiO_2/PANI and (d) Pt/TiO_2/PANI.

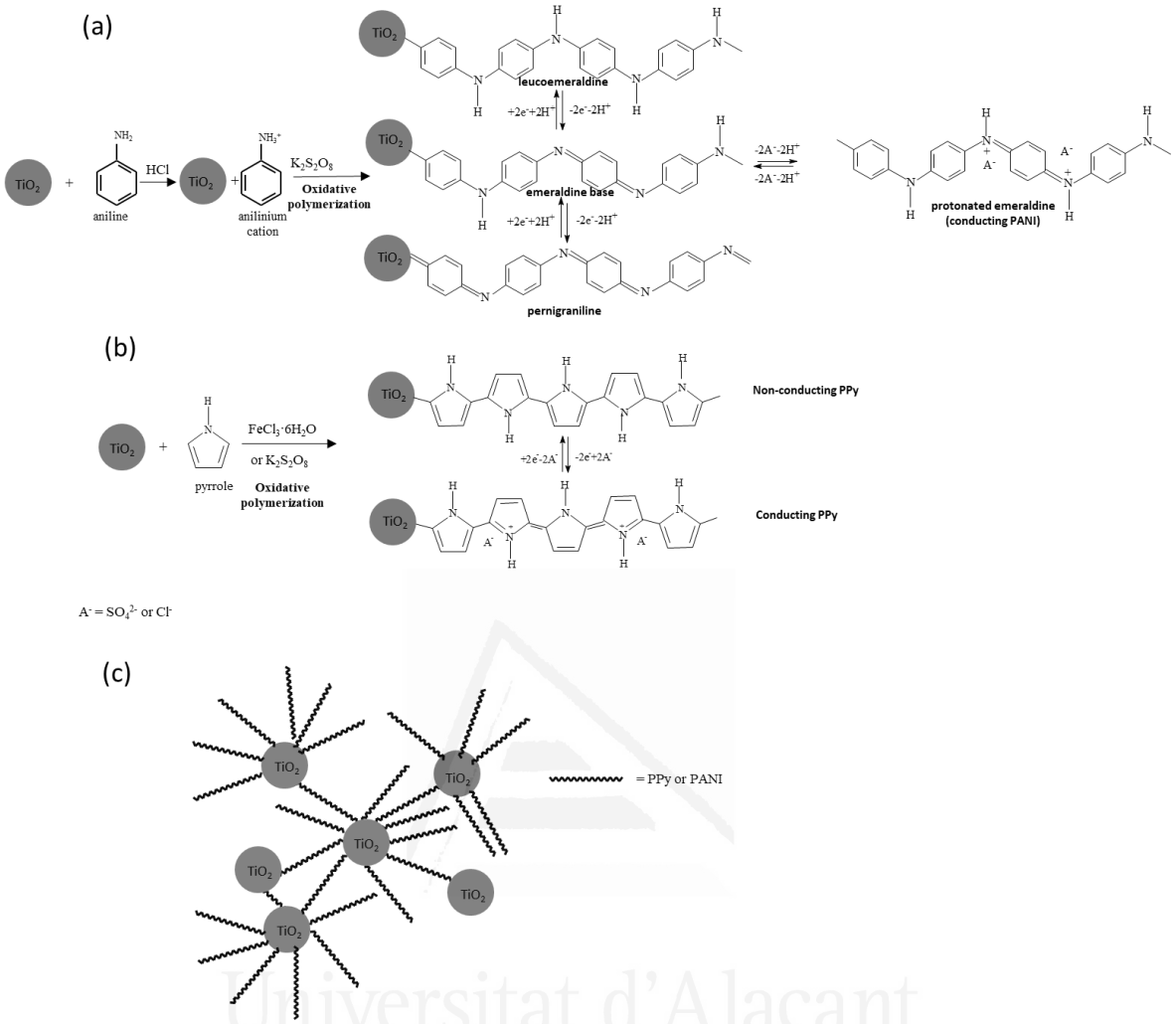

Scheme 9. 1. Scheme showing (a) the synthesis of TiO_2/PANI; (b) the synthesis of TiO_2/PPy and (c) the resulting hybrid TiO_2/polymer material with the polymeric chain interconecting de TiO_2 nanoparticles.

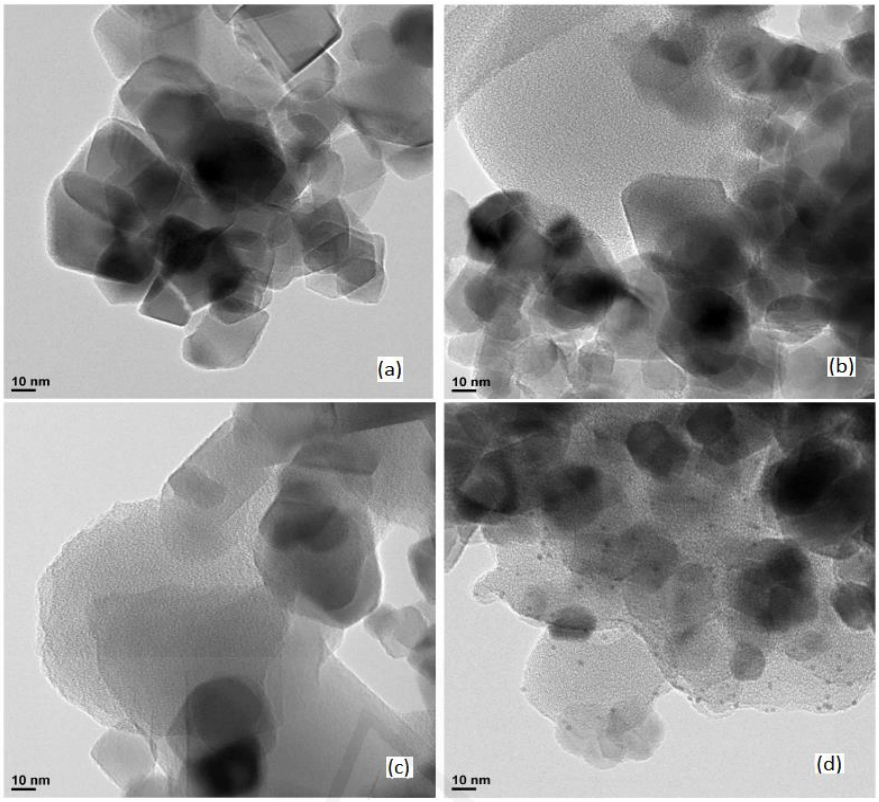

Figure 9. 8. TEM images of (a) TiO_2, (b) TiO_2/PPy/$K_2S_2O_8$/50:50; (c) H_2PtCl_6/TiO_2/PPy/$K_2S_2O_8$/50:50 and (d) Pt/TiO_2/PPy/$K_2S_2O_8$/50:50.

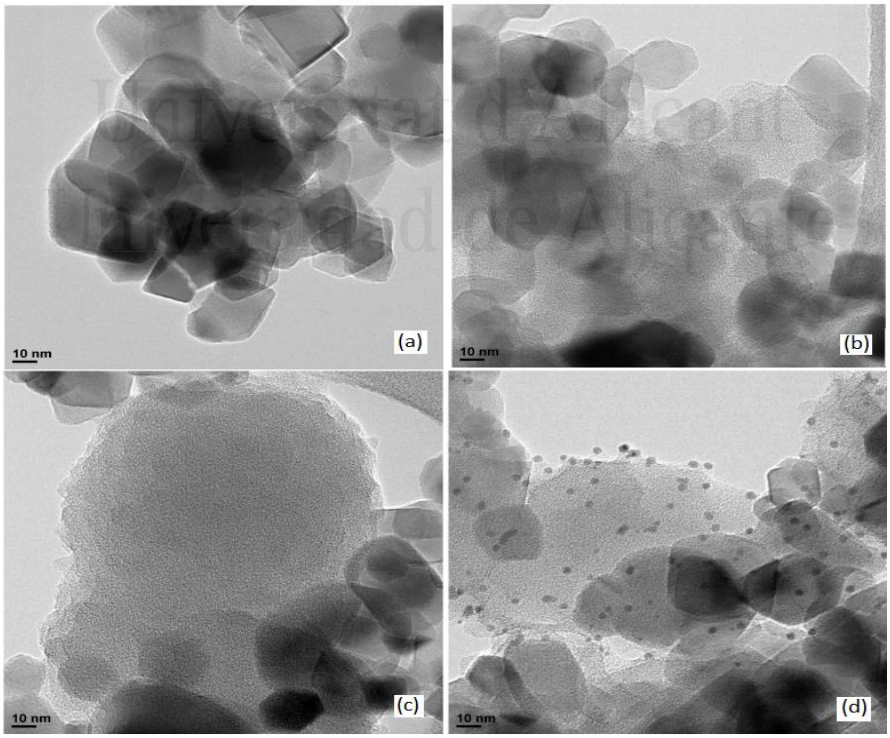

Figure 9. 9. TEM images of (a) TiO_2, (b) TiO_2/PPy/$FeCl_3$/50:50; (c) H_2PtCl_6/TiO_2/PPy/ $FeCl_3$/50:50 and (d) Pt/TiO_2/PPy/$FeCl_3$/50:50.

XPS analysis provides useful information about the surface composition of the different materials. XPS analysis of TiO_2 (Table 9.2) shows the presence of Ti and O and also a considerable amount of C that may come from the precursor used in its preparation [40-42]. Carbon can also result from adventurous hydrocarbon [43]. XPS survey analysis of the composite materials shows the presence of C and N from the polymeric chain and Ti and O from titania. The increase of the polymer percentage in the hybrid materials results in an increase of N and C and a decrease of Ti and O in the three studied series (TiO_2/PANI/$K_2S_2O_8$, TiO_2/PPy/$K_2S_2O_8$ and TiO_2/PPy/$FeCl_3$) (Table 9.2).

High resolution XPS spectra show variations of Ti, O, C and N binding energies of the hybrid materials when compared to the pristine titania and polymers. Ti $2p_{3/2}$ curve fit (Fig. 9.10, Table 9.3) shows the unique contribution of Ti^{4+} at 458.9 eV in pristine TiO_2. In the hybrid materials, the Ti $2p_{3/2}$ binding energy is shifted towards higher values (459.5 eV). No contribution of Ti^{3+} (456 – 457 eV) is shown in any hybrid material, which is in agreement with the literature [44].

Table 9. 2. XPS surface chemical composition (atomic %) of TiO_2, PANI, PPy and hybrid materials.

Sample / Element	C 1s	O 1s	N 1s	Cl 2p	Ti 2p	S 2p	Pt 4f
TiO_2	39.9	47.6	-	-	12.5	-	-
PANI/$K_2S_2O_8$	77.7	7.8	9.6	3.9	-	1.0	-
TiO_2/PANI/$K_2S_2O_8$/60:40	45.7	38.8	3.6	1.5	9.3	1.0	-
TiO_2/PANI/$K_2S_2O_8$/50:50	56.6	27.3	5.9	3.0	6.6	0.6	-
TiO_2/PANI/$K_2S_2O_8$/40:60	58.9	26.5	5.4	2.2	5.4	1.5	-
H_2PtCl_6/TiO_2/PANI/$K_2S_2O_8$/50:50	54.1	22.9	6.2	3.7	12.6	0.4	0.1
Pt/TiO_2/PANI/$K_2S_2O_8$/50:50	41.6	41.1	6.8	1.0	8.1	0.3	0.1
PPy/$K_2S_2O_8$	69.2	18.0	12.2	0.2	-	0.4	-
TiO_2/PPy/$K_2S_2O_8$/60:40	54.5	32.5	5.7	0.2	6.2	0.9	-
TiO_2/PPy/$K_2S_2O_8$/50:50	57.6	29.5	7.2	0.3	4.6	0.8	-
TiO_2/PPy/$K_2S_2O_8$/40:60	60.1	25.5	9.8	0.3	3.5	0.8	-
H_2PtCl_6/TiO_2/PPy/$K_2S_2O_8$/50:50	55.2	30.2	6.7	0.6	6.4	0.7	0.1
Pt/TiO_2/PPy/$K_2S_2O_8$/50:50	50.1	34.3	8.0	0.15	5.6	1.7	0.2
PPy/$FeCl_3$	78.0	6.5	13.2	2.4	-	-	-
TiO_2/PPy/$FeCl_3$/60:40	54.8	28.9	6.0	2.8	7.6	-	-
TiO_2/PPy/$FeCl_3$/50:50	59.8	22.4	8.5	3.5	5.8	-	-
TiO_2/PPy/$FeCl_3$/40:60	61.7	19.2	10.2	3.9	4.8	-	-
H_2PtCl_6/TiO_2/PPy/$FeCl_3$/50:50	59.9	23.3	6.7	4.0	6.0	-	0.1
Pt/TiO_2/PPy/$FeCl_3$/50:50	55.0	27.8	8.3	2.1	6.5	-	0.2

The electron transfer between titania and the polymer depends on both the oxidation state of titanium and the degree of oxidation of the polymeric chain. This can be determined by the binding energy of the N 1s level. Four types of nitrogen may be present: imine (-N=),

neutral amine (-NH-), positively charged nitrogen ($-N^+$) and protonated imine ($=N^+$), with increasing N 1s binding energies, typically located at 398.9, 399.6, 400.9 and 401.8 eV, as the oxidation degree increases. XPS high resolution curve fit of the N 1s level (Fig. 9.11, Table 9.4) shows by the presence of positively charged amine ($-N^+$), this confirming that the conducting form of the polymers have been obtained.

Table 9. 3. XPS analysis of the Ti $2p_{3/2}$ level.

Sample	Energy (eV)	Composition (%)
TiO_2	458.9	100
TiO_2/PANI/$K_2S_2O_8$	459.5	100
H_2PtCl_6/TiO_2/PANI/$K_2S_2O_8$	459.3	100
Pt/TiO_2/PANI/$K_2S_2O_8$	459.2	100
TiO_2/PPy/$K_2S_2O_8$	459.5	100
H_2PtCl_6/TiO_2/PPy/$K_2S_2O_8$	459.4	100
Pt/TiO_2/PPy/$K_2S_2O_8$	459.4	100
TiO_2/PPy/$FeCl_3$	459.5	100
H_2PtCl_6/TiO_2/PPy/$FeCl_3$	459.5	100
Pt/TiO_2/PPy/$FeCl_3$	459.1	100

The formation of the TiO_2/PANI hybrid material does not greatly affects the oxidation degree of the polymeric nitrogen (N^+ moieties percentage is 17 % in the pristine PANI/$K_2S_2O_8$ and 15 % in the hybrid material TiO_2/PANI/$K_2S_2O_8$). On the other hand, pristine polypyrrole is more oxidized than pristine polyaniline. However, the percentage of positively charged nitrogen ($-N^+$) in PPy depends on the oxidant used during the chemical polymerization of pyrrole (93 % with $K_2S_2O_8$ versus 65 % with $FeCl_3$) (Table 9.4). These results reveal that the oxidant used in the polypyrrole synthesis has a considerable influence on the oxidation degree of the polymeric material and consequently, on its final properties. Whereas N1s curve fit is similar in PANI and in the TiO_2/PANI hybrid material (Fig. 9.11a), a significant modification of the nitrogen functionalities is observed in the TiO_2/PPy hybrid materials. The imine (=N-) groups of the pristine polymer are no longer present in TiO_2/PPy/$K_2S_2O_8$, (Fig. 9.11b) and protonated imine ($=N^+$) moieties are detected in TiO_2/PPy/$FeCl_3$ (Fig. 9.11c). The shift of the binding energies of N 1s of PPy to lower binding energies are produced together with a shift of Ti $2p_{3/2}$ to higher binding energies. C 1s and O 1s binding energies are also shifted towards lower binding energies by the presence of TiO_2.

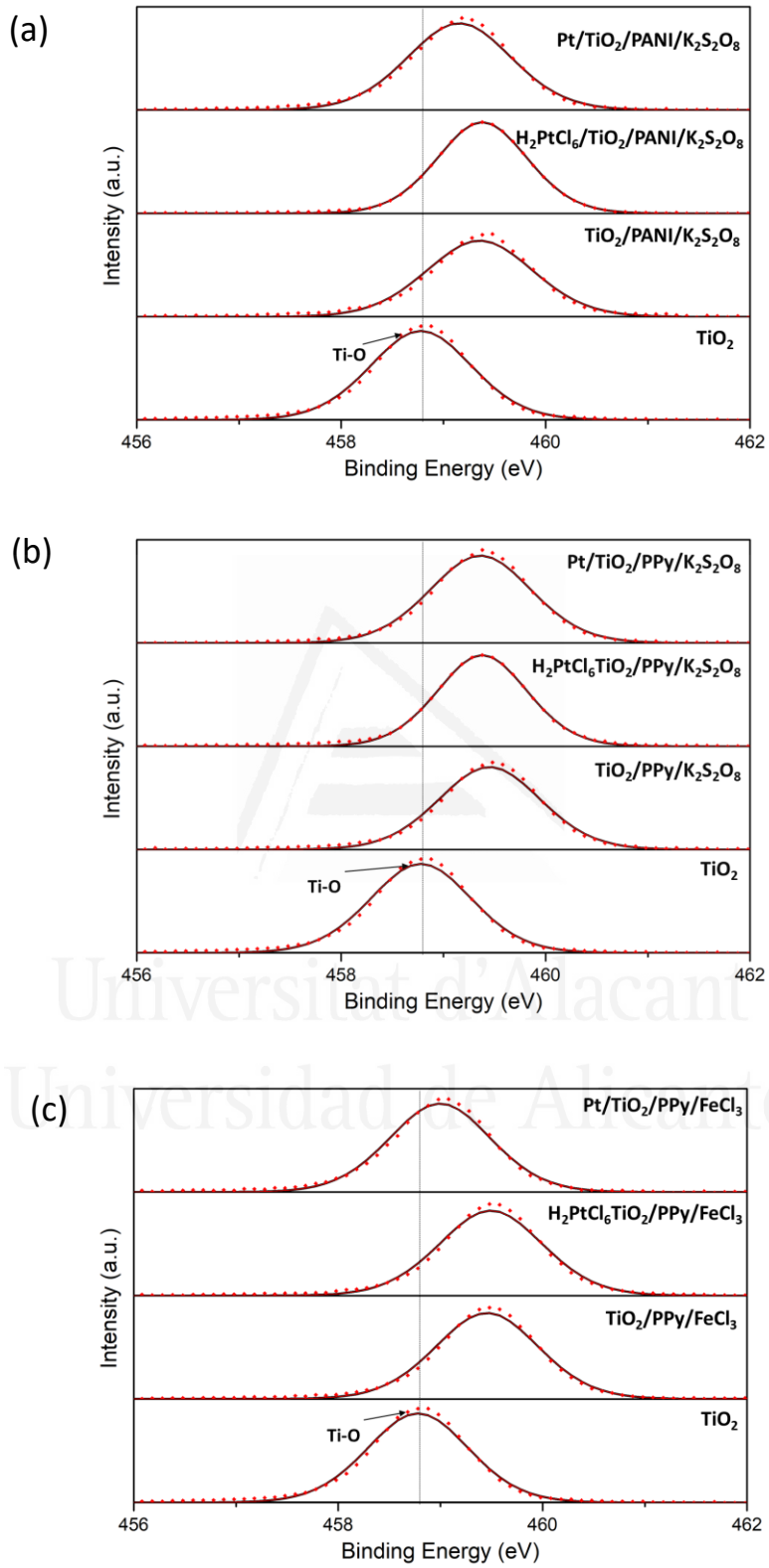

Figure 9. 10. XPS Ti 2p spectra of (a) TiO_2/PANI with $K_2S_2O_8$ and TiO_2/PPy with (b) $K_2S_2O_8$ or (c) $FeCl_3$.

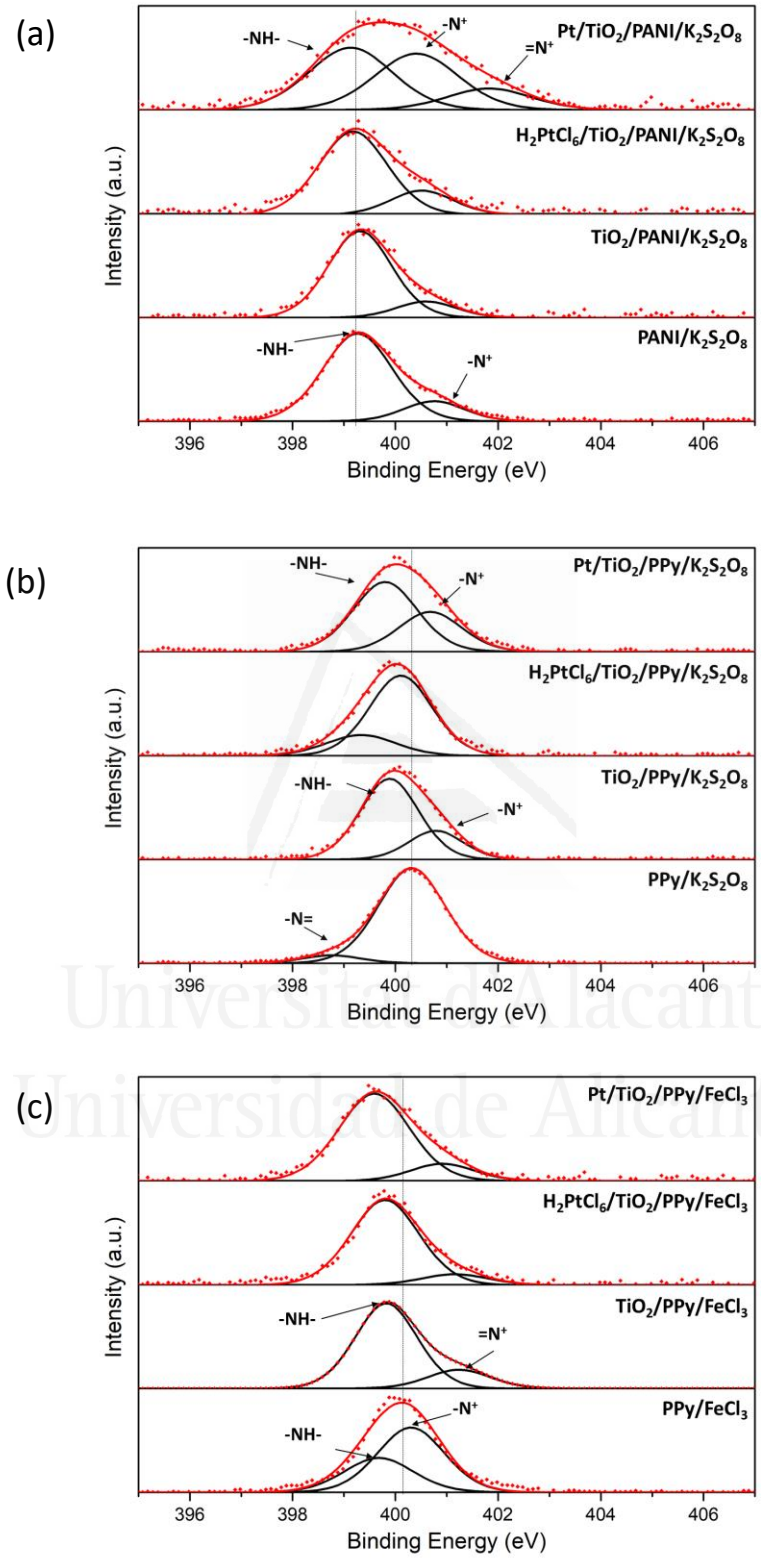

Figure 9. 11. XPS N 1s spectra of (a) TiO_2/PANI with $K_2S_2O_8$ and TiO_2/PPy with (b) $K_2S_2O_8$ or (c) $FeCl_3$.

Table 9. 4. XPS analysis of the N 1s level. Contribution (%) of different nitrogen species.

Sample	Energy (eV)	Species	Composition (%)
$PANI/K_2S_2O_8$	399.3	-NH-	83
	400.7	$-N^+$	17
$TiO_2/PANI/K_2S_2O_8$	399.3	-NH-	85
	400.6	$-N^+$	15
$H_2PtCl_6/TiO_2/PANI/K_2S_2O_8$	399.2	-NH-	79
	400.5	$-N^+$	21
$Pt/TiO_2/PANI/K_2S_2O_8$	399.1	-NH-	45
	400.4	$-N^+$	40
	401.8	$=N^+$	15
$PPy/K_2S_2O_8$	398.7	-N=	7
	400.3	$-N^+$	93
$TiO_2/PPy/K_2S_2O_8$	399.9	-NH-	75
	400.8	$-N^+$	25
$H_2PtCl_6/TiO_2/PPy/K_2S_2O_8$	399.3	-NH-	22
	400.1	$-N^+$	78
$Pt/TiO_2/PPy/K_2S_2O_8$	399.8	-NH-	64
	400.7	$-N^+$	36
$PPy/FeCl_3$	399.7	-NH-	35
	400.3	$-N^+$	65
$TiO_2/PPy/FeCl_3$	399.8	-NH-	81
	401.2	$=N^+$	19
$H_2PtCl_6/TiO_2/PPy/FeCl_3$	399.8	-NH-	90
	401.2	$=N^+$	10
$Pt/TiO_2/PPy/FeCl_3$	399.6	-NH-	85
	400.9	$-N^+$	15

C1s curve fits of the hybrid materials with a 50:50 titania/polymer ratio (Fig. 9.12, Table 9.5) show the presence of C-C, C-H and C-N species from the polymer. Some C-O and C=O moieties are created as a result of the reaction of the polymer surface with water and air [29]. Some of these oxygenated moieties may also correspond to benzoquinone and hydroquinone species in PANI as a result of an excessive oxidation of polyaniline [45]. These O-C and O=C species are also observed in the O 1s high resolution XPS spectra (Fig. 9.13, Table 9.6). O 1s curve fit also shows the presence of hydroxyl groups due to the exposure of Ti^{4+} sites to water in air [7].

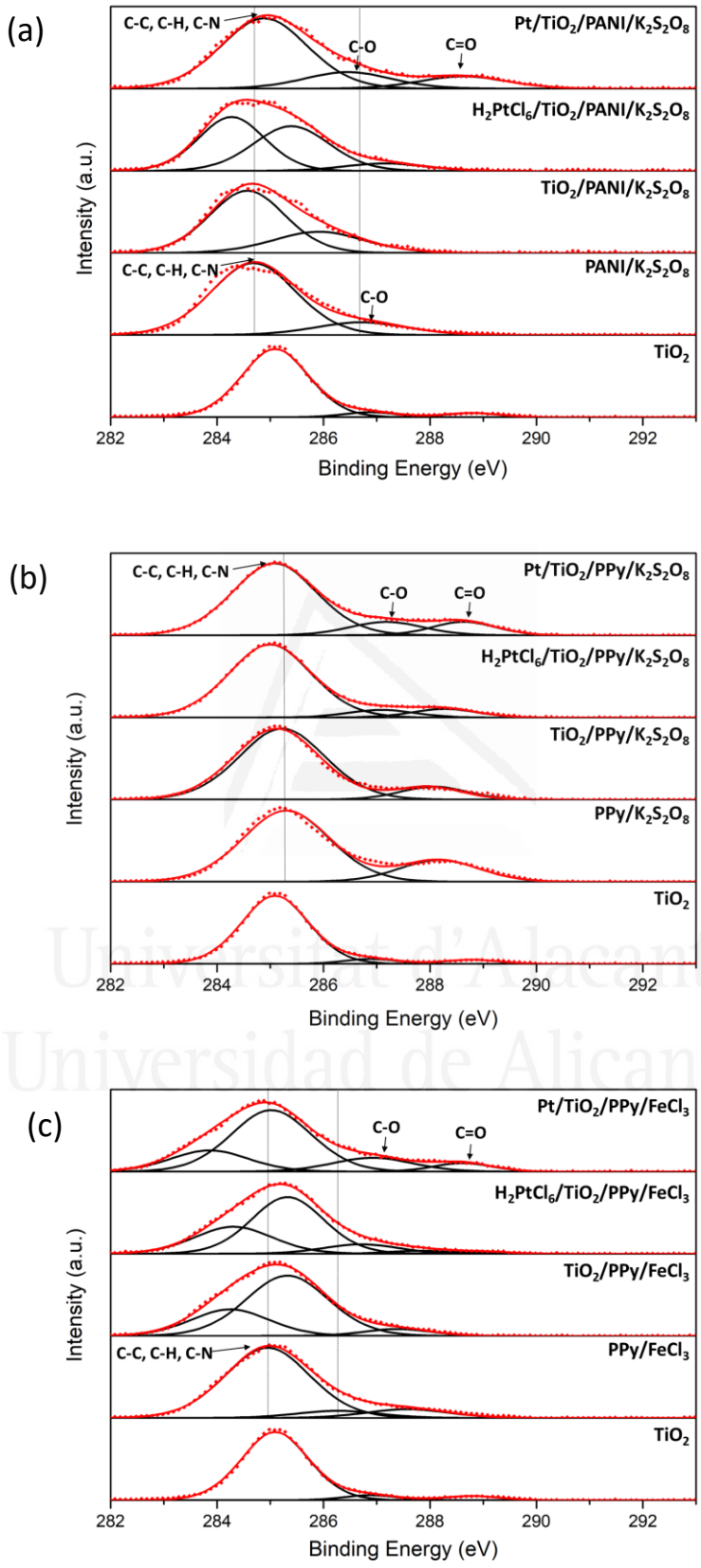

Figure 9. 12. XPS C 1s spectra of (a) TiO_2/PANI with $K_2S_2O_8$ and TiO_2/PPy with (b) $K_2S_2O_8$ or (c) $FeCl_3$.

Table 9. 5. XPS analysis of the C 1s level. Contribution (%) of different carbon species.

Sample	Energy (eV)	Species	Composition (%)
TiO_2	285.1	C-H	90
	286.9	C-O	6
	288.8	C=O	4
$PANI/K_2S_2O_8$	284.7	C-C, C-H, C-N	84
	286.7	C-O	16
$TiO_2/PANI/K_2S_2O_8$	284.6	C-C, C-H, C-N	71
	285.9	C-O	29
$H_2PtCl_6/TiO_2/PANI/K_2S_2O_8$	284.3	C-C, C-H	71
	285.4	C-N	29
	287.2	C=O	21
$Pt/TiO_2/PANI/K_2S_2O_8$	284.9	C-C, C-H, C-N	71
	286.5	C-O	17
	288.6	C=O	12
$PPy/K_2S_2O_8$	285.3	C-C, C-H, C-N	78
	288.2	C=O	22
$TiO_2/PPy/K_2S_2O_8$	285.1	C-C, C-H, C-N	88
	288.0	C=O	12
$H_2PtCl_6/TiO_2/PPy/K_2S_2O_8$	285.0	C-C, C-H, C-N	85
	287.1	C-O	7
	288.3	C=O	8
$Pt/TiO_2/PPy/K_2S_2O_8$	285.1	C-C, C-H, C-N	76
	287.2	C-O	13
	288.6	C=O	11
$PPy/FeCl_3$	284.9	C-C, C-H, C-N	82
	286.3	C-O	8
	287.6	C=O	10
$TiO_2/PPy/FeCl_3$	284.2	C-C, C-H	28
	285.3	C-N	66
	287.4	C=O	6
$H_2PtCl_6/TiO_2/PPy/FeCl_3$	284.3	C-C, C-H	29
	285.3	C-N	57
	286.7	C-O	10
	288.8	C=O	4
$Pt/TiO_2/PPy/FeCl_3$	283.9	C-C, C-H	20
	285.0	C-N	60
	286.9	C-O	14
	288.6	C=O	6

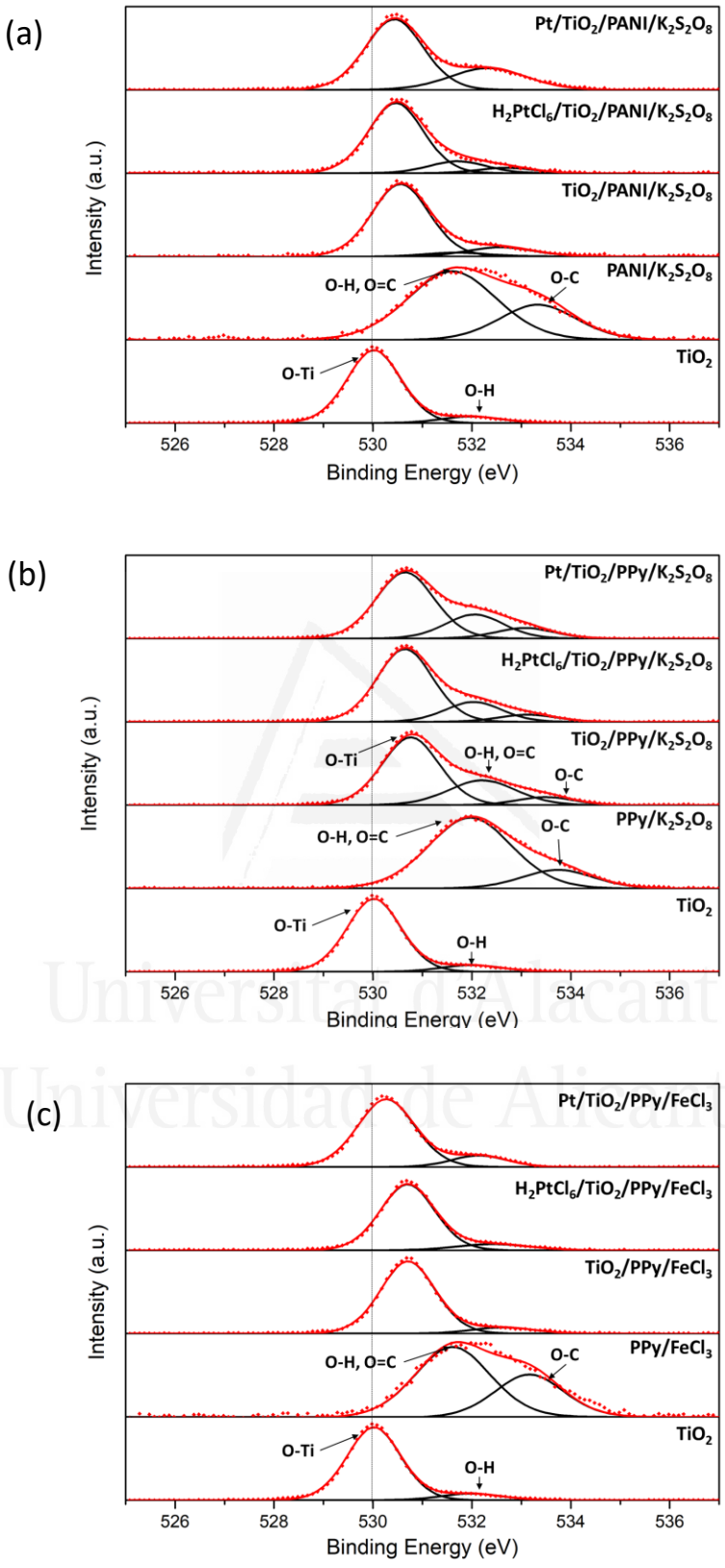

Figure 9. 13. XPS O 1s spectra of (a) TiO_2/PANI with $K_2S_2O_8$ and TiO_2/PPy with (b) $K_2S_2O_8$ or (c) $FeCl_3$.

Table 9. 6. XPS analysis of the O 1s level. Contribution (%) of different oxygen species.

Sample	Energy (eV)	Species	Composition (%)
TiO_2	530.0	O-Ti	91
	532.0	O-H	9
PANI/$K_2S_2O_8$	531.6	O-H, O=C	69
	533.3	O-C	31
TiO_2/PANI/$K_2S_2O_8$	530.6	O-Ti	83
	531.7	O-H, O=C	5
	532.6	O-C	12
H_2PtCl_6/TiO_2/PANI/$K_2S_2O_8$	530.5	O-Ti	79
	531.7	O-H, O=C	14
	532.2	O-C	7
Pt/TiO_2/PANI/$K_2S_2O_8$	530.5	O-Ti	71
	532.3	O-H, O=C	29
PPy/$K_2S_2O_8$	532.0	O-H, O=C	82
	533.7	O-C	18
TiO_2/PPy/$K_2S_2O_8$	530.8	O-Ti	65
	532.2	O-H, O=C	28
	533.5	O-C	7
H_2PtCl_6/TiO_2/PPy/$K_2S_2O_8$	530.6	O-Ti	73
	532.0	O-H, O=C	20
	533.0	O-C	7
Pt/TiO_2/PPy/$K_2S_2O_8$	530.6	O-Ti	66
	532.0	O-H, O=C	24
	533.1	O-C	10
PPy/$FeCl_3$	531.6	O-H, O=C	65
	533.2	O-C	36
TiO_2/PPy/$FeCl_3$	530.7	O-Ti	92
	532.6	O-C	8
H_2PtCl_6/TiO_2/PPy/$FeCl_3$	530.7	O-Ti	88
	532.4	O-H, O=C	12
Pt/TiO_2/PPy/$FeCl_3$	530.3	O-Ti	86
	532.2	O-H, O=C	14

C 1s contributions of PANI/$K_2S_2O_8$ at 284.7 and 286.7 eV (Fig. 9.12, Table 9.5) are shifted towards lower binding energies (284.6 and 285.9 eV) when PANI is a part of the hybrid material (TiO_2/PANI/$K_2S_2O_8$/50:50). In TiO_2/PPy this shift towards less oxidized polymeric carbon is more evident in the presence of $FeCl_3$. Thus, C 1s contributions at 284.9 and 286.3 eV in PPy/$FeCl_3$ are shifted to 284.2 and 285.3 eV in the TiO_2/PPy/$FeCl_3$/50:50 hybrid. There is also a shift of the O 1s contributions in the pristine polymers towards lower binding energies in the hybrid materials (Fig. 9.13, Table 9.6). The shifts of the binding energies of C 1s and O 1s of the polymers to lower binding energies are produced together with a 0.6 – 0.8 eV shift of Ti 2p to higher binding energies in all hybrid materials. This evidences the existence of Ti-C and Ti-O-C interactions in the hybrid material. O 1s curve fit of TiO_2 (Fig. 9.13, Table 9.6) shows a peak at 530.0 eV, which is ascribed to O-Ti bond

in the oxide, and another peak at 532.0 eV which corresponds to the surface hydroxyl (O-H) of water adsorbed on TiO_2. Therefore, hydrogen bond between surface hydroxyl groups in titanium dioxide and nitrogen in the polymer might also take place. The Ti-O-C and Ti-C interactions at the interface between the titanium particles and the polymers may favor the electron transfer in the hybrid materials [9,44,46].

TiO_2 is a non-conducting solid. Otherwise, the hybrid TiO_2/polymer materials showed higher conductivities due to their polymeric counterpart. The oxidation degree of the polymer determines the electrical properties of the hybrid material. Table 9.7 shows considerably high conductivity values of the materials containing PANI and also PPy synthesized with $FeCl_3$. However, the conductivities of the hybrid materials containing PPy synthesized with $K_2S_2O_8$ are considerably lower, which is indicative of a lower degree of oxidation of the pyrrolic N (Scheme 9.1b).

Table 9. 7. Conductivity measured on the materials.

Material	Conductivity ($S \cdot m^{-1}$)
TiO_2	$3.5 \cdot 10^{-5}$
PANI/$K_2S_2O_8$	47.5
TiO_2/PANI/$K_2S_2O_8$	46.2
H_2PtCl_6/TiO_2/PANI/$K_2S_2O_8$	32.5
Pt/TiO_2/PANI/$K_2S_2O_8$	0.26
PPy/$K_2S_2O_8$	$1.2 \cdot 10^{-1}$
TiO_2/PPy/$K_2S_2O_8$	$5.4 \cdot 10^{-2}$
H_2PtCl_6/TiO_2/PPy/$K_2S_2O_8$	$4.5 \cdot 10^{-3}$
Pt/TiO_2/PPy/$K_2S_2O_8$	$6.6 \cdot 10^{-4}$
PPy/$FeCl_3$	130.9
TiO_2/PPy/$FeCl_3$	64.4
H_2PtCl_6/TiO_2/PPy/$FeCl_3$	50.0
Pt/TiO_2/PPy/$FeCl_3$	1.5

However, the percentage of positively charged nitrogen in the polymeric matrix determines not only the redox properties but also the ion exchange ability of the hybrid material. $FeCl_3$ and $K_2S_2O_8$ oxidants not only produce a different degree of oxidation of the polymeric chain, which determines its capability for donating electrons, but they also provide the semioxidized polymeric chain with different counterions which neutralize the positive charge of the N^+ moieties. $K_2S_2O_8$ is responsible for the introduction of O and S moieties detected on both, TiO_2/PPy/$K_2S_2O_8$ and TiO_2/PANI/$K_2S_2O_8$ (Table 9.2). The binding energy of the S 2p peak (168.3 eV) corresponds to sulfate ion, which is produced as a result of the reduction of persulfate ($S_2O_8^{2-}$) to sulfate (SO_4^{2-}), upon its incorporation as a counterion

during the oxidative polymerization of aniline and pyrrole with potassium peroxydisulfate. When ferric chloride is used, chlorine ion is detected in PPy/$FeCl_3$ (Cl 2p at 198.5 eV); but it is also detected on PANI synthesized with $K_2S_2O_8$ in HCl medium. This suggests that Cl from HCl is also introduced as a counterion in PANI. A certain amount of Cl has also been detected on PPy synthesized with $K_2S_2O_8$. In this case, Cl may be ascribed to chloride from the aqueous medium. Neither K from $K_2S_2O_8$ nor Fe from $FeCl_3$ are detected, which confirms that cations do not anchor to the oxidized polymeric chains during the oxidative polymerization of aniline and pyrrole. Chloride and sulfate counteranions are anchored to the semioxidized polymeric chain and therefore they can be potentially exchanged by nitrate present in the aqueous solution (Scheme 9.2). The higher percentage of oxidized amine N^+ moieties, the higher number of counterions (A^- in Schemes 9.1 and 9.2) susceptible of being exchanged by nitrate. From this point of view TiO_2/PPy/$K_2S_2O_8$, which shows a relatively low conductivity (Table 9.7) and only contains sulfate as counterion to neutralize a relatively low percentage of N^+ moieties, is expected to have a limited performance in the adsorption of nitrate from the aqueous solution compared to TiO_2/PPy/$FeCl_3$ and TiO_2/PANI/$K_2S_2O_8$.

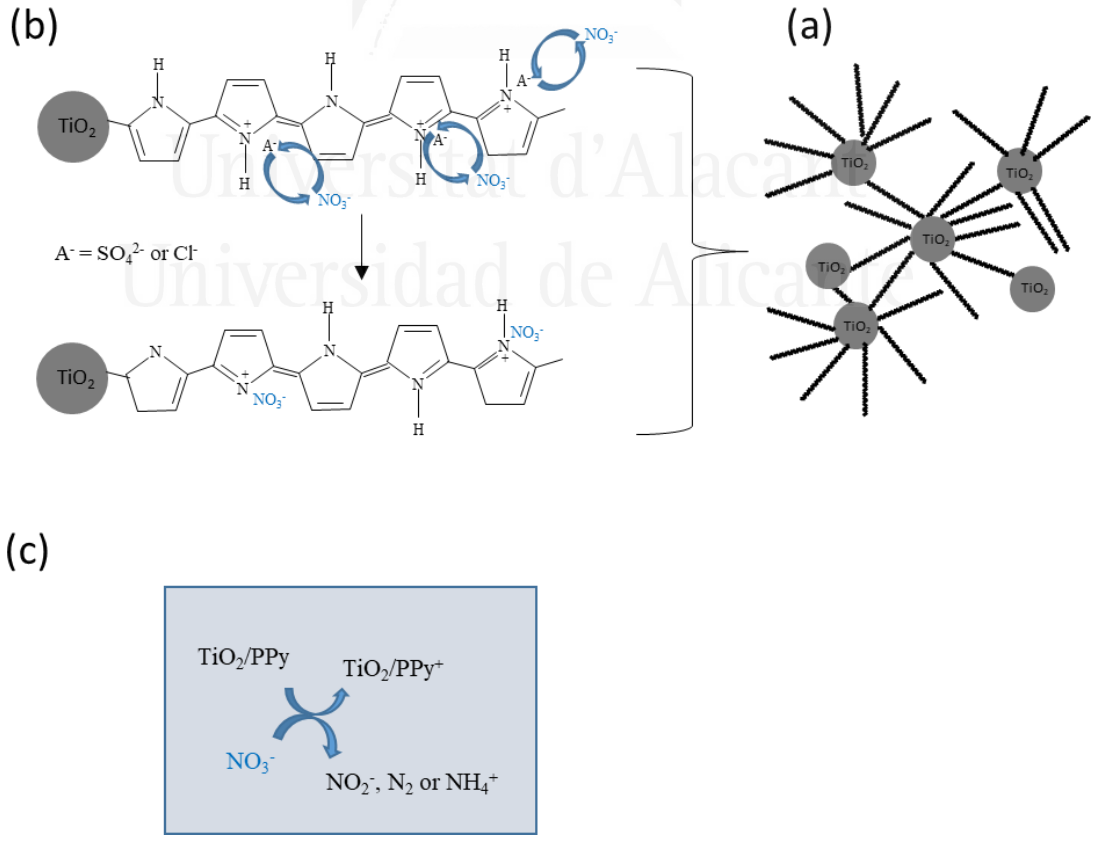

Scheme 9. 2. Scheme showing (a) pyrrole chains interconecting TiO_2 nanoparticles; (b) nitrate exchange with the counteranion (sulfate or chloride) and (c) reduction of nitrate by electrons provided by the polypyrrole.

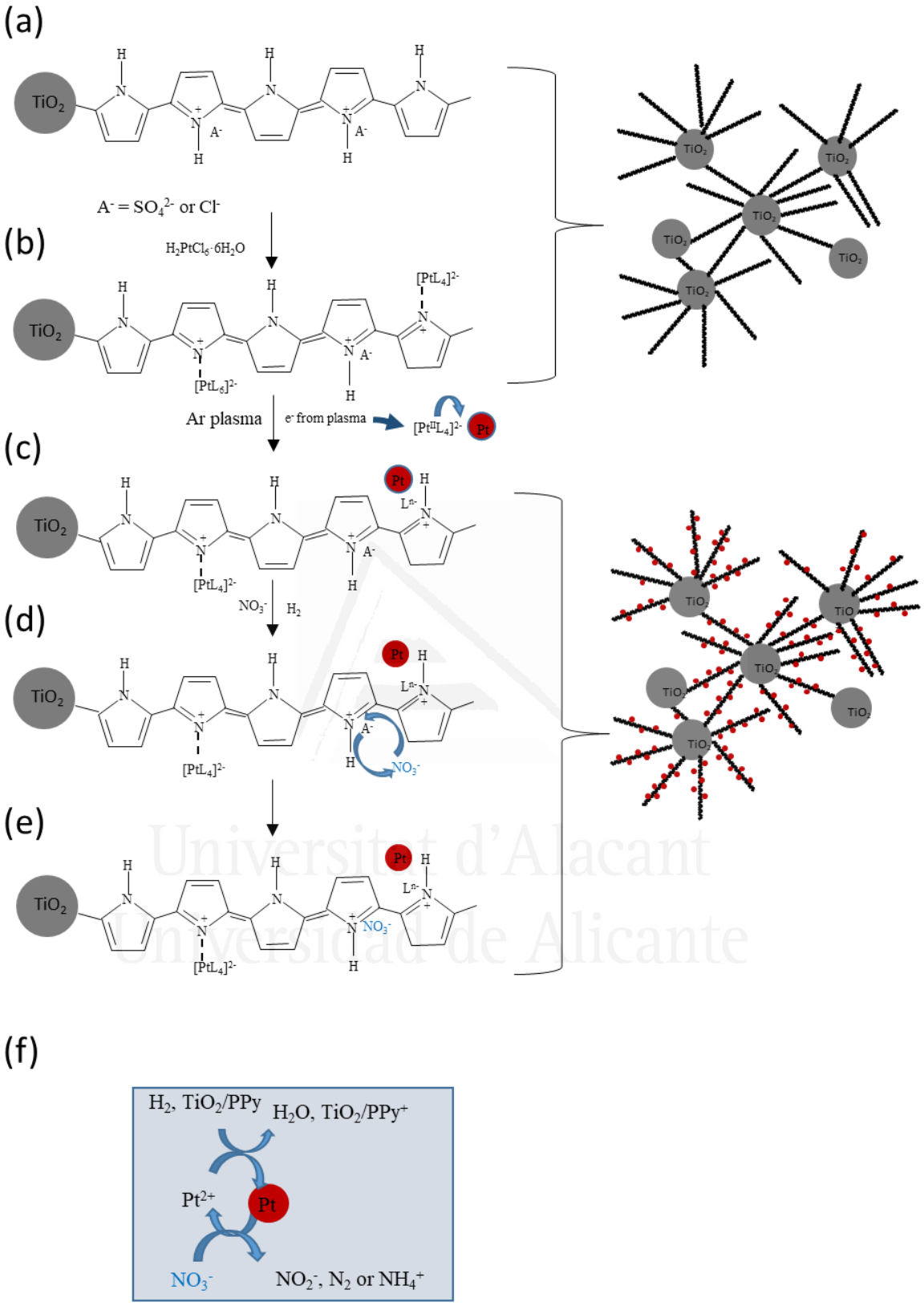

Scheme 9. 3. Scheme showing (a) polypyrrole chains doped with chloride or sulfate anions interconecting TiO_2 nanoparticles; (b) impregnation with a platinum salt precursor producing platinum chlorocomplexes anchored to the pyrrole chain trough the pirrolic nitrogen; (c) platinum nanoparticles generated by electrons in the argon plasma; (d-e) nitrate exchange with the counteranion (sulfate or chloride) and (f) reduction of nitrate by electrons provided by the polypyrrole.

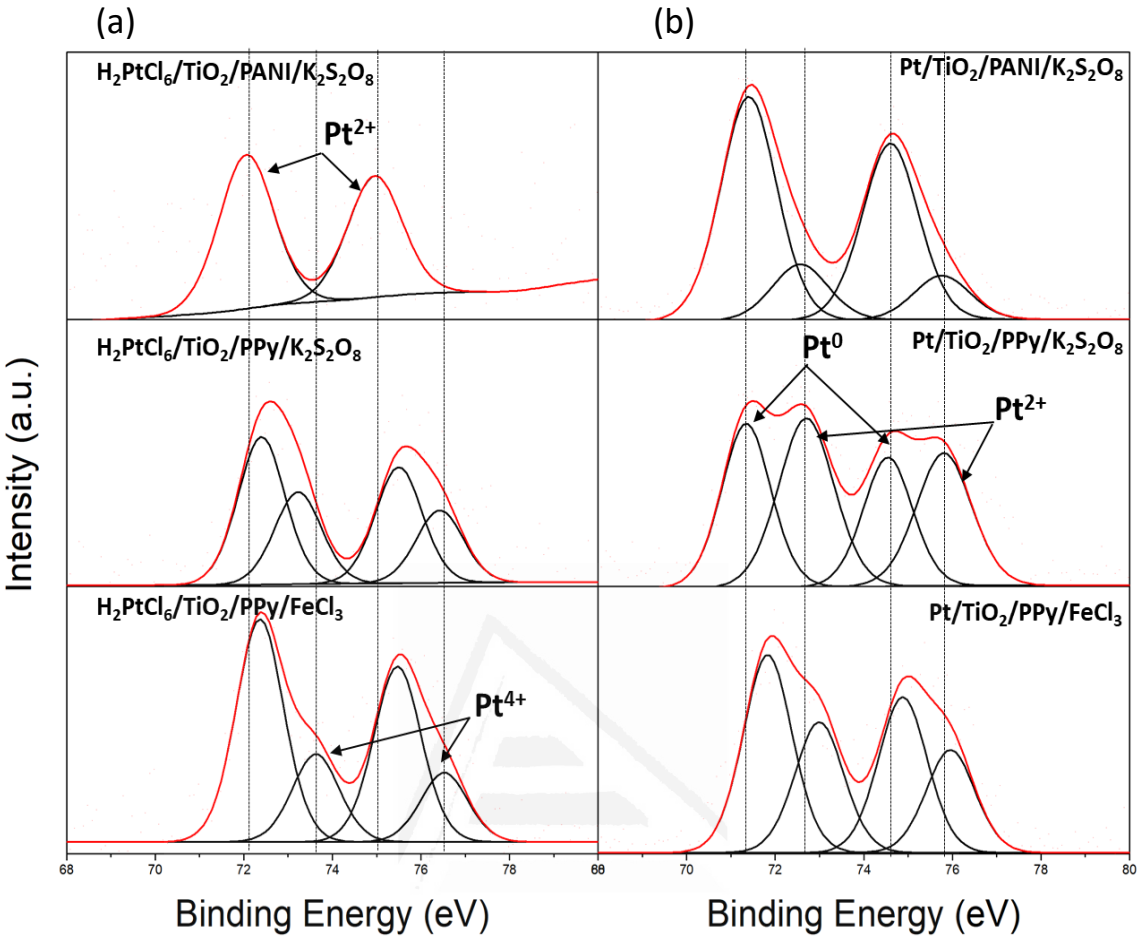

Figure 9. 14. XPS Pt 4f spectra of TiO_2/PANI/$K_2S_2O_8$ and TiO_2/PPy/$FeCl_3$ or $K_2S_2O_8$ (a) after impregnation with H_2PtCl_6 and (b) after a reductive plasma treatment.

As stated before, the goal of this chapter is to prepare metal-free materials able of adsorbing aqueous nitrate and produce its selective reduction to nitrogen. For comparison purposes, the synthesized materials were also used as support of platinum nanoparticles and tested in the catalytic hydrogenation of nitrate. The performance of the metal and the metal-free materials in the removal of nitrate from the aqueous solution was compared.

To prepare the supported platinum catalysts, the hybrid titania/polymer materials were impregnated with hexachloroplatinic acid (H_2PtCl_6) in a first step. As a result, a chloroplatinum complex anchors to the N functionalities of the polymeric chain, as it has been previously reported [47]. During the formation of the coordination compound, Pt^{4+} from H_2PtCl_6 is partially reduced to Pt^{2+}. The reduction of platinum ion is produced by the

electrons coming from the polymeric chain through the N functionality (Scheme 9.3a and 9.3b). This is more evident in the composite with PANI, where only Pt^{2+} is detected after the impregnation of the material with H_2PtCl_6 (Fig. 9.14a), and this is accompanied by an increase in the amount of N^+ functionalities (Fig. 9.11a). This is explained by the fact that, before being treated with the platinum precursor, TiO_2/PANI/$K_2S_2O_8$ is less oxidized (there is a less important percentage of oxidized amine functionalities) than the composites with PPy (Fig. 9.11b and 9.11c). As a result, 100 % of platinum ion is reduced to Pt^{2+} and no contribution of Pt^{4+} is shown in H_2PtCl_6/TiO_2/PANI/$K_2S_2O_8$. However, platinum ions in different oxidation states are present in the composites with PPy after impregnation with H_2PtCl_6 (Fig. 9.14a).

Table 9. 8. XPS analysis of the Pt $4f_{7/2}$ level. Contribution (%) of different platinum species.

Sample	Energy (eV)	Species	Composition (%)
$H_2PtCl_6/TiO_2/PANI/K_2S_2O_8$	72.1	Pt^{2+}	100
$Pt/TiO_2/PANI/K_2S_2O_8$	71.4	Pt^0	80
	72.6	Pt^{2+}	20
$H_2PtCl_6/TiO_2/PPy/K_2S_2O_8$	72.4	Pt^{2+}	60
	73.2	Pt^{4+}	40
$Pt/TiO_2/PPy/K_2S_2O_8$	71.4	Pt^0	44
	72.7	Pt^{2+}	56
$H_2PtCl_6/TiO_2/PPy/FeCl_3$	72.4	Pt^{2+}	77
	73.6	Pt^{4+}	23
$Pt/TiO_2/PPy/FeCl_3$	71.8	Pt^0	59
	73.0	Pt^{2+}	41

The hydrogenation of nitrate requires a noble metal as catalyst. In order to produce metal platinum nanoparticles, the materials impregnated with H_2PtCl_6 were treated in cold Ar plasma in a second step. Formation of platinum nanoparticles implies dissociation of the platinum complexes anchored to the polymeric chain through the nitrogen functionality (-N^+---$[PtL_4]^{2-}$) (Scheme 9.3). As a result, the oxidation state of the polymeric chain is affected as assessed by N 1s contributions: (Fig. 9.11, Table 9.4). The ligands released from the dissociated platinum complex (L^{n-}) could act as counteranions to stabilize the oxidized polymeric chain. In the case of PANI support, platinum ions (as Pt^{2+}) anchored to N^+ moieties located out of the aromatic ring in PANI are more easily reduced to metallic Pt^o by the high energy electrons in the plasma than platinum ions anchored to N^+ located inside the ring in PPy. Therefore, considerably higher amount of metallic platinum is detected on PANI surface (80 %) compared to PPy (44 – 59 %) after plasma treatment (Table 9.8). This significant lower metallic Pt loading than the theoretical value of 1 wt. % together with a

high dispersion of the Pt nanoparticles is in agreement with the absence of Pt peaks in XRD patterns (Fig. 9.5). TEM micrographs showed that the platinum nanoparticles (detected by EDX) of 2 – 5 nm diameter are mainly located on the polymer chains that connect TiO_2 particles (Fig. 9.6d, 9.7d, 9.8d and 9.9d). In all cases, the deposition of platinum nanoparticles lowered the conductivity of the materials (Table 9.7).

3.2. Nitrate removal from water

The mechanism of removing nitrate from water by the synthesized metal-free hybrid materials has been assessed and compared to the hydrogenation of nitrate catalyzed by Pt nanoparticles supported on the titania/polymer hybrid materials.

3.2.1. Reduction of nitrate by metal-free hybrid materials

Aliquots were withdrawn from the nitrate solution in contact with the hybrid TiO_2/polymer hybrid materials at different times (1, 5, 10, 15, 20, 25, 30, 45, 60, 90, 120, 180, 240 and 300 min). The nitrate abatement was rapidly achieved and after 5 min the measured concentrations of nitrate and ammonium remained constant (Fig. 9.15). Nitrite concentrations below 0.1 $mg \cdot L^{-1}$ were detected in all cases. Figure 9.16 shows concentrations measured after 5 minutes of reaction. The metal-free hybrid materials (TiO_2/PPy/$FeCl_3$ and TiO_2/PANI/$K_2S_2O_8$) produce an effective abatement of nitrate from water (almost 70 %) in just 5 minutes (Fig. 9.16a), resulting in measured nitrate concentrations around 30 $mg \cdot L^{-1}$, (Table 9.9) which accomplishes with the legislation (less than 50 $mg \cdot L^{-1}$) [48,49]. However, only 40 % of nitrate is abated in the presence of TiO_2/PPy/$K_2S_2O_8$. These evidences a determinant role of the counterion provided by the oxidant. As PPy synthesis is carried out by the oxidative polymerization of the pyrrole monomer on the TiO_2 in a neutral aqueous medium; either chloride or sulfate anions from the oxidants ($FeCl_3$ or $K_2S_2O_8$) are introduced (Scheme 9.1b). Otherwise, during the PANI synthesis in HCl medium, the anilinium cation is formed in a first step and is then oxidized by the potassium peroxidisulfate (Scheme 9.1a). As a result, both chloride and sulfate counteranions are introduced to neutralize the positively charged polyaniline chain.

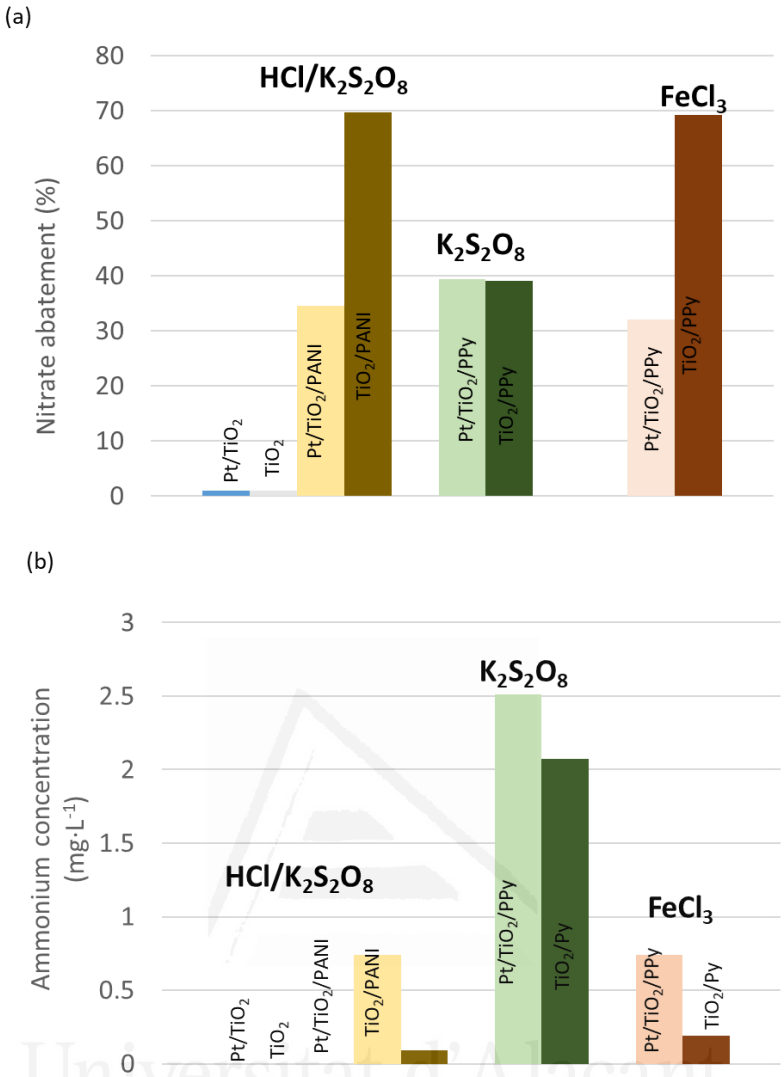

Figure 9. 15. (a) Nitrate abatement and (b) ammonium concentration measured in water in the presence of the different synthesized materials. Oxidant/dopant of PANI:$K_2S_2O_8$; oxidant/dopant of PPy:$FeCl_3$ or $K_2S_2O_8$.

The relative size of the dopant anions has a key role in the exchange with nitrate from the solution. Considering the relative size of the chloride anion (ionic radius 181 pm) and the thermochemical radii of NO_3^- (179 pm) and SO_4^{2-} (258 pm) [50], it is expected the exchange of chloride ion by aqueous nitrate to be easier than the exchange of sulfate ion. Once nitrate has been adsorbed on the polymeric matrix of the material, it must be reduced to assure proper removal without the concern of a further disposal of adsorbed nitrate. XPS revealed the transfer of electrons from titania to the polymer, so the polymer counterpart in the hybrid material is responsible for the reduction of nitrate. Actually, the reduction potentials of nitrate (NO_3^-/NH_4^+, E° = 0.875 V; NO_3^-/N_2, E° = 1.246 V), polyaniline (emeraldine/leucoemeraldine, E° = 0.342 V; pernigraniline/emeraldine, E° = 0.942 V) and

polypyrrole (PPy^+/PPy, E° = 0.150 V) are consistent with the reduction of adsorbed nitrate produced by the electrons coming from the polymeric matrix.

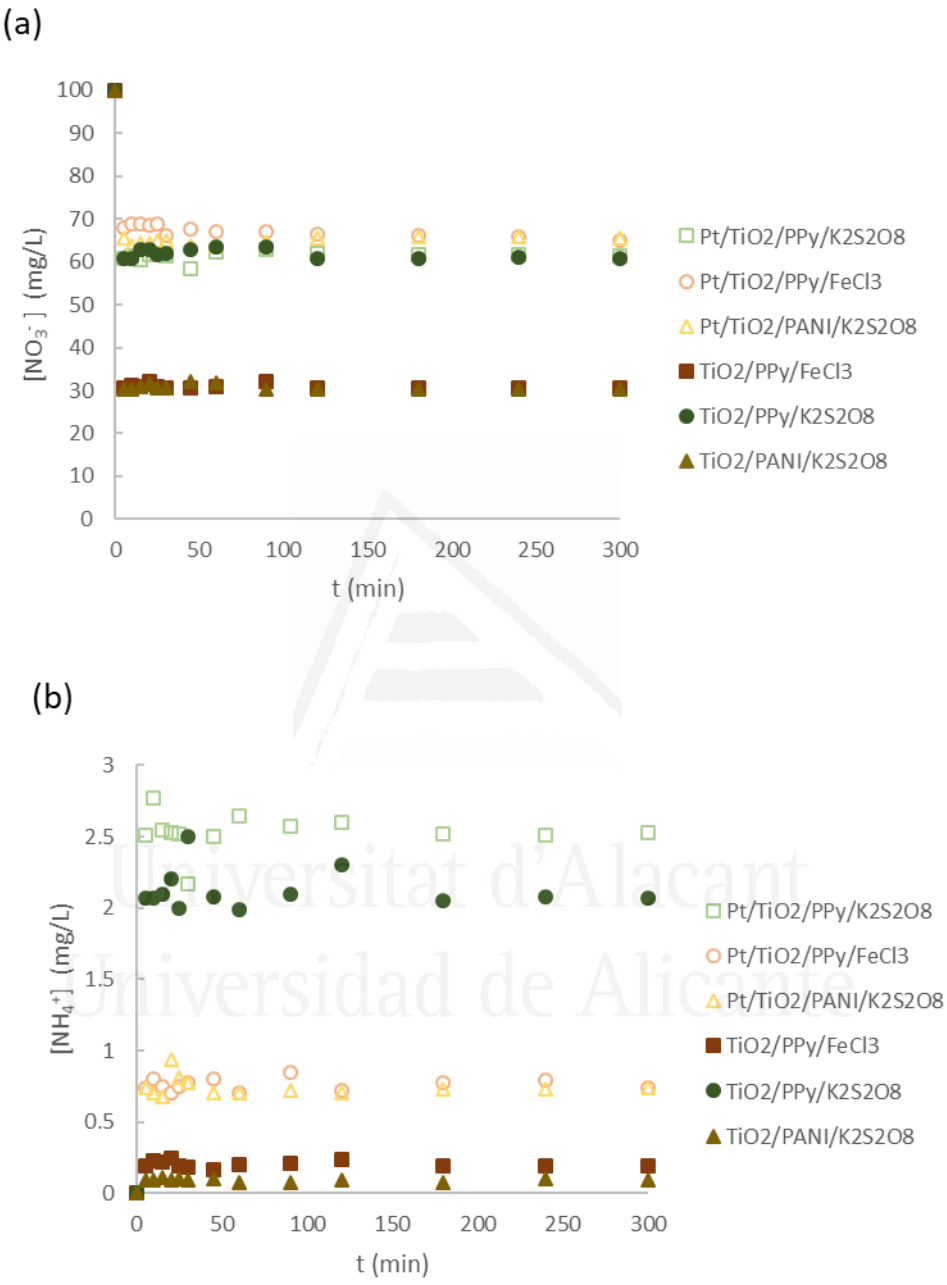

Figure 9. 16. (a) Nitrate concentration and (b) ammonium concentration measured in water at different reacton times in the presence of the different synthesized materials. Oxidant/dopant of PANI:$K_2S_2O_8$; oxidant/dopant of PPy:$FeCl_3$ or $K_2S_2O_8$.

Table 9. 9. Nitrate, nitrite and ammonium concentrations measured in the reactor during three runs. Nitrate conversion and selectivities to nitrite and ammonium.

Sample	Run number	(mg·L^{-1})			(%)		
		$[NO_3^-]$	$[NO_2^-]$	$[NH_4^+]$	$X_{NO_3^-}$	$S_{NO_2^-}$	$S_{NH_4^+}$
Pt/TiO_2	1	99.00	0	0	1	0	0
TiO_2	1	99.00	0	0	1	0	0
$Pt/TiO_2/PANI/K_2S_2O_8$	1	65.47	0.11	0.74	35	0.4	7
	2	66.02	0.08	0.70	34	0.3	7
	3	68.03	0.09	0.68	32	0.3	7
$TiO_2/PANI/K_2S_2O_8$	1	30.25	0.09	0.09	70	0.2	0.4
	2	32.30	0.07	0.08	68	0.1	0.5
	3	33.00	0.05	0.09	67	0.1	0.4
$Pt/TiO_2/PPy/K_2S_2O_8$	1	60.66	0.10	2.51	39	0.3	22
	2	61.42	0.09	2.77	39	0.3	25
	3	61.69	0.10	3.53	38	0.4	25
$TiO_2/PPy/K_2S_2O_8$	1	60.72	0.08	2.07	39	0.3	18
	2	63.84	0.05	2.15	36	0.2	20
	3	64.15	0.07	2.10	36	0.3	20
$Pt/TiO_2/PPy/FeCl_3$	1	67.98	0.09	0.74	32	0.4	9
	2	68.80	0.09	0.80	31	0.4	9
	3	68.94	0.09	0.72	31	0.4	8
$TiO_2/PPy/FeCl_3$	1	30.72	0.09	0.19	69	0.2	0.9
	2	32.50	0.08	0.20	68	0.2	1.0
	3	33.10	0.08	0.19	67	0.2	1.0

However, the mechanism is still unclear. If electrons keep flowing from TiO_2 to nitrate through the conducting polymer, some species must be supplying them, otherwise the continuity will not be there. Challagulla et al. [51] compared the photocatalytic nitrate reduction mechanism over Pt/TiO_2 with the non-photocatalytic nitrate reduction experiments in dark using doped and undoped TiO_2 catalysts both with and without purging of H_2 gas. They stated that the valence band of TiO_2 lies in the suitable range to oxidize species such as hydroxide to hydroxyl radical whereas the conducting band lies in the suitable range to reduce various species like nitrate, nitrite, etc. From our experience, the catalytic reduction of nitrate is being produced by the electrons flowing from TiO_2 through the polymer. Although the precise origin of the continuous electron supply is unclear, it might be plausible that electrons could arise from the photocatalytic oxidation of water, with titania or the whole hybrid acting as a photocatalyst. Nevertheless, further research work is being carried out to unearth the reduction mechanism.

Figure 9.16a shows that the most effective removal of nitrate (around 70 %) is produced by $TiO_2/PANI/K_2S_2O_8$ and $TiO_2/PPy/FeCl_3$. Both materials have chloride counterions and are more oxidized than $TiO_2/PPy/K_2S_2O_8$, as determined by XPS and

conductivity measurements. Consequently, nitrate exchange and nitrate reduction produced by those materials are favored in comparison with TiO_2/PPy/$K_2S_2O_8$. In all cases nitrite (NO_2^-) concentrations are below 0.15 mg·L^{-1} and satisfy the quality standards for potable water (legislation stablishes maximum permitted concentrations of nitrate, nitrite and ammonium less than 50, 0.5 and 0.5 mg·L^{-1}, respectively). These low measured nitrite concentrations confirm that nitrite does not get into the solution followed by re-adsorption by the support. On the contrary, intermediate nitrite is rapidly reduced to ammonium, in the presence of TiO_2/PPy/$K_2S_2O_8$; or to nitrogen, in the presence of TiO_2/PANI/$K_2S_2O_8$ and TiO_2/PPy/$FeCl_3$, where ammonium concentrations below 0.2 mg·L^{-1} are detected.

Recyclability of the hybrid materials was tested. Thus, after 300 min of reaction, when the first run was completed, the materials were separated by centrifugation and put into contact with a 1 mol·L^{-1} solution of NaCl during 30 min under stirring. The purpose of that was to exchange possibly adsorbed nitrate ions with chloride ions and regenerate the polymer counterpart in the hybrid material. Then, the materials were introduced in the reactor containing a fresh nitrate solution for subsequent runs under identical conditions. The measured concentrations of nitrate, nitrite and ammonium measured after 300 min of each run are summarized in Table 9.9. Nitrate conversions achieved with the regenerated materials were only slightly lower than those obtained during the first run. Similar ammonium selectivities were obtained and nitrite was not detected in any case. XRD and TEM of the recovered materials (not shown) remained almost unchanged, so no morphological changes were produced.

3.2.2. Hydrogenation of nitrate catalyzed by Pt supported on the hybrid materials

Catalytic reduction of nitrate (NO_3^-) with dyhidrogen (H_2) progresses through intermediate nitrite (NO_2^-) towards either nitrogen (N_2) or ammonium (NH_4^+) as final products as it is indicated in reactions in chapter I, section 1.2.

As a consequence of hydroxyl formation, there is an increase of the pH of the solution up to 10 – 11, which is unacceptable for drinking water, and favors the selectivity towards ammonium instead of nitrogen [52,53]. This is minimized by buffering the solution with a

CO_2 flow. Considering toxicity of nitrite and ammonium, selective reduction of nitrate towards nitrogen is necessary to accomplish legislation.

Figure 9.16a shows no activity of the platinum catalyst supported on titania. However, between 30 – 40 % of the total nitrate is abated in the presence of the platinum catalysts supported on the hybrid materials, which measured nitrate concentrations over 60 $mg \cdot L^{-1}$ (Table 9.9). ICP-MS results (Table 9.10) show that platinum leaching was not produced as lixiviated platinum was always less than 0.1 %.

Table 9. 10. Concentration of lixiviated (l) and theorical (T) platinum detected by ICP-MS in solution after 300 min of reaction of nitrate reduction with hydrogen.

Sample	(ppb)		(%)
	$[Pt]_l$	$[Pt]_T$	$[Pt]_l/[Pt]_T$
$Pt/TiO_2/PANI/K_2S_2O_8$	15.0	$1.088 \cdot 10^4$	0.14
$Pt/TiO_2/PPy/K_2S_2O_8$	12.5	$1.129 \cdot 10^4$	0.11
$Pt/TiO_2/PPy/FeCl_3$	5.6	$1.129 \cdot 10^4$	0.05

Due to the presence of the conducting polymeric matrix in the composite, the mechanism of reduction of aqueous nitrate catalyzed by platinum nanoparticles supported on the TiO_2/polymer hybrid materials may differ from the reported mechanisms for nitrate reduction with H_2 catalyzed by Pt or Pd supported on TiO_2 [7]. Yoshinaga et al. [54] reported that as palladium is very active for hydrogenation reactions, the nitrate and the nitrite molecules produced by the reduction of nitrate, would be deeply hydrogenated producing ammonium, as shown in 3rd and 4th reactions of reactions in chapter I, section 1.2. However, Figure 9.16 shows higher activity and lower ammonium selectivity when the metal-free hybrid materials are used. Therefore, platinum deposition on all the studied materials decreases nitrate removal efficiency. It is reported [7] that in Pd/TiO_2 systems nitrate is adsorbed at the Lewis acid sites on titania following exchange with OH^- anions. Nitrate is then reduced by Ti_4O_7 species and nitrite is preferentially reduced by Pd. Challagulla et al. [51] reported the competitive nature between nitrate reduction and hydrogen generation in the presence of platinum doped TiO_2. In our experience, no nitrate abatement is significantly produced in the presence of Pt/TiO_2. However, 30 - 40 % of nitrate is removed by the platinum catalysts supported on TiO_2/conducting polymer hybrid materials. In these materials, the electron transfer from the conducting polymer to nitrate ions through the nitrogen functionalities is limited due to the anchoring of the platinum chlorocomplexes (Scheme 9.3d). This results in a considerable decrease of the amount of the adsorbed nitrate.

In this case, nitrate reduction is mainly produced by dihydrogen and catalyzed by the metal platinum nanoparticles dispersed on the hybrid materials. Otherwise, in the metal-free hybrid materials, the electrons are directly transferred from the polymeric matrix to adsorbed nitrate, producing its reduction (Scheme 9.2). The presence of TiO_2 in the composite material not only enhances its thermal properties but also modifies the oxidation state of the polymeric matrix, due to the transfer of electrons from titania to the semi-oxidized polymeric chain. Thus, the reductive ability of the polymeric matrix, that is, its capability of transferring electrons to the adsorbed nitrate ions is increased.

4. CONCLUSIONS

A new route for abating nitrate from water and produce its selective reduction towards nitrogen, avoiding the use of a metal catalyst and gaseous hydrogen, has been developed. This implies the use of titanium dioxide/conducting polymer hybrid materials. During their synthesis, aniline and pyrrole polymerize on titanium dioxide surface connecting titanium dioxide particles. As a result, conducting hybrid materials with enhanced thermal properties are obtained. These materials are capable of adsorbing nitrate and subsequently produce its reduction. The oxidant used during the polymerization of the monomers onto titania plays a key factor as the degree of oxidation of the polymeric chain imparted by the oxidant affects the number of counterions susceptible to be exchanged by nitrogen. The size of the counterion also determines the effective exchange with nitrate. Ti-C and Ti-O-C interactions between the polymers and titanium dioxide allows the electron transfer from titania to the polymer chain, which produce the reduction of the adsorbed nitrate.

Nitrate reduction produced by TiO_2/PPy/$FeCl_3$ and TiO_2/PANI/$K_2S_2O_8$ is considerably more effective than the catalytic hydrogenation produced by platinum nanoparticles supported on these composite materials. In the metal-free composites, the reduction of nitrate is produced by the electrons provided directly by the hybrid material. Otherwise, there is a considerable decrease in the activity of the nitrate reduction reaction produced by the materials containing platinum. The loading of the hybrid materials with platinum results in the blocking of N sites by Pt. Therefore, the transfer of electrons from the material to nitrate adsorbed to the polymeric chain by ion exchange is diminished, and the reduction of nitrate is mainly produced by the dihydrogen dissolved in water and

adsorbed on Pt nanoparticles. Nevertheless, both mechanisms might be having a role in the platinum loaded materials: not only a catalytic hydrogenation is taking place but it could also be a contribution of the electrons provided by the polymer to the reduction of nitrate.

5. REFERENCES

[1] F. Ruiz-Beviá. *J. Catal*. **2004**, *227(2)*, 563-565.

[2] I. Dodouche, D.P. Barbosa, M.C. Rangel, F. Epron. *Appl. Catal., B.* **2009**, *93(1-2)*, 50-55.

[3] O.S.G.P. Soares, M.F.R. Pereira, J.J.M. Órfão, J.L. Faria, C.G. Silva. *Chem. Eng. J*. **2014**, *251*, 123-130.

[4] N. Barrabés, J. Sá. *Appl. Catal., B.* **2011**, *104(1-2)*, 1-5.

[5] O.S.G.P. Soares, E.O. Jardim, A. Reyes-Carmona, J. Ruiz-Martínez, J. Silvestre-Albero, E. Rodríguez-Castellón, J.J.M. Órfão, A. Sepúlveda-Escribano, M.F.R. Pereira. *J. Colloid Interface Sci*. **2012**, *369(1)*, 294-301.

[6] J. Martínez, A. Ortiz, I. Ortiz. *Appl. Catal., B.* **2017**, *207*, 42-59.

[7] J. Sá, J.A. Anderson. *Appl. Catal., B.* **2008**, *77(3-4)*, 409-417.

[8] J. Sá, C. Alcaraz-Agüera, S. Gross, J.A. Anderson. *Appl. Catal., B.* **2009**, *85(3-4)*, 192-200.

[9] M. Radoičić, G. Ćirić-Marjanović, V. Spasojević, P. Ahrenkiel, M. Mitrić, T. Novaković, Z. Šaponjić. *Appl. Catal., B.* **2017**, *213*, 155-166.

[10] C. Janáky, N.R. de Tacconi, W. Chanmanee, K. Rajeshwar. *J. Phys. Chem. B.* **2012**, *116(36)*, 19145-19155.

[11] P. Rajakani, C. Vedhi. *Int. J. Ind. Chem*. **2015**, *6*, 247-259.

[12] R. Arora, U.K. Mandal, P. Sharma, A. Srivastav. *Mater. Today Proc*. **2015**, *2(4-5)*, 2767-2775.

[13] Y.G. Han, T. Kusunose, T. Sekino. *Mater. Sci. Forum*. **2008**, *569*, 161-164.

[14] H. Dong, G. Zeng, L. Tang, C. Fan, C. Zhang, X. He, Y. He. *Water Res*. **2015**, *79*, 128-146.

[15] M. Sangareswari, M.M. Sundaram. *Appl. Water Sci*. **2017**, *7*, 1781-1790.

[16] R. Arora, A. Srivastav, U.K. Mandal. *Int. J. of Modern Eng. Res*. **2012**, *2(4)*, 2384-2395.

[17] M. Radoičić, Z. Šaponjić, I.A. Janković, G. Ćirić-Marjanović, S. P. Ahrenkiel, M.I. Comor. *Appl. Catal., B.* **2013**, *136-137*, 133-139.

[18] M.K. Nowotny, P. Bogdanoff, T. Dittrich, S. Fiechter, A. Fujishima, H. Tributsch. *Mater. Lett*. **2010**, *64(8)*, 928-930.

[19] S. Das, D. Liu, J.B. Park, Y.B. Hahn. *J. Alloys Compd*. **2013**, *553*, 188-193.

[20] Q. Li, S. Wang, Z. Jin, D. Yang, S. Zhang, X. Guo, J. Yang, Z. Zhang. *J. Nanopart. Res*. **2007**, *9*, 951-957.

[21] U. Martínez, B. Hammer. *J. Chem. Phys*. **2011**, *134(19)*, 194703.

[22] I. Salaoru, T. Prodromakis, A. Khiat, C. Toumazou. *Appl. Phys. Lett*. **2013**, *102(1)*, 13506-13509.

[23] V. C. Anitha, A.N. Banerjee, S.W. Joo. *J. Mater. Sci*. **2015**, *50(23)*, 7495-7536.

[24] M.J. García-Fernández, S. Sancho-Querol, M.M. Pastor-Blas, A. Sepúlveda-Escribano. *J. Colloid Interface Sci*. **2017**, *494*, 98-106.

[25] T.A. Skotheim, J.R. Reynolds. *Recent advances in polypyrrole* in *Handbook of conducting polymers. Conjugated polymers: theory, synthesis, properties, and characterization*. 3rd ed. CRC Press: Boca Raton, FL, USA. **2007**.

[26] B. Ohtani, O.O. Prieto-Mahaney, D. Li, R. Abe. *J. Photochem. Photobiol., A*. **2010**, *216(2-3)*, 179-182.

[27] I. Dodouche, F. Epron. *Appl. Catal., B*. **2007**, *76(3-4)*, 291-299.

[28] J. Stejskal, R.G. Gilbert. *Pure Appl. Chem*. **2002**, *74(5)*, 857-867.

[29] R. Buitrago-Sierra, M.J. García-Fernández, M.M. Pastor-Blas, A. Sepúlveda-Escribano. *Green Chem*. **2013**, *15*, 1981-1990.

[30] C.H.B. Silva, A.M. Da Costa-Ferreira, V.R.L. Constantino, M.L.A. Temperini. *J. Mater. Chem., A*. **2014**, *2*, 8205-8214.

[31] M. Hasik, A. Bernasik, A. Adamczyk, G. Malata, K. Kowalski, J. Camra. *Eur. Polym. J*. **2003**, *39(8)*, 1669-1678.

[32] J. Ouyang, Y. Li. *Polymer*. **1997**, *38(15)*, 3997-3999.

[33] A. Nyczyk, A. Sniechota, A. Adamczyk, A. Bernasik, W. Turek, M. Hasik. *Eur. Polym. J*. **2008**, *44(6)*, 1594-1602.

[34] B. Ohtani, Y. Ogawa, S. Nishimoto. *J. Phys. Chem., B*. **1997**, *101(19)*, 3746–3752.

[35] K.J.A. Raj, B. Viswanathan. *Indian J. Chem., Sect. A*. **2009**, *48(10)*, 1378–1382.

[36] S.M. Kumar, P.A. Deshpande, M. Krishna, M.S. Krupashankara, G. Madras. *Plasma Chem. Plasma Process*. **2010**, *30*, 461–470.

[37] A. Drelinkiewicz, A. Zieba, J.W. Sobczak, M. Bonarowska, Z. Karpiński, A. Waksmundzka-Góra, J. Stejskal. *React. Funct. Polym*. **2009**, *69(8)*, 630-642.

[38] A. Katoch, M. Burkhart, T. Hwang, S.S. Kim. *Chem. Eng. J.* **2012**, *192*, 262-268.

[39] X. Li, D. Wang, G. Cheng, Q. Luo, J. An, Y. Wang. *Appl. Catal., B.* **2008**, *81(3-4)*, 267-273.

[40] M.E. Simonsen, H. Jensen, Z. Li, E.G. Søgaard. *J. Photochem. Photobiol., A.* **2008**, *200(2-3)*, 192-200.

[41] J.Yu, X. Zhao, Q. Zhao. *Thin Solid Films.* **2000**, *379(1-2)*, 7-14.

[42] S. Tyagi, D. Rawtani, N. Khatri, M. Tharmavaram. *J. Water Process Eng.* **2018**, *21*, 84-95.

[43] Y. Kitamura, T. Niwa, S. Naya, T. Hattori, Y. Sumida, H. Tada. *Chem. Commun.* **2013**, *49*, 520-522.

[44] N.M. Dimitrijevic, S. Tepavcevic, Y. Liu, T. Rajh, S.C. Silver, D.M. Tiede. *J. Phys. Chem. C.* **2013**, *117(30)*, 15540-15544.

[45] Y. Li, Y. Yu, L. Wu, J. Zhi. *Appl. Surf. Sci.* **2013**, *273*, 135-143.

[46] S. Deivanayaki, V. Ponnuswamy, S. Ashokan, P. Jayamurugan, R. Mariappan. *Mater. Sci. Semicond. Process.* **2013**, *16(2)*, 554-559.

[47] M.J. García-Fernández, M.M. Pastor-Blas, F. Epron, A. Sepúlveda-Escribano. *Appl. Catal., B.* **2013**, *225*, 162-171.

[48] EC (European Community), Official Journal of the European Communities, Council Directive 98/83/EC on the quality of water intended for human consumption, *The Drinking Water Directive (DWD)*, Brussels. **1998**, Annex 1, Part B, 42-44.

[49] USEPA (United State Environmental Protection Agency), *National Primary Drinking Water Regulations*, Washington, DC, **2008**, Title 40, Part 141.

[50] M. Weller, T. Overton, J. Rourke, F. Armstrong. *Inorganic Chemistry*. 7th ed. Oxford University Press, UK. **2018**.

[51] S. Challagulla, K. Tarafder, R. Ganesan, S. Roy. *J. Phys. Chem., C.* **2017**, *121(49)*, 27406-27416.

[52] U. Prüsse, M. Hähnlein, J. Daum, K-D.Vorlop. *Catal. Today.* **2000**, *55(1-2)*, 79-90.

[53] U. Prüsse, K-D.Vorlop. *J. Mol. Catal. A: Chem.* **2001**, *173(1-2)*, 313-328.

[54] I. Mikami, Y. Sakamoto, Y. Yoshinaga, T. Okuhara. *Appl. Catal., B.* **2003**, *44(1)*, 79-86.

General conclusions

The aim of this Doctoral Thesis has been to determine the ability of some conducting polymers (polypyrrole, polyaniline and polythiophene) for removing nitrates from water by adsorption and reduction, preferably without the need of a metal catalyst and producing molecular nitrogen as the only product.

First of all, Ar plasma reduction at room temperature has been demonstrated to be a simple, low time-consuming, green and effective process for the synthesis of polypyrrole-supported Pt catalysts, compared to the wet chemical reduction with borohydride. It has been shown that Ar plasma leads to a more effective reduction of platinum ions in the chloroplatinum complex to metallic platinum compared to reduction with borohydride, due to direct transfer of the abundant electrons in the plasma to platinum ions. Furthermore, another effect of the plasma reduction is the activation of the polypyrrole surface, in such a way that the ulterior exposure to air leads to the creation of carboxylated moieties. It has been found that the platinum nanoparticles supported on polypyrrole, obtained after treatment with argon plasma at 200 W in cycles of 5 min during a total time of 3 h (5 min x 36 times) effectively catalyzed the reaction of reduction of nitrates in water with H_2 producing mainly N_2 and very low amounts of nitrite and ammonium ions.

Using the environmentally-friendly Ar plasma treatment, bimetallic (Pt:Sn) catalysts supported on polypyrrole have been prepared and compared to the monometallic (Pt) catalysts. All the catalysts were effective in the reduction of aqueous nitrate with H_2 at room temperature, and nitrate concentrations in water below the maximum acceptable level of 50 $mg \cdot L^{-1}$ were achieved in all cases, with mono and bimetallic catalysts. However, considering not only the efficiency in nitrate reduction, but also minimized concentrations of the undesired intermediate (nitrite) and by-product (ammonium), the monometallic Pt catalyst seems to be the most effective one.

Nevertheless, nitrate abatement produced by the metal catalysts supported on PPy is less effective than the nitrate removal produced by the metal-free polymer (although high ammonium concentrations are obtained). Platinum nanoparticles anchor to the polypyrrole chain through nitrogen positions. Therefore, electron transfer from polypyrrole to nitrate is direct in absence of platinum but is platinum-mediated in the

platinum catalyst, which shows lower efficiency in the removal of nitrates from water. Besides, the polypyrrole chain seems to be a more effective reductor than dihydrogen. Consequently, reduction of nitrate is more effectively produced by electrons provided by polypyrrole chain than by dihydrogen presumably chemisorbed on platinum nanoparticles.

The mechanisms which govern these processes have been analyzed and it has been found that the oxidant used in the chemical polymerization of pyrrole plays a definitive role in the ability of this polymer to remove nitrate from water. So, it can be concluded that:

a) Ion exchange and redox properties of PPy are affected by the oxidant used in the synthesis, $K_2S_2O_8$ or $FeCl_3$, as they provide different counterions and produce a different degree of oxidation of the pyrrolic chain.

b) The initial oxidation degree of the polymer, imparted by the oxidant, is determinant in the ability of the polymer to produce the reduction of nitrate in aqueous solution by electron transfer from the polypyrrole chain to the nitrate anion. The more reduced the pristine polymeric chain, the more important the electron transfer to nitrate. Consequently, nitrate reduction is more effectively produced by PPy/$FeCl_3$, which is in a more reduced state than PPy/$K_2S_2O_8$.

c) The selectivity of nitrate reduction to nitrogen is also affected by the oxidant. Nitrate is selectively reduced to N_2 in the presence of PPy/$FeCl_3$, whereas the reaction is highly selective to ammonium with PPy/$K_2S_2O_8$. Considering the final concentration of nitrate, nitrite and ammonium, and also the selectivities to nitrite and to ammonium, it can be concluded that PPy/$FeCl_3$ is appropriate to effectively remove nitrates from drinking water in agreement with the European regulations.

Platinum nanoparticles have also been synthesized and supported in polyaniline (PANI), using the same reducing treatment with cold Ar plasma of the platinum salt precursor than in the case of PPy. All the catalysts produced an important abatement of nitrate from water in only 5 min and nitrate ability was maintained after two cycles of the

regenerated catalysts. However, nitrate abatement proceeds by two different mechanisms, depending on the nature of the conducting polymer:

Mechanism A: Nitrate is adsorbed on the platinum complex either forming an adduct or entering the complex as a ligand. This mechanism is favored in PANI, where the nitrogen atom is external to the ring system and steric hindering is minimized.

Mechanism B: There is an ion exchange between Cl^- and/or SO_4^{2-} present in the doped polymers as counterions and NO_3^- from the nitrate aqueous solution. This mechanism is favored in PPy.

In both cases, the adsorption or ion exchange of nitrate is followed by a redox process in which metallic platinum nanoparticles synthesized by argon plasma have a role in the reduction of nitrate to either ammonium (measured) and nitrogen (not measured). Ammonium production was more important when platinum was supported on PPy compared to PANI, but it was maintained constant with reaction time. The location of the nitrogen atom within the aromatic ring in PPy restricts the extension of mechanism A, and favors mechanism B, which involves the reduction of nitrate located next to platinum nanoparticles.

As a result of any of the redox process involving platinum, that is, platinum ions being reduced by electrons coming from plasma and, on the other hand, metal platinum nanoparticles being oxidized as nitrate is reduced, the oxidation state of the polymeric chain changes. This evidence an active participation of the polymer matrix in the redox process.

Redox and ion exchange properties of PPy and PANI doped with $K_2S_2O_8$ have a determinant role in the removal of nitrates from water. However, the nature of each polymer greatly influences the reaction mechanism. Whereas ion exchange between Cl^- and SO_4^{2-} counterions and NO_3^- from water is the main responsible for the effective nitrate removal in PANI, the mechanism for nitrate removal is based in an electron transfer from PPy to nitrate through N located in the pyrrolic ring.

On the other hand, polythiophene (PT) is not able to exchange nitrate unless it is synthesized using an anionic surfactant (sodium dodecyl sulfate, SDS). In this case, ion exchange between counteranions and nitrate is enhanced, and ulterior reduction of nitrate by electrons of thiophene is produced.

Finally, a new route for abating nitrate from water and produce its selective reduction towards nitrogen, avoiding the use of a metal catalyst and gaseous hydrogen, has been developed. This implies the use of titanium dioxide/conducting polymer hybrid materials. During their synthesis, aniline and pyrrole polymerize on titanium dioxide surface connecting titanium dioxide particles. As a result, conducting hybrid materials with enhanced thermal properties are obtained. These materials are capable of adsorbing nitrate and subsequently produce its reduction. The oxidant used during the polymerization of the monomers onto titania plays a key factor as the degree of oxidation of the polymeric chain imparted by the oxidant affects the number of counterions susceptible to be exchanged by nitrogen. The size of the counterion also determines the effective exchange with nitrate. Ti-C and Ti-O-C interactions between the polymers and titanium dioxide allows the electron transfer from titania to the polymer chain, which produce the reduction of the adsorbed nitrate.

Nitrate reduction produced by TiO_2/PPy/$FeCl_3$ and TiO_2/PANI/$K_2S_2O_8$ is considerably more effective than the catalytic hydrogenation produced by platinum nanoparticles supported on these composite materials. In the metal-free composites, the reduction of nitrate is produced by the electrons provided directly by the hybrid material. Otherwise, there is a considerable decrease in the activity of the nitrate reduction reaction produced by the materials containing platinum. The loading of the hybrid materials with platinum results in the blocking of N sites by Pt. Therefore, the transfer of electrons from the material to nitrate adsorbed to the polymeric chain by ion exchange is diminished, and the reduction of nitrate is mainly produced by the dihydrogen dissolved in water and adsorbed on Pt nanoparticles. Nevertheless, both mechanisms might be having a role in the platinum loaded materials: not only a catalytic hydrogenation is taking place but it could also be a contribution of the electrons provided by the polymer to the reduction of nitrate.

Conclusiones generales

El objetivo de esta Tesis Doctoral ha sido determinar la capacidad de algunos polímeros conductores (polipirrol, polianilina y politiofeno) para eliminar nitratos del agua por adsorción y reducción, preferiblemente sin necesidad de un catalizador metálico y produciendo nitrógeno molecular como único producto.

En primer lugar, se ha demostrado que la reducción mediante plasma de Ar a temperatura ambiente es un proceso simple, poco costoso, verde y eficaz para la síntesis de catalizadores de Pt soportados en polipirrol, en comparación con la reducción química con borohidruro. Se ha demostrado que el plasma de Ar conduce a una reducción más efectiva de los iones de platino a platino metálio en el complejo de cloroplatino en comparación con la reducción con borohidruro, debido a la transferencia directa de los abundantes electrones en el plasma a los iones de platino. Además, otro efecto de la reducción con plasma es la activación de la superficie del polipirrol, de tal manera que la exposición posterior al aire conduce a la creación de zonas carboxiladas. Se ha encontrado que las nanopartículas de platino soportadas en polipirrol, obtenidas después del tratamiento con plasma de argón a 200 W en ciclos de 5 min durante un tiempo total de 3 h (5 min x 36 veces), catalizaron eficazmente la reacción de reducción de nitratos en el agua con H_2 produciendo principalmente N_2 y cantidades muy bajas de iones nitrito y amonio.

Utilizando el tratamiento de plasma de Ar, respetuoso con el medio ambiente, se han preparado catalizadores bimetálicos (Pt:Sn) soportados en polipirrol y se han comparado con los catalizadores monometálicos (Pt). Todos los catalizadores fueron efectivos en la reducción de nitrato acuoso con H_2 a temperatura ambiente y se lograron concentraciones de nitrato en agua por debajo del nivel máximo permitido de 50 $mg \cdot L^{-1}$ en todos los casos, con catalizadores mono y bimetálicos. Sin embargo, considerando no sólo la eficiencia en la reducción de nitratos, sino también las concentraciones minimizadas del intermediario no deseado (nitrito) y subproducto (amonio), el catalizador monometálico de Pt parece ser el más efectivo.

Sin embargo, la reducción de nitratos producida por los catalizadores metálicos soportados en PPy es menos efectiva que la eliminación de nitratos producida por el polímero libre de metales (aunque se obtienen altas concentraciones de amonio). Las nanopartículas de platino se anclan a la cadena de polipirrol a través de las posiciones de

nitrógeno. Por lo tanto, la transferencia de electrones desde el polipirrol al nitrato es directa en ausencia de platino, pero se produce a través del platino en el catalizador de platino, el cual muestra una menor eficiencia en la eliminación de nitratos del agua. Además, la cadena de polipirrol parece ser un reductor más eficaz que el dihidrógeno. En consecuencia, la reducción de nitrato es producida más eficazmente por los electrones proporcionados por la cadena de polipirrol que por el dihidrógeno presumiblemente quimisorbido sobre nanopartículas de platino.

Se han analizado los mecanismos que rigen estos procesos y se ha encontrado que el oxidante utilizado en la polimerización química del pirrol juega un papel definitivo en la capacidad de este polímero para eliminar el nitrato del agua. Así pues, cabe concluir que:

a) El intercambio iónico y las propiedades redox del PPy se ven afectadas por el oxidante utilizado en la síntesis, $K_2S_2O_8$ o $FeCl_3$, ya que proporcionan diferentes contraiones y producen un grado diferente de oxidación de la cadena pirrólica.

b) El grado de oxidación inicial del polímero, proporcionado por el oxidante, es determinante en la capacidad del polímero para producir la reducción de nitrato en disolución acuosa por transferencia de electrones de la cadena de polipirrol al anión nitrato. Cuanto más reducida se encuentre la cadena polimérica original, mayor es la transferencia electrónica al nitrato. En consecuencia, la reducción de nitratos se produce de manera más efectiva por PPy/$FeCl_3$, que se encuentra en un estado más reducido que PPy/$K_2S_2O_8$.

c) La selectividad de la reducción de nitrato a nitrógeno también se ve afectada por el oxidante. El nitrato se reduce selectivamente a N_2 en presencia de PPy/$FeCl_3$, mientras que la reacción es altamente selectiva a amonio con PPy/$K_2S_2O_8$. Teniendo en cuenta la concentración final de nitrato, nitrito y amonio, así como las selectividades de nitrito y amonio, puede concluirse que el PPy/$FeCl_3$ es adecuado para eliminar eficazmente los nitratos del agua potable de acuerdo con la normativa europea.

Las nanopartículas de platino también se han sintetizado y soportado en polianilina (PANI), utilizando el mismo tratamiento de reducción con plasma frío de Ar

de la sal de platino precursora que en el caso del PPy. Todos los catalizadores produjeron una reducción significativa de nitrato en agua en sólo 5 min y la capacidad de reducir nitrato se mantuvo después de dos ciclos con los catalizadores regenerados. Sin embargo, la reducción de nitratos tiene lugar a través de dos mecanismos diferentes, dependiendo de la naturaleza del polímero conductor:

Mecanismo A: El nitrato se adsorbe en el complejo de platino ya sea formando un aducto o entrando en el complejo como un ligando. Este mecanismo es favorecido en la PANI, donde el átomo de nitrógeno es externo al anillo, minimizándose el impedimento estérico.

Mecanismo B: Se produce un intercambio iónico entre Cl^- y/o SO_4^{2-} presentes como contraiones en los polímeros dopados y el NO_3^-, procedente de la disolución acuosa de nitrato. Este mecanismo es favorecido en el PPy.

En ambos casos, la adsorción o el intercambio iónico de nitrato es seguido por un proceso redox en el cual las nanopartículas metálicas de platino sintetizadas por plasma de argón tienen un papel en la reducción de nitrato a amonio (medido) y a nitrógeno (no medido). La producción de amonio se produjo de manera más importante cuando el platino se encontraba soportado en PPy en comparación con PANI, pero se mantuvo constante con el tiempo de reacción. La ubicación del átomo de nitrógeno dentro del anillo aromático en el PPy restringe la extensión del mecanismo A y favorece el mecanismo B, que implica la reducción del nitrato ubicado junto a las nanopartículas de platino.

Como resultado de cualquiera de los procesos redox que involucran al platino, los iones de platino son reducidos por electrones provenientes del plasma y, por otro lado, las nanopartículas de platino metálico se oxidan cuando el nitrato se reduce, con lo que el estado de oxidación de la cadena polimérica cambia. Esto evidencia una participación activa de la matriz polimérica en el proceso redox.

Las propiedades redox y el intercambio iónico de PPy y PANI dopados con $K_2S_2O_8$ tienen un papel determinante en la eliminación de nitratos del agua. Sin embargo, la naturaleza de cada polímero influye enormemente en el mecanismo de reacción. Mientras que el intercambio iónico entre los contraiones Cl^- y SO_4^{2-} y el NO_3^- del agua

es el principal responsable de la eliminación efectiva de nitratos en la PANI, el mecanismo para la eliminación de nitratos se basa en una transferencia de electrones desde el PPy al nitrato a través del N ubicado en el anillo pirrólico.

Por otro lado, el politiofeno (PT) no es capaz de intercambiar nitrato a menos que se sintetice utilizando un tensioactivo aniónico (sulfato de dodecil sodio, SDS). En este caso, se mejora el intercambio iónico entre los contraiones y el nitrato y se produce una posterior reducción de nitrato por electrones del tiofeno.

Finalmente, se ha desarrollado una nueva vía para disminuir el nitrato del agua y producir su reducción selectiva hacia el nitrógeno, evitando el uso de un catalizador metálico y de hidrógeno gaseoso. Esto implica el uso de materiales híbridos de dióxido de titanio/polímero conductor. Durante su síntesis, la anilina y el pirrol se polimerizan en la superficie del dióxido de titanio conectando las partículas de dióxido de titanio. Como resultado, se obtienen materiales híbridos conductores con propiedades térmicas mejoradas. Estos materiales son capaces de adsorber nitrato y posteriormente producir su reducción. El oxidante utilizado durante la polimerización de los monómeros sobre titania es un factor clave ya que el grado de oxidación de la cadena polimérica producido por el oxidante afecta al número de contraiones susceptibles de ser intercambiados por nitrógeno. El tamaño del contraión también determina el intercambio efectivo con el nitrato. Las interacciones Ti-C y Ti-O-C entre los polímeros y el dióxido de titanio permiten la transferencia de electrones desde la titania hacia la cadena polimérica, lo que produce la reducción del nitrato adsorbido.

La reducción de nitratos producida por TiO_2/PPy/$FeCl_3$ y TiO_2/PANI/$K_2S_2O_8$ es considerablemente más efectiva que la hidrogenación catalítica producida por nanopartículas de platino soportadas en estos materiales compuestos. En los materiales compuestos libres de metal, la reducción del nitrato se produce por los electrones proporcionados directamente por el material híbrido. Por otra parte, hay una disminución considerable en la actividad de la reacción de reducción de nitratos producida por los materiales que contienen platino. La incorporación de platino en los materiales híbridos conlleva el bloqueo de sitios N por Pt. Por lo tanto, la transferencia de electrones del material al nitrato adsorbido a la cadena polimérica por intercambio iónico disminuye y la reducción de nitrato se produce principalmente por el dihidrógeno disuelto en el agua

y adsorbido en las nanopartículas de Pt. Sin embargo, ambos mecanismos podrían estar teniendo un papel en aquellos materiales que contienen platino: no solo se produce una hidrogenación catalítica, sino que también es posible que haya una contribución de los electrones proporcionados por el polímero a la reducción del nitrato.

Annex 1. List of Abbreviations / Lista de Abreviaturas

A^-	counter-ion
Ar	argon
B	benzenoid rings in PANI structure
BET	Brunauer-Emmett-Teller equation
C^+	cations from the electrolyte solution
CTAB	CetylTrimethylAmmonium Bromide
DSC	Differential Scanning Calorimetry
$FeCl_3$	ferric chloride / iron (III) chloride
$FeCl_3 \cdot 6H_2O$	ferric (III) chloride hexahydrate
FTIR-ATR	Fourier Transform Infrared Spectroscopy - Attenuated Total Reflectance
H_2	dihydrogen
H_2O_2	hydrogen peroxide
$H_2PtCl_6 \cdot 6H_2O$	hexachloroplatinic acid hexahydrate
ICP-MS	Inducted Coupled Plasma Mass Spectrometry
$K_2S_2O_8$	potassium peroxydisulfate
MCL	Maximum Contaminant Level
MFC	Mass Flow Controller
N_2	dinitrogen
N_2O	nitrous oxide
$NaBH_4$	sodium borohydride
NH_4^+	ammonium
NO_2^-	nitrite
NO_3^-	nitrate
OH^-	hydroxyl ions
PANI	polyaniline
PPy	polypyrrole
PT	polythiophene
Pt	platinum
Q	quinoid rings in PANI structure
RF	Radio Frequency
SDS	Sodium Dodecyl Sulfate
Sn	tin

$SnCl_2 \cdot 2H_2O$	tin (II) chloride dihydrate
st	stretching
TEM	Transmission Electron Microscopy
TGA	ThermoGravimetric Analysis
TX	polyethylene glycol terc-octyphenil ether - Triton X -
WHO	World Health Organization
XPS	X-ray Photoelectron Spectroscopy
XRD	X-Ray Diffraction
δ	in-plane bending
δ_{oop}	out-of-plane bending

A^-	contraión
Ar	argón
B	anillos bencenoicos en estructura PANI
BET	Ecuación Brunauer-Emmett-Teller
C^+	cationes de la disolución de electrolitos
CTAB	bromuro de cetiltrimetilamonio
DSC	calorimetría diferencial de barrido
$FeCl_3$	tricloruro de hierro
$FeCl_3 \cdot 6H_2O$	tricloruro de hierro hexahidratado
FTIR-ATR	espectroscopía infrarroja con transformada de Fourier en el modo de reflectancia total atenuada
H_2	dihidrógeno
H_2O_2	peróxido de hidrógeno
$H_2PtCl_6 \cdot 6H_2O$	ácido hexacloroplatínico hexahidratado
ICP-MS	espectrometría de masas por plasma de acoplamiento inductivo
$K_2S_2O_8$	peroxidisulfato de potasio
MCL	máximo nivel de contaminante
MFC	controlador de flujo másico
N_2	nitrógeno
N_2O	óxido nitroso

$NaBH_4$	borohidruro de sodio
NH_4^+	amonio
NO_2^-	nitrito
NO_3^-	nitrato
OH^-	iones hidroxilo
PANI	polianilina
PPy	polipirrol
PT	politiofeno
Pt	platino
Q	anillos de quinona en la estructura de la PANI
RF	radiofrecuencias
SDS	sulfato de dodecil sodio
Sn	estaño
$SnCl_2 \cdot 2H_2O$	dicloruro de estaño dihidratado
st	tensión
TEM	microscopía electrónica de transmisión
TGA	análisis termogravimétrico
TX	polietilenglicol terc-octifenil éter - Tritón X -
WHO	organización mundial de la salud (OMS)
XPS	espectroscopía fotoelectrónica de rayos X
XRD	difracción de rayos X
δ	flexión en el plano
δ_{oop}	flexión fuera del plano

Annex 2. List of Equations

Annex 3. List of Figures

Figure 9.15. (a) Nitrate abatement and (b) ammonium concentration measured in water in the presence of the different synthesized materials. Oxidant/dopant of PANI:$K_2S_2O_8$; oxidant/dopant of PPy:$FeCl_3$ or $K_2S_2O_8$

Figure 9.16. (a) Nitrate concentration and (b) ammonium concentration measured in water at different reacton times in the presence of the different synthesized materials. Oxidant/dopant of PANI:$K_2S_2O_8$; oxidant/dopant of PPy:$FeCl_3$ or $K_2S_2O_8$

Annex 4. List of Schemes

Annex 5. List of Tables

Curriculum Vitae & List of Publications

María Jesús García Fernández nació el 12 de Agosto de 1985 en Novelda, Alicante. Estudió Licenciatura en Química en la Universidad de Alicante (2003 – 2008) y obtuvo el Título de Máster en Ciencia de Materiales en 2013 en la misma universidad, bajo el nombre *"Síntesis de catalizadores metálicos soportados en polipirrol mediante plasma de baja presión para su aplicación en la eliminación de nitratos en agua"*. El trabajo de fin de Máster fue desarrollado en el Laboratorio de Materiales Avanzados del Departamento de Química Inorgánica – Instituto Universitario de Materiales de la Universidad de Alicante. La Tesis Doctoral ha sido desarrollada en el Laboratorio de Materiales Avanzados del Departamento de Química Inorgánica de la Universidad de Alicante.

Durante la etapa de doctorado realizó una estancia de 3 meses en Poitiers, Institut de Chimie des Milieux et Matériaux de Poitiers (IC2MP-CNRS-Université de Poitiers), Francia.

PUBLICACIONES

- R. Buitrago-Sierra, M.J. García-Fernández, M.M. Pastor-Blas, A. Sepúlveda-Escribano, ***"Environmentally friendly reduction of a platinum catalysts precursor supported on polypyrrole"***, *Green Chemistry*. **2013**, *15*, 1981-1990.

- M.J. García-Fernández, R. Buitrago-Sierra, M.M. Pastor-Blas, O.S.G.P. Soares, M.F.R. Pereira, A. Sepúlveda-Escribano, ***"Green Synthesis of polypyrrole-supported metal catalysts: application to nitrate removal in water"***, *RSC Advances*. **2015**, *5*, 32706-32713.

- M.J. García-Fernández, R. Buitrago-Sierra, M.M. Pastor-Blas, A. Sepúlveda-Escribano, ***"Plasma-assisted preparation of polypyrrole-supported catalysts Application to nitrate removal in water"***, Artículo del libro "Recent advances within the field of materials science in Spain", *Publicacions Universitat d'Alacant*. **2015**, 366-380. ISBN: 978-84-9717-346-9.

- M.J. García-Fernández, S. Sancho-Querol, M.M. Pastor-Blas, A. Sepúlveda-Escribano, ***"Surfactant-assisted synthesis of conducting polymers. Application***

to the removal of nitrates from water", *Journal of Colloid and Interface Science*. **2017**, *494*, 98-106.

- M.J. García-Fernández, M.M. Pastor-Blas, F. Epron, A. Sepúlveda-Escribano, ***"Proposed mechanisms for the removal of nitrate from water by platinum catalysts supported on polyaniline and polypyrrole"***, *Applied Catalysis B: Environmental*. **2018**, *225*, 162-171.

- J.J. Villora-Picó, V. Belda-Alcázar, M.J. García-Fernández, E. Serrano, A. Sepúlveda-Escribano, M.M. Pastor-Blas, ***"Conducting polymer-TiO_2 hybrid materials: application in the removal of nitrates from water"***, *Langmuir*. **2019**, *35*, 6089-6105.

- J.J. Villora-Picó, M.J. García-Fernández, A. Sepúlveda-Escribano, M.M. Pastor-Blas, ***"Metal-free abatement of nitrate contaminant from water using a conducting polymer"***, *Chemical Engineering Journal*. **2021**, *403*, 126228-126240.

CONGRESOS

- *IX Jornadas Científicas de Instituto Universitario de Materiales IUMA 2013*; Alicante, España 24-25 Enero, 2013. ASISTENCIA.

- *Escuela de Verano (2ª Escuela hispano-italiana de Catálisis) SECAT 2013*; Sevilla, España 24-25 Junio, 2013. ASISTENCIA.

- M.J. García-Fernández, M.M. Pastor-Blas, A. Sepúlveda-Escribano, ***"Reducción de nitratos en agua utilizando un catalizador de platino-estaño soportado en polipirrol"***. *SECAT 2013*; Sevilla, España 26-28 Junio, 2013. PÓSTER.

- M.J. García-Fernández, M.M. Pastor-Blas, A. Sepúlveda-Escribano, ***"Reducción de nitratos en agua utilizando un catalizador de PPy-Pt:Sn"***. *XVII Jornadas de Investigación Departamental San Alberto Magno*; Alicante, España 11-15 Noviembre, 2013. PÓSTER.

- *X Jornadas Científicas de Instituto Universitario de Materiales IUMA 2014*; Alicante, España 23-24 Enero, 2014. ASISTENCIA.

- M.J. García-Fernández, M.M. Pastor-Blas, A. Sepúlveda-Escribano, ***"Síntesis de catalizadores de platino soportado en polipirrol y polianilina para la eliminación de nitratos del agua"***. *X Jornadas Científicas de Instituto Universitario de Materiales IUMA 2014*; Alicante, España 23-24 Enero, 2014. PÓSTER.

- *10th International Symposium on the Characterization of Porous Solids – Pre-symposium School*; Alicante, España 8-10 Mayo, 2014. ASISTENCIA.

- M.J. García-Fernández, M.M. Pastor-Blas, A. Sepúlveda-Escribano, ***"Síntesis de catalizadores metálicos soportados sobre polímeros conductores y su utilización en la eliminación de contaminantes"***. *Jornadas Doctorando Universidad de Alicante*; Alicante, España 22 Mayo, 2014. ORAL.

- *I Encuentro de Jóvenes Investigadores de la SECAT – JJ.II. SECAT 2014*; Málaga, España 22-24 Junio, 2014. ASISTENCIA.

- M.J. García-Fernández, M.M. Pastor-Blas, A. Sepúlveda-Escribano, ***"Síntesis de catalizadores de platino soportado en polipirrol y polianilina para la eliminación de nitratos del agua"***. *I Encuentro de Jóvenes Investigadores de la SECAT – JJ.II. SECAT 2014*; Málaga, España 22-24 Junio, 2014. FLASH ORAL + PÓSTER.

- M.J. García-Fernández, M.M. Pastor-Blas, A. Sepúlveda-Escribano, ***"Síntesis de catalizadores de platino soportado en polipirrol y polianilina para la eliminación de nitratos del agua"***. *XVIII Jornadas de Investigación Departamental San Alberto Magno*; Alicante, España 10-14 Noviembre, 2014. PÓSTER.

- M.J. García-Fernández, M.M. Pastor-Blas, A. Sepúlveda-Escribano, ***"Synthesis of polypyrrole with two different oxidants for its application in the abatement of***

nitrate from water". *XI Jornadas Científicas de Instituto Universitario de Materiales IUMA 2015*; Alicante, España 22-23 Enero, 2015. PÓSTER.

- M.J. García-Fernández, M.M. Pastor-Blas, A. Sepúlveda-Escribano, ***"Synthesis of polypyrrole with two different oxidants for its application in the abatement of nitrate from water"***. *XX Jornadas de Investigación Departamental*; Alicante, España 25 Noviembre, 2015. PÓSTER.

- M.J. García-Fernández, M.M. Pastor-Blas, A. Sepúlveda-Escribano, ***"Synthesis and characterization of conducting polymer/TiO_2 hybrid materials for its application in the abatement of nitrate from water"***. *XX Jornadas de Investigación Departamental*; Alicante, España 25 Noviembre, 2015. PÓSTER.

- *XII Jornadas Científicas de Instituto Universitario de Materiales IUMA 2016*; Alicante, España 21-22 Enero, 2016. ASISTENCIA.

- M.J. García-Fernández, M.M. Pastor-Blas, A. Sepúlveda-Escribano, ***"Synthesis and characterization of conducting polymer/TiO_2 hybrid materials for its application in the abatement of nitrate from water"***. *XII Jornadas Científicas de Instituto Universitario de Materiales IUMA 2016*; Alicante, España 21-22 Enero, 2016. PÓSTER.